WARWICK
THE UNIVERSITY OF WARWICK

A Thesis Submitted for the Degree of PhD at the University of Warwick

Permanent WRAP URL:
http://wrap.warwick.ac.uk/101423

Copyright and reuse:
This thesis is made available online and is protected by original copyright.
Please scroll down to view the document itself.
Please refer to the repository record for this item for information to help you to cite it.
Our policy information is available from the repository home page.

For more information, please contact the WRAP Team at: wrap@warwick.ac.uk

warwick.ac.uk/lib-publications

Chromatin Remodelling During Plant-Pathogen Interactions

by

Emmanouil Mastorakis

A thesis submitted in partial fulfilment of the
requirements for the degree of
Doctor of Philosophy in Life Sciences

2013-2017

School of Life Sciences, University of Warwick

Supervisor: Dr. Vardis Ntoukakis

CHROMATIN REMODELLING DURING PLANT-PATHOGEN INTERACTIONS

Dedication

I dedicate this work to my family who have provided me with unparalleled support for as long as I can remember

Table of Contents

List of Figures

List of Tables

Author's declaration

I hereby certify that this thesis is presented in accordance with the regulations for the degree of Doctor of Philosophy. It has been composed by myself and has not been submitted in any previous application for any degree. The work in this thesis has been undertaken by myself except where otherwise stated.

Dr. Sophie Piquerez from the Ntoukakis group (University of Warwick, UK) has been closely involved in many of the experiments presented here, as an advisor and collaborator.

Dr. Selena Gimenez-Ibanez (University of Warwick, Coventry, UK & National Centre of Biotechnology CSIC, Madrid, Spain) cloned all of the *Pseudomonas syringae* effectors presented in Chapter 5 and performed the effector screen using the FRAP method under my guidance and assistance. Additional data from Dr. Gimenez-Ibanez have been used in this chapter as indicated. The project presented in Chapter 5 also benefited from work conducted by undergraduate students such as Charles Greenspon, Oscar Guerra and James Coleman.

Emmanouil Mastorakis

PhD candidate

Student ID: 0920695

University of Warwick

Coventry

United Kingdom

Acknowledgements

A four year-long journey could not be complete without the help of several fellow travellers.

To my awesome friends in the lab Bea, Chrysa, Alonso, Arsheed, Steph, Ruth, Jack and Ranjith I owe massive gratitude for being amazing friends and colleagues. I learned many things from each and every one of them.

To Vardis I would like to say a big 'Thank you' for all the support and for giving me the chance as his first PhD student to work on extremely interesting, challenging and ambitious projects.

Last but not least, this work has been a tight collaboration with Sophie. Through daily cooperation, struggle, brainstorming, moments of discovery & despair, she has been the key person to unlock most of the skills that I applied on a daily basis. Learning from her exemplary persistence, resourcefulness and intelligence were the compass I needed on this rocky journey!

Abbreviations

Term	Definition
35S	Cauliflower Mosaic Virus (strong promoter)
AcCoA	Acetyl Coenzyme A
bp	Base pair
Br/Bromo	Bromodomain
CBB	Coomassie Brilliant Blue
Chr/Chromo	Chromodomain
cDNA	Complementary DNA
dpi	days post infection
EMS	Ethyl Methane Sulfonate
ETI	Effector-Triggered Immunity
FA	Formaldehyde
FRAP	Fluorescence Recovery After Photobleaching
g	Gram
g	Centrifugal force unit
HAT	Histone Acetyltransferase
HDAC	Histone Deacetylase
kb	Kilobase
kDa	kilo Daltons
PAMPs	Pathogen Associated Molecular Patterns
PCR	Polymerase Chain Reaction
PEG	Polyethylene Glycol
PRR	Pattern Recognition Receptor
PTI	PAMP-Triggered Immunity
ROS	Reactive Oxygen Species
rpm	rounds per minute
RPM	Revolutions per minute
SA	Salicylic Acid
SAGA	Spt-Ada-Gcn5 acetyltransferase
SWI/SNF	SWItching-defective/Sucrose Non-Fermenting
T-DNA	Transfer DNA

Summary

Plants - including commercially important crops - are exposed to numerous pathogens often resulting in significant loss of yield. Understanding the underlying mechanisms of pathogen recognition and defence strategies is key in successfully ensuring food security. Research on plant-pathogen interactions has mainly focused on the gene networks after pathogen perception as well the identification of resistance genes. Latest research suggests that chromatin remodelling, including nucleosome displacement and DNA or histone-modifying enzymes are important in plant immunity. This thesis focuses on chromatin remodelling as the mechanism by which plants mount an effective immune response. The thesis also investigates the role of histone acetylation as one of several chromatin remodelling mechanisms. Histone acetyltransferases (HATs) and histone deacetylases (HDACs) are two classes of histone modifying enzymes that antagonistically govern the acetylation levels of histones in gene promoters and gene bodies ultimately affecting gene expression. HAG1 was identified as an important positive regulator of plant immunity in the interaction with *Pst* DC3000. A proteomic approach allowed the identification of TOPLESS family members as HAG1 interactors. Considering that chromatin remodelling is an important aspect of plant immunity, it was hypothesised that pathogens have evolved mechanisms to interfere with such processes. To this end, this thesis will present a comprehensive approach towards identifying *Pst* DC3000 Type-III effectors with the ability to interfere with chromatin remodelling. HopO1-1 was initially identified as an effector with chromatin binding properties, however, further experiments pointed more strongly towards this effector's involvement in processes such as translation and photosynthesis. Overall, this thesis contributes towards a better understanding of the roles of histone acetylation and HAG1 histone acetyltransferase in plant immunity and sheds light into which *Pst* DC3000 effectors could be potentially involved in chromatin remodelling processes.

Chapter 1 - Introduction

1.1. Biotechnology promises to tackle global food security problems

Food and agriculture globally are estimated to be a $5 trillion industry experiencing continuous growth (Denis, 2015). The socioeconomic and environmental impact of agribusiness represents 10% of global consumer spending, 20% of employment as well as 30% of greenhouse-gas emissions. By current trends, with an exponentially growing world population expected to reach 10 billion people by 2050, caloric demands for both human and animal feed will double. In order to meet this growing demand, food production must continue to increase, despite a sizeable improvement in productivity improvement observed over the past 50 years (Fuglie et al., 2012). However, agriculture today faces important challenges, which render this objective a difficult task. The increased agricultural activity suggests that 40% of water demand in 2030 is unlikely to be met, whilst the continuous loss of arable land and changing climates are some of the most highlighted and well-studied problems. In addition, approximately 26% of the worldwide crop production each year is lost due to pests and pathogens even before harvest. With rapidly advancing global trades, changing climates and agricultural intensification, the spread of plant diseases is expected to increase further. Different geographies may face some of these problems to different levels, nevertheless, the above considerations represent global issues (Bebber et al., 2013). Altogether, this means that increases in food production will largely rely not only on increasing current agricultural efforts, but also on the development of existing technologies to improve output from the same amount of arable land. The four staples, which feed more than half the population includes wheat (*Triticum aestivum*), maize (*Zea mays*), banana (*Musa acuminata*) and rice (*Oryza sativa*). Importantly, the challenges facing these ma-

jor crops includes emerging infectious diseases throughout both developing and developed countries (Fisher et al., 2012).

Crop plants are exposed to a wide-range of pests and pathogens, such as bacteria, fungi, oomycetes, viruses, nematodes, and insects, but only in certain interactions does this culminate in disease. For example, wheat faces a threat by the virulent Ug99 strain of wheat stem rust fungus (*Puccinia grimness g. sp. tritici*) (Singh et al., 2015), while Panama disease (fungus *Fusarium oxysporum*) is an important issue in bananas (Churchill, 2011). Potato and tomato are challenged by late blight disease caused by the oomycete *Phytopthora infestans,* which is known for the 1.25 million deaths during the Irish potato famine in 1845, but also for being a modern-day problem for farmers (Haverkort et al.,2008; Haas et al., 2009).

In the absence of genetic resistance in crops, food production heavily relies on chemical control of pathogens, a critical element in pest management. Although pesticides are a testament of the improved productivity in the past few decades allowing the quadrupling of food grain production from the 1950s to 2000s, there are many reported hazards of these chemicals, which are driving the requirement for more sustainable approaches. Initially, lime sulfur was introduced in the 1800s and fungicides interfering with the metabolic processes of fungi were introduced in the 1900s. Since then, use of fungicides has seen a continuous rise in all markets of the world, and has further increased during pathogen outbreaks in different parts of the world. Rice blast, for example, the most economically important disease in Japan faces recurrent outbreaks once to twice every decade leading to the introduction of multiple types of fungicides for the protection of blast-susceptible rice varieties (Hirooka et al., 2013). This highlights the inevitable vicious cycle of chemical control and pathogen resistance in modern-day agriculture.

The burden of chemical-based pest management has been studied

extensively showing the detrimental effects of pesticides on human health and environment. In fact, the World Health Organization (WHO) has reported that there is no population segment that is completely protected against exposure to pesticides and the associated health effects, although there are high-risk countries shouldering a disproportionate level of this burden (WHO, 1990).

Briefly, certain chemicals have been found to mimic or antagonise natural hormones in humans and have been linked to immune suppression, reproductive abnormalities and cancer (Brouwer et al., 1999; Crisp et al., 1998). Meanwhile, such pesticides have also been found to contaminate ground and surface water through runoff from treated plants and soil, while their effect on heavily treated soils can cause beneficial soil microorganisms to decline. Pesticide sprays can also directly affect non-target vegetation and non-target organisms damaging wildlife overall (Aktar et al., 2009).

Furthermore, limitations in conventional breeding approaches for a large group of crops is an additional factor driving the necessity for genetic engineering of crops. For example, banana, which is the staple food in more than 50 countries exists as a sterile triploid selected from the wild making its breeding a challenging process and is, therefore, propagated vegetatively. This lack of genetic diversity makes banana trees highly susceptible to changing biotic and abiotic stresses (Cronauer-Mitra and Krikorian, 1987).

All the above highlight the need for a more sustainable approach, which would allow for durable endogenous resistance to reduce dependence on chemical-based approaches. There is already a significant amount of evidence to support the potential of biotechnological approaches in meeting this challenge. In general, biotechnology is capable of overcoming production constraints that are more difficult or intractable

by conventional breeding. Thus, it can provide farmers with disease-free planting materials by creating inherently resistant crops.

Starting off with the first signs of human intervention on agriculture dating back to 10,000 BC, domestication of crops with desirable traits led to selection of specific cultivars (Abbo et al., 2014). In addition, in the beginning of the 20th century, with an increased understanding of inheritance principles through Gregor Mendel's research, classical breeding methods resulted in the generation of commercial hybrid crops. In the 1950s, with the discovery of DNA as the genetic material and the development of genetic engineering technologies, engineered plant varieties became a reality. Using *Agrobacterium tumefaciences* as a vector, desired genes have been transferred to crops of interest, resulting in desirable phenotypes. The first commercial example of genetic engineering came with pharmaceutical company Celgene's Flavr Savr tomato, which became the first ever food crop with approval for commercial production after being modified for increased firmness and longer shelf life (Redenbaugh, 1992). This was followed by the approval of Bt corn, genetically engineered to resist herbicides by producing Bt toxin resulting in easier cultivation. In addition, Monsanto introduced the first of a group of glyphosate-resistant crops also known as Roundup Ready crops in the 1980s (Homrich et al., 2012). Another significant development is Golden Rice, which was developed to address the problem of vitamin A deficiency in high-risk populations, where the death toll is approximately 500,000 people annually. Provitamin A pathway genes have been genetically introduced into rice and in fact, one gene has a bacterial origin, highlighting that in addition to across-plant species gene transfer, gene transfer across-kingdoms can also find real-world applications in modern agriculture (Paine et al., 2005; Schaub et al., 2005). More recently, 'golden bananas' were generated as a proof of concept and were field-trialled in Australia to test the success of biofortification of this crop to contain higher levels of

provitamin A (Paul et al., 2017).

There is also a plethora of well-characterised examples of gene transfer into crops translating research in model organisms to crops. For example, the EF-Tu receptor (EFR), which is restricted to the *Brassicaceae* genus, was shown to confer broad spectrum bacterial resistance in the *Solanaceae* genus (Lacombe et al., 2010), whilst ongoing projects involve the same strategy applied in potato, lettuce, apple and citrus (2Blades-Foundation, 2004). Narusaka *et al* (2013) also demonstrated the activity of nucleotide binding and leucine rich repeat (NB-LRRs) proteins in taxonomically distinct families by transferring Brassicaceae-specific *RPS4* and *RRS1* to tomato (*Solanum lycopersicum*) and tobacco (*Nicotiana benthamiana*). These examples show that the downstream elements of R genes are highly conserved and this supports the current strategies of resistance gene transfer between different crop species. Lastly, the application of such strategies has relied for years on the extensive study of plant immunity by employing model patho-systems such as the one consisting of the model plant *Arabidopsis thaliana* and the Gram-negative bacterium *Pseudomonas syringae*.

1.2. The *Arabidopsis thaliana - Pseudomonas syringae* pathosystem

Arabidopsis thaliana has proved to be an indispensable tool in characterising biological processes in plants, empowered by a huge library of well-described Arabidopsis mutants generated by T-DNA insertion or EMS mutagenesis. This system lends itself to both forward and reverse genetics, which have led to the identification of important proteins involved in defence such as FLS2 (FLAGELLIN SENSING2) (Gomez-Gomez and Boller, 2000) and BAK1 (BRASSINOSTEROID INSENSITIVE1-ASSOCIATED KINASE1) (Chinchilla et al., 2007). Arabidopsis can be infected by multiple pathogens, which has allowed the study of plant-pathogen interactions including plant-bacterium (e.g. *Pseudonomas sy-*

ringae) and plant-fungus (e.g. *Magnaporthe oryzae*) and plant-oomycete (e.g. *Phytophthora infestans*) interactions.

P. syringae, specifically, can infect different plant species thus further strain classification into pathovars (*pv*.) is based on host specificity. As an example, *P. syringae* DC3000 *pv*. tomato was first identified from tomatoes in California and is known to infect this plant causing bacterial speck disease and resulting in great yield and financial losses (Scofield et al., 1996). Interestingly, *P. syringae* has been found to have a dual lifestyle whereby the pathogen initially grows at the leaf surface (epiphytically), gradually entering the leaf tissue through stomata or wounds. This is followed by aggressive multiplication at which stage host cell death is observed, also known as necrosis. The pathogen is thus described as a hemibiotroph as it avoids killing the host until the later stages of infection, which is in contrast to necrotrophic pathogens known to kill the host for the purposes of obtaining nutrients (Xin and He, 2013). Additionally, *Pst* DC3000 *pv*. tomato is able to establish infection in Arabidopsis, which resulted in its popularisation as a model species across multiple research groups allowing researchers to expand our knowledge of plant-bacteria interactions (Koornneef and Meinke, 2010).

Research on *Pst* DC3000 has revealed that its virulence relies on the production of toxins, phytohormones and protein effectors encoded in the *Pst* DC3000 genome, which are delivered through a Type III secretion systems (Lindeberg et al., 2008). Overall, this pathosystem has aided in the discovery of defence mechanisms on the host side as well as virulence mechanisms on the pathogen side, both of which form the basis of the evolutionary arms-race between host and pathogen.

1.3. Current understanding of the plant immune system

All multicellular eukaryotes can become susceptible to pathogens. Whilst animals have developed innate and adaptive immunity, plants rely

entirely on an innate system and the ability of individual cells to mount immune responses upon pathogen detection by cell surface or intracellular immune receptors (Jacob et al., 2013). In this way, the plant immune system has evolved to protect the host against a variety of pathogens. However, the diverse strategies employed by pathogens make it a bigger challenge for plants to successfully respond to infection. Our current understanding of a plant-pathogen interaction and co-evolution is summarised in the zig zag model, proposed by Dangl and Jones, which describes the quantitative output of the plant immune system throughout the course of the infection. This model is heavily based on the *Arabidopsis thaliana-P.syringae* interaction. Specifically, in Phase 1, the presence of a pathogen is rapidly recognised by the plant. Recognition takes place through pattern recognition receptors (PRRs) on the surface of the plant plasma membrane. The ligands of PRRs are highly conserved pathogen structures known as pathogen-associated molecular patterns (PAMPs) and some of the most famous studied examples include bacterial flagellin or its synthetic derivative, the 22-amino acid epitope, flg22 (Felix et al., 1999b); elongation factor Tu (EF-Tu) or its synthetic derivative, the 18-amino acid epitope, elf18 (Kunze et al., 2004). Notably, different receptors are responsible for the recognition of different PAMPs. Experiments involving immunological techniques and binding assays have shown that a 175kDa transmembrane leucine rich receptor (LRR) kinase known as FLS2 is essential for the recognition of flg22 in *Arabidopsis thaliana* and tomato (Felix et al., 1999a). Similarly, EF-Tu is recognised by the LRR-kinase called EFR leading to converged downstream PTI responses (Kunze et al., 2004). The formation of immune receptor complexes between proteins and PRRs is necessary for normal perception of PAMPs and signal transduction. *In vivo* phospho-labelling experiments showed the *de novo* phosphorylation of both FLS2 and the co-receptor BAK1 within 15 seconds of flg22 elicitation, suggesting that extracellular receptors are poised

to detect the presence of PAMPs and can do so in a rapid and robust manner (Schulze et al., 2010). Pattern recognition receptors (PRRs) are receptor kinases (RKs), which also contain a cytosolic kinase domain and a variable ectodomain with leucine-rich repeats (LRRs) as in the case of FLS2 and EFR. Others such as CERK1 (CHITIN ELICITOR RECEPTOR KINASE 1) contain LysM motifs or other ligand-binding domains. Downstream RKs are proteins known as plant receptor-like cytoplasmic kinases (RLCKs), which have been recognised as important regulators of immunity (Lin et al. 2013). For example, the RLCK BIK1 (BOTRYTIS-INDUCED KINASE 1) is a common downstream interactor for RKs including FLS2, EFR, CERK1 and BAK1. Following phosphorylation and activation, BAK1 subsequently phosphorylates its two known substrates RBOHD and CDPKs (Lin et al., 2014). Hyperphosphorylation is observed upon PAMP perception, which is likely to further activate BIK1, facilitating the onset of PAMP-triggered responses such as production of reactive oxygen species (ROS) and phosphorylation of RBOHD (Kadota et al., 2014). Additional PTI (PAMP-triggered immunity) responses include but are not limited to the strengthening of the cell wall by callose deposition (Luna et al., 2011), the production of reactive oxygen species (ROS), Ca^{2+} influxes, MAPK (mitogen-activated protein kinases) and CDPK (cyclin-dependent protein kinases) cascade activation leading to further downstream gene activation (Boller and Felix, 2009; Boudsocq et al., 2010; Ma and Berkowitz, 2007; Tena et al., 2011).

In phase 2, effector-triggered susceptibility (ETS) ensues when pathogens deliver into the host cell and the apoplast multiple effector proteins. Effectors interfere with PTI processes and can thus enhance the pathogen's virulence and colonisation (Jones and Dangl 2006).

In phase 3, direct or indirect effector recognition by host proteins leads to effector triggered immunity (ETI). The proteins involved in effector recognition typically are intracellular immune receptors known as NB-

LRRs (Nulceotide-Binding-Leucine Rich Repeat) and resemble Nod-Like Receptors (NLRs) found in mammals (Matzinger, 2007). Upon intracellular detection of pathogen effectors, ETI ensues, leading to increased disease resistance and involving a hypersensitive cell death response (HR) at the site of infection. This aims to effectively prevent the pathogen from spreading to other tissues (Jones and Dangl 2006).

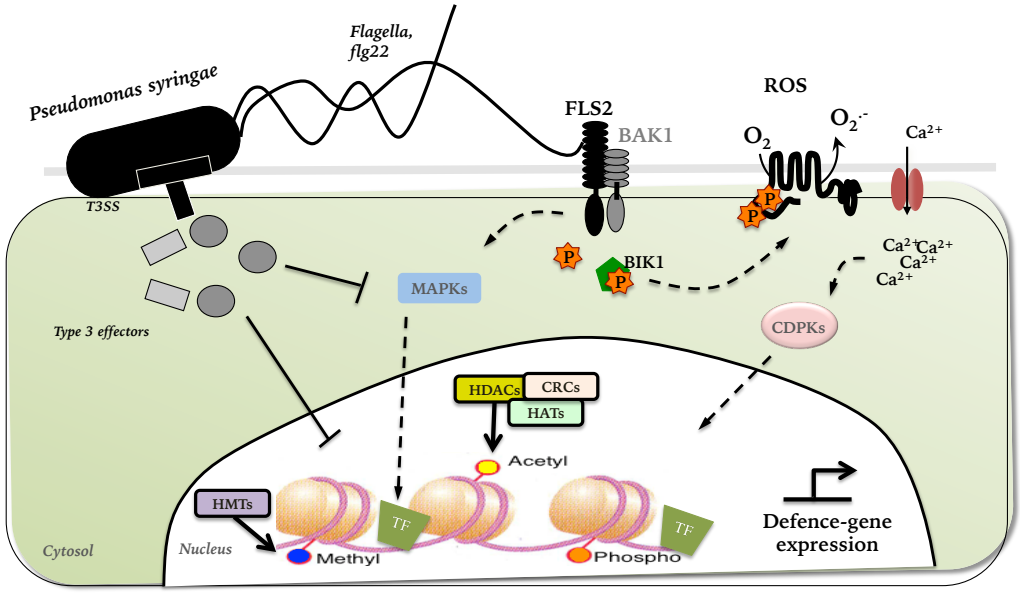

Figure 1.1. The plant immune system. PAMPs such as flagella or its epitope, flg22, are recognised by plasma membrane-associated receptors such as FLS2. Dimerisation with BAK1 is known to occur immediately after PAMP perception. Downstream events include interaction and trans-phosphorylation with BIK1. The latter together with CDPKs further phosphorylates RBOHD protein to facilitate the release of ROS at the extracellular space. Meanwhile, calcium influx takes place leading to the activation of CDPKs, which mediates nuclear processes such as gene activation. Genes such as *NHL10* and *PHI1* are known to be partially or completely dependent upon CDPKs, respectively. At the same time, MAPKs are activated leading to gene activation. *FRK1* is an example of MAPK-dependent gene. It is unknown whether MAPKs and CDPKs are able to directly phosphorylate histones, however, in the case of MAPKs, direct targets such as histone deacetylases (HDACs) or transcription factors have been reported. Different enzymes are involved in chromatin remodelling such as histone acetyltransferases (HATs), HDACs, histone methyltransferases (HMTs) and chromatin remodelling complexes (CRCs). These responses are part of PAMP-triggered immunity, which can be targeted by effectors delivered into the cell via a Type III Secretion System (T3SS) found in bacterial pathogens such as *Pseudomonas syringae* DC3000 *pv*. tomato. Suppression of PTI results in effector-triggered susceptibility (ETS). The figure does not include nucleotide-binding leucine-rich repeat (NB-LRR) proteins, which are involved in the recognition of effectors leading to effector-triggered immunity (ETI). Adapted from multiple sources referenced in the main text.

In phase 4 of the proposed zig-zag model, natural selection on both sides of this evolutionary arms race drives the formation of diversified ef-

fector genes capable of avoiding or inhibiting ETI and the subsequent evolution of new resistance genes to trigger ETI once again. It is believed that microbial pathogens evolve faster than plants, however, defence mechanisms evolved by plants have been found to be effective allowing the host to keep up with the fast-evolving virulence strategies of pathogens.

1.4. PTI outputs contribute towards a robust defence response

PAMP-triggered immunity (PTI) is usually effective at stopping pathogen growth due to a rapid and robust set of responses, which includes the production of ROS, increases in intracellular Ca^{2+}, CDPK and MAPK signalling cascades, callose deposition, closing of stomata and downstream activation of defence genes, among other mechanisms (Nicaise et al., 2009; Tena et al., 2011).

Production of ROS is known to increase rapidly after pathogen attack establishing local and systemic resistance. In addition, ROS can directly strengthen host cell walls through cross-linking of glycoproteins (Bradley et al., 1992). The plasma membrane-bound NADPH oxidase also known as RBO (respiratory burst oxidase) is involved in the production of ROS such as superoxide after the transfer of electrons to molecular oxygen. In Arabidopsis, 10 *AtRboh* genes exist and the expression of these is significantly induced after recognition of bacterial and fungal pathogens (Bolwell et al., 1998; Chittoor et al., 1997). It is also known that ROS serve diverse signalling processes during disease resistance, which explains why on one hand, double mutants *atrbohD/atrbohF* display reduced HR, whilst on the other hand, a *atrbohF* single mutant is more resistant to a weak virulent strain of the oomycete *Hyalopernonospora parasitica* with enhanced HR. However, some of this diversity is due to the fact that not all ROS responses are localised in the plasma membrane, rather some are localised in the chloroplast or can also take place in the root (Torres et al., 2002).

Ca^{2+} influx is another PTI response with multiple known functions. A Ca^{2+} gradient exists across the plasma membrane whereby extracellular Ca^{2+} is higher in resting plant cells. Upon elicitation of plant cells, cytosolic Ca^{2+} rapidly increases and is perceived by calmodulin and calcium dependent protein kinases resulting in their activation. In addition, Ca^{2+} is believed to function as a potentiator of reactive oxygen intermediates (ROI) and nitric oxide (NO) production thus contributing to the hypersensitive response (HR) overall. In relation to this, CDPKs phosphorylate RBOHD and contribute to ROS production (Dubiella et al., 2013; Lecourieux et al., 2002; Lecourieux et al., 2006). Another important role of Ca^{2+} influx is to activate downstream calcium-dependent protein kinases (CDPKs). Specifically, Boudoscq *et al* (2010) showed that four CDPKs were critical for the transcriptional reprogramming that occurs in plant immune signalling. Interestingly, in the same study, using an in-gel kinase assay with histone H3 as a substrate, activation of CDPKs was observed as early as 15 minutes after flg22 elicitation. This was solely dependent upon Ca^{2+} ions as the phosphorylation was not seen in the presence of a Ca^{2+} chelator.

Interestingly, CPK4, 5, 6 and 11 were found to re-localize to the nucleus, interacting with WRKY TFs, resulting in the phosphorylation of WRKY8, 28 and 48 during ETI induced by RPS2 or RPM1 R proteins (Gao et al., 2013).

Signalling of PAMP perception can also be relayed downstream by MAPKs. These enzymes are involved collectively in signalling cascades whereby they phosphorylate downstream kinases giving rise to a nomenclature such as MAPKs, MAPK kinases (MAPKKs) and MAPKK kinases (MAPKKKs) (Pitzschke et al., 2009). A phosphorylation cascade that consists of MEKK1 (MAPKKK), MKK4 & MKK5 (MAPKK) and MPK3 & 6 (MAPK) is activated following elicitation by flg22 (Asai et al 2002). Knockout mutations in *mpk3* and *mpk6* mutants result in increased *Botry-*

tis cinerea (necrotrophic fungus) susceptibility (Kliebenstein et al., 2005), although MPK3 was found to be a negative regulator of inducible defences in the interaction with *P. syringae* (Frei dit Frey et al., 2014). A number of genes have been found to be induced in a MAPK-dependent manner such as *FRK1* (*FLG22-INDUCED RECEPTOR KINASE1*) (Asai et al., 2002; Boudsocq et al., 2010). Interestingly, the activation of some defence genes is dependent on MAPKs as well as CDPKs, as for example, *NHL10* (*NDR1/HIN1-LIKE 10*), whilst others are CDPK-dependent as in the case of *PH1* (*PHOSPHATE- INDUCED 1*)(Boudsocq et al., 2010). MAPKs can localise to the nucleus to phosphorylate nuclear proteins involved in transcription as in the case of MKS1 a phosphorylation substrate of MPK4 both *in vivo* and *in vitro* (Qiu et al., 2008). A recent example came from Latrasse *et al* (2017) who showed the direct interaction of MPK3 and HD2B (HDAC) in response to PAMP-perception. Another example is that MPK3 phosphorylates VIP1 (VirE1-INTERACTING PROTEIN 1) after flg22 perception and as a bZIP (basic leucine zipper) transcription factor, VIP1 induces the expression of *PR1* among other defence genes (Pitzschke and Hirt, 2009). The role of MAPK cascades has been demonstrated in the context of hormonal signalling, specifically in Systemic Acquired Resistance (SAR), which provides the plant systemic protection in a salicylic acid (SA)-dependent manner (Durrant and Dong, 2004a). Higher levels of SA and enhanced resistance to *P. syringae* were found in *mpk4* mutants, however, this was due to the function of MPK4 as a positive regulator of jasmonic acid (JA) responses and it is known that these two hormonal pathways are regulated in an antagonistic manner (Brodersen et al., 2006; Petersen et al., 2000). In all, MAPKs have a well-established role in inducing transcription in basal conditions and in response to stresses and their activities couple upstream PAMP receptors and downstream regulators of immunity.

As mentioned earlier, pathogens are able to subvert immune processes such as PTI responses of the host, leading to enhanced susceptibility. Numerous examples of this have been recorded.

HopAI1 was shown to inactivate MPK3 and MPK6 by de-phosphorylating threonines through a unique phosphothreonine lyase activity leading to the suppression of two independent downstream evens such as the re-inforcement of cell wall defences as well as PAMP-induced transcriptional activation of specific genes. *Pst* DC3000 *pv*. tomato lacking HopAI1 was less virulent, whilst the MAPK-dependent *FRK1* gene among others was not induced as strongly in transgenic plants expressing HopAI1 (Zhang et al., 2007)

AvrPto and AvrPtoB are two very well-studied effectors capable of suppressing PTI responses by targeting the PRR complex consisting of FLS2 and BAK1 that forms after flg22 perception. CERK1 is also targeted by AvrPtoB (Gimenez-Ibanez et al., 2009).

HopM1 is an effector from *Pst* DC3000 that alters proteasome specificity in Arabidopsis MIN7 in a post-translational manner resulting in the destabilization of MIN7. AtMIN7 is an ADP-ribosylation factor-guanine nucleotide exchange factor (ARF-GEF) regulating vesicle trafficking and is believed to recycle or mobilise immunity-related plasma-membrane proteins (e.g. FLS2) allowing plants to perceive or respond to the pathogen. In *min7* mutants lacking AtMIN7, susceptibility is increased, but also rescues the growth of *Pst* DC3000 lacking HopM1 (Nomura et al., 2006; Ustun et al., 2016).

Another example of effector-mediated interference of immune signalling is HopAO1. Following elf18 perception by the EF-TU RECEPTOR (EFR) the receptor is phosphorylated in multiple tyrosine residues. Phosphorylation of Y836 is necessary to induce downstream signalling in response to *P. syringae* infection, however, HopAO1 effector, a tyrosine phosphatase was found to reduce EFR phosphorylation (Bretz et al.,

2003; Espinosa et al., 2003). HopAO1 expression led to 50% reduction in the phosphorylation of EFR upon elf18 treatment. As a result, in the presence of HopAO1, dampening of immune responses such as MAPK activation and ROS production was observed and was followed by increased bacterial growth (Macho et al., 2014).

1.5. Effector-triggered immunity

In response to these virulence strategies, plants have developed mechanisms allowing the recognition of effectors and the establishment of a hypersensitive response (HR), which aims to effectively stop the spread of the pathogen. HR development is part of ETI and relies on NB-LRRs, which are particularly important in plant immunity, as exemplified by a significantly larger group of NB-LRRs in plants amounting to 125 in Arabidopsis (Col-0 ecotype) as opposed to approximately 20 in mammals (Jones and Dangl, 2006). In addition, the NB-LRR gene family is one of the largest within plants and contains genes that are polymorphic and evolve rapidly due to the presence of transposable elements within NB-LRR gene clusters (Baumgarten et al., 2003). NB-LRRs are predicted to be cytoplasmic allowing the monitoring of plant proteins that are potential targets of effector proteins (McHale et al., 2006). NB-LRR classification is based on their N-terminal structural features, whereby, TIR-NB-LRRs contain N-terminus with homology to the Toll and interleukin receptors, whereas non-TIR-NB-LRRs are also known as CC-NB-LRRs due to the presence of a coiled-coil domain in their N-terminus (Dangl and Jones, 2001; Van der Biezen and Jones, 1998).

A well-known example of TIR-NB-LRR pair consists of RRS1-R and RPS4. Briefly, the bacterial effectors PopP2 (from the Gram-negative root pathogen *Ralstonia solanacearum*) and AvrRps4 (from *P. syringae* pv. *pisi*) are recognized by the same pair of NB-LRRs consisting of RPS4 (*Resistance to Pseudomonas syringae 4*) and RRS1-R (*Resistance to Ralstonia*

solanacearum 1). The latter is atypical in that it consists of an additional C-terminal WRKY DNA-binding domain, which is traditionally known to exist in WRKY proteins that are transcription factors binding DNA at specific sequences (Deslandes et al., 2003). In addition, Pop2, which belongs to the YopJ family and has acetyltransferase activity is able to acetylate RRS1 in leucine 1221 thus weakening its DNA-binding affinity and leading to the activation of cell death. AvrRps4 on the other hand does not acetylate RRS1, but leads to cell death in a yet unknown mechanism (Deslandes et al., 2003; Sarris and Jones, 2015).

1.6. Phytohormone signalling in plant immunity

During plant defence, different plant hormones contribute towards effective defence against the pathogens. Classic phytohormones include abscisic acid (ABA), auxins (AUX), cytokinins (CKs), ethylene (ET) and gibberellins (GAs), but also smaller signalling molecules including brassinosteroids (BRs), jasmonates (JAs) and salicylic acid (SA) (Pieterse et al., 2012). Crosstalk exists between the different hormonal pathways. For example, jasmonates appear to play a role in conferring resistance to necrotrophic pathogens, whilst SA is more important against (hemi)biotrophs (Glazebrook, 2005). The active JA-isoleucine is perceived by a coreceptor complex between the F-box protein CORONATINE-INSENSITIVE 1 (COI1) and JAZ proteins (Sheard et al., 2010). Arabidopsis mutants lacking COI1 have increased susceptibility to necrotrophic fungi such as *Alternaria brassicicola* and *Botrytis cinerea* (Lorenzo et al., 2003; Thomma et al., 1998), while resistance to the hemibiotrioph *P. syringae* is higher. This is consistent with elevated SA levels in the same mutant supporting an antagonistic relationship between the two pathways (Kloek et al., 2001). Furthermore, failure to accumulate SA, either by means of reduced biosynthesis, such as in the case of the *sid2* mutants (*SALICYLIC ACID INDUCTION DEFICIENT* 2), a gene

encoding an isochorismate synthase or by means of constitutive degradation of SA in transgenic plants expressing the bacterial gene nahG, leads to increased susceptibility to hemibiotrophic pathogens such as *P. syringae* (Abreu and Munne-Bosch, 2009).

Salicylic acid is a small phenolic compound that acts as a signalling molecule (Vlot et al., 2009). There is a tight interplay between growth and immunity, in which SA is known to play an important role considering that accumulation of SA results in stunted growth but increased resistance e.g. in *mpk4* mutants, whereas failure to accumulate SA results in decreased resistance and sometimes increased growth (Ishihara 2008). Therefore, SA is an underpinning molecule for the trade-off between growth and resistance to pathogens.

The isochorismate (IC) and phenylalanine ammonia-lyase (PAL) pathways use chromate to produce SA (Dempsey 2011) in species such as tobacco, tomato, pepper and others (Catinot et al., 2008; Kim and Hwang, 2014; Sadeghi et al., 2013; Uppalapati et al., 2007; Wildermuth et al., 2001). Mutants in either of these pathways show impaired induction of SA accumulation after pathogen infection (Huang 2010). Salicylic acid production takes place in the chloroplasts as isochorismate synthase (ICS) converts chorismate into isochorismate (IC) (Wildermuth et al., 2001) followed by conversion to SA (Dempsey et al., 2011). SA perception is achieved through SA receptors such as the recently identified NPR (*NON-EXPRESSOR of PATHOGENESIS-RELATED GENES*) family members, NPR1, 3 and 4 (Fu et al., 2012; Wu et al., 2012). NPR1 is also a transcriptional coactivator (Pajerowska-Mukhtar et al., 2013) regulating about 95% of the genes that are responsive to the SA-analog compound known as benzothiadiazole (BTH) (Mou et al., 2003; Wang et al., 2010b).

SA is also responsible for the acquisition of systemic immunity to further infection, which is also known as systemic acquired resistance (SAR). This can occur even at a distal site from the infection site and it

can be achieved even with exogenous application of salicylic acid or its analogs (Durrant and Dong, 2004b). This 'priming' phenomenon allows faster response to subsequent challenge. For example, *npr1* mutants are deficient in SAR and cannot become primed for enhanced gene expression, whereas mutants such as *sni1* and *edr1* show constitutive priming along with the developmental cost associated with continuously up-regulated defence responses, such as smaller plant size (Conrath, 2011; Frye and Innes, 1998; Mosher et al., 2006).

SA is also involved in preventing bacterial entry into plant tissue via stomatal closure, which occurs soon after the pathogen has been in contact with the plant (Melotto et al., 2006). This is a process that *P. syringae* DC3000 *pv.* tomato can hijack, leading to the reopening of closed stomata, which is mediated by the phytotoxin coronatine. Specifically, coronatine is used as a mimic of JA-Ile that binds COI1/JAZ leading to 26S-mediated proteasomal degradation of the JAZ transcriptional repressors. Repression of JA responsive genes occurs at resting state by JAZ repressor proteins together with the adaptors and co-repressors NINJA and TOPLESS, interacting with and suppressing MYC TFs. Upon infection and release of coronatine into the host cells, expression of JA-dependent genes is no longer blocked and at the same time the SA pathway is inhibited. The affinity of COR for the COI1/JAZ complex is in fact greater than JA-Ile making it a very potent virulence factor. The end result is suppression of SA-responses and increased bacterial colonization (Chini et al., 2007; Sheard et al., 2010; Thines et al., 2007).

1.7. Massive transcriptional changes occur during infection

One of the most notable outputs in response to infection is the rapid transcriptional reprogramming leading to differential expression of a large number of genes involved in a plethora of cellular processes. At the transcriptomic level, it has been shown that approximately 1/10 of

the Arabidopsis genome exhibits differential expression within an hour after perception of flg22 (Zipfel et al., 2004) and up to 1/3 of the Arabidopsis genome during infection with the necrotrophic fungus *Botrytis cinerea* within the first 48 hours (Windram et al., 2012). These massive transcriptomic changes are known to be accompanied by the activity of transcription factors and the RNA polymerase machinery as well as changes in the architecture of chromatin, which is a highly dynamic macromolecule (Lusser, 2002; Smale, 2014).

In Arabidopsis, RNA polymerase II is known to be activated by cyclin-dependent kinase (CDK)-mediated phosphorylation at the C-terminal domain (CTD). Thus, phosphorylation of RNA pol II is recognised as an important mechanism for the rapid induction of defence gene expression (Li et al., 2014b).

The activation of genes in response to stress is partially mediated through direct DNA-binding transcription factors. Perhaps the most famous TF family in plant immunity is known as WRKY family (Rushton et al., 2010). A complex regulatory network arises from positive and negative feedback and feedforward loops allowing rapid signal amplification and regulation of the immune response. The WRKY domain has received its name from the almost invariant W-R-K-Y sequence, which on specific occasions may be replaced by W-R-R-Y, W-S-K-Y, W-K-R-Y or W-K-K-Y. Binding to DNA is determined by the specific DNA sequence TTGACC/T also known as 'W Box'. These proteins are involved in multiple biological processes, but it is noteworthy that many WRKY TFs are key regulators - positive or negative - of plant immunity. As an example, ETI response to the barley powdery mildew (*Blumeria grimness* f. sp. *horde*) relies on the recognition of AVR10 effector by the host R protein MLA (MILDEW-RESISTANCE LOCUS A), which then physically associates with WRKY1/2 (Shen et al., 2007). In addition, WRKYs are embedded within MAPK signalling pathways, as for example WRKY33, which is found in a complex

with MPK4 and upon activation by PAMPs the complex dissociates allowing the WRKY-dependent activation of *PAD3* (*phytoalexin deficient 3*), necessary for the production of camalexin, a secondary metabolite with antimicrobial activity.

Part of the massive transcriptional reprogramming upon PAMP perception involves suppression of nuclear encoded chloroplast-targeted genes (NECGs) and is followed by production of photosynthesis-derived ROS in the chloroplast. The transcriptional responses within the first two hours after PAMP perception were related to chloroplast functions such as ROS production, photosynthesis and synthesis of salicylic acid (de Torres Zabala et al., 2015; Lewis et al., 2015). In addition, photosynthetic process were shown to be important in the expression of flg22-inducible NECGs (Sano et al., 2014).

1.8. Chromatin remodelling in regulation of gene expression

Transcription is a complex process that involves multiple proteins acting on the DNA, however, the DNA macromolecule is not always readily accessible to all these factors mentioned above. Specifically, the genetic material of eukaryotic cells is tightly packed inside the nucleus to a millionth of its length into a hierarchical structure consisting of proteins and DNA, known as chromatin. Chromatin consists of DNA organised around proteins known as histones that assemble into octameric structures called nucleosomes. This structure is important for nuclear processes involving DNA such as repair, recombination, replication as well as transcription. Chromatin is very dynamic and its structure at the macro- and micro-scale may vary significantly to accommodate the processes that are taking place at any time (Lusser et al., 2001). The histones are highly conserved throughout eukaryotic organisms and are characterised by a small size ranging from 11 to 21 kDa. Histones H2A, H2B, H3 and H4 are very small, have a globular shape and are very basic. Two copies of H2A and

H2B forming a tetramer and two H3/H4 dimers come together to create nucleosomes (Kornberg, 1974). Approximately 147 base pairs of DNA wrap around each nucleosome. Nucleosome-free, linker DNA, is found between adjacent nucleosomes and linker histone H1 is found in this space in stoichiometric amounts compared with nucleosomal particles (Routh et al., 2008). The roles of the linker H1 are confined to nucleosome stability preventing nucleosome sliding and also contributing towards higher-order chromatin assembly, which is largely attributed to its high lysine content giving the protein a net positive charge (Clark and Kimura, 1990; Subirana, 1990). *In vitro* studies have shown that H1, and its variant H5, make contact with the nucleosome, mainly with H2A using their C-termini, while their N-termini neutralise the negative charge of the linker DNA leading to higher-order compaction. The C-terminal part of the core histones, the histone fold, is approximately 70 amino acids long and is highly conserved between the four histones. Histone fold extensions are responsible for histone-histone interactions to define the nucleosomal particle as well as contribute to binding of the DNA macromolecule (Luque et al., 2014). The N-terminal tails of the core histones protrude from this octameric structure in an outwards fashion as shown by crystallographic analyses (*Fig. 1.2*) (Luger et al., 1997). These tails are rich in amino acids, such as lysines, which can be covalently modified. The ability of histones to bear post-translational modifications was recognised in the 1960s, but it was not until the 1980s that a functional role was attributed to these modifications. Since then, the study of histone N-terminal modifications has been a very exciting and complex topic of research. Several types of modification have been identified with most research being focused on acetylation, methylation, phosphorylation, ubiquitination and ADP-ribosylation. A total of more than 200 other modifications have been discovered mostly due to recent advances in mass spectrometry (Macek et al., 2006). These post-translational modifications

serve a multitude of roles in nuclear processes, while a major advantage is their reversibility allowing rapid responses to changing environmental cues (Hamon and Cossart, 2008). Most notably, these modifications can strongly and rapidly affect the packaging of DNA into nucleosomes and subsequently influence all processes where DNA acts as a template.

Acetylation of histones, the addition of acetyl groups onto lysine residues on histone tails, is known to affect chromatin structure and gene expression. Acetylation is associated with a loosened interaction between histones and DNA and increased levels of transcription (Sterner and Berger, 2000). This can be explained by various mechanisms. First, at a smaller scale, the negatively charged DNA interacts strongly with the positively charged histone tails, and the addition of a negatively charged acetyl group can neutralise the charge difference and weaken this interaction leading to a more accessible DNA. At a larger scale, the same effect of acetylation can lead to higher-order conformational changes of chromatin. Third, acetylation can also occur in non-histone proteins. Examples include the HMG (High Mobility Group) proteins, other transcriptional activators and even HATs and HDACs (Spange et al., 2009). In these cases, non-histone acetylation affects protein-protein interactions. Fourth, acetyl groups have been found to act as docking sites for proteins interacting with histones. For example, several HATs (Gcn5, PCAF, CBP/p300) contain bromodomains, a conserved domain that binds acetylated lysines and can mediate the recruitment and propagation of acetylation on the same nucleosomes. Overall, it has been established that in animals and plants, through these mechanisms, acetylation almost always is associated with more 'open' chromatin and increased gene activation (Kouzarides, 2007). Lysines found at the core region of histones are also post-translationally modified. For example, lysine H3K56 was recently found to be acetylated. This modification is facing towards the major

groove of DNA, thus is in an optimal conformation to influence the histone-DNA interaction (Xu et al., 2005).

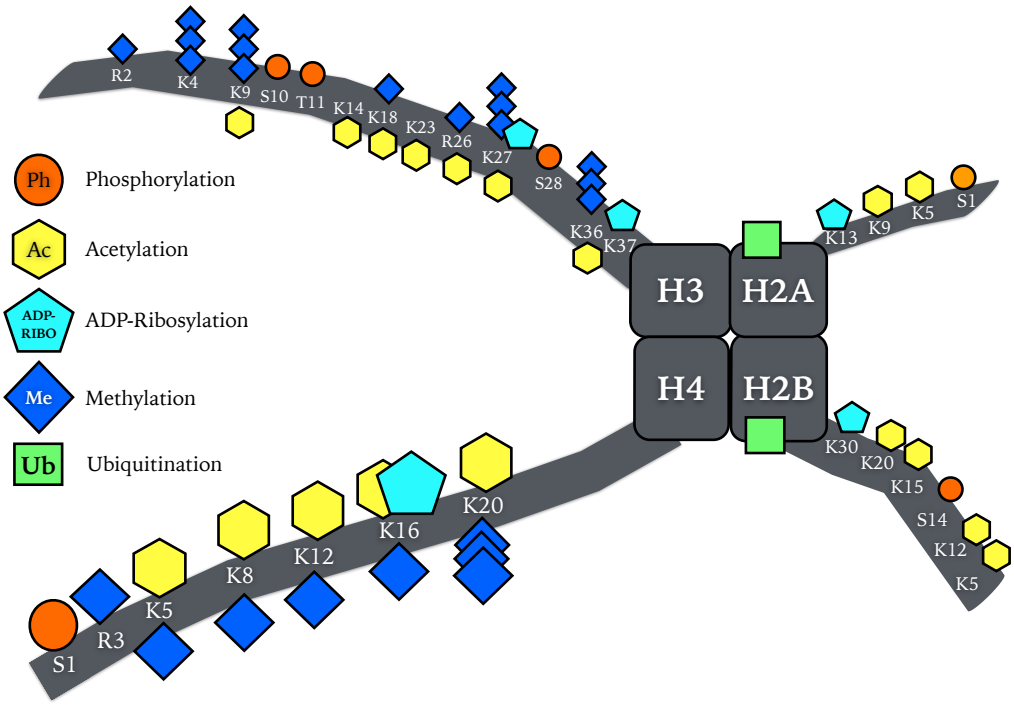

Figure 1.2. Post-translational histone modifications in plants. Histone modifications occur at the N-terminal tails and the core region of histones H2A, H2B, H3 and H4. Two copies of each create an octameric structure known as the nucleosome. For simplicity only one copy of each histone is shown. Modifications such as phosphorylation, methylation (mono-, di- and tri-methylation), ADP-ribosylation, acetylation and ubiquitination can occur on different or on the same residues, but not simultaneously. Ubiquitination is mostly identified at the C-ter part of the histones H2A(K^{120}) and H2B(K^{119}). Phosphorylation is found on Tyrosines (Tyr, T) and Serines (Ser, S). These modifications have been identified in planta using methods such as mutagenesis, *in vitro* reactions, mass spectrometry, western blotting and others. Adapted from multiple sources (Earley et al., 2007; Kouzarides, 2007; Lusser, 2002; Messner et al., 2010)

The remarkable property of histones being post translationally modified to a larger extent than any other known protein by the addition of many different PTMs (Kouzarides, 2007) raises the question of what is the function of these in gene expression as well as how these PTMs are interpreted by the transcription machinery upon different stresses. The balance of different histone modifications is governed by multiple enzymes that can deposit them, recognise or bind them, and remove them, which gives rise to the colloquial terms: 'writers', 'readers' and 'erasers'

of chromatin, respectively (Strahl and Allis, 2000). Genetic and biochemical evidence has elucidated the roles of histone PTMs in chromatin-related processes. The histone code, proposed by Strahl and Allis (2000) supports that transcription is in part regulated by the modifications mentioned before and that these are critical in recruiting other proteins with specific protein domains and a variety of functions involved in altering chromatin structure and/or altering transcription (Jenuwein and Allis, 2001). In other words, the histone code describes the complex language of how the different PTMs act in concert and may affect each other directly (e.g. by steric hindrance) or indirectly through the action of 'writers', 'readers' and 'erasers' of chromatin. Specifically, *in vitro* acetylation of H3 by GCN5 at lysine 14 (H3K14ac) is dependent upon specific consensus motifs in the same way as protein kinases, such as MAPKs are proline-directed Serine/Threonine (Ser/Thr) kinases obeying the S/T-P motif (Pereira et al., 2011). Crystal structures of GCN5 enzyme with its substrate H3 has revealed that GCN5 acetylation of H3K14 is dependent on the G-K14*-X-P motif where the acetylated lysine is preceded by a glycine and followed by a proline (Rojas et al., 2004; Trievel et al., 1999). It is also important to note that the close proximity of most of these modifications could positively or negatively affect the ability of these enzymes to further modify their target residues. In support of this, it was found that H3S10 phosphorylation (H3S10ph) enhanced the acetylation of H3K14 by GCN5 (Trievel et al., 1999). Furthermore, H3K9 methylation is a known repressive mark and can affect adjacent H3S10ph negatively, thus indirectly inhibiting H3K14ac and excluding acetylation of H3K9 at the same time. Deacetylation of H3K9ac could in the same way promote methylation of the same site.

The histone code is an appealing hypothesis as it can explain the opposing roles of many modifications. For example, although acetylation is normally associated with a more relaxed chromatin conformation and

increased gene expression, in several cases, heterochromatic areas in flies and silent loci in yeast are rich in acetylated H4K12 (Braunstein et al., 1996; Turner et al., 1992). Similarly, H3S10ph is associated with chromosome condensation as well as immediate early gene induction after mitogenic stimulation (Sawicka and Seiser, 2012). A possible explanation to these paradoxical examples could be that these marks are read by distinct sets of histone modifying enzymes leading to a variety of possible downstream responses. In addition, the presence of a modification does not always imply an immediate function, rather it could imply transcriptional priming. Bivalent chromatin marks are such an example, which are present at the promoters of the developmental HOX genes that specify the anteroposterior development in vertebrates. In this example, activating marks (H3K4me3) are co-present with repressive marks (H3K27me3), suggesting a model of transcriptional regulation where the genes are primed for activation but held in check by a negative mark and the fate of transcription depends on upstream signals such as developmental or environmental cues. Similarly, robust regulation of transcription can be ensured by the co-localisation of different activating marks as in the case of acetylated forms of H3 and H3K4me3 (Bernstein et al., 2006; Tee et al., 2014).

Type of PTM	H3 K4	H3 K9	H3 K14	H3 K27	H3 K79	H3 K122	H4 K5	H4 K20	H2A K4	H2A K7	H2B K5	H2B K11
Mono-methylation	●	●		●	●			●			●	
Di-methylation	●	○		○	●							
Tri-methylation	●	○		○	○● Context-dependent			○			○	
Acetylation		●	●	●		●	●		●	●		●

Table 1.1. Effect of histone marks on gene expression. Green circles indicate gene activation; red circles indicate gene repression. H3K70me3 is a histone mark with a context-dependent effect on transcription. Empty boxes indicate that the modification has not been described on that residue. PTM, post-translational modification. Adapted from

multiple sources (Alvarez et al., 2010; Berger, 2007; Jenuwein and Allis, 2001; Kouzarides, 2007)

Chromatin largely exists in two states - euchromatin and heterochromatin; the first is described by a looser architecture, associated with increased transcriptional activity and the latter by a more condensed one, which does not favor transcription. Generally, highly active genes are found in euchromatin, while genes under repression are buried in heterochromatin, inaccessible to transcription factors and the RNA polymerase machinery (Lusser, 2002). Many genes may be activated upon a particular signal and thus their chromatin context can change significantly. Modification of histones has been shown to influence the activity of a gene, for example, acetylation is important for the activation of gene expression (Durrin et al., 1991; Yoshida et al., 1995). Generally, the post-translational addition of acetyl groups onto proteins can have a variety of roles. For example, (i) the affinity of a protein for DNA is reduced, (ii) the localisation of a protein may change upon acetylation, (iii) the stability of a protein may increase i.e. through prevention of ubiquitin-mediated degradation and (iv) the interaction with other proteins may change. In the case of histones, which are basic proteins and thus have high affinity for the negatively charged DNA macromolecule, (v) this affinity may be reduced upon addition of the positively charged acetyl groups on lysine residues of histones (Glozak et al., 2005). This leads to a loosening of the histone-DNA interaction and a more relaxed chromatin structure.

Eukaryotic nuclei have been found to contain transcriptional hotspots also known as transcription factories. These were found using fluorescence recovery after photobleaching (FRAP) experiments, whereby the kinetics of a GFP-tagged protein of interest are measured after photobleaching a fluorescent area with high-power laser at the same wavelength of fluorescence. The rate of fluorescence recovery in this area is then calculated as adjacent GFP-tagged molecules naturally diffuse into

that space. Proteins involved in chromatin-interacting processes, like gene transcription, DNA replication, DNA repair and histones, bind directly or indirectly to DNA leading to slow recovery (Day et al., 2012). FRAP analysis has been shown to be a strong *in vivo* approach to study the mobility and transient immobilisation of nuclear proteins associated with DNA (Stasevich and McNally, 2011). A study monitored RNAPII in living cells using FRAP showing that at least two populations of RNAPII can be observed, the majority described by a very short recovery time, whilst a transcriptionally engaged pool of RNAPII was found to have a longer recovery time (Dundr et al., 2002). This finding pointed towards the existence of distinct transcription centers ('hotspots') inside the nucleus, which are characterised by the enrichment of transcription factors and RNAPII to allow more efficient transcription.

Transcription factor binding is coordinated by genetic and epigenetic mechanisms. For example, TFs are known to bind DNA in a DNA sequence-specific manner, however, methylated DNA or histone modifications can act as docking sites for TFs thus providing an alternative mode of TF binding. Similarly, methylated DNA or modified histones can occlude the binding of a TF in a context-dependent manner (Klose and Bird, 2006). The importance of histone acetylation is further emphasised by the observation that histones are first acetylated and then nucleosome eviction takes place as in the case of yeast *PHO5* promoter, which is known to be regulated in response to the level of inorganic phosphate in the growth medium (Reinke and Horz, 2003). Another example includes *HSP82* gene which is transiently acetylated at the promoter region prior to nucleosome eviction (Zhao et al., 2005). This is further supported by the fact that chromatin remodelling complexes such as SWI/SNF contain bromodomains, which act as 'reader' domains recognising and binding acetylated histones, suggesting that histone loss is dependent on acetylation before nucleosome replacement can occur (Steger and Workman, 1996).

As a consequence, acetylation of histones appears to allow easier loss of nucleosome ahead of the polymerase machinery and their re-incorporation behind the polymerase machinery (Svejstrup, 2003).

DNA methylation is a well-established epigenetic mechanism with a key role in gene expression in response to stresses. It involves the covalent binding of a methyl group to the fifth carbon in a cytosine nucleotide ring of a DNA molecule and often occurs in cytosines linked to guanine via a phosphodiester bond denoted altogether as CpG. Specifically in plants it can also be found in the context of CpG, CpHG (whereby H represents A,C or T) and CpHH and it is particularly abundant representing approximately 30% of the nucleotides in plants (Gruenbaum et al., 1981). In a similar way to the other mechanisms, DNA methylation can be highly dynamic in response to environmental changes and different methylation patterns are observed throughout a plant's development (Finnegan et al., 2000). In *A. thaliana,* the centromeric regions and other loci were found to have reduced levels of DNA methylation following infection with *P. syringae* (Pavet et al., 2006).

Another level of regulation of gene expression is the enrichment of genomic areas with a distinct set of histone variants. For example, Stroud *et al* (2012) showed that the histone variant H3.1 is strongly enriched in areas of the genome that were more silent and were co-present with repressive modifications such as H3K27me3, H3K9me and DNA methylation. By contrast the histone variant H3.3 is more commonly found in actively transcribed regions, correlating with modifications that promote gene expression such as H3K4me and H2Bub as well as transcriptionally engaged RNA polymerase II. Crucial enzymes in the displacement and deposition of histone variants are ATP-dependent chromatin remodellers.

The discovery of the first ATP-dependent chromatin remodellers was made in yeast mutant screens. Specifically, some of the *swi* (switch) and *snf* (sucrose non-fermenting) mutations resulted in impaired gene ac-

tivation in many different pathways (Sudarsanam and Winston, 2000; Workman and Kingston, 1998). Later studies revealed that those genes encoded subunits of the same SWI/SNF complex and their mutation resulted in phenotypes similar to those observed in histone and other chromatin mutants. Now, SWI/SNF is known to be a major player in chromatin remodelling across species. After the biochemical purification of the complex it was revealed that the remodelling mechanism requires energy from ATP in order to displace nucleosomes resulting in increased accessibility of DNA-binding sites.

1.9. Histone acetylation and GCN5 in other systems

Following the discovery of chromatin remodelling enzymes in yeast, the other main class of co-activators, Gcn5 (homolog of plant HAG1), was also discovered through similar genetic screens in yeast and was linked to chromatin-related pathways after it was shown to be identical with the p55 subunit of a histone acetyltransferase complex initially purified from *Tetrahymena* (Cote et al., 1998; Georgakopoulos and Thireos, 1992; Kruger et al., 1995). Gcn5 complexes preferentially acetylate histone H3 N-terminal tails. Two biochemically distinct complexes were first identified in yeast, where Gcn5 is the catalytic component. These include the Ada and SAGA (Spt-Ada-Gcn5 Acetyltransferase) complexes (Grant et al., 1997). Other complexes in yeast and other organisms are shown in *Table 1.2* demonstrating similarities such as the presence of adaptor proteins (ADAs) together with GCN5 across species, as well as that these complexes are usually composed of many proteins. In plants, very little is known with regards to the composition of a HAG1 complex apart from the interaction of HAG1 with ADA2a and ADA2b. Importantly, SAGA complexes, like other HATs, have pairwise preferences for histones as substrates, for example, H2B and H3 are targets for Gcn5 in yeast (Grant et al., 1997).

Organism	HAT	Complex	Main Components	Estimated Complex Size
S. cerevisiae	Gcn5	HAT-A2	Ada2,3 and more	200 kDa
		ADA	Ada2,3 and more	900 kDa
		SAGA, SAGA-like (SLIK)	Ada1-5, Spt, TAFII, Tra1	1200 kDa
	Esa1	NuA4	Tra1 and more	1300 kDa
H. sapiens	hGCN5	SAGA	Ada, Spt, Tra, TAFII and more	2000 kDa
D. melanogaster	GCN5	SAGA	ADA2B,3, SPT, TRA1 and more	800kDa
		ATAC	ADA2A,3 and more	700 kDa
T. thermophila	HAT1	Monomeric enzyme		56 kDa
A. thaliana	HAG1	Unknown	ADA2A*, ADA2B*	Unknown

Table 1.2. Major HAT complexes identified in different model organisms. In the case of HAG1 in *A. thaliana*, although the full complex has not been described yet, interaction with ADA2A and ADA2B has been confirmed. Collated from multiple sources referenced in the main text.

In yeast, highly optimised biochemical approaches allowed researchers to purify and characterize the various modules of the SAGA complex giving rise to a 21-protein complex with four main modules (*Fig. 1.3*). These include the histone acetylation (HAT) module that consists of Ada3, Ada2, Sgf29 and Gcn5. The de-ubiquitination (DUB) module is composed of Sgf11, Sgf73, Sus1 and Ubp8, which performs the de-ubiquitination reaction. The SPT module is responsible for the assembly of the pre-initiation complex during transcription and consists of Spt3, Spt7, Spt20, Ada1, Tra1 and Chd1/Chr5. TAF is a co-activation module and is known to have roles in the structural integrity of the complex (Koutelou et al., 2010; Samara and Wolberger, 2011).

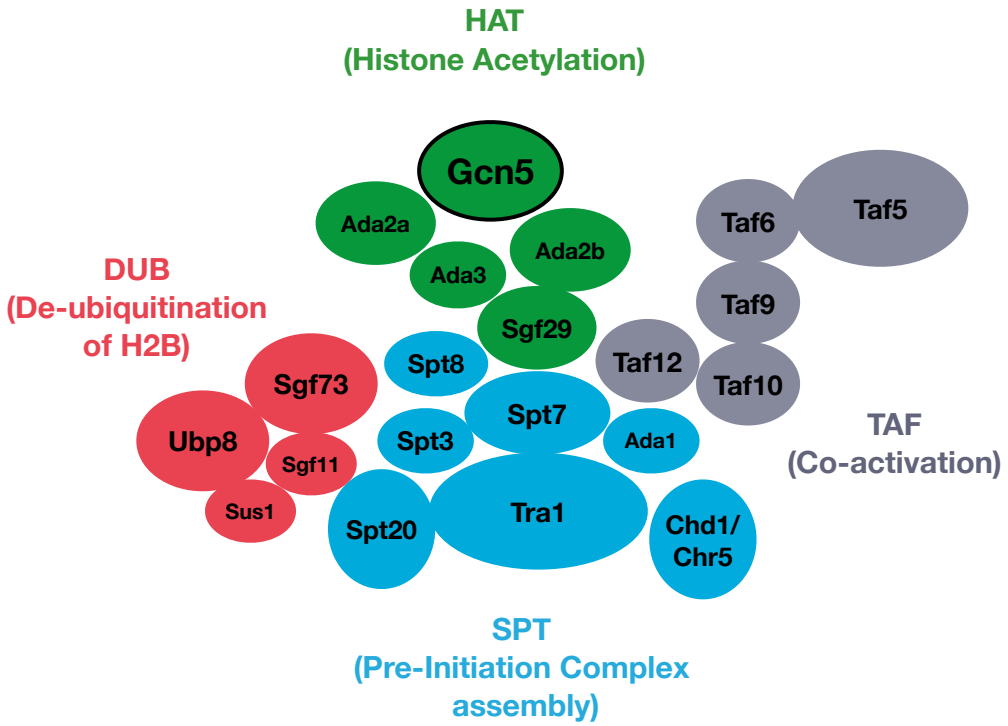

Figure 1.3. Yeast SAGA complex has multiple modules with different functions. SAGA is a multi-protein complex with multiple functions performed by its different modules. The HAT module is responsible for the histone acetyltransferase activity with Gcn5 being the catalytic component. The DUB module removes ubiquitin molecules from histone H2B, while SPT and TAF modules play important roles in facilitating transcription, through assembly of the pre-initiation complex and co-activation processes. Modified from (Koutelou et al., 2010; Samara and Wolberger, 2011)

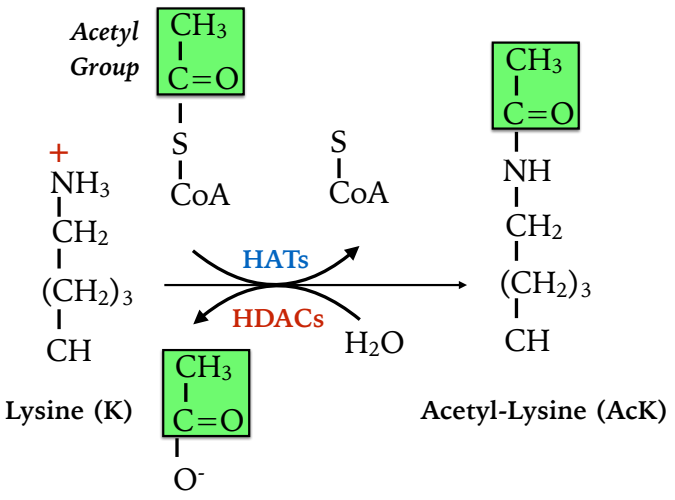

Figure 1.4. Acetylation/De-acetylation reaction of lysine/acetyl-lysine. HATs catalyse the transfer of an acetyl group from acetyl-CoA onto a lysine residue forming the byproduct coenzyme A with a thiol group (CoASH). HDACs catalyse the reverse reaction with the input of a water molecule. It should be noted that different HATs use different amino acids to catalyse the transfer of the acetyl group. Modified from Kim and Yang (2011).

In yeast, it has been shown that E173 of GCN5 acts as the general base responsible for de-protonating the lysine of a histone. This is a requirement for the transfer of an acetyl moiety onto the target lysine. Upon completion of the reaction coenzyme-A with a thiol group (CoASH) is formed (Tanner et al., 1999) (*Fig. 1.5*).

Although there is no study in HAG1 showing which amino acid is responsible for the catalytic activity, the existing literature on GCN5 from other eukaryotes suggested that the highly conserved 8-amino acid sequence highlighted in *Figure 1.4* was identified as part of a core region sufficient for catalysis of the acetylation reaction in yeast (Gregory et al., 1998; Wang et al., 1998). Further studies using mutagenesis and *in vitro* and *in vivo* HAT reactions also pinpointed that the glutamic acid (E173 in yeast, E121 in *Tetrahymena*, E582 in human) inside the highly conserved HAT domain of GCN5 is responsible for the enzymatic activity. This corresponds to E289 in *A. thaliana* HAG1 within the catalytic HAT domain as shown in *Figure 1.5*.

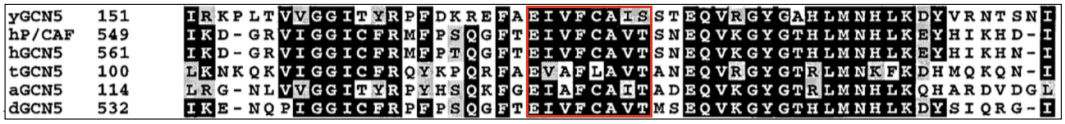

Figure 1.5. Sequence alignment of HAT domains in different model organisms. Yeast GCN5, human P/CAF, human GCN5, Tetrahymena GCN5, Arabidopsis GCN5, Drosophila GCN5 protein sequences are shown. The catalytic domain for each protein is highlighted with a red square and is highly conserved across all organisms (Modified from (Trievel et al., 1999) .

1.10. Chromatin remodelling in plant defence

Several examples of proteins involved in chromatin remodelling have been found to be important for biotic stress responses in plants. SPLAYED is an ATP-dependent chromatin remodeller, and HISTONE MONOUBIQUITINATION1 is a RING-finger E3 ligase and both were required for resistance to necrotrophic fungal pathogens (Dhawan et al., 2009; Walley et al., 2008). In addition, *sdg8* mutants impaired in H3K36me3 deposition also displayed lower resistance to necrotrophic

fungal pathogen infection (Berr et al., 2010). Furthermore, Arabidopsis Trithorax 1 (ATX1), another histone methyltransferase, directly regulates the transcriptional activity of WRKY70, a positive regulator of salicylic acid (SA)-mediated defence signalling (Alvarez-Venegas et al. 2007). Components of the Arabidopsis SWR1-like complex, which is responsible for the replacement of histone H2A with the histone variant H2A.Z, are required for the repression of SA-dependent defence genes (March-Diaz et al., 2008).

In another example, histone monoubiquitination, histone variants and a chromatin remodeller act together on the same pathway ensuring that defence genes are activated only after infection. For example, in rice, defence genes are kept silent in the absence of pathogen attack and this is held in check by the presence of histone variants at the promoters of the pathogenesis-related gene *OsPBZc* and the LRR *OsSIRK1* gene. The mechanism by which these genes are kept silent is explained by the action of SWI/SNF ATPase BRHIS1, the expression of which is downregulated upon infection by the rice blast fungus. Therefore, the interaction between BRHIS1 and histone variants of H2A and H2B is lost allowing the expression of the underlying genes. Given the enrichment in histone monoubiquitination, these genes are poised for expression until BRHIS1 repression is relieved (Li et al., 2015).

1.11. Histone acetylation in plant immunity

In addition to the chromatin remodelling mechanisms mentioned above, histone acetylation has been shown to have various roles in immunity. The levels of histone acetylation are controlled antagonistically by histone acetyltransferases (HATs) and histone deacetylases (HDACs) and there are at least 12 and 18, respectively, in Arabidopsis (Pandey et al., 2002) (*Table 1.3*). Three extra HAT genes can be identified, but are not included in the 12 canonical HATs; *At1g77540*, which belongs to the

GNAT family (Tyler et al., 2006), *IDM1* (Qian et al., 2012) and *SNS1* (Umezawa et al., 2013), which encode a HAT domain, but do not belong to any of the four families by homology. Studies have shown the role of most plant HATs/HDACs in a variety of biological processes as well as identified their *in vitro* (Earley et al., 2007) and *in vivo* specificities i.e. which histones and specific lysines they target for acetylation/deacetylation as listed in *Table 1.3*.

	Family	Enzyme Name	Accession No.	Specificity	Details	References
Histone Acetyltransferases (HATs)	GNAT	HAG1	*At3g54610*	H3K9K14	Development, Abiotic stresses	*Earley et al 2007*
		HAG2	*At5g56740*	H4	-	*Earley et al 2007*
		HAG3	*At5g50320*	H3K14, H4K8	DNA repair	*Fina et al 2015*
		At1g77540	*At1g77540*	-	-	*Tyler et al 2006*
	MYST	HAM1	*At5g64610*	H4K5	Flowering time	*Xiao et al 2013*
		HAM2	*At5g09740*			
	CBP	HAC1	*At1g79000*	H3K9K14	Priming of PTI	*Singh et al 2014*
		HAC2	*At1g67220*	-	-	-
		HAC4	*At1g55970*	-	Expressed as pseudogene	*Pandey et al 2002*
		HAC5	*At3g12980*	-	Development	*Li et al 2014*
		HAC12	*At1g16710*	Multiple	-	*Earley et al 2007*
	TAFII250	HAF1	*At1g32750*	-	Affects root-transformation	*Crane et al 2007*
		HAF2	*At3g19040*	H3 and H4	Response to light	*Bertrand et al 2005*
	No family	IDM1	*At3g14980*	H3K14K18K23	Prevents DNA methylation	*Qian et al 2012*
		SNS1	*At1g26470*	Unknown	Abscisic Acid	*Umezawa et al 2013*
Histone Deacetylases (HDACs)	RPD3/HDA1	HDA2	*At5g26040*	-	-	-
		HDA5	*At5g61060*	14-3-3 proteins	Localises in ER	*Alinsug et al 2012*
		HDA6	*At5g63110*	-	Jasmonic acid pathway	*Devotto et al 2002*
		HDA7	*At5g35600*	-	Female gametophyte development	*Cigliano et al 2013*
		HDA8	*At1g08460*	-	-	-
		HDA9	*At3g44680*	H3K9	Salt and drought stress	*Zheng et al 2016*
		HDA10	*At3g44660*	H3K9K14K18	Development	*Liu et al 201a*
		HDA14	*At4g33470*	α-tubulin	Microtubule metabolism	*Tran et al 2012*
		HDA15	*At3g18520*	-	Chlorophyll biosynthetic genes	*Liu et al 201a*
		HDA17	*At3g44490*	-	-	-
		HDA18	*At5g61070*	H2,H3,H4	Cell differentiation	*Liu et al 201b*
		HDA19	*At4g38130*	H3K9,H4K5	JA/ET and SA pathway	*Servet et al 2010*
	HD2	HD2A	*At3g44750*	-	Leaf polarity	*Yoshihisa et al 2007*
		HD2B	*At5g22650*	-	Seed dormancy	*Yano et al 2013*
		HD2C	*At5g03740*	-	Salt stress	*Sridha et al 2006*
		HD2D	*At2g27840*	-	Development and Abiotic stress	*Han et al 2016*
	SIR2	SRT1	*At5g55760*	-	-	-
		SRT2	*At5g09230*	H3K9 (rice)	SA biosynthesis	*Wang et al 2010*

Table 1.3. List of histone acetyltransferases (HATs) and histone deacetylases (HDACs) in the Arabidopsis genome. Sequence homology identifies several families for the HATs and HDACs. Information on the *in vitro* and *in vivo* specificities of these enzymes as well as the biological processes they are involved in are listed here. This table is not exhaustive and shows representative information for each enzyme. The data shown here refers to Arabidopsis unless otherwise stated.

Although not many studies have focused on the roles of these enzymes in plant immunity, this is mostly attributed to the fact that single HAT or HDAC mutations rarely result in increased susceptibility or increased resistance to pathogens. Some exceptions to this observation have

resulted in the identification of certain HATs as important regulators of immunity. The first example is known as Elongator Protein 3 (ELP3) or HAG3 and was found to positively regulate immune responses by accelerating defence gene expression and this was dependent upon its HAT activity. It was also found that ELP3 does not have a role in the establishment of SAR (Defraia et al., 2013; DeFraia et al., 2010).

PTI priming is important in allowing the plant to respond to future infections in a more robust manner than in previous encounters with pathogens. Interestingly, in Arabidopsis, HAC1 histone acetyltransferase was shown to play a vital role in priming responses triggered by flg22 treatment. The same was seen after infection with *Pseudomonas syringae* DC3000 *hrcC* strain, which contains a defective T3SS and is unable to deliver any effectors into the host cell and always results in a weaker infection (Deng and Huang, 1999; Singh et al., 2014). Specifically, HAC1 was found to be required in the context of repetitive abiotic stress-induced plant resistance to *P. syringae* infections, in up-regulating expression of PTI marker genes as well as in establishing activating histone modifications and RNAPII occupancy. However, given that *hac1* mutants did not display major differences from wild-type plants in bacterial resistance, it is likely that HAC1 plays a smaller role in immunity in a non-priming context (Singh et al., 2014).

In rice, HDT701 histone deacetylase, member of the HD2 subfamily, is a negative regulator of plant innate immune responses, by deacetylating H4 histone in the promoters of defence genes. Its role was tested in the context of infection by the fungal pathogen *Magnaporthe oryzae*, and upon silencing of HDT701 increased transcript levels of PRR and other defence-related genes and increased ROS responses after PAMP treatment were observed (Ding et al., 2012).

SIRTUIN2 (SRT2) is a histone deacetylase involved in immunity through repressing SA biosynthesis, specifically *PAD4* and *SID2* genes. In

line with this, *srt2* mutants were more resistant, while over-expressing lines were more susceptible to *Pst* DC3000 (Wang et al., 2010a).

One of the most well-studied histone deacetylases in the context of immunity in Arabidopsis is HDA19, a negative regulator of plant immunity. *HDA19* expression is shown to be up-regulated upon infection by *Pst* DC3000, *hda19* mutants are more resistant to infection by this pathogen. HDA19 negatively regulates plant immunity by repressing an important family of defence-related genes known as *Pathogenesis-Related* (PR) genes (Choi et al., 2012).

HDA19 is also an important deacetylase as it physically interacts with TOPLESS (TPL), a major transcriptional corepressor protein. TPL is thus responsible for recruiting the deacetylase to specific gene promoters to induce gene repression (Chini et al., 2007; Long et al., 2006). Although there has been no report showing the direct involvement of a plant histone acetyltransferase acting within same pathway as HDA19 and TPL, there have been studies showing a genetic interaction between the *TPL, HDA19* and *HAG1/GCN5*. Specifically, Long *et al* (2006) showed that *hda19-1* and *hda19-2* seedlings grown at 29°C displayed phenotypes similar to mutant *tpl-1* plants but when *hda19*$^{-/-}$*tpl-1*$^{+/-}$ mutants were grown at 24°C (a temperature at which *tpl-1* mutation is recessive) it was observed that more seedlings showed cotyledon fusion defects suggesting that HDA19 acts on an overlapping set of genes as TPL during embryo development. In triple mutants of *tpl-1 hda19-1 hag1-3,* it appeared that the introduction of a mutated *HAG1* gene (*hag1-6*) resulted in *hda19-1*-like phenotypes further suggesting that *hag1-3* mutation can suppress *tpl-1* phenotypes even in the absence of *HDA19*. Overall, this was the first report placing these three genes within same pathway.

Furthermore, evidence suggesting that a HAT such as HAG1 may be acting opposite of TPL and HDA19 on the same set of genes, comes from studies in auxin responses, whereby auxin responsive genes are kept

silent by the concerted action of AUX/IAA repressors as well as TPL, which is again responsible for recruiting HDA19. This repression is reversed upon increase of auxin levels leading to the expression of the underlying auxin responsive genes. Transcription is then further enhanced by the bZIP11-mediated recruitment of ADA2b; the interaction of these two proteins was shown by Weiste *et al* (2014). It is therefore, hypothesised that ADA2b recruitment is accompanied by recruitment of HAG1/GCN5, although this has not been experimentally verified.

In all, current evidence strongly suggests that HDA19 and HAG1 may work antagonistically on the same set of genes, albeit in various multiple pathways. The involvement of TPL in both examples mentioned above (Long et al. 2006; Weiste et al. 2014) also provides a mechanistic basis for supporting this model (*Fig. 1.6*).

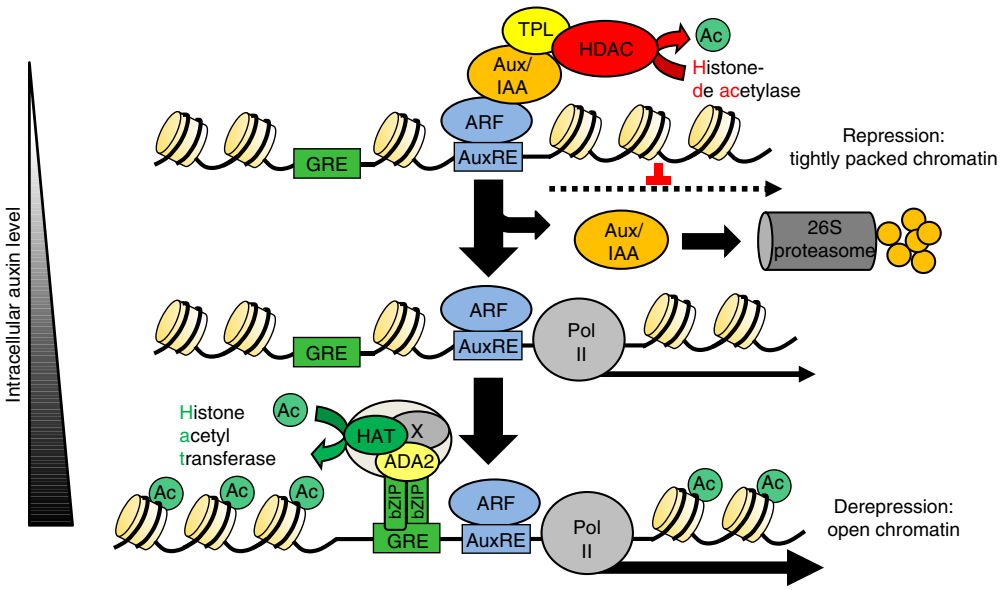

Figure 1.6. Proposed model of the function of the interaction of TPL with HATs/HDACs in the context of auxin-mediated transcription. In auxin-limiting conditions, auxin-responsive genes are repressed by AUX/IAA proteins, TPL and HDA19, which ensures de-acetylation of those promoters. With increasing levels of auxin, ubiquitin-mediated degradation of the repressors leads to increased transcription of the underlying genes and further recruits co-activators such as ADA2b and a GCN5-containing complex (HAT) to ensure higher levels of auxin-mediated transcription. Taken from Weiste *et al* (2014).

1.12. HAG1 is an important co-activator of transcription

GCN5 is a highly conserved protein across all kingdoms. Its roles in regulating developmental processes have been recorded in fruitfly (*Drosophila melanogaster*), where *gcn5* mutants are defective in metamorphosis and oogenesis (Carre et al., 2005), while mice with mutations in *GCN5* fail to survive beyond embryo stage (Xu et al., 2000). In addition, in yeast *gcn5* mutants slower growth is observed (Georgakopoulos and Thireos, 1992). Arabidopsis T-DNA insertion mutants such as *hag1-6* (Col-0 background) show pleiotropic effects, including dwarfism, loss of apical dominance, aberrant meristem function, root and leaf development, short petals and stamens, floral organ identity, and lower expression of light-regulated and cold-responsive genes. As an example of the roles of HAG1 in development, it was found that HAG1 determines floral meristem activity through the well-described WUSCHEL (WUS)/AGAMOUS (AG) pathway (Vlachonasios et al. 2003; Bertrand et al. 2003; Long et al. 2006; Kornet and Scheres 2009).

HAG1 contains a bromodomain, which makes it a reader of acetylated lysines. Two T-DNA insertion mutants, *gcn5-1* and *gcn5-2* are found in the bromodomain-coding region and the latter mutation leads to reduced histone H3 acetylation (Benhamed et al., 2008; Bertrand et al., 2003). In fact, *E.coli*-expressed HAG1 has *in vitro* acetyltransferase activity with a strong preference towards H3K14 (Earley et al., 2007). Through chromatin immunoprecipitation coupled with a promoter ChIP, it was found that HAG1 associates with approximately 40% of the Arabidopsis promoters. Using hag1 mutants lacking the bromodomain, the authors showed that only 11% of the target genes appeared to require the bromodomain (Benhamed et al. 2008), suggesting that HAG1 employs other mechanisms in addition to its bromodomain to ensure recruitment to chromatin.

HAG1 is also known to acetylate non-histone proteins in plants and other species. For example, HAG1 is reported to acetylate ADA2 and in particular at a site unique to plant homologs not present in fungal or animal homologs (Kornet and Scheres, 2009; Mao et al., 2006). This highlights that HAG1 may be involved in additional mechanisms involving gene expression, that is, through changing the activity of its interactors. Given that ADA2 is an interactor of HAG1 and that the activity of HAG1 depends on this interaction (Grant et al., 1999), acetylation of ADA2 may be part of a self-regulation mechanism for HAG1.

1.13. SAGA complex in plants

The interaction between HAG1 and ADA2 has been shown by *in vitro* and in yeast-two-hybrid experiments. ADA2 proteins are integral parts of so-far identified GCN5-containing complexes. In *A. thaliana,* ADA2a mutations appear to result in wild-type-like phenotype, suggesting a distinct set of target genes for this adaptor (Hark et al., 2009). In contrast, mutations in the ADA2b protein (Stockinger et al., 2001) lead to pleiotropic effects in development, similar to the phenotypes observed in *gcn5* mutants (*Fig. 1.7*). These phenotypes include a small, dark green and curly leaves with small stature and infertility similar to *hag1* mutants. The root system is also significantly shorter than wild type seedlings (*Fig. 1.7e*). A dose-dependent effect can be seen, whereby heterozygous *ada2b* mutants display wild-type like phenotypes, but *ada2b* homozygous mutants display the full effect of the mutation. In double *ada2a ada2b* mutants (*Fig. 1.6e*) apical dominance appears to be completely lost similar to *ada2b* (*PROPORZ1*, *prz1-1*) and *gcn5* single mutants. ADA2b is also required to modulate histone acetylation in response to auxin, which may account at least in part for these phenotypes (Anzola et al., 2010).

The above observations suggest that in *A. thaliana* Ws-0 (Wassilewskija), HAG1 is part of at least two separate complexes, potentially

one associated with ADA2a and another associated with ADA2b, although it is still possible that plant GCN5-containing complex involves both adaptor proteins. To date there has been no report showing *in vivo* the interaction of all three proteins, contrary to studies in other systems where purification of GCN5-containing complexes has allowed us to fully characterize their composition (*Table 1.2*).

Figure 1.7. Developmental phenotypes of *AtGCN5*, *AtADA2a* and *AtADA2b* mutants. A-C, Seedlings grown in agar; D-E, mature rosette plants grown on soil. Adapted from Hark *et al* (2009) and Vlachonasios *et al* (2003).

1.14. HAG1 is involved in abiotic and biotic stresses in plants

Vlachonasios *et al* (2003) investigated cold acclimation of plants through the induction of C-repeat/DRE binding factors (CBFs), which are regulators of cold-regulated (COR) gene expression. CBFs were induced in both *gcn5* and *ada2b* mutants in the same way as in wild type plants, however, subsequent transcription of COR genes was impaired. In addition, ADA2b has been found to interact with the DNA-binding domain of CBF1. These findings suggest a model in which CBF1 requires SAGA components for the activation of COR gene transcription in response to cold stress (Mao et al., 2006; Stockinger et al., 2001; Vlachonasios et al., 2003).

HAG1 was found to interact with the phosphatase PP2C-6-6, resulting in its de-phosphorylation *in vitro*. The interaction was shown by yeast-two hybrid and further confirmed by bimolecular fluorescence complementation (BiFC) (Servet et al., 2008). In addition, mutants of PP2C-6-

6 showed that this phosphatase is involved in salt induction of stress-inducible genes, whilst in mutants lacking a full-length HAG1 protein, up-regulation of stress-inducible genes was observed under non-induced conditions. This was also correlated with a marked reduction of H3K14 and H3K27 acetylation in the *gcn5* mutant and by contrast, *pp2c-1* and *pp2c-2* mutants had higher acetylation in these lysine residues. These experiments suggested a mechanism by which PP2C-6-6 is capable of dephosphorylating HAG1 resulting in its inactivation upon stress to allow the activation of salt stress-responsive genes. Although this may come in contrast to the role of HAG1 as a co-activator of transcription, it is possible that the activity of HAG1 is highly dynamic and context dependent. This study also showed that environmental signals can be relayed to chromatin-associated proteins through signalling proteins such as phosphatases, further suggesting the existence of an opposing mechanism, whereby HAG1 is phosphorylated by a putative kinase leading to its activation (Servet et al., 2008).

Multi-protein complexes such as SAGA complex consist of proteins with a variety of protein domains. As mentioned, GCN5 itself contains a catalytic ('writer') HAT domain and a bromodomain, which acts as a recognition ('reader') domain. Modifications on histone tails can be read by protein domains, which further adds to the complexity of the histone code. In humans, TAF1, the largest subunit of TFIID complex, which is involved in the assembly of transcription machinery contains two adjacent bromodomains that recognise diacetylated H4 (Jacobson et al., 2000). Despite bromodomains, which are found in HATs and the SWI/SNF family of chromatin remodelling proteins, multiple other 'reader' domains (*Table 1.4*) exist. Chromodomains (Chr; chromatin organization modifier) recognise methylated lysines and can be found in histone methyltransferases such as SUV39H1 (de la Cruz et al., 2005; Marfella and Imbalzano, 2007). The ISWI family of ATP-dependent chromatin remod-

ellers have a SANT domain, which only recognises and binds unmodified histones (Boyer et al., 2004). The PHD (Plant Homeodomain) finger domain initially identified in the Arabidopsis protein HAT3.1 and subsequently found in many human proteins such as the transcriptional co-activators p300, CBP and Trithorax-group proteins, allows these chromatin-associated proteins to bind to H3K4me3 (Aasland et al., 1995). The EAR (Ethylene-responsive element binding factor-associated amphiphilic repression) motif mediates transcriptional repression in plant gene regulation and is identified by the consensus sequence patterns of either LxLxL or DLNxxP. It is found in repressors known to respond to developmental and environmental signals at the transcriptional level, for example NINJA (Novel Interactor of JAZ) acts as a transcriptional repressor recruiting TOPLESS and TPL-related proteins (TPRs) (Pauwels et al., 2010).

3D Ribbon Structure	Domain	Proteins Examples	Target
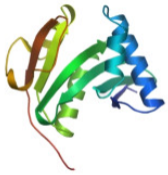	HAT	HAG1, HAC1	Lysines
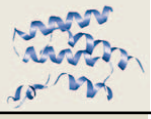	Bromo	HAG1, SWI/SNFs	Acetylated Lysines
	SANT	ADA2 ISWI	Unmodified Histones
	Chromo	SUV39H1	Methylated Lysines
	PHD finger	p300, CBP	H3K4me3, Arginine
	EAR motif	NINJA	Corepressors (TPL), Chromatin modifiers (HDA19)

Table 1.4. Important protein domains in chromatin-associated proteins. HAT, histone acetyltransferase; Bromo, bromodomain; SANT; Chromo, chromodomain; PHD finger, plant homeodomain; EAR, ethylene responsive element. Ribbon structure for HATs were taken from van den Burg *et al* (2009) and the rest were taken from Liu *et al* (2012)

These examples highlight the plethora of protein domains that are employed in gene regulation and that by understanding the composition of multi-protein complexes and the domains found within, we can predict and test specific functions of those complexes.

1.15. Chromatin remodelling mechanisms targeted by pathogens

The importance of chromatin remodelling mechanisms has been demonstrated in both plants and animals and is further highlighted by the fact that pathogens have evolved strategies to hijack such mechanisms so as to establish successful colonisation of their host. For example, *Listeria monocytogenes* is a food-borne pathogen that causes listeriosis in humans and animals (Low and Donachie, 1997). A protein effector, known as LntA is found specifically in the virulent strains of *L. monocytogenes*. LntA directly interacts with the chromatin remodelling complex BAHD1, which normally represses IFN responses. Upon infection with LntA-expressing bacteria there was induced expression of IFN-λ, due to effector-mediated derepression of BAHD1 leading to higher levels of host colonisation (Lebreton et al., 2011). In another example, direct trimethylation of H3K14 by the RomA effector from *Legionella pneumophila*, the causative agent of pneumonia and Legionnaires' disease was detected in infected lung epithelial cells and macrophages. Interestingly, H3K14me3 is a mark that has not been identified in mammals in any other context, which suggests that the pathogen evolved a unique mechanism to block the acetylation of H3K14 and repress gene expression (Rolando et al., 2013). OspF and OspB, two effectors from *Shigella flexneri*, a pathogen of the large intestine in humans, were proposed to both target the Retinoblastoma (Rb) protein. Considering that Rb is an important regulator of gene expression, as a recruiter of chromatin modifying proteins (Macaluso et al., 2006), *S. flexneri* is interesting in that it has evolved two independent effectors targeting the same pathway to ensure diminished inflammatory cytokine

production (Zurawski et al., 2009). These examples highlight the breadth of virulence strategies targeting chromatin remodelling processes that can be employed by pathogens with the aim of increasing colonisation. Interestingly, the effector HopAI1 from *P. syringae* has nuclear localisation and it is likely that it could employ its phospho-Thr lyase activity on histones, thus altering chromatin modification status and gene expression.

In plants, a very well characterised class of pathogen effectors is known as transcription-activator-like (TAL) effectors from the Gram-negative bacterium *Xanthomonas*. These function as transcriptional activators of host genes, thus acting as virulence factors. The mechanism of action is based on the binding of these effectors on DNA sequences using a central domain of tandemly arranged nearly identical repeats of approximately 34 amino acids. TAL effector AvrBs3 is known to bind to the conserved UPA box TATATAAACCN2–3CC in more than 20 pepper genes to induce their transcription. Specifically, *Xanthomonas campestris pv. vesicatoria* bacteria expressing *AvrBs3* induced a hypersensitive response in pepper plants, which coincided with an AvrBs3-dependent hypertrophy of the mesophyll tissue. The same phenotype was observed when *avrBs3* gene was transiently expressed in tobacco plants (Boch and Bonas, 2010; Marois et al., 2002). This highlights the fact that the outputs of nuclear processes are often linked to immunity phenotypes and interference of these is a common strategy among plant pathogens.

Another interesting virulence strategy comes from the Agrobacterium protein 6b, which contributes towards crown gall formation and is known to associate with various host nuclear proteins including histone H3 (Terakura et al 2007; Tinland et al 1990). It has been proposed that 6b acts as histone chaperone, however, more recent structural studies revealed a putative ADP-ribosyltransferase activity (Wang et al 2011) suggesting that this protein may interfere with host transcription through modifying histone H3.

Pathogen-mediated modulation of histone acetylation was recently shown by Kong *et al* (2017) who found that the soybean pathogen *Phytophthora sojae* employs the cytoplasmic effector PsAvh23, which then acts to disrupt the structural integrity of the SAGA complex. Specifically, by binding to ADA2 and interfering with the complex assembly, the pathogen is able to alter H3K9 levels and increase host colonisation. This further highlights the importance of acetylation in immunity, the role of HAG1 as an important player in mounting immune responses and that this pathway is an attractive target for pathogens.

1.16. Context of this work

As explained in the introductory sections above, multiple mechanisms of chromatin remodelling have been described in plant immunity, however, our understanding of the exact role of histone acetyltransferases is still lacking. Pathogens are known to have evolved strategies to interfere with the different defence mechanisms of plants, including chromatin remodelling processes. Despite its importance, research into how *Pst* DC3000 is able to subvert such processes in *A. thaliana* is still limited.

In this work, we aimed to identify important regulators of histone acetylation with a role in plant immunity by taking a reverse genetics approach. The results of this screen are presented in Chapter 3 along with evidence supporting the importance of HAG1 histone acetyltransferase in conferring plant resistance. To further characterise this HAT, a biochemical approach was followed in Chapter 4, specifically by attempting to identify its interacting partners so as to describe its mechanism of action in greater detail. Chapter 5 explored the possibility of *Pst* DC3000 effectors interacting with chromatin remodelling processes of *A. thaliana* by screening a large number of T3S effectors for nuclear localisation and chromatin binding capacity. This chapter focused on HopO1-1, a putative ADP-ribosyltransferase with potential chromatin binding ability. Mass

spectrometry was used to identify potential interactors of this effector in *A. thaliana* and *N. benthamiana* revealing that this effector is unlikely to be involved in chromatin-related processes, but may interfere with photosynthetic processes, actin polymerisation and protein synthesis.

Chapter 2 - Materials & Methods

2.1. Material and Growth conditions

2.1.1. Plant material

Arabidopsis thaliana plants used in this project are in Col-0 ecotype background, unless otherwise stated, and listed in supplementary *Table 2.1 (Refer to Appendix)*. To obtain adult Arabidopsis plants, seeds were sown in Arabidopsis mix (F2 Compost, grit, Intercept) and stratified for 2-3 days at 4°C, then pots were transferred into a growth chamber (Aral-ab) with controlled humidity, temperature and light (60% humidity, 22°C, 10 hours light/14 hours dark, 100µmol m^{-2} s^{-1} light intensity) for 2 weeks. Seedlings were then carefully transplanted into P24 trays with Arabidopsis mix and grown for a further 3-4 weeks. For *in vitro* work, seeds were sown on plates with 4.3g/L Murashige-Skoog (MS) salts (Duchefa Biochemie), 10g/L sucrose (Sigma), 5g/L Phytagel (Sigma) and 25mg/L Nystatin (to avoid contamination by fungi) and were allowed to grow for 2 weeks in a controlled environment chamber.

2.1.2. Bacterial cultures

Stocks were kept in 20% glycerol at -80°C. For selection on agar plates LB (Luria Bertani) appropriate antibiotics were used to plate *E. coli* and Agrobacteria and grown for 1 day at 37°C or 2 days at 28°C, respectively. *Pseudomonas syringae* strains were plated on Kings B media with appropriate antibiotics (Rifampicin 100µg/mL, Kanamycin 25µg/mL) for 2 days at 28°C. For inoculation of all liquid cultures, single colonies were picked into 10mL of the appropriate medium, antibiotics and temperature with shaking at 220rpm and grown overnight.

Plant Line	Gene Mutated	Genetic Modification	Details	Line	Source
Columbia (Col-0)	-	None	-	-	-
fls2	*FLS2 (At5g46330)*	Point Mutation	(G1064R)	*fls2-17*	Gomez-Gomez et al 2000
hag1-6	*HAG1 (At3g54610)*	T-DNA	-	-	
hag1-5	*HAG1 (At3g54610)*	T-DNA	-	-	
hda19	*HDA19 (At4g38130)*	T-DNA	-	-	
sid2-1	*SID2 (At1g74710)*	Point Mutation	-	-	
hag1-6 x sid2-1	*HAG1 and SID2*	T-DNA	-	-	Ntoukakis group
hag1-6 x hda19	*HAG1 and HDA19*	T-DNA	-	-	Ntoukakis group
hag1-6 x NahG	*HAG1*	T-DNA	-	-	Ntoukakis group
NahG	NahG (*P.syringae* sp. ND6)	T-DNA	-	-	
hag1-6 np::HAG1-FLAG	*HAG1 (At3g54610)*	T-DNA	C-ter FLAG	(Line A10)	Ntoukakis group
hag1-6 np::HAG1-FLAG	*HAG1 (At3g54610)*	T-DNA	C-ter FLAG	(Line K31)	Ntoukakis group
hag1-6 np::HAG1-FLAG	*HAG1 (At3g54610)*	T-DNA	C-ter FLAG	(Line K34)	Ntoukakis group
Col-0 *35S::GFP-H2B*	*H2B*	T-DNA	N-ter GFP	-	Ntoukakis group
Col-0 *DEX::HopO1-1-HA*	*HopO1-1* (*P. syringae* DC3000 T3E)	T-DNA	C-ter HA	-	Selena-Gimenez Ibanez
Ler *TPL-HA*	*TOPLESS*	T-DNA	C-ter 6xHA	-	Szemenyi *et al* 2003/Beynon group

Table 2.1: Plant genotypes used in this project.

2.1.3. Transformation of *Agrobacterium tumefaciens* with plasmid

Constructs of interest were transformed into *Agrobacterium tumefaciens* GV3101 using the electroporation method. After electroporation, the bacteria were incubated for 2 hours in LB without antibiotics and then

plated under sterile conditions in LB plates with appropriate selection for two days. Rifampicin and Gentamicin (20 µg/mL) were used to select for the Agrobacterium strain and further selection was used according to the plasmid used.

2.1.4. *Agrobacterium tumefaciens* for *N. benthamiana* transient expression

Cells from overnight cultures were harvested by centrifugation at 3,500 rpm, washed twice in agro-infiltration buffer (10mM MES pH 5.6, 10mM $MgCl_2$) and OD_{600} was adjusted to 0.4 for single-construct infiltration and to 0.8 for double-construct infiltration reaching a final OD_{600} 0.4 for each construct. The cultures were syringe-infiltrated in *Nicotiana benthamiana* leaves using a 2 ml syringe. Harvesting or imaging of tissue occurred 2-3 days post infiltration.

2.2. Molecular Biology

2.2.1. Traditional cloning

For bacterial expression of HAG1 the destination vector pOPIN-M (N-ter 6x His and 1x MBP, IPTG-inducible T7 promoter) was chosen. HAG1 ORF sequence was amplified from Arabidopsis Col-0 cDNAs using primers VN92 and VN93 to introduce cloning sites *KpnI* and *PmeI* respectively. The resulting fragment was ligated into pGEM®-T Easy sub-cloning vector and transformants were selected using the X-gal/IPTG system. Mutagenesis to generate putative catalytic inactive HAG1 versions was made on the cDNA version of the gene in this vector. Two point mutations were made on HAG1 generating E289Q and E289H. HAG1 ORFs for WT and the two point mutants were digested from pGEM®-T Easy vector with *KpnI* and *PmeI* and ligated (DNA ligase by NEB) overnight at 16ºC into POPIN-M expression vector, which was then transformed into *E. coli* and

selected on plates with Ampicillin (100 µg/mL). Clones were confirmed by colony PCR and sequencing. *Note*: a *KpnI* site within HAG1 ORF was removed by site-directed mutagenesis resulting in a synonymous mutation, in order to successfully clone into pOPIN-M vector.

2.2.2. PCR purification

PCR purification kit (Qiagen) was used for reactions that gave a single band of the expected size. When multiple amplicons were identified on an agarose gel, a razor blade was used to excise only the band of the expected size. The fragment was purified using a Gel extraction kit (Qiagen).

2.2.3. Colony PCR

Positive transformants were tested using a colony PCR. A colony was picked and mixed in 100µL of water. 1µL of this mixture was used in the PCR as DNA template.

2.2.4. Site-directed mutagenesis

To generate the point mutants E289Q and E289H in *HAG1* a site-directed mutagenesis protocol based on 'Agilent Quickchange site-directed mutagenesis kit' was adapted with the following specifications. Wild type *HAG1* cDNA in pGEM®-T Easy sub-cloning vector was used. Mutagenic primers were designed to anneal to the same strand on the plasmid with a size of 25-45 base pairs and melting temperature (T_m) above 78°C. For primer design, the following formula was used: $T_m = 81.5 + 0.41 \times (\%GC) - (675/N) - \%MM$, where: %GC is a whole number, N is the primer length, %MM or mismatch is a whole number representing the number of bases being mutated as a percentage of the whole primer sequence. Twelve amplification cycles were used as this was a point mutation, as opposed to single amino acid mutations and multiple amino acid

changes, which require 16 or 18 cycles respectively. High fidelity polymerase (Phusion®) was used with 100-150ng of template DNA. The PCR conditions were [95°C for 30 sec] x 1, [95 °C for 30 sec, 55 °C for 60 sec, 68 °C for 60 sec/kb] x12, [68 °C for 5 minutes] x 1. Dpn1 enzyme was used to remove methylated DNA. Standard PCR clean-up was used (QIAGEN) remove protein from the sample. *E. coli* TOP10 electrocompetent cells were transformed using 1-2µL of the *Dpn1*-treated sample. At least three positive clones were sequenced to account for low mutagenesis efficiency.

2.2.5. Plant genotyping

To verify the presence of T-DNA insertions in mutants and transgenic Arabidopsis plants, genotyping was performed after crude extraction of genomic DNA. Briefly, a small leaf disc was taken from an adult plant and ground in 5% Chelex-100 (Bio-Rad) in water. The sample was boiled at 100°C for 10 minutes and 1µL of the clear lysate was used as a template in the PCR reaction. *sid2-1* mutants bear a point mutation, which was confirmed by amplification of a 500bp fragment using primers VN336 and VN337 and subsequent digestion with the enzyme *MfeI* (NEB). The point mutation leads to the creation of the palindromic digestion site 5'- CAATTG - 3', which results into two separate bands after running on gel electrophoresis, contrary to wild type, which was resistant to enzyme digestion.

2.2.6. Gateway cloning

For *in planta* expression of *HAG1* the destination Gateway vectors pEG202 (N-ter FLAG, 35S promoter) and pEG302 (C-ter FLAG, native promoter cloned with gene) were chosen (Earley et al., 2006). Both the *HAG1* genomic sequence with a native promoter and *HAG1* cDNA were cloned from plant genomic DNA and cDNA library, respectively. First,

genomic *HAG1* was PCR-amplified from high quality genomic DNA. The amplification of the 4,400 bp fragment (3,700 bp gene plus 719 bp native promoter) was achieved using primers VN88 and VN91. Phusion DNA polymerase (NEB) with proof-reading ability was used to avoid PCR-induced mutations. Similarly, the 1,700 bp *HAG1* cDNA was amplified in the same way. Resulting fragments were PCR-purified and served as templates for a second amplification to introduce the second half of the *attB* recombination sites, followed by PCR purification. A BP reaction was performed using pDONR-Zeo® as the target vector and BP clonase 2 enzyme mix (Invitrogen). Proteinase K treatment at 37°C was used to eliminate protein from the sample before the transformation pDONR-Zeo-HAG1 into *ccdb*-sensitive *E. coli* cells, which were then selected in Zeocin. Positive clones were checked by colony PCR using the universal primers M13F, M13R and *HAG1*-specific primers VN100-107. After extracting plasmid DNA from positive clones, LR reactions were performed using 150ng of pEarleyGate vectors 202 (for cDNA) and 302 (for gDNA), 150ng of pDONR-Zeo-HAG1 vector, supplemented with LR clonase 2 enzyme mix (Invitrogen). Proteinase K treatment, transformation and colony PCR were performed as before with the difference that selection was made in Kanamycin (100 µg/mL). Positive clones were sent for sequencing.

2.3. Biochemistry

2.3.1. Protein immunoprecipitation

A protocol published by Piquerez *et al* (2014) was used for the immunoprecipitation of plant-expressed proteins when nuclear enrichment was not necessary. Briefly, plant material was pulverised into a fine powder using liquid nitrogen and proteins were extracted in Buffer C (2% w/v PVPP, 1% IGEPAL® CA-630) at a ratio 4:1 v/w. Starting plant material

varied from 1-2 grams for the identification of expressed protein to 30-40 grams for the immunoprecipitation of large protein complexes and subsequent mass spectrometry. Protein extracts were filtered through Miracloth (Millipore) and mixed with 15-30μL of appropriate affinity resin (GFP-Trap, HA Agarose, FLAG). In the case of FLAG resin, 1% BSA was used to block the beads beforehand. Immunoprecipitation was performed at 4°C for 2-3 hours on a rotating wheel. Beads were washed 5-6 times with Buffer D. Elution of FLAG-tagged proteins was performed in Buffer D using 0.25mg/ml FLAG peptide (DYKDDDDK) as a competitor. The process was repeated 2-3 times at room temperature and each time the supernatants/eluates were collected into the same tube. The eluates were further concentrated using the highly unspecific protein binding Strataclean beads (Agilent Genomics) at room temperature.

2.3.2. Protein Immunoprecipitation after nuclear enrichment

To extract nuclear proteins a nuclear enrichment protocol was followed. First, plant tissue was flash frozen in liquid nitrogen and pulverised into a fine powder. Proteins were extracted using nuclei extraction HONDA buffer containing 1.25% Ficol (GE Healthcare), 2.5% Dextran T40 (Sigma), 440mM sucrose, 0.5% TritonX-100. HONDA buffer was added at a ratio 2:1 volume buffer/tissue weight. Nuclei were burst using lysis buffer containing 1% SDS , 10mM EDTA, 50mM Tris-HCl and sonicated (Low power, 3x30sec ON, 60 sec OFF) to break the chromatin. Immunoprecipitation was performed on the lysate diluted 10 times in IP buffer (16.7mM Tris-HCl, 1.2mM EDTA, 167mM NaCl, 1.1% TritonX-100) for 4 hours at 4°C in a rotating wheel after the addition of appropriate resin. Beads were washed thoroughly with beads-washing buffer containing 1.1% TritonX-100 to remove specific binding followed by detergent-free washes to remove traces of detergent prior to mass spectrometry analysis. A small aliquot (10% of the sample) was used for

immunoblotting to confirm successful immunoprecipitation, while the rest of the beads were used for on-beads trypsin digestion and mass spectrometry.

2.3.3. HAT activity of HAG1 purified from *N. benthamiana*

FLAG-tagged *HAG1* cDNAs (WT, E289Q, E289H) were transiently expressed in *N.benthamiana* and immunoprecipitated as described in Piquerez *et al* (2014) without elution from FLAG resin. The histone acetyltransferase reaction was performed on the beads. A fluorescence-based HAT kit was purchased from Active Motif. Controls without substrate and Acetyl-CoA were included to account for background activity. The reaction was performed at 37°C for 3 hours with shaking (300rpm). The reaction was stopped by addition of STOP solution, followed by DEVELOPER solution. The resulting fluorescence was measured at an excitation wavelength of 360nm and emission at 465nm using a plate reader (TECAN Genios) after preparing each reaction in triplicate wells in a 96-well plate.

2.3.4. Expression of recombinant HAG1 in *E.coli*

For expression of recombinant *HAG1* from *E.coli*, TOP10 cells containing IPTG-inducible 6xHis-MBP-HAG1 (WT, E289Q, E289H) were first streaked on 100 µg/mL ampicillin plates and single colonies were used for inoculation of a pre-culture. The next day, 500µL from the pre-culture were inoculated into 50mL of LB and grown for 2-3 hours. When OD_{600} reached 0.6, 2mM IPTG was added and the cells were grown for 3 more hours at 37°C. The cultures were cooled to 4°C and harvested by centrifugation at 4,000rpm. Supernatants were boiled in 1x SDS at 90°C for 10 minutes and loaded on SDS-PAGE, transferred onto a PVDF membrane and blotted with αHis antibody (Sigma).

2.3.5. On-beads trypsin digestion

Immunoprecipitated proteins were prepared for mass spectrometry by performing on-beads trypsin digestion. Starting with 45µL of immunoprecipitated material, reduction of cysteine double bonds was achieved in 10mM DTT at 60°C incubation for 15 minutes. Alkylation of the cysteine bridges was done in 20mM Iodoacetamide (IAA) and incubation in the dark for 30 minutes. Digestion with 0.5mg/mL (Promega) and overnight incubation at 37°C. A low pH was obtained by addition of formic acid at 0.1% final concentration. A clear solution of tryptic digest was obtained after filtration through a 0.22 μm Costar® Spin-X® centrifuge tube filter (Sigma- CLS8169) before transferring to a glass vial for mass spectrometry analysis. Samples were kept at -20°C until analysed by MS.

2.3.6. In-gel trypsin digestion

Immunoprecipitated HAG1-FLAG after nuclear enrichment was eluted from FLAG resin and concentrated using Strataclean beads (Agilent) according to Piquerez *et al* (2014). After running on 12% SDS-PAGE and staining with colloidal Coomassie Blue the lanes (control and test sample) were cut into five pieces, then into smaller cubes and placed into individual Protein-LoBind (Eppendorf) tubes. Gel pieces were washed in 50% ethanol in 50mM ammonium bicarbonate and dehydrated in 100% ethanol. Disulphide bonds were reduced with 10mM DTT in 50mM ammonium bicarbonate and alkylated with 55mM Indoleacetic Acid (IAA) in 50mM ammonium bicarbonate. A trypsin concentration of 2.5ng/µL was used overnight at 37°C. To stop the reaction and lower the pH of the sample, a final concentration of 2.5% formic acid was obtained before several sonication cycles to extract digested peptides from the gel pieces. The resulting extract was dried and resuspended in 40µL 0.05% trifluo-

roacetic acid in 2.5% acetonitrile followed by several rounds of sonication. A clear solution of tryptic digest was obtained after filtration through a 0.22 μm Costar® Spin-X® centrifuge tube filter (Sigma- CLS8169) before transferring to a glass vial for mass spectrometry analysis. Samples were kept at -20°C until analysed by MS.

2.3.7. Measuring Histone Acetylation Levels

For the quantification of histone acetylation levels by western blot, 10 day-old seedlings were transferred to 16-well plates containing liquid MS for 5 days and then treated with flg22 (100nM)(Peptone). Seedlings were collected at various time points and flash frozen. After grinding the frozen tissue into fine powder, proteins were extracted at a ratio 5:1 v/w in 1x SDS buffer with 50mM DTT and boiled at 95°C for 10 minutes. Protein concentration was determined using BioRadUltra (Expedeon) appropriate for detergent-rich samples. Equal amounts of protein were loaded on 15% SDS-PAGE gel along with 4 µL of protein marker (ThermoFisher Scientific). Proteins were transferred onto a PVDF membrane overnight at 30V at 4°C. Antibodies against histones and histone modifications were purchased from Millipore and used at the following concentrations for 1 hour at room temperature (H3K9K14Ac 1:5000, H3K9Ac 1:5000, H3K14Ac 1:5000, H3 1:10,000) in 5% milk TBS-T. Secondary anti-rabbit HRP (Sigma) was used at 1:10,000.

2.3.8. Mass spectrometry parameters

For on-beads digested samples, an aliquot containing 2 μL of extracted peptides from each sample was analysed by means of nanoLC-ESI-MS/MS using the Ultimate 3000/Orbitrap Fusion instrumentation (Thermo Scientific) using a 120 minute LC separation on a 50 cm column. For in-gel digested samples, an aliquot containing 20 μL of extract-

ed peptides from each sample was analysed by means of nanoLC-ESI-MS/MS using the Ultimate 3000/Orbitrap Fusion instrumentation (Thermo Scientific) with a 30-minute LC separation on a 25 cm column. The data were used to interrogate the *Arabidopsis thaliana* or *Nicotiana benthamiana* database (supplied by The Sainsbury Laboratory, Norwich), *Pseudomonas syringae* and the common Repository of Adventitious Proteins (http://www.thegpm.org/cRAP/index.html) using uninterpreted MS/MS ions searches within Mascot software (http://www.matrixscience.com/). Scaffold software was used to analyse and visualise the results from Mascot search.

2.3.9. Statistical analysis of proteomic data

Scaffold uses spectral counting for quantification. Peptides are matched with the spectra identified during the experiment. For the purposes of protein identification, Scaffold uses a ProteinProphet™ model, assigning the peptide exclusively to the protein with the most evidence. The result is that the peptide has a weight of 1 in one protein and a weight of zero in all other proteins. Normalisation between samples to compare abundances of a protein was performed by adjusting "unweighted spectrum counts" to a normalised "quantitative value". In the case of missing values, a minimum value of 1 was used to allow for statistical analyses and determination of fold-change. When three or more replicates were present in each category, a T-Test was performed to obtain p-values of each interaction, which were then used for the construction of volcano plots.

Antibody Name	Target Protein/Epitope	Company	Concentration
Primary Antibody			
α-FLAG (Mouse)	FLAG tag	Sigma	1:10,000
α-H3 (Rabbit)	Histone H3 (no PTM)	Millipore	1:10,000
α-H4 (Rabbit)	Histone H4 (no PTM)	Millipore	1:4,000
α-H3Ac (Rabbit)	Histone 3 Lys 9/14 (Acetylated)	Millipore	1:5,000
α-H3K9Ac (Rabbit)	Histone 3 Lys 9 (Acetylated)	Millipore	1:5,000
α-H3K14Ac (Rabbit)	Histone 3 Lys 14 (Acetylated)	Millipore	1:5,000
α-p44-ERK/p42	Phosphorylated MPK6,3,4	Cell Signalling	1:5,000
α-His (Mouse)	His-tag	Sigma	1:10,000
α-HA	HA-tag	Sigma	1:2,000
α-GFP	GFP-tag	ChromoTek	1:2,000
Secondary Antibody			
α-Mouse-HRP (Goat)	Mouse IgG	Sigma	1:10,000
α-Rabbit-HRP	Rabbit IgG	Sigma	1:10,000
TrueBlot™	Non-denatured proteins	Sigma	1:10,000
Affinity Resin			
GFP Beads	GFP-tag	ChromoTek	
HA Beads	HA-tag	ChromoTek	
FLAG Beads	FLAG tag	Sigma	

Table 2.2: Antibodies used in this project

2.4. Physiological assays

2.4.1. Reactive oxygen species (ROS) production

To measure the production of reactive oxygen species in different genotypes a previously described method was used (Boutrot et al., 2010). Briefly, approximately 12 leaf discs per genotype were taken from leaves 5 and 7 from adult *A. thaliana* plants using a No. 1 cork borer, placed into a white 96-well plate and kept overnight on distilled water. Assay solution with luminol (100µM final), horseradish peroxidase (10µg/mL) and flg22

(100nM) was freshly prepared the next day. Luminescence was recorded using a High Resolution Photon Counting System (Photek) for 1 hour after treatment.

2.4.3. Mitogen-Activated Protein Kinase (MAPK) activation assay

Seedlings were grown on solid MS for two weeks and then transferred on liquid MS. Seedlings were then treated with 100 nM flg22 solution and flash frozen in liquid nitrogen at different time points. Frozen tissue was ground and proteins extracted in MAPK extraction buffer (Tris-HCl, EDTA, NaCl, Sodium Fluoride, Sodium Molybdate, Sodium Orthovanadate, 1% IGEPAL® CA-630) for 10-15 minutes. The lysates were cleared by centrifugation at 16,000g for 10 minutes. After protein quantification (Bradford), proteins were boiled in 1x SDS loading dye containing 50mM DTT for 10 minutes at 90°C. Approximately 160µg of total protein were separated on a 12% SDS-PAGE. The semi-dry method was used for transferring the proteins onto a PVDF membrane (GE Healthcare). Primary antibody α-phospho-p44/42 MAPK (Erk1/2) (Thr202/Tyr204) from Cell Signalling was used according to manufacturer's instructions to identify the double phosphorylation of the activation loop of MAPK3,4 and 6 (pTEpY). Primary antibody was added to 5% BSA in TBS-Tween 20 at 1:5000 using a peroxidase-conjugated goat anti-rabbit IgG (Sigma) as a secondary antibody. The PVDF membranes were stained with Coomassie Brilliant Blue (CBB) to assess equal loading.

2.4.4. Bacterial infection

Overnight cultures of appropriate strains were washed and resuspended in 10mM $MgCl_2$. For the infiltration method, cells were diluted serially to an OD_{600} 0.001 with 10mM $MgCl_2$. Hand-infiltration took place immediately into leaves from 4-5-week old Arabidopsis plants using a 1

mL syringe. Samples were collected 2-3 dpi. For the spraying method the OD_{600} was adjusted to 0.1 and 0.02% Silwet-L77 was added. After homogenous spraying of 4-5-week old Arabidopsis plants (30mL culture per 24 plants), lids were added to the trays to maintain high humidity. Samples were harvested 2-3 dpi.

2.4.5. Quantification of bacteria in infected leaves

Infected tissue was collected as leaf disc using No. 4 cork borer such that 2 leaf discs equalled $1cm^2$. Two leaf discs were placed into a 1.5mL tube containing 200mL 10mM MgCl2 and ground using a tissue lyser (brand) at frequency of 28MHz for 30 seconds twice. An additional 800µL of $MgCl_2$ solution was added. Serial dilutions were made in a 96 well plate first at a 1:1 dilution (10^{-1}) and then 1:9 serial dilutions (10^{-2}, 10^{-3}, 10^{-4}, 10^{-5}, 10^{-6}, 10^{-7}) were made. 10µL of these were spotted onto Kings B plates with appropriate antibiotic selection. Two days later single colonies were counted.

2.4.6. PTI and ETI elicitation prior to mass spectrometry

A. thaliana hag1-6 plants complemented with HAG1-FLAG construct downstream a native promoter (*np::HAG1-FLAG*) were grown to adult stage. For PTI induction, plants were sprayed with 1µM flg22 solution and leaf tissue was harvested after 1 hour, while for ETI induction, plants were sprayed with *Pst* DC3000 *AvrRpt2* at OD_{600} 0.1 and leaf tissue was harvested after 4 hours. Mock treatment included spraying with water and harvesting after 1 hour. In all cases, 0.02% Silwet L-77 was used. Harvested tissue was placed into a 1% formaldehyde solution and were vacuum-infiltrated 3-5 times 5 minutes to crosslink protein-protein and DNA-protein interactions. The reaction was quenched using 0.125 M

glycine. Tissue was thoroughly dried on kitchen paper and flash frozen in liquid nitrogen.

2.4.7. Chlorophyll fluorescence imaging

Photosystem II chlorophyll fluorescence imaging of Arabidopsis rosettes was performed as described in de Torres Zabala *et al* (2015) using a CF Imager (Technologica Ltd., Colchester, UK). *P. syringae* strains DC3000 WT and DC3000 ΔHopO1-1 were used to infect Col-0 adult plants. Infection was made by hand-infiltration of a OD_{600} 0.15 culture. Plants were immediately placed in the chamber for 40 min post inoculation and then dark adapted for 20 min. This was followed by a saturating light pulse (6349 µmol m^2 s^{-1} for 0.8 s) to maximum obtain dark-adapted fluorescence (Fm). Actinic light was applied at the same light intensity as plant growth (120 µmol m^2 s^{-1}) for 15 min, followed by a saturating pulse to obtain maximum light adapted fluorescence (Fm'). The plants were left for a further 24 min in actinic light before returning to the dark for 20 min. At this point the cycle of measurements (59 min duration) was repeated 23 times. Fm, Fm' and Fo (minimal fluorescence with fully oxidised PSII centres) were used to calculate chlorophyll fluorescence parameters related to photosystem II photochemistry, specifically Fv/Fm (maximum dark adapted quantum efficiency). The temperature was kept constant at 20 °C.

2.5. Cell Biology

2.5.1. Fluorescence Recovery After Photobleaching (FRAP)

For the FRAP experiments, root tips (1cm long) from Arabidopsis seedlings were treated with water or flg22 solution (100nM or 1µM) and imaged immediately. For experiments with leaf tissue, 1mm in diameter leaf discs were taken from *N. benthamiana* treated in the same way. All

FRAP experiments were performed on a confocal microscope (Zeiss LSM710 and LSM880). Specific confocal microscope settings: A pre-scan on GFP-tagged histones or effectors was acquired at an excitation wavelength 488nm and emission 533nm. After adjusting laser power and gain to avoid any saturation of signal, a bleaching pulse of 5 iterations (laser power 100%, speed 200-500 pxls/ms) with a bleaching area of 1µm was made. For image acquisition, the laser power was reduced to 1% to avoid acquisition bleaching on the fluorescent signal. A Z-stack of 15-24 slices of 1µm thickness was obtained, once every 60 seconds. FRAP data were analysed in the following way: three regions were selected; bleached region (ROI), unbleached region to account for the recurrent loss of fluorescence owing to imaging bleaching and a background region to account for background intensity levels. Using the following formula the variation of intensity on the bleaching depth was also normalised.

$$\frac{I(t) - I(t_{bleach})}{1 - I(t_{bleach})} = I(norm)$$

Images were processed using ImageJ to first create a Z-project resulting in a single Z-stack image from multiple Z-slices. Then, the plug-in 'StackReg/Rigid Body' was used to align the different images over time to allow fluorescence quantification of the ROI. Prism was used for curve fitting.

2.5.2. Protoplast preparation and transfection

Arabidopsis leaf mesophyll protoplasts were generated following the protocol by Yoo *et al* (2007). Leaves 5, 6 and 7 from 24 Col-0 plants grown to 4-weeks old were chosen and removed from the plant. Thin leaf strips of 0.5mm width were placed into 15ml enzyme solution passed through 0.45mm filters. The enzyme solution initially consisted of 20mM MES, 0.4% w/v Macerozyme R10 (Duchefa-Biochemie), 1.5% w/v Cellulase R10 (Duchefa-Biochemie), 0.4M mannitol, 20mM KCl and after warming the solution to 30°C, BSA was added to a final 0.1% and 10mM

$CaCl_2$. The leaf tissue was vacuum infiltrated and incubated for 2.5 hours at room temperature with occasional gentle shaking. Protoplasts were diluted with equal volume of W5 buffer (2mM MES, 154mM NaCl, 125mM $CaCl_2$, 5mM KCl). Protoplasts were counted using a Fuchs-Rosenthal haemocytometer and diluted in MMG (4mM MES, 0.4M mannitol, 15mM $MgCl_2$) to a concentration of 300,000 protoplasts/mL for the transfection. *HAG1* cDNA was cloned from pDONR-Zeo® into p2FGW7 vector with an N-terminal GFP tag using an LR reaction. For the transfection, 1µg of plasmid per construct was added for the PEG transformation (PEG4000 40% w/v from Sigma, 0.2M mannitol, 100mM $CaCl_2$). After a wash with W5 and one with WI buffer (4mM MES, 0.5M mannitol, 20mM KCl) the protoplasts were incubated overnight in a growth chamber. Protoplasts were imaged the next day using in a confocal microscope to assess intact protoplasts and nuclear localisation of GFP-HAG1.

Chapter 3 - HAG1 is required for plant immunity

3.1. Context of this chapter

A significant transcriptional reprogramming is well-known to occur in plants within minutes following pathogen or PAMP perception; specifically ~5% (~1,100 genes) of the Arabidopsis genome is differentially regulated after elicitation with flg22 (Moore et al., 2011; Navarro et al., 2004; Thilmony et al., 2006; Zipfel et al., 2004). The majority of these genes (966) were found to be upregulated within 30 minutes of elicitation, whereas only 202 genes were down-regulated, leading to a significant net increase in gene expression after PAMP perception. These transcriptional changes were specific to PAMP-mediated perception as mutants lacking a functional FLS2 receptor, failed to initiate a significant transcriptional response (Zipfel et al., 2004).

Considering the degree of transcriptional reprogramming, it is reasonable to hypothesise that significant changes occur in the chromatin structure to allow an overall increase in the transcription levels. Chromatin organisation is established, maintained and altered according to developmental cues and environmental stimuli by the combined action of a variety of chromatin remodelling mechanisms. Nucleosome sliding (Alvarez et al., 2010), covalent modification of histones (Lusser, 2002) and histone variants exchange (Kumar and Wigge, 2010) are the major mechanisms responsible for the remodelling of chromatin.

In recent years, advances in confocal microscopy techniques have facilitated the *in vivo* study of chromatin dynamics and chromatin-associated proteins in great detail to determine important aspects of transcription and chromatin regulation such as histone mobility and transcription factor binding properties (Mueller et al., 2010). A well-established method known as Fluorescence Recovery After Photobleaching (FRAP) has been key in exploring the dynamics of fluorescent-tagged proteins in-

volved in cellular processes, including chromatin binding and remodelling. In FRAP experiments, cells are stably or transiently transfected with a protein of interest fused to a fluorescent protein such as GFP. Once expression is established as a visible fluorescence signal through a confocal microscope, a targeted high-power laser beam at the same wavelength of excitation, photo-bleaches a region of interest (ROI) leading to irreversible removal of the fluorescent signal in the selected area.

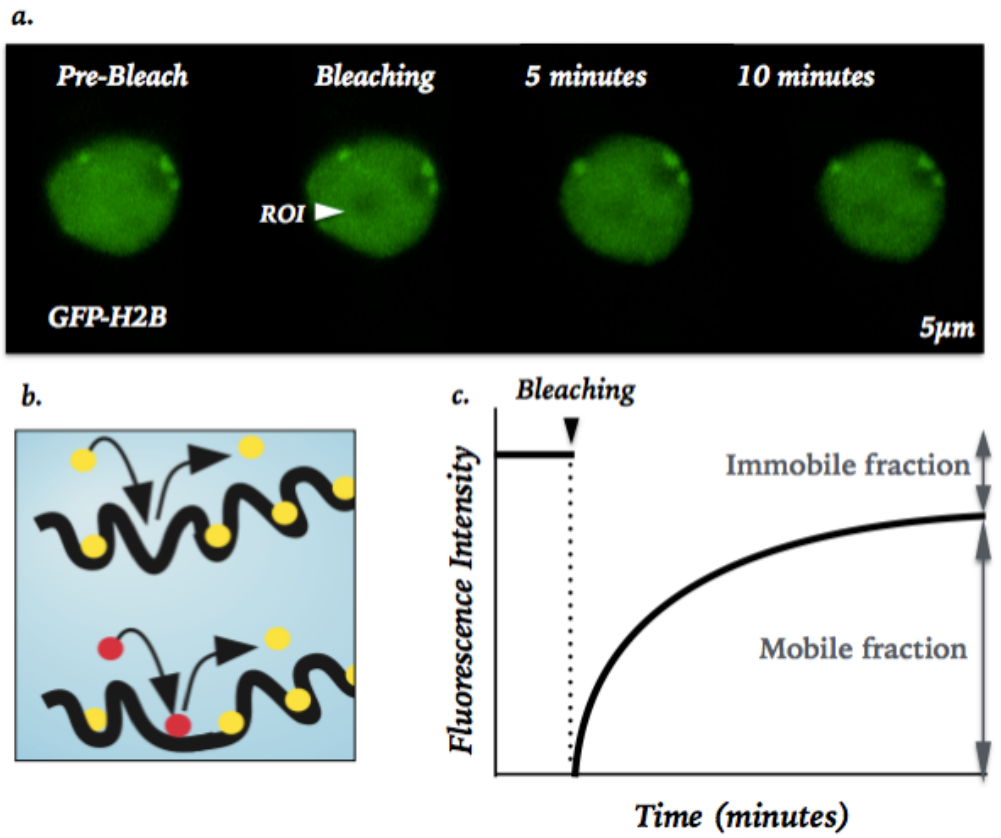

Figure 3.1. Principles of Fluorescence Recovery After Photobleaching (FRAP) experiments. (a) *A. thaliana* leaf expressing a *35S::GFP-H2B* construct. A fluorescent nucleus is bleached and the recovery of fluorescence at the region of interest (ROI, white arrow) is recorded over time. Multiple slices of the nucleus at the z-axis are obtained to generate a vertical stack of images for each time point, which are later compressed into one image per time point during analysis (*image was obtained by E. Mastorakis*); (b) DNA (black line) is wrapped around histones (yellow and red circles). Fluorescence recovery of GFP-tagged histones depends on the chromatin structure, which can be highly dynamic. A more relaxed conformation of chromatin allows faster exchange of nearby histones (red) within the chromatin fraction; (c) fluorescence intensity of the bleached spot (ROI, shown by white arrow) is calculated and plotted after accounting for total loss of fluorescence due to bleaching from image acquisition. Complete recovery cannot be achieved due to some permanently photo-bleached molecules, known as the 'immobile' fraction . 'b' and 'c' were obtained from Mistel *et al* (2001).

As fluorescent molecules move dynamically inside the living cell, fluorescence in the photo-bleached ROI can recover at a rate that directly depends on the mobility of the protein of interest. Time-lapse imaging immediately after bleaching allows the rate of fluorescence recovery to be measured providing quantitative information on the mobility of the protein and by extension, its protein binding properties (*Fig. 3.1*) (Misteli, 2001).

In functional terms, chromatin status is an important determinant of the accessibility of chromatin-associated proteins such as transcription factors and the RNA polymerase machinery (Alajem et al., 2015; Gaspar-Maia et al., 2011; Gaspar-Maia et al., 2009). In various eukaryotic model organisms the process of cellular differentiation is accompanied by global changes in chromatin organisation ranging from a euchromatic state in undifferentiated cells, such as embryonic stem cells, to a heterochromatic state in differentiated cells, such as somatic cells (Kouzarides, 2007). In plants, cell differentiation is also accompanied by changes in chromatin structure, while histone modifications have also been implicated in this process (Rosa et al., 2014). For example, the *Arabidopsis thaliana* root consists of the meristematic zone found at the tip, where cells actively divide and are highly undifferentiated. Above the meristematic zone, cell division stops and cells increase in length throughout the elongation zone and start to differentiate until they reach complete differentiation status in the maturation zone (*Fig. 3.2a*) (Dolan et al., 1993). Using the FRAP method, Rosa *et al* (2014) demonstrated a decrease in histone mobility from the meristematic to the differentiation zone. Interestingly, cells treated with Trichostatin (TSA), a chemical inhibitor of several histone deacetylases, resulted in faster histone mobility and higher histone acetylation levels, whereas in the histone acetyltransferase mutant *hag1-6* lower histone acetylation levels led to slower histone mobility. Most notably, hyperacetylation caused by TSA not only increased histone mobility but

also altered the expression of a meristem marker (*RHD6*) in cells from the differentiation zone (Rosa et al., 2014). These results implicated histone acetylation in the process of differentiation, but most importantly provided a functional link between chromatin mobility and histone modifications in plants, whereby higher acetylation levels are correlated with higher histone mobility and a more relaxed chromatin conformation.

In addition to developmental cues, biotic or abiotic stress can also lead to rapid changes in chromatin dynamics, mediated by different chromatin remodelling processes. Studies with cultured animal cells have shown that the perception of PAMPs such as lipopolysaccharide (LPS), synthetic bacterial lipoproteins (sBLP) and fungus-derived molecules lead to nucleosome eviction and a rapid increase of histone H3 acetylation and phosphorylation serving as positive marks for defence gene expression. For example, the promoter of *IL-2* gene (encoding cytokines involved in innate defence), is occupied by a single nucleosome, which is evicted upon LPS perception (Weinmann et al., 1999) and this is also correlated with a general increase in H3 acetylation and phosphorylation at promoters of defence genes (Weinmann et al., 2001). There has been no report linking the rapid deposition of activating histone marks with PAMP perception in plants. However, several reports showed the role of acetylation in abiotic stress responses. For example, H3K9, H3K14 and H4 acetylation, which are known to activate transcription (Lusser et al., 2001), were enriched on the promoter and coding regions of salt-stress inducible genes before and after high salt treatment (Kaldis et al., 2011). Other reports have shown that treatment with the synthetic analogue of SA resulted in histone acetylation of defence genes in leaves distal to the infection (Jaskiewicz et al., 2011). In addition, the mutant lacking ADA2b, a major interactor of the histone acetyltransferase HAG1 (Hark et al., 2009), displayed lower levels of H3K9/14 and H4 acetylation compared to wild type, although it should be noted that these findings are in the con-

text of salt-stress, a type of abiotic stress (Kaldis et al., 2011). Along the same lines, HAG1 has been found to play a role in light-regulated gene expression (Benhamed et al., 2006; Benhamed et al., 2008), further supporting the dynamic nature of histone acetylation in a variety of biological processes.

The acetylation levels are balanced by the antagonistic actions of HATs and HDACs. Interestingly, genetic evidence suggests that the histone deacetylase HDA19 works opposite HAG1 in the regulation of light-responsive genes. Furthermore, *hda19* mutants have a shorter hypocotyl and higher H3K9, H3K27, H4K5 and H4K8 levels on those genes, while double mutants lacking both HAG1 and HDA19 show a reversal of this photomorphogenic phenotype (Benhamed et al., 2006). However, this is not the only report suggesting an antagonistic relationship between *HAG1* and *HDA19*, which were found to interact genetically, acting on the same pathway for shoot differentiation (Long et al., 2006). Strangely, although there is no evidence for a direct role of HAG1 in plant immunity, the role of HDA19 in plant immunity has become more clear in the past few years. An important process regulated by HDA19 is the repression of SA responses. Specifically, *PR1* and *PR2 (PATHOGENESIS RELATED)* genes, which are normally induced after infection by *Pseudomonas syringae* or treatment with PAMPs and salicylic acid are more highly expressed in *hda19* mutants (Makandar et al., 2006). The enrichment of histone acetylation at the promoters of these genes was also important for their up-regulation. Mutants lacking HDA19 showed increased resistance to *Pst* DC3000 along with increased SA content and *PR* gene expression (Mosher et al., 2006). Mutating the SA-biosynthetic gene *SA-INDUCTION DEFICIENT 2* (*SID2)* or introducing the bacterial encoded gene for an SA-degrading salicylate hydroxylase (NahG) into wild type plants leads to lower SA levels and increased bacterial growth (Delaney et al., 1994; Wildermuth et al., 2001). The same sid2/NahG mutations in *hda19* mutant

background reversed the resistant phenotype of *hda19* mutants, suggesting that SA is essential for the resistance conferred by the lack of HDA19 (Choi et al., 2012). In this line of thinking it is unknown whether a histone acetyltransferase is working opposite HDA19 to locally restore the acetylation levels at the promoters of SA genes such as *PR1* and *PR2* to ensure their activation upon infection. In all, these responses result in global transcriptomic changes, which have been described in detail (Zipfel et al., 2004), however, it still remains unclear how chromatin remodelling affects the expression of defence responsive genes. This chapter explores the role of histone acetylation as a chromatin remodelling mechanism in the context of plant immunity.

3.2. Main findings

In this chapter we investigated how PAMP perception leads to chromatin remodelling in plants. Initial findings using FRAP elucidated that the chromatin of both *A. thaliana* and *N. benthamiana* plants exhibits dynamic remodelling within minutes following flg22 perception. Histone acetylation was found to increase after flg22 elicitation suggesting a role of this mark in the dynamic remodelling observed by FRAP. A susceptibility screen of Arabidopsis HAT mutants infected with *Pst* DC3000 revealed that mutations in *HAG1* lead to increased bacterial colonisation. Additional experiments confirmed that the PAMP-induced increase in histone acetylation is impaired in *hag1* mutant Arabidopsis plants. Introducing mutations (*sid2-1, hda19)* or transgenes (NahG) affecting salicylic acid levels suggested that the role of HAG1 in immunity is mostly independent of salicylic acid responses.

3.3. Results

3.3.1. Chromatin Remodelling occurs after PAMP perception

To investigate responses during PAMP-triggered immunity at the chromatin level, *A. thaliana* Col-0 seedlings stably expressing GFP-tagged histone H2B were challenged with flg22 and immediately imaged using a confocal microscope before conducting a FRAP experiment (*Fig. 3.2a and 3.2c*). Fluorescent nuclei from leaf cells were bleached and fluorescence recovery was recorded over a period of 40 minutes with images taken once every minute. Nuclei from the differentiation and maturation zone were tested. As *Figure 3.2c* shows, flg22 perception leads to an increase of GFP-H2B mobility. As early as 5 minutes after treatment with flg22 or water, the respective recoveries appear to be distinctively different. Flg22 perception in roots was in line with studies showing that immune responses also occur at the root tissue (Robatzek et al., 2006). To obtain further evidence that chromatin remodelling also occurs in leaf cells as in other plant systems, the same FRAP experiment was repeated in *N. benthamiana* leaves transiently expressing GFP-H2B (*Fig. 3.2b*). In agreement with the results obtained in *A. thaliana*, flg22 treatment resulted in significantly higher histone mobility confirming that PAMP perception alters histone mobility (*Fig. 3.2d*). For technical reasons such as low fluorescent signal and chlorophyll autofluorescence, the experiment could not be conducted in *A. thaliana* leaf nuclei expressing GFP-tagged H2B. Overall, our experiments provided evidence for flg22-induced chromatin 'opening'.

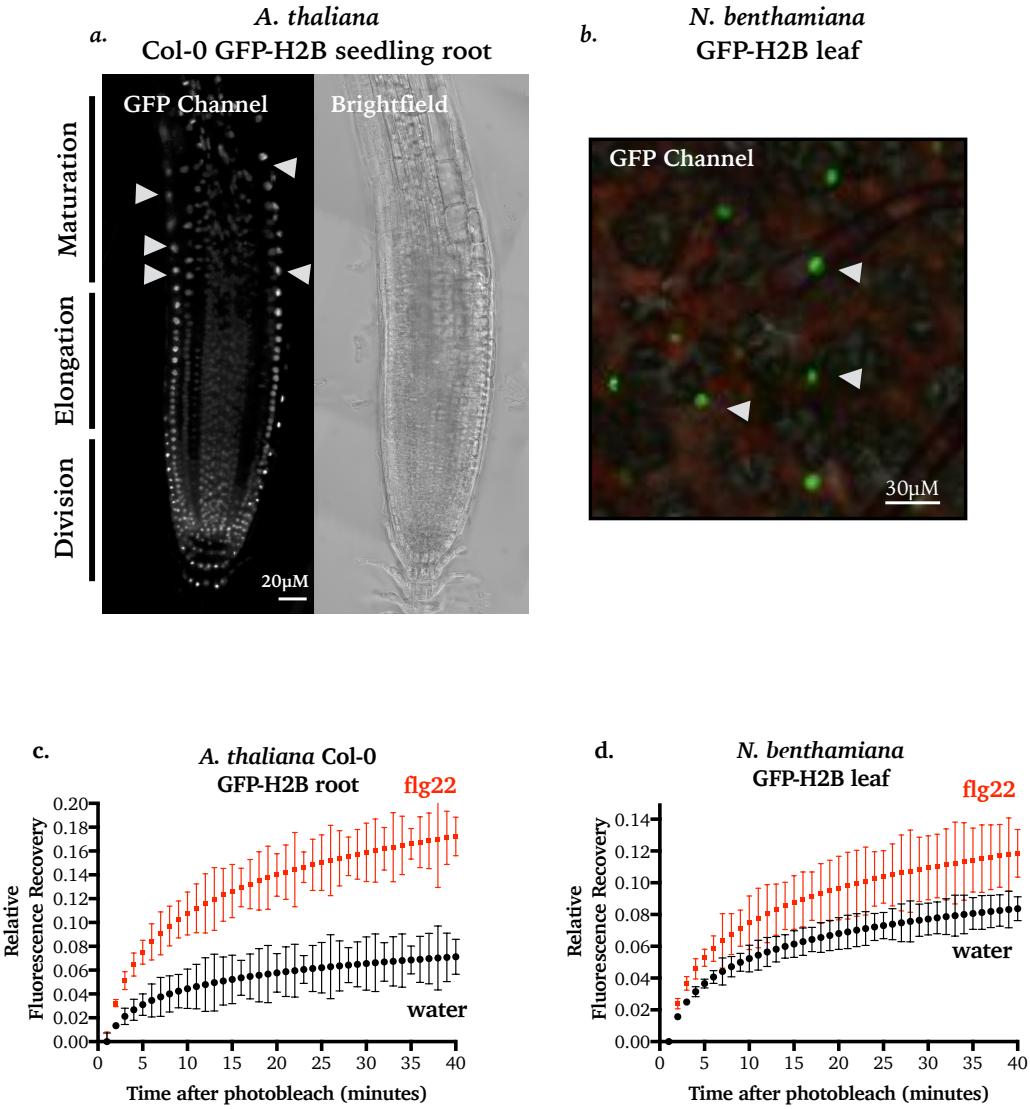

Figure 3.2. Perception of flg22 leads to opening of the chromatin. a,c. Roots from *A. thaliana* seedlings stably expressing GFP-H2B. The different root zones are shown. Maturation zone cells were tested in the FRAP experiments as shown by white arrows. White arrows also show the nuclei tested in *N. benthamiana* by FRAP. **b,d.** *N. benthamiana* leaves transiently expressing GFP-H2B. A x10 lens was used to check that transformation efficiency rates were high. flg22 (100nM) treatment of root tips or leaf discs was followed by immediate imaging, photo-bleaching and fluorescence recovery measurement.

3.3.2. Global histone acetylation increases after flg22 perception

Having established that chromatin remodelling and more specifically, a relaxation of the chromatin structure takes place within minutes after the perception of flg22, we attempted to elucidate the molecular mechanism underlying this rapid and dynamic remodelling of chromatin. Chromatin remodelling mechanisms can lead to either more compacted or more relaxed chromatin allowing or blocking access to transcription factors or other chromatin-associated proteins and it is known that increased histone acetylation is linked with increased gene expression and a more open chromatin conformation (Eberharter and Becker, 2002). Therefore, we first asked whether the global levels of histone acetylation would increase immediately after flg22 perception. To test this, Col-0 seedlings were treated with flg22 and samples were harvested at different time points within 1 hour after elicitation. Western blots using antibodies against acetylated lysines 9 (H3K9Ac) and/or 14 (H3K14Ac) on histone H3 were performed and a rapid increase in both histone marks was shown (*Fig. 3.3*). The changes in both histone marks are taking place within 5-10 minutes after flg22 elicitation in a global fashion. A peak at 15 and 30 minutes is observed for H3K14Ac and H3K9K14Ac respectively, while H3K9Ac levels remain constant from 5 to 60 minutes after flg22 treatment.

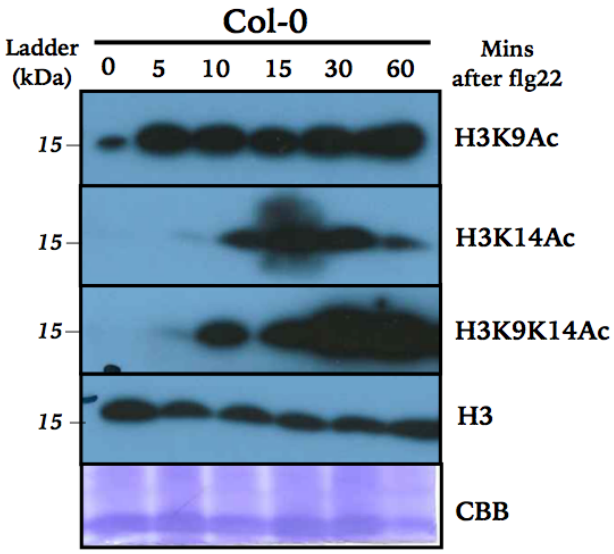

Figure 3.3. Global histone acetylation levels increase after flg22 perception. Arabidopsis Col-0 seedlings were elicited with 100nM flg22 and samples were taken at various time points (min) after elicitation. Total protein extracts were run on a 15% SDS gel and transferred onto a PVDF membrane. Blots were incubated with antibodies against single acetylation (αH3K9Ac, αH3K914Ac), dual acetylation (αH3K9K14Ac) and total unmodified H3 (αH3) to assess equal loading. CBB, Coomassie Brilliant Blue. The ladder is denoted by kDa.

3.3.3. Bacterial susceptibility screen of HAT mutants

The rapid enrichment of acetylated positions H3K9 and H3K14 after flg22 perception suggests either a rapid deposition by HATs or reduced removal by HDACs. We focused on identifying which HAT(s) could be important for immunity and potentially be responsible for the flg22-induced acetylation effect.

Figure 3.4. *Arabidopsis thaliana* HAT mutants. 4-week old HAT homozygous T-DNA insertion mutants were collected. Developmental phenotypes in size, color and leaf shape are observed. Scale bars represent 1cm.

To achieve this, single T-DNA insertion mutants for most HAT genes were obtained from publicly available seed stock centres and PCR-genotyped to ensure homozygosity. The mutants displayed a variety of developmental phenotypes with differences in size and leaf shape, for example, *hag1-6* is smaller with curly leaves, *hac4-1* is also smaller, while *hag5-1* is a bigger plant than Col-0 (*Fig. 3.4*). Growth of *Pst* DC3000 after spray inoculation revealed a susceptibility phenotype for *hag1-6* mutant, almost to the same level as the *fls2* mutant (Zipfel et al., 2004). The screen showed no statistically different phenotype of increased or decreased resistance in any other mutant (*Fig. 3.5*).

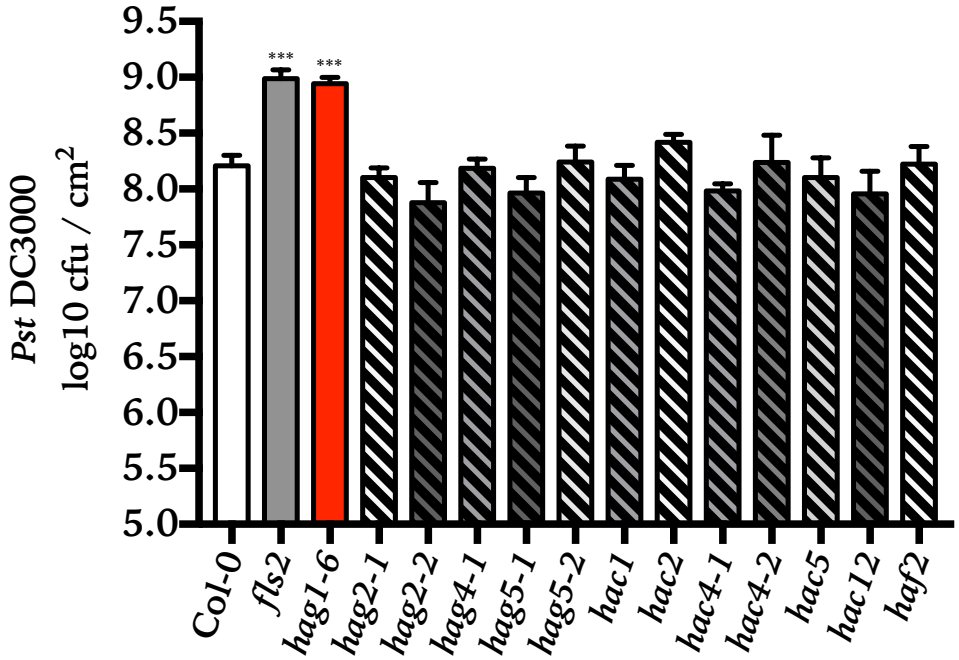

Figure 3.5. Screen of HAT mutants for altered susceptibility to *Pst* DC3000. T-DNA insertion mutants in various HAT genes were obtained. 4-5 weeks old plants were spray-infected with *Pst* DC3000 and leaf tissue was harvested 3 days post infection. Asterisks denote statistical significant differences (*** for $p<0.0001$) of columns compared to Col-0 based on unpaired parametric t-tests. The error bars represent the standard error of the mean (SEM) for 6 technical replicates. *NB: haf2 mutant is not shown in Figure 3.4.*

3.3.4. HAG1 loss leads to increased susceptibility to *Pst* DC3000

To confirm the susceptibility phenotypes of *hag1-6* and further elucidate the role of HAG1 in plant immunity we expanded the susceptibility screen on additional available T-DNA insertion mutants of the *HAG1* gene (*Fig. 3.6*) and two well-known interactors of HAG1, ADA2 and ADA2B (also known as PRZ1) (Grant et al., 1997; Hark et al., 2009). HAG1 protein contains a highly conserved HAT domain, responsible for the enzymatic activity as well as a bromodomain, which regulates binding to acetylated histones (Servet et al., 2010b). There are various mutants available, but we chose to work with two representative knock-outs, *hag1-6* and *hag1-5* (also known as *gnc5-5)*. While *hag1-6* mutation leads to truncation of both domains, the weaker mutation *hag1-5* only lacks the bromodomain (*Fig. 3.6*).

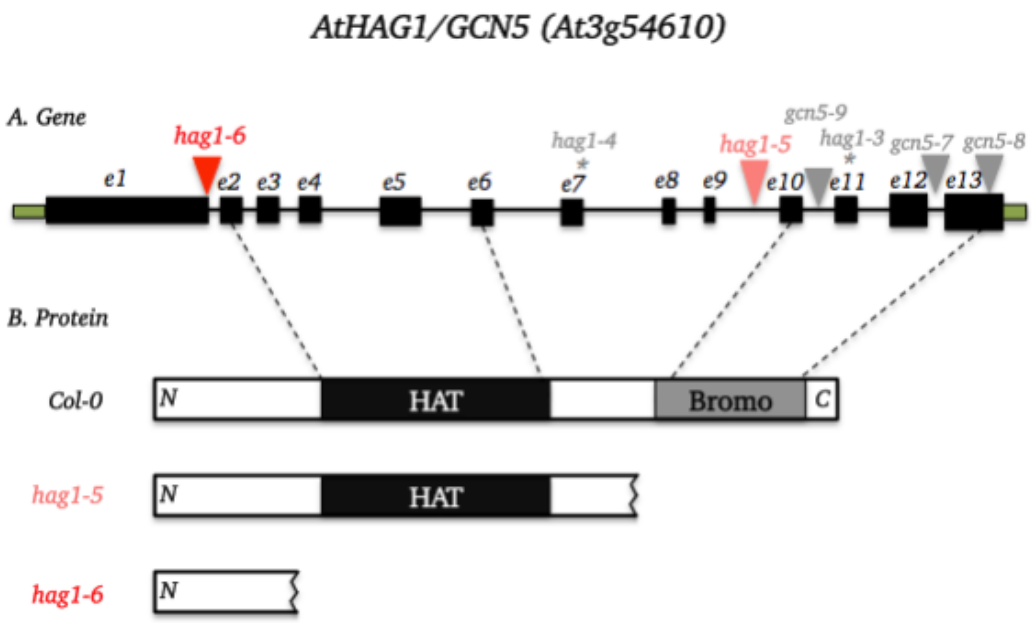

Figure 3.6. *HAG1* gene and HAG1 protein structures. A. Wild type *HAG1* is 4,700 base pairs long and consists of 13 exons (labelled with the letter 'e') 12 introns. Several T-DNA insertion mutations exist for *HAG1* genes as shown by triangles and point mutations as shown by asterisks. **B.** The full-length protein is 63kDa. Exons 2 to 6 give rise to a highly conserved enzymatic domain, responsible for the HAT activity, while exons 10 to 13 give rise to the bromodomain at the C-terminus that is responsible for binding to acetylated histones. As a result of the T-DNA insertions in *hag1-6* and *hag1-5* mutants, a fully truncated and a partially truncated protein are predicted resulting in lack of both domains or only the bromodomain, respectively.

The *hag1-6* mutant displays developmental phenotypes such as smaller size, and delayed flowering (Servet et al., 2010b), while at the seedling stage the roots are shorter, but more abundant (*Fig. 3.7a and 3.7d*). There is no clear developmental phenotype in the weaker allele *hag1-5* or in the heterozygous *hag1-6* mutant (*Fig. 3.5a*). Complementing *hag1-6* with the full length HAG1 gene expressed from a native promoter (1kb upstream the ORF) restores the size to Col-0 level (*Fig. 3.7a*).

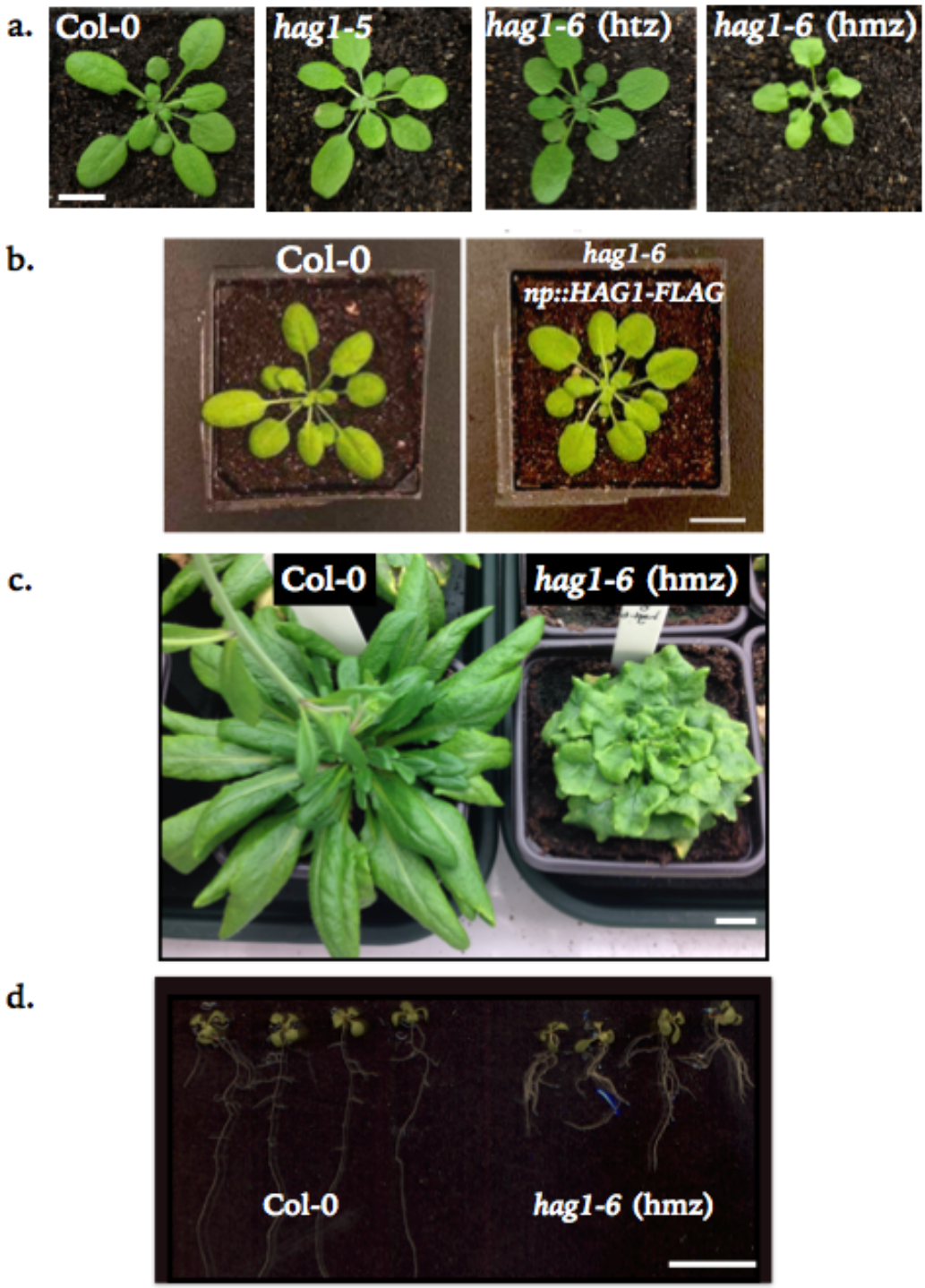

Figure 3.7. Morphological phenotypes of T-DNA insertion mutants of the *HAG1* gene. a. 4 week-old plants grown in soil; b. 5-week old plants grown in soil; c. 8 week-old plants (flowering stage); d. 2 week-old seedlings grown vertically on solid MS medium. Scale bars represent 1cm. htz, heterozygous; hmz, homozygous.

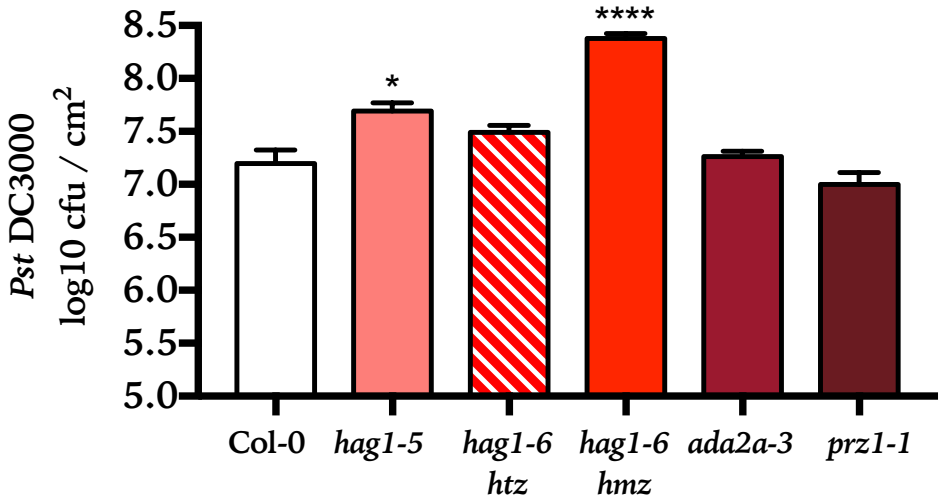

Figure 3.8. Bacterial growth in various *hag1* mutants including known interactors of HAG1. 4-weeks old plants were screened for susceptibility to *Pst* DC3000 after syringe-infiltration. Asterisks denote statistical significant differences (* for $p<0.05$, **** for $p<0.00005$) of columns compared to Col-0 based on unpaired parametric t-tests. The error bars represent the standard error of the mean (SEM). htz: heterozygous; hmz: homozygous. The mutants *ada2a-3* and *prz1-1* represent mutations in *ADA2A* and *ADA2B* genes, whose products are two established interactors of HAG1.

In all cases, mutations in *HAG1* led to consistently increased bacterial proliferation upon syringe infiltration of the *Pst* DC3000, suggesting that even when PTI responses are bypassed, immunity appears to be compromised in *hag1-6* and *hag1-5* mutants (*Fig 3.8*). We tested the susceptibility of *ada2a-3* and *prz1-1* mutants, representing two major interactors of HAG1 (ADA2 and ADA2B) (Anzola et al., 2010; Hark et al., 2009) and did not identify any difference.

We also wanted to uncouple the developmental phenotypes of *hag1-6* from the immunity phenotypes. To this end, we used the mutants *hag1-5* and heterozygous *hag1-6* plants. Mutants heterozygous for *hag1-6* mutation do not display any developmental phenotypes, and although the susceptibility is not significantly increased, it has been consistently higher than wild type in all of our experiments. Interestingly, *hag1-5* mutant does not have any developmental phenotypes, but is more susceptible to *Pst* DC3000, suggesting that the bromodomain of HAG1 is important for its

role in immunity. We also confirmed that both *hag1-5* and *hag1-6* mutants are affected in the deposition of acetylation onto histones by determining the global H3 acetylation levels in resting conditions (*Fig. 3.9*). Interestingly, the levels of H3 acetylation appear to correlate well with the level of disease resistance to *Pst* DC3000, whereby lower acetylation levels coincided with lower resistance.

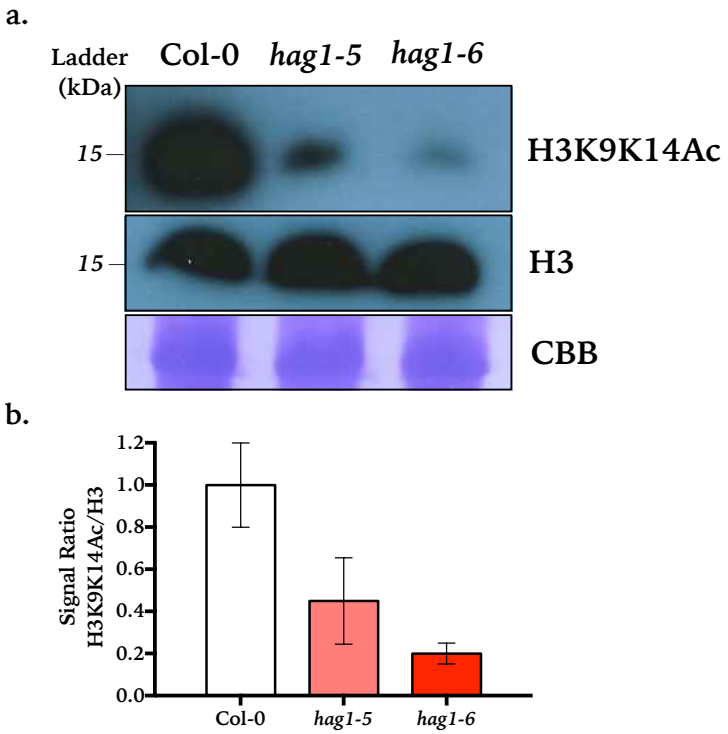

Figure 3.9: Histone H3 acetylation levels are reduced in *hag1-5* and *hag1-6* mutants. a. Western blots showing the levels of dual acetylation in H3 Lys9 and Lys14. Crude extracts from adult plant leaf tissue were loaded on 15% SDS gels, transferred onto PVDF membranes and blotted with αH3K9K14Ac antibody or αH3 (no modification); b. The relative acetylation levels were calculated as the ratio of the H3K9K14 signal to H3. A representative blot is shown with the error bars representing the standard deviation arising from two independent experiments. Using ImageJ, the intensity of each band was calculated resulting in the graphs of the ratios of acetylated to non-acetylated histone. CBB, Coomassie Brilliant Blue.

3.3.4. The *hag1-6* mutant fails to acetylate histone H3 after flg22 perception

The disease susceptibility tests identified HAG1 as a positive regulator of plant immunity, however, it remained to be seen whether HAG1 contributes to the flg22-induced histone acetylation. To test this, we repeated the flg22-induced histone acetylation experiments including the

mutant *hag1-6*. Following flg22 elicitation, the levels of H3K9 acetylation in the *hag1-6* mutant appear to be reduced in comparison to the wild-type Col-0 plants (*Fig. 3.10*). There was also no induction in the *hag1-6* mutants. In order to test whether *hag1-6* mutants are impaired in general recognition of flg22, we tested the production of reactive oxygen species (ROS) (*Fig. 3.11*) and MAPK activation (*Fig. 3.12*) after flg22 treatment.

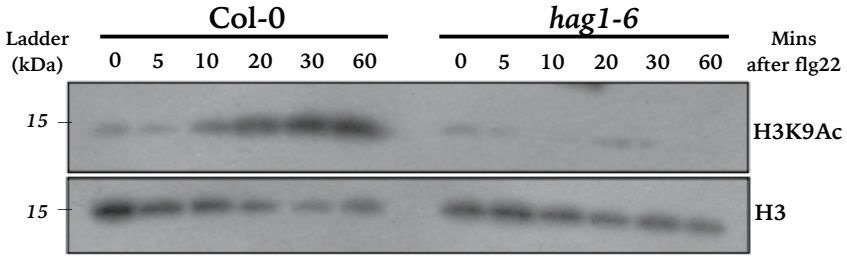

Figure 3.10: Impaired flg22-induced histone acetylation in *hag1-6* mutant. Arabidopsis Col-0 and *hag1-6* seedlings were elicited with 100nM flg22 and samples were taken at the indicated time points. Total proteins were extracted, run on 15% SDS gels and transferred onto PVDF membranes. Blots were made using antibodies for single acetylation (αH3K9Ac and no modification αH3) to ensure equal loading. Ladder is denoted by kDa.

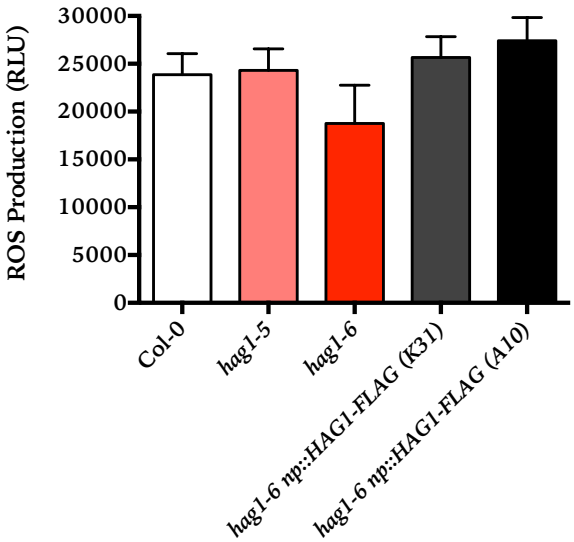

Figure 3.11: Reactive oxygen species (ROS) production in *hag1* mutants is not significantly impaired. Leaf discs from adult plants were collected and placed in water overnight. Peroxidase-luminol solution replaced the water the next day and 100nM flg22 was used to elicit PAMP-triggered immunity. Cumulative photon count was measured for 30 minutes after elicitation and expressed as relative light units (RLUs). Unpaired parametric t-tests assuming populations with same standard deviation were performed in pairs. Two complemented lines of *hag1-6* are shown, K31 and A10.

The total ROS production was not significantly affected (*Fig. 3.11*), while MAPKs showed similar levels of activation to Col-0 as seen by the similar band intensity between Col-0 and *hag1-6* plants elicited with flg22 (*Fig. 3.12, top panel*). Taken together, these results support the idea that PTI outputs upstream chromatin remodelling are not impaired in the *hag1-6* mutant. In addition, the timing of events, activation of MAPKs at 15 mins and acetylation of H3 after 15 mins in Col-0 further supports a model in which histone acetylation is a PTI output found downstream of MAPK activation (*Fig. 3.12*).

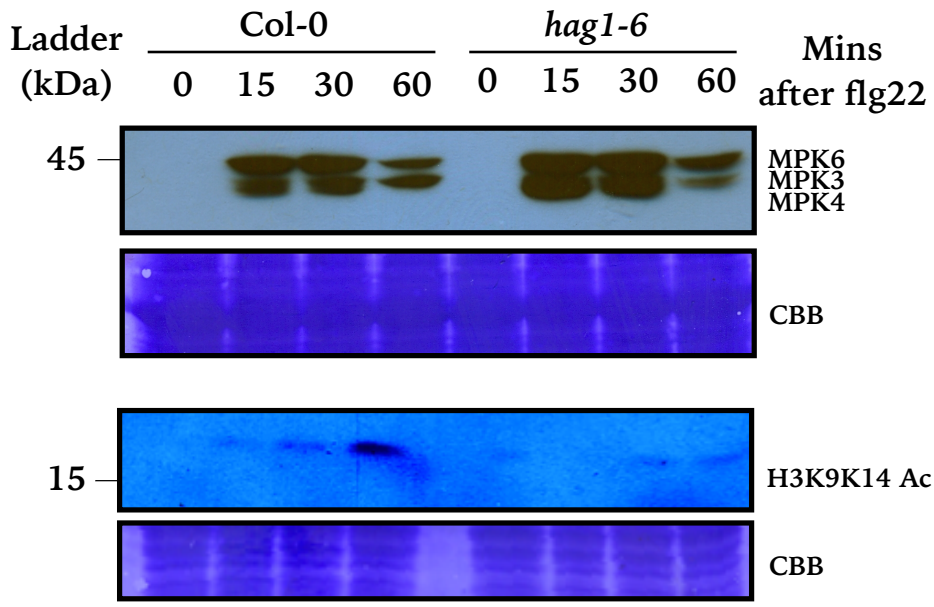

Figure 3.12: MAPK activation is not affected in *hag1-6* mutant. Col-0 and hag1-6 seedlings were treated with 100nM flg22, total proteins were loaded on a 12% SDS-PAGE gel, transferred onto a PVDF membrane and blotted with α-p44-ERK/p42 and αH3K9K14Ac, after cutting the membrane at corresponding protein sizes. CBB, Coomassie Brilliant Blue. Ladder is denoted by kDa.

3.3.1. *hag1-6* mutant phenotype is not due to SA responses

Mutants with impaired resistance to hemi-biotrophic pathogens often display impaired induction of SA-responses. To test whether the susceptibility phenotype of the *hag1-6* mutant could be explained by im-

paired SA responses, we generated crosses between *hag1-6* and SA-deficient mutants. *sid2-1* mutants and NahG-expressing plants were chosen because the first constitutes a biosynthetic SA mutant, whereas the second is able to produce SA, but SA is constantly degraded by the bacterial protein NahG. The *hda19* mutant was chosen considering the previously published role of HDA19 as a negative regulator of SA responses (Choi et al., 2012). The introduction of NahG partially rescues the *hag1-6* phenotype, which suggests that *hag1-6* size is only partially attributed to impairment in SA, although actual SA levels were not tested. Meanwhile, there is no difference after the introduction of *sid2-1* and *hda19* in the *hag1-6* background (*Fig. 3.13*). *hda19* is more resistant to *Pst* DC3000 as previously described and the double *hda19 hag1-6* mutant displays the same level of resistance (*Fig. 3.12*). This suggests that HAG1 does not act on the same set of SA-related genes as HDA19 as this scenario would require the reversal of the *hda19* phenotype to Col-0 levels upon introduction of *hag1-6*. Similarly, introduction of *hag1-6* mutation in NahG and *sid2-1* plants leads to increased susceptibility to *Pst* DC3000 *(Fig. 3.14)*. This implies that the increased susceptibility in the double mutants is due to additional roles of HAG1 in immunity that do not overlap with the SA-related processes affected by *sid2-1* and NahG mutations.

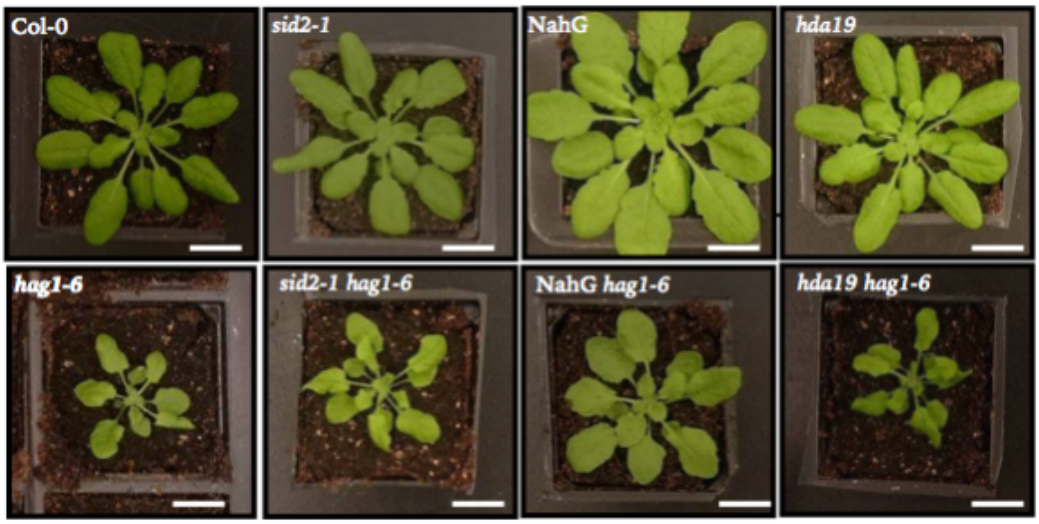

Figure 3.13: Morphological phenotypes of *hag1-6* mutants crossed to *sid2-1*, NahG and *hda19* plants. 4-weeks old plants grown in soil. Scale bar represents 1cm.

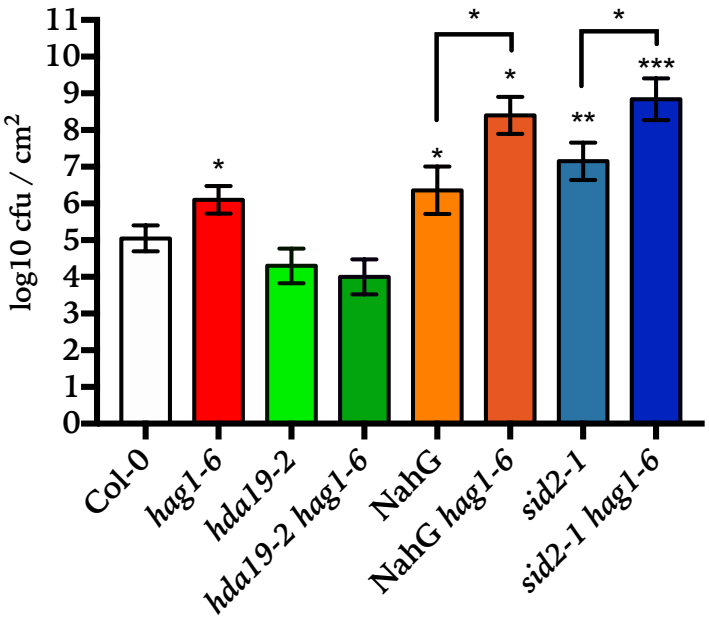

Figure 3.14: HAG1 is not involved in SA responses. 5-weeks old plants were screened for susceptibility to *Pst* DC3000 after spray infection. Asterisks denote statistical significant differences (* for $p<0.05$, ** for $p<0.005$, *** for $p<0.005$) of columns compared to Col-0 based on unpaired parametric t-tests. The error bars represent the standard error of the mean (SEM).

3.4. Discussion

It is known that for transcriptional activation to occur, local relaxation of chromatin at the corresponding promoters has to happen to allow easier access of transcription factors and other chromatin-binding proteins to DNA. This is often characterised by the presence of activating histone marks such as H3K4me3, H3K9ac, H3K14ac as well as reduced nucleosome occupancy (Clark and Felsenfeld, 1991; Eberharter and Becker, 2002). The aim of this chapter was to establish whether such mechanisms of chromatin remodelling take place during pathogen perception. We used the FRAP assays in both *A. thaliana* and *N. benthamiana* to identify dynamic changes in the chromatin conformation and identified an opening of the chromatin in cells treated with flg22. It should also be noted that the significance level of the recovery rates with or without flg22 was different in

each plant species due to different cell types being tested, which are known to have different chromatin status to begin with (Rosa et al., 2014). Nevertheless, the flg22-induced chromatin remodelling is apparent in both systems. It would be interesting to solidify this phenotype in Arabidopsis leaves, which is a more physiologically relevant tissue as *Pst* DC3000 is a foliar pathogen. However, the presence of FLS2 receptor as well as PTI responses in the roots is well-documented and immune responses in roots are important as well considering the vast array of plant-microbe interactions that take place in the rhizosphere (Millet et al., 2010; Robatzek et al., 2006). One could argue that the recovery of fluorescence is at least partially due to *de novo* synthesis of histones. However, it has already been described that this is not the case as there is no significant fluorescence recovery within the time frame of 1 hour, following bleaching of the entire nucleus (Rosa et al., 2014). Further evidence supporting that recovery is not due to *de novo* histone synthesis can be found in *Supplementary Figure S3.1,* showing that upon bleaching of the whole nucleus, there is minimal recovery. In addition, Rosa *et al* (2014) demonstrated already that the *hag1-6* mutant displays slower chromatin dynamics in resting state. We used a biochemical approach to further show that *hag1-6* was unable to acetylate the histones before and after elicitation with flg22, thus linking the chromatin dynamics with the process of histone acetylation. We could test the ability of *hag1-6* mutants (expressing H2B-GFP) to induce rapid chromatin remodelling following flg22 perception. Using DNase I, one could examinee the state of the chromatin before and after elicitation with flg22, as this enzyme will be able to find more places to digest the DNA in case of a more euchromatic chromatin.

Another interesting experiment would be to pretreat wild type plants with chemical inhibitors of histone acetyltransferases to test directly the involvement of these enzymes in chromatin remodelling and to quantitatively dissect the contribution of HATs in the total chromatin re-

modelling from other remodelling enzymes such as ATP-dependent chromatin remodellers. Generic HAT inhibitors, however, would fail to identify the contribution of HAG1 alone due to potential lack of specificity. To specifically inhibit the action of HAG1 alone, we could consider testing highly specific chemical inhibitors that have been developed for GCN5 such as g-butyrolactone (Biel et al., 2004). Importantly, the *hag1-6* mutant susceptibility to *Pst* DC3000 is not due to impaired perception of flg22 since the ROS production and the MAPK activation resembles that of the wild-type Col-0 plants. Even though we have not tested the levels of FLS2 receptor and other major receptors or signalling components, microarray experiments in the Ntoukakis group have shown no difference in *FLS2* expression levels in *hag1-6* mutant before or 1 hour after flg22 treatment, further validating that *hag1-6* mutants are not impaired in important components of immunity (*unpublished data from the Ntoukakis lab*).

Although not tested so far, follow-up experiments in the Ntoukakis Lab *(data not shown)* have shown that the complemented lines of *hag1-6 (Fig. 3.7b)* are as susceptible to *Pst* DC3000 as Col-0 plants.

The global increase in H3K9 and H3K14 acetylation was shown to occur after flg22 perception (*Figs. 3.3, 3.9, 3.10*) and could be considered as a previously unidentified PTI output. H3K9 and H3K14 are the major acetylation targets of HAG1 as previously described (Earley et al., 2007; Servet et al., 2010a), which further supports the active role of HAG1 in PTI. However, additional H3 lysines residues are targets of HAG1 in Arabidopsis and other plant species, such as H3K27 (Benhamed et al., 2006) and H3K36 (Mahrez et al., 2016) and could thus be tested in the future. One hypothesis is that each HAG1-dependent H3 lysine acetylation is involved in different biological processes. By testing for additional lysine residues acetylated after flg22 we could, first, shed light into any additional HATs being involved in immunity as we already have an indication of the *in vitro* and *in vivo* specificities of some Arabidopsis HATs from other

studies (*Table 1.1*). Second, it would help us determine whether repressive marks are removed upon flg22 treatment if we used appropriate antibodies for those histone marks. Although a global increase in acetylation is observed, the dynamics of histone acetylation after flg22-perception are anticipated to be more complicated. For example, Latrasse *et al* (2017) analysed the H3K9ac landscape before and after flg22 treatment using ChIP-seq. Their analysis revealed a class of 731 genes that exhibited hyper-acetylation after flg22 and included mostly defence genes; a class of 13,159 genes with no obvious changes in the acetylation pattern; and a third class of 787 hypoacetylated genes involved in metabolic processes, chloroplast and plastid organization. These findings are in line with our results and would support a model in which flg22 leads to *de novo* acetylation of a group of genes, whilst a separate group of genes is deacetylated, and these two groups are respectively regulated by HATs and HDACs, which are likely to be HAG1 and HD2B.

Furthermore, it would be highly informative to measure the levels of histone acetylation throughout the course of a real infection with *Pst* DC3000. This could allow us to determine whether this pathogen can affect the histone acetylation status of the host at the later stages of infection. Based on the results from this chapter, histone acetylation is part of the immune signalling cascade, which makes it a potential target for pathogens. Therefore, we can hypothesise that pathogens such as *Pst* DC3000 have evolved mechanisms to interfere with the process of histone acetylation or deacetylation. In fact, a recent study showed that PsAvh23 effector from the oomycete *Phytophthora infestans* is able to interfere with the assembly of ADA2 and GCN5 in soybean, ultimately resulting in decreased H3K9 acetylation of defence-related loci and increased susceptibility (Kong et al., 2017). In the same line of thinking, we could measure the acetylation levels in Col-0 plants a few hours after infection with *Pst* DC3000. If there is an effect, we could test whether this is effec-

tor-dependent by using a *Pst* DC3000 *hrcC* strain, which is unable to deliver effectors into the host and further pinpoint the effector(s) involved by using *Pst* DC3000 strains with single-effector deletions.

It is also known that gene knock-out mutations result in visible phenotypes about 10-20% of the time, which is due to redundancies, alternative network routes and the robustness of interaction networks (Hopkins, 2008). Redundancy between different HATs is, therefore, a major consideration for big enzyme families, which is evident as a lack of phenotype in single HAT mutants (*Fig. 3.4 and Fig. 3.5*). For example, the MYST family histone acetyltransferases HAM1 and HAM2 were found to be redundant in the formation of male and female gametophytes as single mutants in each gene were not affected, while double HAM1/HAM2 mutants displayed arrested cell division during gametogenesis (Latrasse et al., 2008). We could hypothesise that additional HATs are responsible for the acetylation of H3K9 and H3K14 after flg22. However, the western blots (*Fig. 3.10 and Fig. 3.12*) showing absence of this phenotype in *hag1-6* mutant together with the susceptibility phenotypes in the HAT screen (*Fig. 3.5*) strongly suggest that HAG1 is the major enzyme responsible for these marks, it is required for immunity and its absence cannot be compensated by the activity of other HATs. This strengthens the importance of HAG1 as a positive regulator of immunity.

It would be interesting to further investigate upstream processes leading to the HAG1-dependent acetylation of histones after flg22 perception. In animal studies, PAMP-induced phospho-acetylation of H3 was found to be MAPK dependent using chemical inhibitors of known MAPKs (Cao et al., 2008). In plants, flg22 perception leads to MAPK and CDPK-dependent gene activation (Boudsocq et al., 2010) We could test whether flg22 leads to acetylation of histones in the same way in MAPK and CDPK mutants. Flg22-induced phosphorylation of histone H3 was found to be CDPK-dependent, as it was abolished by EGTA, a Ca^{2+} chelator (Boud-

socq et al., 2010). One hypothesis is that the HATs involved in the acetylation of histones during PTI are activated by upstream kinases. To this day, there is no clear evidence that HATs are activated in such a way; a yeast-2-hybrid screen showed that HAG1 interacts with phosphatase PP2C-6-6, making it a potential target for de-phosphorylation leading to its inactivation. In fact, T-DNA mutations in this phosphatase gene lead to higher global acetylation levels (Servet et al., 2008). Additionally, several CDPKs have been found to localise to the nucleus in the presence of AvrRpt2 or AvrRpm1, and subsequent phosphorylation of WRKY transcription factors has been reported (Gao et al., 2013). Finally, it is known that multiple MAPKs (MPK3, 4, 6 amongst others) are activated by being phosphorylated immediately after flg22 perception (Asai et al., 2002; Ligterink et al., 1997). Perhaps similar mechanisms exist for the direct activation of HATs or indirectly through phosphorylation of HAT interactors.

Another aspect that may be interesting to molecular plant pathologists is the dissection of the pathways downstream different PAMP receptors. We could repeat the same experiment with different PAMPs including bacteria-derived elf18 or peptidoglycan, fungi-derived chitin and host-derived molecules such as pep1 (Zipfel, 2008). Similar increases in the histone phospho-acetylation levels was observed in Weinmann *et al* (2001) after treatment with different elicitors suggesting that perception of PAMPs converges to conserved downstream pathways including the rapid modification of histones.

The significance of this chapter's results can be placed in the context of recent results supporting the notion that the temporal induction of PTI responses can determine the outcome of the infection. In *Atelp3-10* mutants lacking a functional histone acetyltransferase ELP3 (Elongator or HAG3) the induction of major SA-responsive genes was delayed compared to wild type and this led to increased bacterial colonisation (Defraia et al., 2013).

Using FRAP we could endeavour to investigate how the chromatin binding kinetics of HAG1-GFP change after flg22 perception. In other words, HAG1-GFP would be expected to be more closely associated with chromatin following flg22 perception in order to contribute towards increased histone acetylation. To this end, a more informative experiment would involve ChIP-seq experiments on HAG1-FLAG following treatment with flg22. Microarray experiments in our lab have also been performed to elucidate the defence genes targeted for acetylation by HAG1 before and after flg22 perception by using Col-0 and *hag1-6* mutants. Highly informative in this would be the use of the *hag1-6* heterozygous mutants as it would allow us to more quantitatively dissect the roles of HAG1 in immunity. Coupling ChIP to a transcriptomic analysis could provide further granularity into which genes specifically are acetylated by HAG1, as we have so far only observed a global increase in histone acetylation with no further information as to whether this involves defence genes. Latrasse *et al* (2017), however, recently improved our understanding of which genes are acetylated and which genes are deacetylated after flg22 perception. The bacterial growth phenotypes of *hag1-6* crossed with SA mutants cannot fully answer whether HAG1 targets SA genes, such as *PR1* and *PR2* for acetylation. The susceptibility phenotypes of the *hag1* double mutants suggested that HAG1 is not a negative regulator of SA-responses, contrary to HDA19 (Choi et al., 2012). To further shed light on a possible role of HAG1 in SA responses, qPCR experiments before and after infection should be conducted in the single and double mutants or alternatively on key SA-responsive genes. In the scenario where HAG1 positively regulates SA responses, *hag1-6* plants would be expected to have lower expression of *PR1* and *PR2* than Col-0 and introducing *hag1-6* in *hda19* background would restore the levels of *PR1* and *PR2* to wild type. Measuring SA-levels, however, is a better indicator of changes in SA metabolism and would be a more appropriate experiment than using SA

marker genes. Alternatively, ChIP-PCR experiments could be conducted using the complemented lines (expressing a C-ter FLAG tag; *Fig. 3.7b*) to identify whether HAG1 is associated with the promoters of SA-responsive genes. ChIP-PCR experiments would be crucial not only in identifying which genes are acetylated in after flg22 elicitation by HAG1, but also where along the gene histone acetylation is taking place (i.e. promoter, or gene body).

Chapter 6, Figure 6.1 presents a model of our understanding arising from experiments of the current chapter and highlights that HAG1 may be activated by yet unknown upstream enzymes (potentially MAPKs or CDPKs) and is responsible for flg22-induced histone acetylation.

Therefore, with the current data and current knowledge gaps we questioned how HAG1 is able to positively regulate immune responses, which encouraged us to proceed with a biochemical approach to characterise a putative HAG1 complex during immunity.

Chapter 4 - HAG1 complex in plant immunity

4.1. Context of this Chapter

Histone acetyltransferase enzymes have been thoroughly studied in different model organisms including humans, fruitfly and yeast. The chromatin remodelling mechanisms in these systems are highly conserved and many of the proteins involved show a high degree of conservation in terms of protein sequence, mechanism of action, target substrates and even interacting partners (Koutelou et al., 2010). Since its discovery in yeast through genetic studies, as a general co-activator of transcription, the histone acetyltransferase GCN5 (the homolog of *A. thaliana* HAG1) has been at the centre of studies in chromatin remodelling and more specifically, histone acetylation. In most of these organisms, GCN5 associates with two adaptor proteins known as ADA2 and ADA3 forming the acetylation module of a large (approximately 2MDa) multi-protein complex known as SAGA (Grant et al., 1997). The lysine specificity of yeast GCN5 HAT activity was found to expand upon association in native complexes with the adaptor proteins ADA2 and ADA3, which highlights the importance of adaptor proteins in supporting the roles of a central enzymatic subunit of a larger multi-protein complex (Grant et al., 1999). The studies that elucidated the composition of GCN5 complexes involved purification of the complex from yeast giving rise to our in-depth understanding of the proteins that constitute the SAGA complex as well as the roles of each module within SAGA (*refer to Fig. 1.3*). One of the most interesting findings is that SAGA can be actively recruited onto promoters to activate transcription upon specific environmental stimuli such as hormonal treatment. For example, upon binding to glucocorticoids in the cytosol, glucocorticoid receptor (GR) translocates to the nucleus and mediates transcriptional reprogramming through SAGA (Pruett et al., 2003). Wallberg *et al* (2000) showed that yeast strains with mutations in ADA

proteins are also defective in hormone-dependent gene activation and that GR recruits the SAGA complex leading to chromatin remodelling through histone acetylation. This highlights that coactivator complexes like SAGA can be rapidly recruited by DNA-binding factors upon specific stimuli that normally lead to extensive transcriptional changes. Another interesting finding came from the discovery of a multi-protein complex similar in size and substrate specificity but chromatographically different from SAGA, known as SLIK (SAGA-like). These two complexes differ in that only SAGA contains the Spt8 subunit, whilst only SLIK contains the Rtg2 subunit (Pray-Grant et al., 2002). The presence of two slightly different SAGA complexes was found to allow better response to metabolic stresses in yeast grown in different conditions. This study implicated GCN5-containing complexes in regulating stress-response genes and suggested that slight modifications (i.e. through mutation of *Rtg2*) in the composition of such complexes led to significant changes in the functions of the complex, highlighting that multi-protein complexes can be highly dynamic in their composition and function.

Our understanding of HAG1 complexes in plants is not as advanced as in other systems. Interactors of HAG1 have been identified genetically or through yeast two-hybrid screens, but the complex composition in plants remains elusive.

HAG1 and ADA2a in both Arabidopsis and maize have been found to interact with each other *in vitro* and *in vivo,* while this also involved interaction with the transcription factor Opaque-2 (Bhat et al., 2004; Bhat et al., 2003). Furthermore, recent research provided evidence for the recruitment of the wheat *(Triticum aestivum)* TaGCN5 onto target glutenin genes by the transcription factor TaGAMyb. By performing chromatin immunoprecipitation coupled to PCR (ChIP-PCR) TaGCN5 was found to physically interact with the transcription factor TaGAMyb, facilitating its association with glutenin gene promoters during wheat endosperm devel-

opment leading to higher H3K9 and H3K14. This interaction was further confirmed in Arabidopsis by ectopically expressing TaGCN5 (Guo et al., 2015). This study showed the recruitment of GCN5, subsequent enrichment of the acetylation marks and quantitative transcript increase of target genes. However, this study did not attempt to place TaGCN5 in the context of a putative SAGA complex (i.e. by identifying other putative interactors of HAG1). Through other studies and a variety of experimental approaches, a number of proteins have been found to interact with HAG1, many of which are chromatin-related proteins and DNA-binding transcription factors (Servet et al., 2008). For example, interaction between HAG1 and the transcription factor EML was reported (Gao et al., 2007). Therefore, several examples exist showing the recruitment of HAG1 onto specific target genes can be mediated by interaction with sequence-specific DNA-binding transcription factors or via adaptor proteins.

An important example of transcription factor-mediated recruitment of HATs/HDACs comes from studies in auxin-responses. In the absence of auxin, expression of auxin-responsive genes is repressed by the AUX/IAA proteins, which are able to recruit the transcriptional repressor TOPLESS (TPL) and through this protein further recruitment of histone deacetylase HDA19 takes place. Upon higher auxin concentration ubiquitin-mediated degradation of AUX/IAA repressors takes place enabling expression of genes targeted by auxin-response factors such as ARF-TF (Liu and Karmarkar, 2008; Szemenyei et al., 2008). Weiste *et al* (2014) proposed an antagonistic mechanism of the same pathway whereby transcription factors interact with ADA2b likely resulting in the recruitment of a HAG1-complex onto auxin-responsive genes. The recruitment of HAG1 was not shown experimentally, but this model is particularly interesting as it provides a mechanistic description of the antagonistic roles of plant HATs and HDACs on the same set of genes in response to external

cues and involves TOPLESS, HDA19 and HAG1, whereby studies have previously shown the interaction of these genes (Long et al., 2006).

4.2. Main findings

This chapter aims to identify the molecular mechanism by which HAG1 positively contributes to disease resistance to *Pst* DC3000. We used a biochemical approach to characterize HAG1 complex in Arabidopsis. The proteomic analysis confirmed several known components of SAGA complex such as ADA2a and ADA2b and revealed ADA3 and CHR5 as interactors of HAG1 for the first time in plants. The interaction with members of the TOPLESS family point towards a model in which the co-repressors negatively regulate HAG1 until pathogen perception takes place, at which point the interaction is lost allowing HAG1 to acetylate target genes. Additional interactors with roles in chromatin or DNA binding properties further suggest that HAG1 has a large variety of interactors, which reflects that HAG1 is a versatile HAT with roles in different processes.

4.3. Results

4.3.2. HAG1 is a nuclear protein with histone H3 binding capacity

For the molecular characterisation of HAG1 protein, *HAG1* gene was cloned from *A. thaliana* Col-0 plants. Both the cDNA of *HAG1* and the genomic sequence of *HAG1* including a native promoter (700bp upstream) were cloned with a N-ter 1xFLAG (35S promoter, CaMV) and a C-ter 1xFLAG with the native promoter, respectively. *FLAG-HAG1* (cDNA) was transiently expressed in *N. benthamiana* plants after agro-infiltration and the resulting protein was shown to co-immunoprecipitate with histone H3 (*Fig. 4.1*), while expression of GFP-tagged HAG1 (35S

promoter, CaMV) in protoplasts showed a clear nuclear localisation (*Fig 4.2*). These results suggested that the cloning product of HAG1 is a nuclear HAT with histone binding capacity instilling confidence in continuing with the molecular characterisation of the interactors of HAG1.

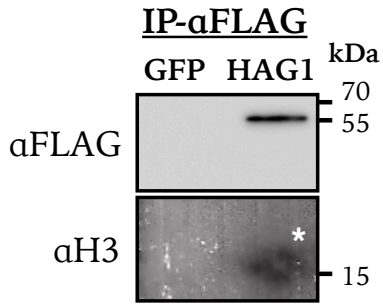

Figure 4.1. Transiently-expressed HAG1 interacts with histone H3. FLAG-tagged HAG1 (cDNA) and FLAG-tagged GFP were agro-infiltrated in *N. benthamiana* leaves and tissue was harvested 2 dpi. FLAG co-immunoprecipitation was performed on enriched nuclear extracts followed by immunoblotting using αFLAG and αH3 antibodies. The asterisk denotes the band corresponding to H3. Ladder is denoted by kDA.

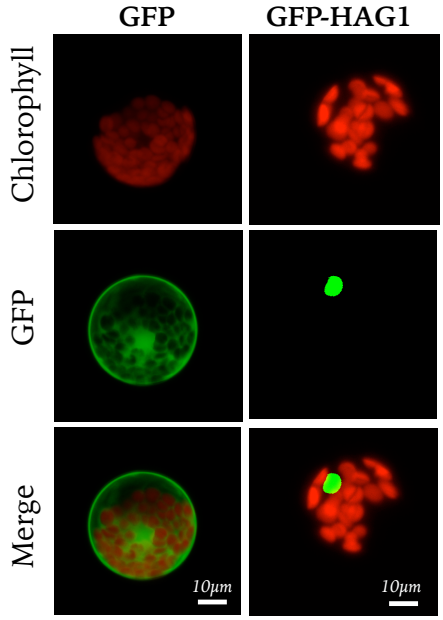

Figure 4.2. Protoplast-expressed HAG1 localises to the nucleus. Leaf protoplasts generated from 4-week old Arabidopsis Col-0 plants were transfected with free GFP or GFP-HAG1 and imaged the next day. Autofluorescence channel to detect chlorophyll (430nm - 662nm) and GFP channel (520nm - 560nm) to detect GFP fluorescence were used.

4.3.2. HAG1 is successfully purified and interacts with nuclear proteins

To proceed with the biochemical characterisation of HAG1 complex in Arabidopsis plants, *hag1-6* mutants complemented with the full-length genomic *HAG1* gene (native promoter and C-ter FLAG-tag) were grown to adult stage. Approximately 30g of leaf tissue was cross-linked with formaldehyde to stabilise protein:protein and DNA:protein interactions as performed in previous biochemical purifications of large protein complexes (Grant et al., 1998). Nuclear enrichment and FLAG-immunoprecipitation were performed before running the resulting purification on SDS-gel. After observing a clear band at the expected size both on the immunoblot and Coomassie stained gel, the samples were prepared for mass spectrometry (MS) analysis after following an in-gel trypsin digestion protocol to digest proteins into smaller peptides (*Fig 4.3*).

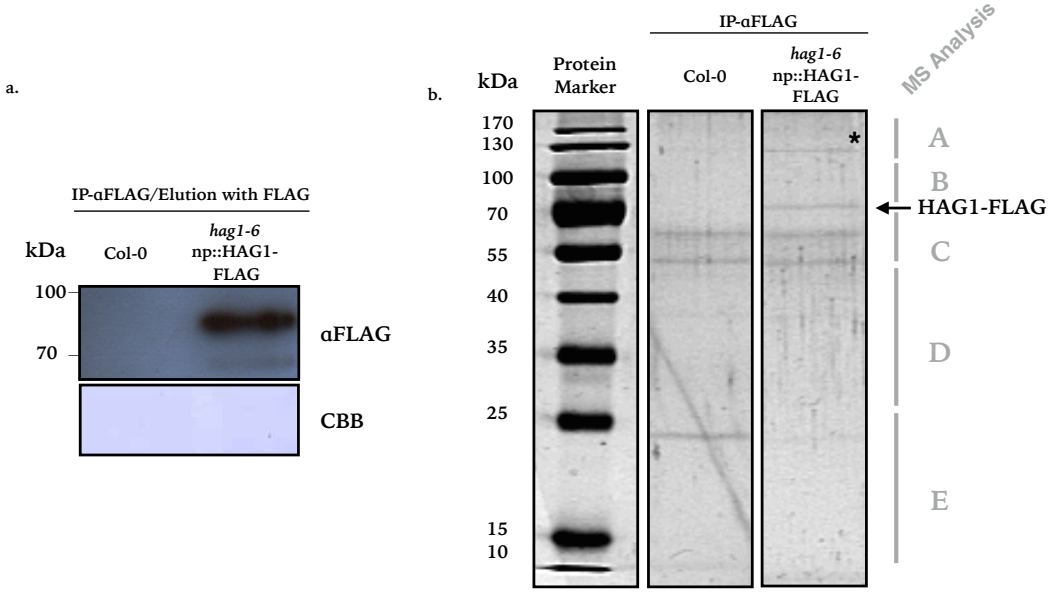

Figure 4.3: Stably-expressed HAG1 is successfully purified. HAG1-FLAG expressed in transgenic Arabidopsis, after immunoprecipitation with αFLAG beads and elution with FLAG peptide. (a) 10% of the eluate was loaded on a 12% SDS-PAGE, transferred onto a PVDF membrane and immunoblotted with αFLAG antibody. No proteins are visible after staining with Coomassie Brilliant Blue (CBB), because most proteins are eluted; (b) 90% of the eluate was loaded on a different 12% SDS-PAGE and the gel was stained with colloidal CBB. Bands identified only in the HAG1-FLAG sample are noted with an asterisk, while the band corresponding to HAG1-FLAG protein is shown with an arrow. The gel fragments labelled A-E were cut and prepared for trypsin digestion and mass spectrometry. Ladder is denoted by kDa.

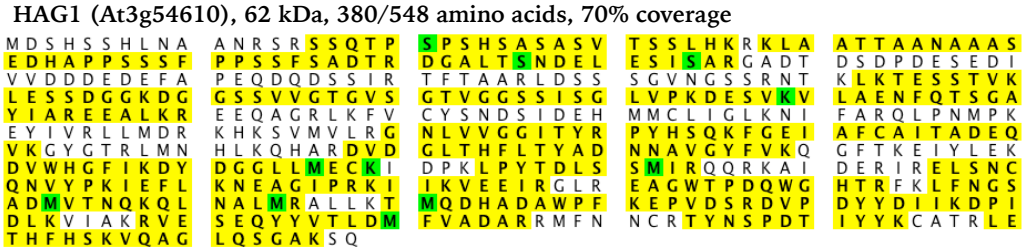

Figure 4.4: Stably-expressed HAG1 is purified and detected successfully by mass spectrometry using in-gel digestion protocol. HAG1 sequence coverage is highlighted in yellow for peptides that were identified at least once. 36 exclusive unique peptides, 60 exclusive unique spectra, 93 total spectra and 380/568 amino acids (70% coverage). Post-translational modifications were identified such as Lysine (K) methylation, Serine (S) phosphorylation and Lysine (K) acetylation highlighted in green. Methionine (M) is frequently identified in an oxidised form, which arises during the sample processing.

Peptide	Times identified	Modification
(R)SSQTP**S**PSHSASASVTSSLHK(R)	3	$[_{p}S^{21}]$
(R)KLAATTAANAAASEDHAPPSSSFPPSSFS	5	
(K)LAATTAANAAASEDHAPPSSSFPPSSFSA	2	
(R)DGALT**S**NDELESI**S**AR(G)	4	$[_{p}S^{76}]$,$[_{p}S^{84}]$
(K)LKTESSTVK(L)	2	
(K)LESSDGGKDGGSSVVGTGVSGTVGGSSIS	4	
(K)DGGSSVVGTGVSGTVGGSSISGLVPK(D)	3	
(K)DESV**K**VLAENFQTSGAYIAR(E)	3	$[_{ac}K^{188}]$
(K)VLAENFQTSGAYIAREEALK(R)	3	
(R)GNLVVGGITYRPYHSQK(F)	9	
(K)FGEIAFCAITADEQVK(G)	3	
(R)DVDGLTHFLTYADNNAVGYFVK(Q)	2	
(K)DVWHGFIK(D)	1	
(K)DYDGGLLMEC**K**(I)	6	$[_{me}K^{368}]$
(R)ELSNCQNVYPK(I)	4	
(K)NEAGIPR(K)	1	
(R)KIIKVEEIR(G)	9	
(R)EAGWTPDQWGHTR(F)	4	
(K)LFNGSADMVTNQK(Q)	2	
(K)QLNALMR(A)	1	
(K)TMQDHADAWPFKEPVDSR(D)	10	
(R)DVPDYYDIIK(D)	4	
(K)RVESEQYYVTLDMFVADAR(R)	5	
(R)TYNSPDTIYYK(C)	1	
(R)LETHFHSK(V)	1	
(K) VQAGLQSGAK(S)	1	

**** Phosphorylation detected as addition of 80 Da, Oxidation as +60 Da, Acetylation as +80 Da***

***** Modified sites are shown in bold and underlined***

Table 4.1: Identified peptides and post-translational modifications on stably-expressed HAG1 using in-gel digestion protocol. Peptides identified in HAG1 sequence. Modified residues are shown in bold and underlined within the peptide sequence. Methionine (M) oxidation, which occurs upon sample processing for mass spectrometry is not shown in this table (Perdivara et al., 2010).

The analysis showed a 70% sequence coverage for our bait, HAG1. *Table 4.1* shows the results of a representative IP-MS experiment, including the number of times each peptide was identified and their post-translational modifications occurring on HAG1 protein. Interestingly, multiple post-translational modifications were identified along the protein sequence including methylation and acetylation on lysine residues as well as phosphorylation on serine residues (*Fig. 4.4 and Table 4.1*). Methionine oxidation is commonly found in samples processed for MS and does not indicate a functionally relevant modification (Perdivara et al., 2010). The presence of these modifications suggests an additional level of HAG1 regulation through post-translational modification of the protein in line with previous findings (Servet et al., 2008).

The list of interactors identified using the in-gel digestion method (*Fig. 4.3b*) contained 6 proteins exclusively identified in the HAG1-FLAG sample. Among these was the previously published interactor ADA2. Newly identified interactors included TOPLESS (TPL), Chromatin Remodeller 11 (CHR11), Tudor 1, Transportin1 and DDB1A protein (*Table 4.2-Experiment 4*). Considering the low number of interactors as well as the relatively faint band of HAG1-FLAG on the gel, we attempted to follow an on-beads trypsin digestion protocol (*Fig. 4.5*) in order to overcome common limitations of in-gel proteomic analysis such as cost, time, contamination and protein abundance (Turriziani et al., 2014).

4.3.3. Identification of HAG1-interactors during PTI and ETI

Performing the on-beads digestion protocol resulted in a greater abundance of HAG1 interactors as anticipated, which can be seen in *Table 4.2*. The simplicity of this methodology allowed us not only to verify the interactors identified by the in-gel digestion protocol and to identify more interactors of HAG1, but to also describe interactions, which are specific to PTI or ETI-responses. To be more specific, previous experiments had

suggested the involvement of HAG1 in PAMP-triggered immunity contributing to increased acetylation of H3K9 and H3K14 within minutes of flg22 perception (*Chapter 3*). Therefore, our hypothesis was that a HAG1-complex is responsible for this response and that this complex is different in composition from the HAG1-complex that is recruited at the promoters of genes in resting conditions. This would allow a shift of histone acetylation from a set of genes active in resting conditions to a set of genes that are upregulated during PTI. Similarly, it can be hypothesised that at later stages of infection, plant responses are supported by the expression of a different set of genes, likely to be acetylated by a distinct HAG1-complex. To this end, we aimed to identify the presence of different HAG1-interacting partners, which would be specific to flg22 elicitation (PTI-specific; 1 hour post-treatment) or *Pst* DC3000 *AvrRpt2* (ETI-specific; 4 hours post-infection) infection. The timing of 1 hour for flg22 treatment was based on previous results showing that acetylation is still high at the 1 hour mark (*Fig. 3.3*), but also based on microarray experiments showing that approximately 10% of the genome is differentially expressed 1h after flg22 treatment (Zipfel et al., 2004)

The different stages of our experimental procedure are outlined in *Figure 4.5*. Briefly, plants were sprayed with $MgCl_2$ as a control treatment or sprayed with 1µM flg22 solution or spray-infected with *Pst* DC3000 *AvrRpt2 (Step 1)*. The choice of AvrRpt2 was based on its ability to induce ETI. Then, formaldehyde treatment was applied in order to crosslink proteins between them as well as with DNA *(Step 2)*. A nuclear enrichment protocol was found to be necessary in order to minimise "contamination" by non-nuclear proteins *(Step 3)*. Immunoprecipitation using an appropriate resin *(Step 4)* was followed by on-beads trypsin digestion *(Step 5)* and the samples were processed for MS analysis *(Step 6)*.

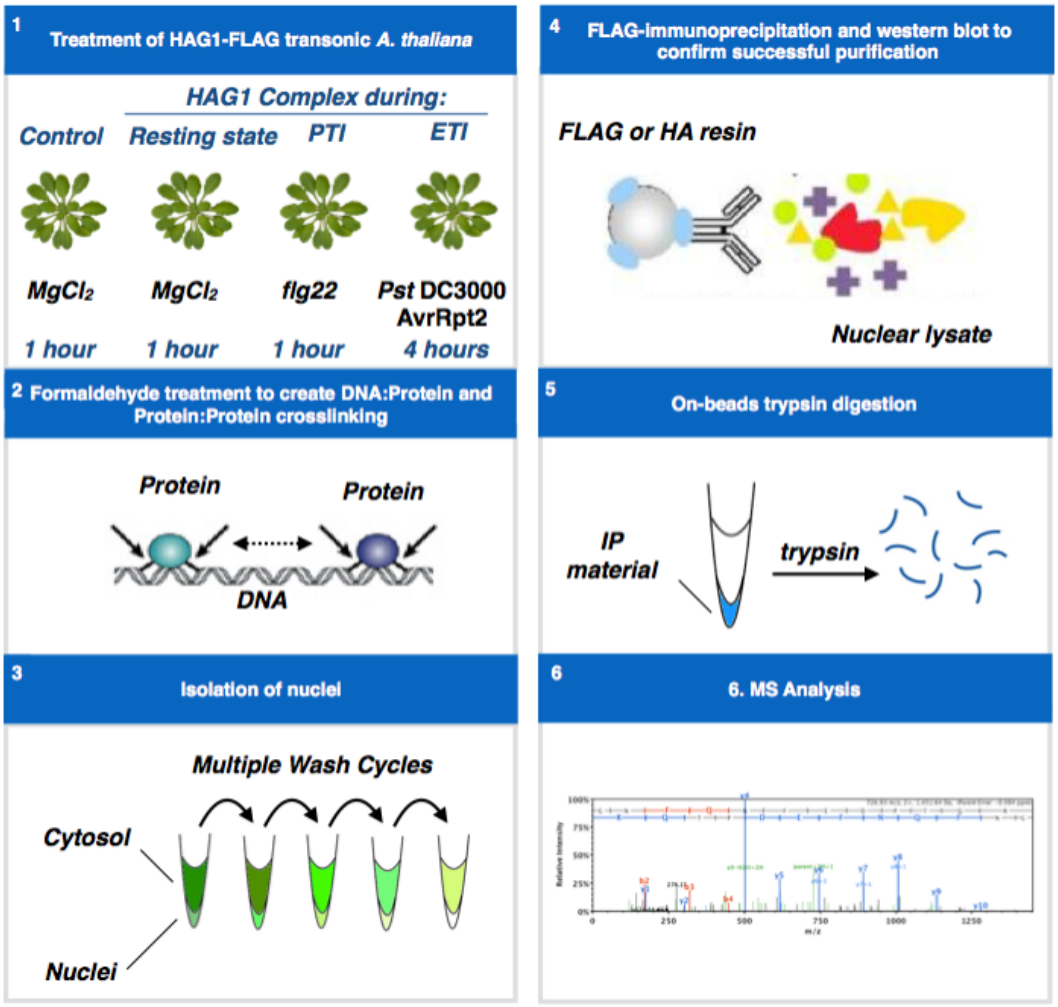

Figure 4.5: Experimental design for the identification of HAG1 complex. Step 1 involves spraying of each solution onto 48 5-week old plants for each treatment. A 10mM $MgCl_2$, a 1µM flg22 and an OD_{600} 0.1 bacteria suspension (*Pst* DC3000 *AvrRpt2*) was used. At the end of 1 hour or 4 hours, the rosette was separated from the roots, placed in a 1% formaldehyde solution and vacuum infiltrated. Steps 1-5 can be completed on Day 1, while step 6 is performed on Day 2. Optimisation and protocol adaptations may be required at multiple steps to account for problems such as low levels of protein expression. For example, modifications may include starting with a different amount of plant material (Step 1), longer cross linking times (Step 2), more wash cycles to eliminate abundant non-nuclear proteins (Step 3), longer incubation with beads to maximise immunoprecipitation of larger complexes (Step 4), longer trypsin digestion to ensure cross linked material has been digested (Step 5) and using a longer separation column during MS analysis for very complex IP samples(Step 6). 'Control' refers to Col-0 plants; whilst 'HAG1 complex' refers to hag1-6 mutants complemented with *HAG1* gene

As *Table 4.2* shows, following the 'on-beads trypsin digestion protocol' (*Experiments 1-3 and 5*) yielded a significantly higher number of interactors in comparison with the 'in-gel trypsin digestion protocol' (*Experiment 4*). The interactions with the highest level of significance (p-value) are ADA2a, ADA2b, TOPLESS and TOPLESS-RELATED 1. It is known that ADA2a and ADA2b associate with HAG1 *in planta* (Mao et al., 2006),

which highlights that the integrity of HAG1 protein is maintained in our transgenic plants and further supports the validity of the interactions observed. Interestingly, ADA3 was identified in at least 2 experiments providing strong evidence for the interaction of HAG1 with ADA3. This is the first time that ADA3 is shown to interact with HAG1 in plants confirming results from other experimental models (Grant et al., 1997). In line with previously identified interactors of GCN5 in yeast, we confirmed in these experiments the interaction with CHROMATIN REMODELLER 5 (CHR5), which is believed to be part of the Spt module of the SAGA complex in yeast (*Fig. 1.3*) (Pray-Grant et al., 2005).

Members of the TOPLESS family, TPL and TPR1, 2, 4 were strongly enriched in all biological replicates with the exception of TPR3 that was not found in our results. The presence of TPL family proteins was particularly encouraging given the already established genetic interaction between *HAG1* and *TPL* genes. In addition, given the roles of TPL and related proteins in immunity, the findings warranted further investigation.

In agreement with previous findings that histone acetyltransferases and chromatin remodelling proteins are often found in the same complex acting in concert with each other (Neely and Workman, 2002), our results showed novel interactors of HAG1 which are involved in chromatin remodelling processes such as histone acetylation (HAC1), ATP-dependent chromatin remodelling (PKL, CHR11, CHR2) and histone deacetylation (HD2B).

Current understanding of SAGA composition in various models includes a variety of proteins with DNA-binding or chromatin-binding proteins such as ADA2a and ADA2b, which have already been described above. Most notably, RNA Pol α, PHD finger, TFIIB, Zn finger (CCCH), WD-40, Global TF1, Nucleic Acid Binding, ING1, Zn Knuckle (CCHC) and WRKY1 were also identified in our experiments and an interaction of HAG1 with these proteins points towards different mechanisms by which

HAG1 could be recruited onto target genes. Overall, our MS analyses revealed that most of the putative HAG1 interactors presented here also have domains involved in chromatin or DNA binding (*Supp. Fig. S4.3*).

Probability Legend:
over 95%
80% to 94%
50% to 79%
20% to 49%
0% to 19%

			Exp 1 On-Beads				*Exp 2* On-Beads				*Exp 3* On-Beads				*Exp 4* In-Gel		*Exp 5* On-Beads			
			COL-0	$MgCl_2$	flg22	AvrRpt2	COL-0	$MgCl_2$	flg22	AvrRpt2	COL-0	$MgCl_2$	flg22	AvrRpt2	COL-0	HAG1-FLAG	No sample	$MgCl_2$	flg22	AvrRpt2	
				HAG1-FLAG				HAG1-FLAG				HAG1-FLAG						HAG1-FLAG			*p-value*
BAIT	HAG1	*AT3G54610*	0	37	49	54	0	37	21	54	0	61	52	50	0	62	-	17	20	25	0.017
Published Interactors	ADA2A	*AT3G07740*	0	3	9	10	0	4	0	0	0	14	15	14	0	0	-	0	0	0	0.052
	ADA2B	*AT4G16420*	0	4	3	2	0	4	0	1	0	14	12	8	0	3	-	0	0	1	0.056
	ADA3	*AT4G29790*	0	0	2	2	0	1	0	0	0	4	2	3	0	0	-	0	0	0	0.180
	CHR5	*AT2G13370*	0	1	0	0	0	0	0	0	0	2	2	0	0	0	-	0	0	0	0.310
TOPLESS Family	TOPLESS	*AT1G15750*	3	7	4	2	0	6	0	4	3	9	8	9	0	1	-	1	3	3	0.046
	TPR1	*AT1G80490*	4	6	2	1	0	5	0	3	1	9	7	9	0	0	-	0	2	2	0.075
	TPR2	*AT3G16830*	3	3	2	1	0	4	0	1	0	6	3	3	0	0	-	1	1	3	0.110
	TPR4	*AT3G15880*	2	2	2	1	0	3	0	2	0	3	0	2	0	0	-	0	0	2	0.170
Chromatin Remodelling	HAC1	*AT1G79000*	0	0	0	1	0	0	0	0	0	2	2	0	0	0	-	0	0	0	0.260
	PKL	*AT2G25170*	0	1	0	0	0	0	0	0	0	2	0	2	0	0	-	0	0	0	0.300
	CHR11	*AT3G06400*	0	1	1	3	0	1	0	0	1	1	3	0	0	1	-	0	0	0	0.200
	CHR2	*AT2G46020*	0	1	1	3	0	1	0	0	1	4	2	1	0	0	-	0	0	0	0.320
	HD2B	*AT5G22650*	1	0	2	2	0	1	0	1	0	2	1	1	0	0	-	1	2	1	0.140
Proteins with chromatin binding, DNA binding, protein modification domains	ARGAH2	*AT4G08870*	0	0	1	0	0	0	0	0	0	0	0	0	0	0	-	1	2	3	0.550
	Tudor1	*AT5G07350*	0	1	1	1	0	1	1	1	0	0	0	0	0	3	-	8	9	8	0.270
	PHD finger	*AT1G77800*	0	1	4	3	0	2	0	0	0	6	5	2	0	0	-	0	0	0	0.120
	RNA Pol α	*ATCG00740*	0	1	0	0	0	0	0	0	0	0	0	0	0	0	-	1	0	2	0.550
	TFIIB	*AT2G41630*	0	1	1	0	0	0	0	0	0	0	3	0	0	0	-	0	0	0	0.270
	SMP2	*AT4G37120*	0	1	5	7	0	0	0	0	1	12	9	3	0	0	-	5	4	7	0.140
	HMGB2	*AT1G20693*	0	1	1	3	0	1	0	0	0	1	0	1	0	0	-	0	0	0	0.500
	Zn Finger (CCCH)	*AT3G27700*	1	1	0	1	0	0	0	0	0	2	2	1	0	0	-	0	0	0	0.170
	WD40-Transducin	*AT3G63460*	0	3	1	1	0	0	0	0	0	0	0	0	0	0	-	2	0	3	0.270
	Cyclophilin-like	*AT2G36130*	0	2	0	0	0	0	0	1	1	3	2	1	0	0	-	2	3	3	0.340
	Cyclophilin71	*AT3G44600*	0	1	0	0	0	1	0	0	0	1	2	1	0	0	-	0	0	0	0.200
	WLIM1	*AT1G10200*	0	1	1	1	0	0	0	0	0	2	0	0	0	0	-	0	0	0	0.270
	Global TF B1	*AT1G65440*	2	8	2	2	3	10	0	3	10	29	23	24	0	0	-	0	1	2	0.210
	CwfJ-like protein	*AT5G56900*	0	3	0	0	0	1	0	2	2	10	5	6	0	0	-	0	0	2	0.210
	RNA binding plectin	*AT4G25740*	0	1	0	0	0	0	0	0	0	0	0	0	0	0	-	3	5	3	0.550
	Nucleic Acid Binding	*AT2G02570*	0	0	1	2	0	1	0	0	1	4	1	1	0	0	-	0	0	0	0.210
	ING1	*AT3G24010*	0	1	0	0	0	0	0	0	0	3	2	1	0	0	-	0	0	0	0.260
	Zn Knuckle (CCHC)	*AT5G49400*	0	0	0	2	0	0	0	0	0	2	1	0	0	0	-	0	0	0	0.410
	WRKY1	*AT2G04880*	0	0	0	1	0	0	0	1	0	3	0	0	0	0	-	0	0	0	0.440
	LRR	*AT3G20820*	2	7	0	0	0	0	0	2	0	1	2	2	0	0	-	5	4	7	0.510
	PP2A	*AT3G09880*	0	1	1	0	0	0	0	0	0	0	0	1	0	0	-	2	2	6	0.550
	Protein Kinase	*AT3G13670*	0	0	0	2	0	0	0	0	0	3	2	2	0	0	-	0	0	0	0.220
	Protein Kinase	*AT1G67580*	0	1	0	0	0	0	0	0	0	2	2	1	0	0	-	0	0	0	0.190
Nuclear Import/ Export	Transportin1	*AT2G16950*	0	3	0	0	0	2	0	0		1		1	0	2	-	1	1	2	0.430
	NRP1	*AT2G03440*	0	2	2	1	0	0	0	1	0	0	0	0	0	0	-	0	1	1	0.290
	NUA	*AT1G79280*	0	1	0	0	0	0	0	0	0	0	0	0	0	0	-	1	1	2	0.430
Other proteins	ACX1	*AT4G16760*	0	3	0	0	0	0	0	0	0	0	0	0	0	0	-	3	2	6	0.550
	ATMIN7	*AT3G43300*	0	1	0	0	0	0	0	0	0	0	0	0	0	0	-	3	2	6	0.550
	PLD	*AT3G15730*	0	1	0	0	0	0	0	0	0	0	1	2	0	0	-	1	2	3	0.330
	SRP30	*AT1G09140*	0	1	0	0	0	1	0	0	0	3	4	1	0	0	-	0	0	0	0.190
	CXIP4	*AT2G28910*	0	1	2	1	0	1	0	0	1	4	2	1	0	0	-	0	0	0	0.230
	SHM4	*AT4G13930*	0	3	0	0	0	0	0	0	0	0	0	0	0	0	-	0	0	1	0.550
	DDB1A	*AT4G05420*	0	1	0	0	0	0	0	0	0	0	0	0	0	2	-	1	1	2	0.550
	MFP2	*AT3G06860*	0	6	0	0	0	0	0	0	0	0	0	0	0	0	-	14	19	21	0.550

Table 4.2: Major interactors of HAG1. The most significant interactors are shown from all MS analyses performed. The number of exclusive unique peptide hits is shown along with a color code indicating the peptide probability. The interactors are grouped into different groups based on whether their interaction with HAG1/GCN5 has been previously described and in terms of their function. The significance level of each interacting protein is shown as a p-value, calculated for the first three experiments. The most significant p-values are highlighted in green. Control (Col-0) and different treatments are shown (MgCl2, flg22, [*Pst* DC3000] *AvrRpt2*) are shown. Experiment 4 represents the only biological replicate that followed in-gel digestion. The gene number is also shown next to the protein number.

Furthermore, proteins with post-translational modification properties were identified such as the phosphatase PP2A and two independent protein kinases. These could suggest that HAG1 or other subunits of the HAG1 complex are regulated by a phosphorylation/de-phosphorylation mechanism.

The volcano plot in *Figure 4.6* shows the distribution of all proteins in our MS results with the most significant interactors clustered on the right side of the graph. Fold change is plotted on the log2 scale (x-axis) and p-values are plotted on the log10 scale on the vertical axis. *Figure 4.7* 'zooms-in' at the most significant interactors of HAG1 with the majority of these represented also in *Table 4.2*.

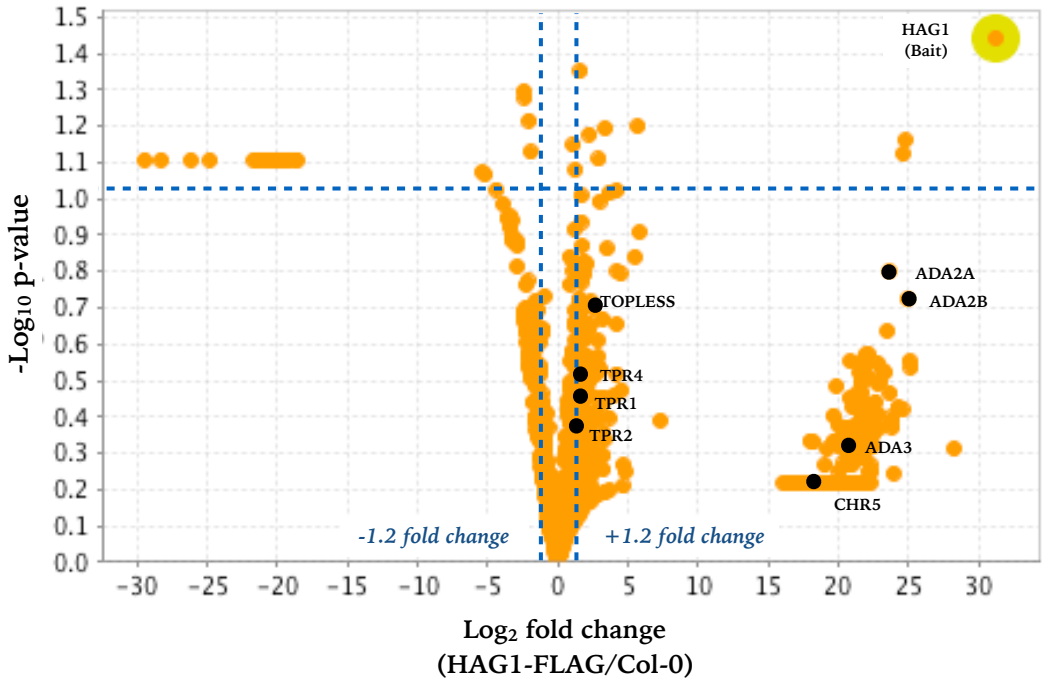

Figure 4.6: Volcano plot of HAG1 interactors. The volcano plot demonstrates magnitude and significance of the protein comparisons between HAG1-FLAG group (pooled treatments) and Col-0 group. The -log10 (Benjamini-Hochberg corrected p-value) is plotted against the Log2 (fold change: HAG1-FLAG/Col-0). The vertical axis indicates -Log10 (p-value) and the horizontal axis indicates Log2 fold change. The non-axial vertical lines denote ±1.2 fold change, while the non-axial horizontal line denotes a significance threshold of p=0.05 prior to logarithmic transformation. Annotated black dots indicate the presence of the major interactors of HAG1 whilst all other interactors are shown in orange.

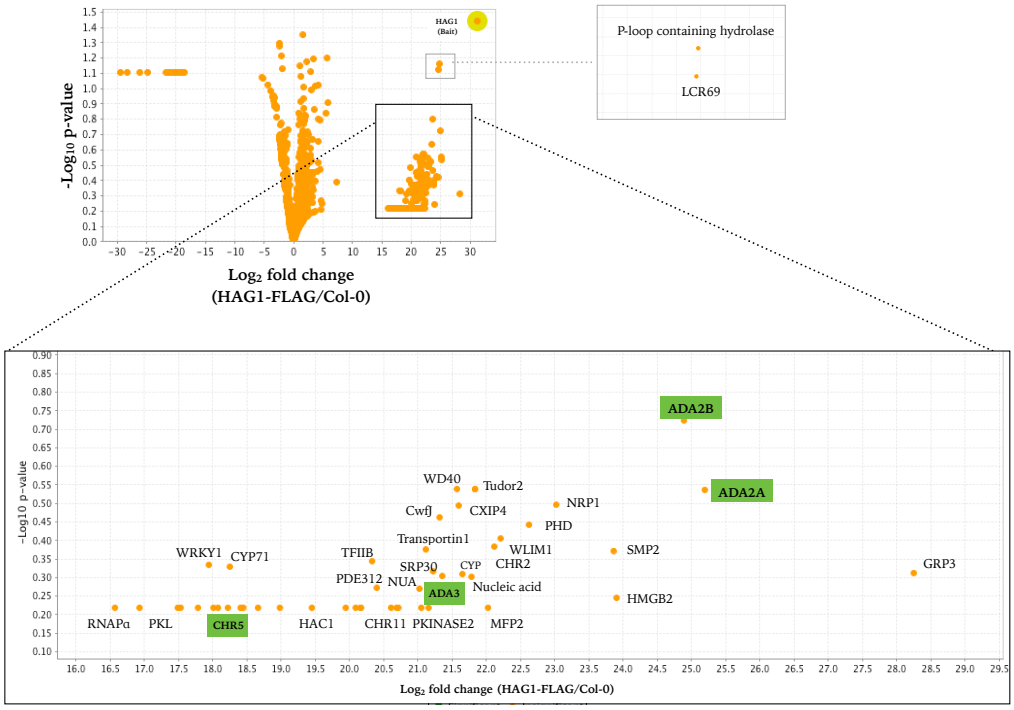

Figure 4.7. Zoomed-in volcano plot of HAG1 interactors. The volcano plot demonstrates magnitude and significance of the protein comparisons between HAG1-FLAG group (pooled treatments) and Col-0 group. This is the zoomed-in version of Figure 4.6. The -Log10 (Benjamini-Hochberg corrected p-value) is plotted against the Log2 (fold change: HAG1-FLAG/Col-0). The vertical axis indicates -Log10(p-value) and the horizontal axis indicates Log2 fold change.

4.3.4. PTI/ETI-specific interactors of HAG1

The results presented in *Table 4.2* provide an overview of HAG1 interactors, but do not provide a quantitative assessment of these interactions after flg22 perception or during *P. syringae* infection, which would allow us to test the hypothesis that the composition of HAG1 complex changes during PTI or ETI. The enrichment or depletion of interactors would suggest a change in the activity of HAG1 complex during immune responses. In our MS analyses we observed a high degree of bait and interactor variation among the treatments, but also between the different experiments. In order to semi-quantitatively assess whether there is an enrichment or depletion of these interactions in each of the conditions tested, we used Scaffold (proteome software) (Searle, 2010) to obtain the

quantitative value from each interactor. Quantitative values are used by Scaffold as a method for normalising spectral counts for each MS sample. Although this method allows samples with different abundances to be more easily compared, this method can only be employed as a semi-quantitative approach. For this reason, we decided to perform this analysis on the closest interactors of HAG1, for which the normalization bias would be smaller due to a closer stoichiometry to the bait.

The quantitative value of each interactor was then normalised to the quantitative value of HAG1, which allowed us to identify quantifiable changes in the level of each interactor with respect to bait (HAG1) levels. *Figure 4.9* shows the normalized quantitative values for the closest interactors of HAG1. For the interactors ADA2A, ADA2B, ADA3 and CHR5 there is no clear pattern of enrichment or depletion across the different conditions, but we noticed that members of the TOPLESS family converged towards a pattern in which stronger interaction with HAG1 was observed in resting conditions, whilst the interaction appears to be lost after flg22 perception or at later stages of infection with *Pst* DC3000 *AvrRpt2*.

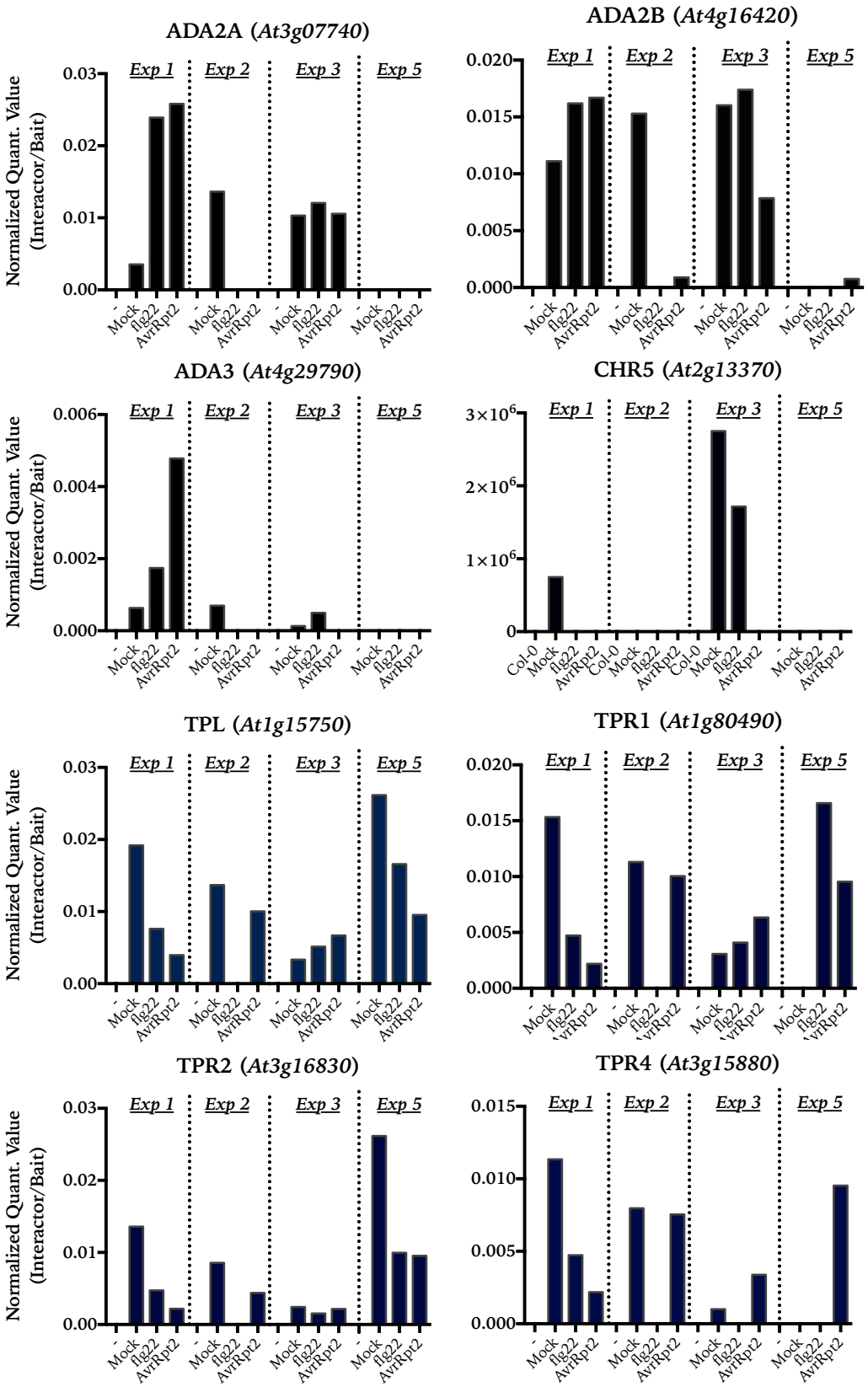

Figure 4.8. Enrichment or depletion of major interactors of HAG1. The most significant interactors of HAG1 were quantitatively analysed to determine enrichment of depletion of each interaction in each condition. The quantitative values of each interactor (as calculated by Scaffold) were normalized to the quantitative value of HAG1 (bait). Relative values are shown as a result of the normalization. The experiment numbers correspond to the experiment numbers in *Table 4.2*.

4.3.5. Members of TOPLESS-family co-immunoprecipitate with HAG1 only after HAG1 immunoprecipitation

After obtaining evidence that members of the TOPLESS family may have a dynamic relationship with HAG1 we attempted to investigate the interaction more closely. We obtained Arabidopsis plants stably expressing the constructs *TPL*::TPL-HA or *TRP1*::TPR1-HA (Zhu et al., 2010) (from Prof. Jim Beynon Lab) and checked for the expression of each of these proteins by performing immunoprecipitation followed by immunoblotting. After seeing a strong expression pattern for TPL as opposed to TPR1, for which we did not see a band at the expected size (both at 124kDa) *(Fig. 4.9)*, we chose to pursue immunoprecipitation followed by mass spectrometry in the TPL-expressing plants. We were also more inclined to work with the TPL-expressing plants as we found stronger evidence for interaction between TPL and HAG1 as seen in all of our experiments collectively, but also in Experiment 4 (*Table 4.2*), where TPL co-immunoprecipitated with HAG1 in the more stringent 'in-gel digestion' method.

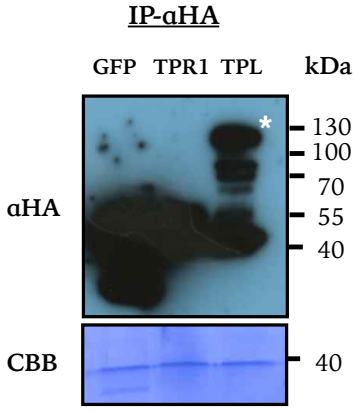

Figure 4.9: TOPLESS and TPR1 expression. Stable transgenic *A. thaliana* plants expressing GFP-HA, TPR1-HA or TPL-HA were grown to adult stage and total protein s were extracted. HA-immunoprecipitation was followed by immunoblotting using αHA antibody. The asterisk denotes the band corresponding to expected size of the protein. Ladder is denoted by kDa.

As *Figure 4.10a* shows TPL-HA-expressing plants have broader leaves and a shinier leaf surface. After following the same protocol as with the HAG1 MS procedure, but this time using HA resin *(Fig. 4.5)*, we obtained a TPL protein coverage of approximately 21% (*Fig. 4.11*). We also observed a phosphorylation site at Ser-214. The results from two biological replicates showed that very few

proteins co-immunoprecipitate with TPL, none of these proteins has been previously described, but HAG1 was not amongst these interactors.

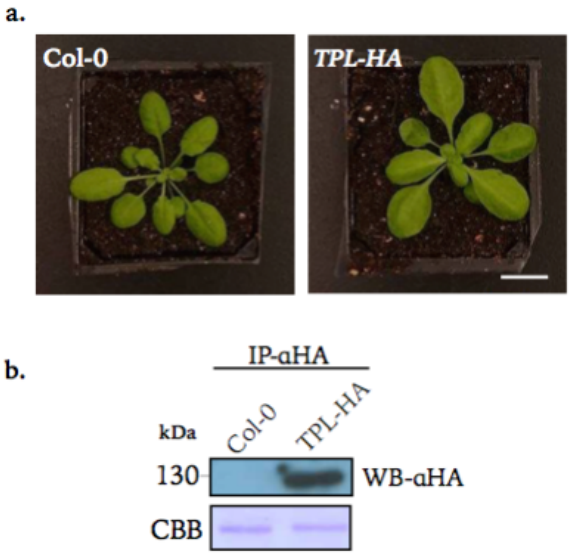

Figure 4.10: TOPLESS immunoprecipation. TPL-HA is expressed in the stable transgenic Arabidopsis line, after immunoprecipitation with αHA beads. (a) TPL-HA-expressing plants appear to have wider leaves and a more shiny leaf surface as compared to wild-type Col-0 plants; (b) 10% of the beads solution was loaded on a 10% SDS-PAGE, transferred onto a PVDF membrane and blotted with αHA antibody. Ladder is denoted by kDa.

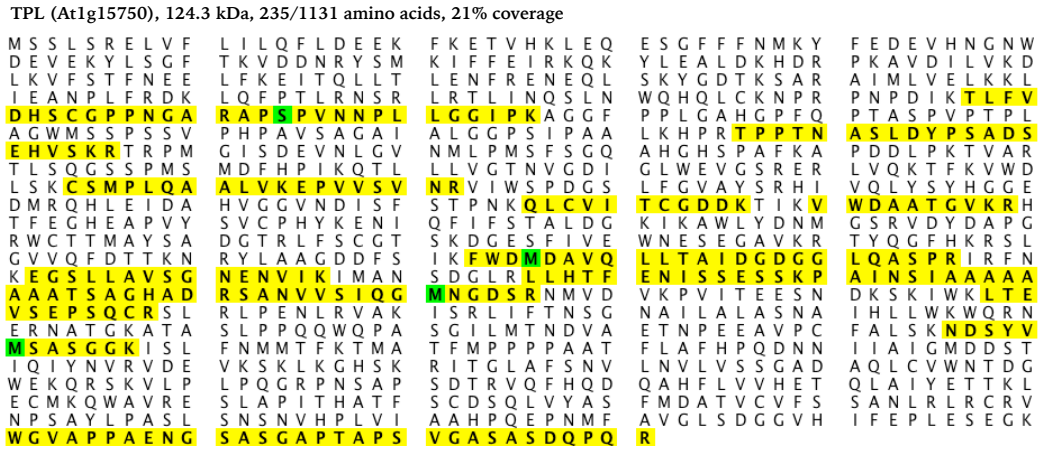

Figure 4.11: Coverage of TPL protein sequence. Representative biological replicate of TPL-HA pull-down and subsequent proteomic analysis. Illustration of coverage of TPL sequence by peptides identified in MS analysis of HA immunoprecipitation. Peptides are highlighted in yellow and green indicates post-translational modification e.g. M = methionine oxidation, S = serine phosphorylation

Probability Legend:
over 95%
80% to 94%
50% to 79%
20% to 49%
0% to 19%

		Exp 1			*Exp 2*		
		On-Beads			On-Beads		
		COL-0	$MgCl_2$	AvrRpt2	COL-0	$MgCl_2$	AvrRpt2
			TPL-HA			TPL-HA	
TOPLESS (Bait)	***AT1G15750***	0	12	11	0	26	28
TPR1	***AT1G80490***	0	0	0	0	16	16
TPR2	***AT3G16830***	0	0	0	0	11	7
TPR4	***AT3G15880***	0	0	0	0	0	9
Catalase 3	***AT1G20620***	0	0	0	0	3	3
RAS-related nuclear protein-1	***AT5G20010***	0	0	0	0	2	0
Histone H2A 7	***AT5G27670***	0	0	0	0	0	2
GRP17, ATGRP17, ATGRP-7	***AT5G07530***	0	0	9	0	0	0
DUF1216	***AT3G28830***	0	0	7	0	0	0
Regulator of Vps4 activity in the MVB pathway	***AT4G29440***	0	0	5	0	0	0

Table 4.3: Major interactors of TPL. The results from two biological replicates involving TPL immunoprecipitation and MS. The number of exclusive unique peptide hits is shown along with a color code indicating the probability of the peptide. Control (Col-0) and different treatments ($MgCl_2$, [*Pst* DC3000] *AvrRpt2*) are shown.

4.4. Discussion

4.4.1. Core interactors of HAG1

This chapter attempted to identify the mechanism by which HAG1 positively contributes towards plant immunity. Our understanding of HAG1 in plants and its homolog GCN5 in other model organisms suggested that this enzyme requires the collaboration of other nuclear proteins in order to target specific genes for histone acetylation at their promoter or gene body. In yeast, the huge multi-protein complex known as SAGA has been described already, but the HAG1 complex in plants has not been previously characterised. Research in plant HAG1/GCN5 has identified a few interactors, without any attempts to place all these interactors in the context of a multi-protein HAG1 complex.

We managed to identify the two most well described interactors of HAG1, ADA2a and ADA2b, confirming data from other studies (Hark et al., 2009; Vlachonasios et al., 2003). In yeast, Ada3 interacts with Gcn5 (HAG1 homolog), however, a similar interaction has not been described

so far *in planta*. Due to an incomplete Arabidopsis genome annotation, it was believed that no ADA3 existed in plants (Vlachonasios et al., 2003). However, based on more recent studies the locus AT4G29790 was identified as the homolog to yeast Ada3 (Moraga and Aquea, 2015). This strongly suggests that HAG1 is not only interacting with ADA2a and ADA2b, but may also depend on its interaction with ADA3 to perform its function. The *ada3* phenotypes have not been so far described, but it could be expected that the mutant would display impaired histone acetylation and possibly increased susceptibility to *Pst* DC3000. However, it should be noted that *ada2a* and *ada2b* (*prz1-1*) mutants did not display a disease susceptibility phenotype (*Fig. 3.8*). For the purposes of solidifying some of the interactions observed in this set of experiments, it would also be valuable to perform IP followed by MS in transgenic lines of ADA2a, ADA2b or ADA3, in order to fully characterize HAG1 complex, although the time commitment and resource investment for these experiments should be recognised.

Next, we queried our MS results for modifications on HAG1 to find evidence for regulation of HAG1 activity at the post-translational level. Previous publications have pointed towards the presence of a phosphorylation/dephosphorylation mechanism - the latter being governed by PP2C phosphatase - leading to change of HAG1 activity (Servet et al., 2008). Furthermore, GCN5 in humans has been reported to be post-translationally modified in its bromodomain, HAT domain and PCAF domain (not present in HAG1) (*Fig. 4.13A*) and this includes acetylation and phosphorylation at multiple sites. In our experiments, we found evidence for the post-translational modification of HAG1 at various sites (Table 4.1) including phosphorylation (Ser-21, Ser-76, Ser-84), methylation (Lys-368) and acetylation (Lys-188). However, there was no clear evidence to suggest that these modifications were dynamic, in other words, they did not appear to change during PTI or ETI. By contrast, a recent

study by Latrasse *et al* (2017) showed that MAPK3 phosphorylates the HDAC HD2B upon flg22 perception leading to its re-localization from the nucleolus to the nucleus and ultimately affecting chromatin remodelling.

Figure 4.12: Human GCN5, ADA2A and ADA2B can be modified by multiple types of PTMs. Acetylation, methylation and ubiquitination occur in Lysines (K), Phosphorylation occurs in Serines (S), Threonines (T) and Tyrosines (Y). The data were obtained from www.phosphosite.org

It is known that human GCN5, ADA2A and ADA2B can be modified at various sites with various types of post-translational modifications.

It is, therefore, likely that in the case of HAG1, one of the kinases mediating HAG1 phosphorylation could be any of the two protein kinases identified in our MS results (AT3G13670; AT1G67580). In order to test this hypothesis, *in vitro* phosphorylation experiments could be performed using HAG1 as substrate. To prove the *in vivo* interaction between HAG1 and any of these kinases, split-YFP experiments, that have proven extremely useful in the past, could also be used here (Servet et al., 2008).

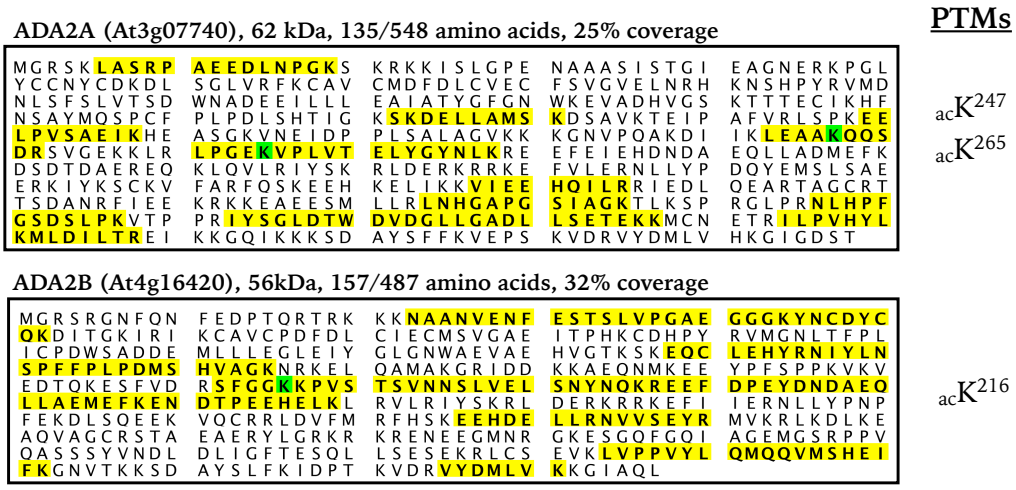

Figure 4.13: ADA2 proteins sequence coverage and post-translational modifications. ADA2a and ADA2b show a high coverage and are also acetylated in 2 and 1 lysines, respectively. A representative experiment is shown.

Interestingly, in our MS results, we also found evidence for the post-translational modification of ADA2a (Lys247, Lys265) and ADA2b (Lys216) (*Fig. 4.8*), which could likely be mediated by HAG1 given the close interaction with the HAT, as well as due to the fact that GCN5 has been found to also have non-histone substrates for acetylation (Kornet and Scheres, 2009; Mao et al., 2006). ADA2A and ADA2B in humans are post-translationally modified at several sites, but acetylation is only found for ADA2A (*Fig. 4.13*). The N-terminal regions of ADA2a and ADA2b are predicted to interact with HAG1, whilst a middle fragment is known to bind to the HAT domain of HAG1 (Servet et al. 2010). Therefore, it could be argued that these acetylation sites appear to coincide with the middle-fragment predicted to interact with the HAT domain. The significance of these acetylation sites may be that they regulate the interaction with HAG1 adding another level of regulation in the activity of HAG1, which could be context dependent. Again, we did not find evidence that these acetylation sites are dynamic (i.e. dependent on flg22 perception).

A large proportion of the interactors listed in *Table 4.2* contain protein domains involved in chromatin binding according to search queries using the 'conserved domain' tool *(Supp. Figure S4.3)*. This provides

greater confidence in our MS results, given that we would expect HAG1 interactors to employ chromatin-binding domains to associate with chromatin.

The SAGA complex in other model organisms consists of the HAT module (ADA module), TAF module, DUB module and SPT module. As mentioned, we have identified 3 members of the HAT module (ADA2a, ADA2b, ADA3). We also identified CHR5, a homolog of Chd1 (Moraga and Aquea, 2015), which is believed to belong to to the SPT module. The presence of a full SPT module cannot be confirmed on the basis of these findings, but we can speculate that the interaction with this chromatin remodeller serves certain purposes. To be more specific, CHR5 contains a SNF2 domain, involved in transcription regulation as well as tandem chromodomains, involved in binding methylated H3K4 (*Fig. 4.14*). Specifically, chromodomain 2 of Chd1 in yeast was required for optimal SAGA HAT activity *in vitro* and for the acetylation of H3K9 and H3K14 at the *GAL1-10* promoter *in vivo* (Pray-Grant et al., 2005). Therefore, CHR5 may constitute an additional mechanism by which HAG1 is recruited or tethered onto chromatin.

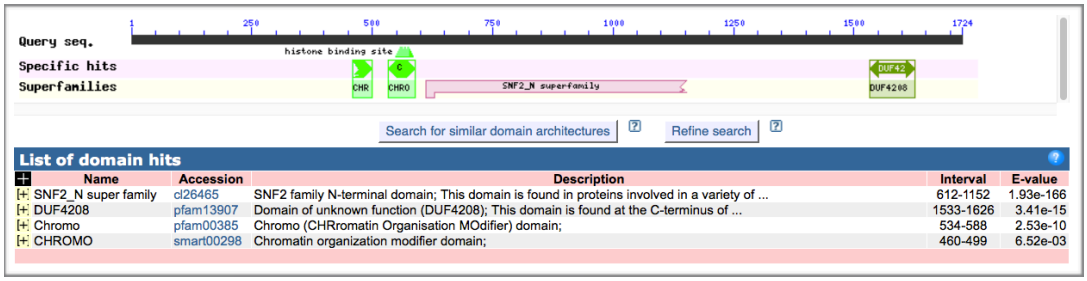

Figure 4.14: Domains identified in *A. thaliana* Chromatin Remodeller 5. A domain search in NCBI for CHR5 (At2g13370) identified three types of domains; SNF2 family N-terminal domain, a domain of unknown function (DUF4208) and a chromodomain.

We also did not identify interaction with certain proteins published previously for HAG1. Previous studies have focused on the direct interaction of HAG1 and other proteins such as the bZip transcription factor OPAQUE in maize (Bhat et al., 2004) or the transcription activator EML in Arabidopsis (Gao et al., 2007). AtADA2b was shown to interact with

the transcription factor AtCBF1, to promote cold-responsive gene expression (Mao et al., 2006). In rice, Zhou *et al* (2017) described the interaction of ADA2-GCN5 with the transcription factor WOX11 in the context of root meristem development. Although these interactions were not identified in our experiments, we did identify other transcription activators or transcription factors. PHD finger protein (AT1G77800) containing a PHD (Plant Homeodomain) Zn finger domain is involved in binding methylated lysines on histones. TFIIB (AT2G41630) and RNA pol α subunit (ACG00740) are part of the RNA polymerase machinery and GCN5 is known to interact with this multi-protein machinery (Roberts and Winston, 1997). Other Zn finger-containing proteins (AT1G65440) were found as well as DNA-binding proteins (AT4G25740, AT2G02570) including the WRKY1 transcription factor (AT2G04880) involved in disease resistance and abiotic stresses but there was no enrichment upon PTI or ETI, according to our experiments. All these interactions warrant further investigation as they could shed light into the different ways that HAG1 contributes to developmental processes as well as responses to abiotic and biotic stresses.

We did not find compelling evidence to support the presence of a deubiquitination module (DUB), in contrast to studies in yeast. Other mechanisms for histone deubiquitination in the context of plant immunity have been described in Arabidopsis, although these have not been linked to HAG1 (Zou et al., 2014). It is possible that a DUB module in plants may be lacking or is different to the one in yeast.

Yeast studies have shown that SAGA is implicated in processes relating to the nuclear pore, potentially facilitating the export of mRNA directly after transcription. Yeast protein Sus1 is part of the highly conserved mRNA export machinery and was subsequently shown to interact with various subunits of SAGA. A role of SAGA in this process is further supported by findings showing that SAGA-regulated genes are confined to

the nuclear periphery upon their transcription in a Sus1-dependent manner (Cabal et al., 2006; Rodriguez-Navarro et al., 2004). Interestingly, we have identified three proteins with potential roles in nuclear import/export. These include Transportin1 (AT2G16950) with roles in miRNA loading (Cui et al., 2016), NRP1 (AT2G03440), which is induced by *Pst* DC3000 (Audenaert et al., 2002) and NUA (AT1G79280), which is involved in mRNA export (Xu et al., 2007). We did not observe enrichment in flg22 or *Pst* DC3000 conditions for any of these potential interactors.

4.4.2 HAG1 and TOPLESS family members interaction

Perhaps the most interesting finding in our MS data is that HAG1 interacts with members of the TOPLESS family. Specifically, interaction with all members was identified except for TPR3, which may be attributed to sequence differences between the different members. An alignment suggests that the five members have many differences in their protein sequence *(Supp. Fig S4.1)*.

With regards to the finding that TOPLESS family member interaction with HAG1 is disturbed following flg22 elicitation or *Pst* DC3000 *AvrRpt2* infection, we could hypothesise that the underlying mechanism involves ubiquitin-mediated degradation of the co-repressor proteins. This is similar to the model proposed by Weiste *et al* (2014) who showed that in low auxin concentrations, repression of auxin-responsive genes takes place due to the action of AUX/IAA proteins, TPL and HDA19; however, upon increasing auxin levels the co-repressors are degraded in a ubiquitin-mediated manner. Zhu *et al* (2010) showed that TPR1 associates with HDA19 *in vivo* to repress *DND1, 2 (Defense No Death)* among other genes to negatively regulate R-protein-mediated immune responses (Zhu et al., 2010).

We did not identify an interaction between HAG1 and TPL upon immunoprecipitation of TPL-HA. However, given that none of the identified interactors have been described before (or published TPL interactors were not identified here), we could argue that the experiment has not been successful and requires further optimisation such as, for example, to be performed at a larger scale or with a different construct or biochemical tag. Another way to further consolidate the interaction between HAG1 and members of the TOPLESS family, would be to co-express the two proteins in leaf protoplasts or transiently in *N. benthamiana,* which has already been performed in the Ntoukakis lab confirming the MS findings in *N. benthamiana.* Recent experiments in the Ntoukakis lab showed that this interaction is not direct. Specifically, Y2H experiments confirmed that HAG1 does not directly interact with TPL (*data not shown here*). In line with our findings no interaction between HAG1 and TPL by Y2H was found in a large interaction screen published previously (Causier et al., 2012). This appears to be supported by the fact that HAG1 does not have an EAR motif (Tiwari et al., 2004), which is required for interaction with TOPLESS proteins. In addition, a direct interaction of HDA19 with TPL is lacking as well, although these two proteins are known to act together. Therefore, both of these HATs/HDACs are most likely to be interacting with TPL indirectly.

Furthermore, two proteins that are present in the same complex would be expected to display similar FRAP kinetics (Franks et al., 2016), thus investigating the FRAP kinetics of TOPLESS and HAG1 could provide insights into whether these proteins are in the same complex. One limitation is that TOPLESS interacts with NINJA (Pauwels et al., 2010), yet we did not identify NINJA as one of the interactors of HAG1. This may suggest that TPL exists in different complexes, whereby one contains HAG1 and is involved in regulating HAG1 role in defence responses, and another one contains NINJA and is involved in JA signalling. Most impor-

tantly, a valuable experiment would be to generate double transgenic lines expressing HAG1 and TPL with different tags and performing ChIP before and after flg22 treatment to determine whether the two proteins act on the same promoters.

4.4.3. Limitations and future experiments

Most of our current knowledge on large multi-component protein complexes comes from biochemical experiments involving high quantity and high quality affinity purification of the protein of interest and interacting partners. Almost exclusively, studies with this objective have employed strong cross linking agents to stabilise protein-protein and DNA-protein interactions, in an attempt to maximise the number of purified interactors and to also create a snapshot of protein networks in living systems. One potential limitation arising from this methodology is the identification of false positive interactions between proteins functioning in close proximity. In support of the cross-linking technique, the Allis lab who were responsible for several seminal papers in histone acetylation and the characterisation of the SAGA complex, also employed cross-linking agents such as formaldehyde. Two additional significant aspects of the experimental procedure include the quantity of material and the purification method. We attempted to scale up the purification by extracting protein from at least 70 rosettes per treatment resulting in at least 30g of plant tissue. To put this into perspective, purifications from yeast to characterise the SAGA complex involved cultures ranging from 5-20 litres. This is significantly higher than the 30g of plant tissue employed in our experiments and highlights that the identification of multi protein complexes (potentially >1MDa in size) may require very large quantities of plant tissue. To our knowledge not many studies in plant research have attempted to fully characterize multi-protein chromatin remodelling com-

plexes or have attempted to purify nuclear protein at this scale. Lastly, the Allis lab have employed a very robust, multi-column biochemical purification approach involving Ni^{2+}-NTA agarose, MonoQ column, Superose and GST-Glutathione Sepharose column (*Suppl. Figure S4.4*)(Grant et al. 1997), allowing high quality complex purification (Kuo et al., 1996; Tanner et al., 1999). This could suggest that a complete characterisation of HAG1 complex in plants could benefit from a more stringent purification method at a larger scale.

In addition, one limitation in our experiments is that it is impossible to know whether HAG1 molecules that we immunoprecipitated are chromatin-bound or are free in the nucleoplasm. It is likely that the two populations of HAG1 would be significantly different in their interacting partners. Therefore, it is likely that this limitation is contributing to the complexity of our results. To circumvent this limitation and obtain greater granularity, one option would be to perform chromatin immunoprecipitation, allowing only chromatin bound molecules of HAG1 to be pulled down, although a technical limitation is once again the requirement for larger amounts of plant tissue.

One observation for the MS results is the absence of histones as interacting partners, despite the fact that these are the most well-known substrates of HAG1/GCN5 and the identification of HAG1-H3 interaction by Co-IP and immunoblotting (*Fig. 4.1*). This is attributed to the high frequency of lysine residues in the protein sequence of histones offering multiple digestion sites for trypsin. The resulting peptides following trypsin treatment (which digests after an arginine or lysine unless this residue is followed by a proline) are too small to be identified by MS (Olsen et al., 2004). To circumvent this, alternative enzymes with different digestion sites could be used such as chymotrypsin, which cleaves after phenylalanine, tryptophan or tyrosine unless this residue is followed by a proline (Appel, 1986). This would also allow us to identify post-

translational modifications on histones and specifically determine whether there is an enrichment of acetylation in the flg22-treated or *Pst* DC3000-infected samples.

In the future, to obtain further granularity as to which part of HAG1 contributes to the interactions observed here, we could employ transgenic lines expressing a truncated version of HAG1, specifically lacking the bromodomain. This would allow us to identify, which proteins interact with the bromodomain of HAG1. This set of experiments could be complemented by Y2H experiments attempting to test pairwise interactions of identified interactors from the results presented here and in which the bromodomain of HAG1 is required for these interactions.

Having established that HAG1 is required for the establishment of flg22-induced H3 acetylation we would like to show the *in vitro* and *in vivo* enzymatic activity of HAG1. To this end, we have generated two different constructs of HAG1 with substitution mutations at E289. The selection of Glu-289 as the catalytic residue was based on studies in other model organisms, which pointed towards this residue as responsible for the acetyltransferase activity (Tanner et al., 1999; Wang et al., 1998). After performing site-directed mutagenesis, we generated two putative catalytic inactive mutants, namely E289Q and E289H. The selection of Gln (Q) and Histidine (H) was also based on previous experiments in the literature, showing complete loss of enzymatic activity in the presence of these residues. More specifically, the best candidate for this was glutamine because it has no charge and thus is not able to accept a proton (H^+) from the targeted lysine. In addition, Gln has a similar structure as Glu and according to Tanner *et al* (1999), the substitution does not seem to affect protein folding. The choice of histidine was also supported by previous studies (Wang et al., 1998). First, an attempt to confirm *in vitro* the loss of enzymatic activity in the mutants was made by performing immunopurification of FLAG-HAG1 (WT, E289Q, E289H) from *N. benthamiana* after

transient expression. Immunopurification was followed by a fluorimetric HAT assay. The result suggested that optimisation of the HAT assay is required as the background signal in the control sample was very high. The mutated versions of HAG1 were nuclear localised, which suggests that the protein folding is not affected (*Supp. Fig. S4.2; HAT activity data not shown*). As an alternative, a more sensitive approach to identify the HAT activity of wild-type and mutated HAG1 would involve a radioactive HAT assay in which radio-labelled carbon is used to monitor the rate of Ac-CoA transfer onto the substrate (i.e. histone) (Brownell and Allis, 1995).

In addition, we also attempted to test the *in vivo* activity of HAG1 by testing the expression levels of classical defence genes (*FRK1, PHI1, NHL10*) in protoplasts. Specifically, this involved expressing RFP-HAG1 (WT, E289Q, E289H) in protoplasts from Col-0 and *hag1-6* plants. Following protoplast transfection, the efficiency of transformation was determined by confocal microscopy to ensure that HAG1 is successfully expressed and localises to the nucleus (*Supp. Figure S4.2*). The protoplasts were then treated with water or *flg22* and samples were processed for qPCR. These initial attempts did not result in successful experiments (*data not shown*), but ongoing attempts aim to ask what the function of HAG1 could be in defence-gene induction. We hypothesise that non-transfected *hag1-6* protoplasts will display reduced expression of classical defence genes after flg22 treatment and that complementation with wild-type HAG1 would restore expression to Col-0 levels. The complementation should also depend on the enzymatic activity of HAG1, such that the mutated versions of HAG1 would be unable to fully restore defence gene expression in *hag1-6* mutants.

We have also generated transgenic plants expressing the mutated versions of HAG1 in Col-0 and *hag1-6* backgrounds. Although we have confirmed that complementation of *hag1-6* plants with wild-type *HAG1* restores the developmental and immunity phenotypes, experiments to de-

termine whether mutated HAG1 is able to restore these phenotypes are still under way. Our hypothesis is that introducing mutated HAG1 into *hag1-6* plants will result in no phenotype restoration or partial restoration at best. The latter could be justified by the fact that a putative SAGA complex could be fully reconstituted in the presence of a full-length HAG1 protein, albeit lacking catalytic acetyltransferase activity.

Furthermore, an alternative method to identify changes in the composition of a putative SAGA complex after *flg22* elicitation or *Pst* DC3000 infection is to perform native PAGE, which would allow the identification of an intact HAG1-containing complex in the different conditions. Studies involving native PAGE experiments continue to improve our understanding of SAGA complex composition in other systems (Kassem et al., 2017) and it is likely that this would also be highly informative in our attempt to fully characterize the Arabidopsis HAG1 complex. Initial attempts to identify a HAG1 complex in native conditions in our lab were unsuccessful, suggesting that further optimisation of the method is required (*data not shown*).

Overall, as explained in greater detail in Chapter 6, Figure 6.2 and Figure 6.3, we have managed to shed light into the potential composition of a SAGA complex in plants and to suggest a model in which the composition may be dynamic depending on the conditions that the plant is exposed to.

Chapter 5 - Identifying bacterial effectors with roles in chromatin remodelling

5.1. Context of this chapter

Many studies have explored the plethora of mechanisms by which pathogens establish infection. *Pseudomonas syringae* DC3000 *pv*. tomato relies on a repertoire of approximately 30 effectors, which are translocated via a type III secretion (T3S) system into host cells leading to effector-triggered susceptibility (Cui et al., 2015). The presence of a large number of effectors allows targeting of a range of sub-cellular compartments in order to subvert a variety of host cellular functions and promote virulence. The targeting of multiple host processes ranges from signal transduction inhibition, to influencing hormone signalling, to interfering with chromatin-related processes (Xin and He, 2013). In recent years, different strategies of interference with host nuclear processes have been described in plant pathogens, for example, TAL effectors from Xanthomonas have been identified as transcription factors acting in a highly specific manner on plant host DNA sequences (Boch et al., 2014).

Pst DC3000 was shown to employ effector HopU1, an ADP ribosyltransferase (ADP-RT) to subvert host immunity (Fu et al., 2007). Fu *et al* (2007) showed that infection of Arabidopsis Col-0 leaves with *Pst* DC3000 lacking HopU1 is weaker than wild-type *Pst* DC3000 in terms of bacterial growth. In experiments that employed *Pst* DC3000 expressing a catalytically inactive HopU1, bacterial virulence was reduced leading to the conclusion that the ADP-ribosyltransferase enzymatic activity of HopU1 is responsible for these phenotypes. In addition, two-dimensional (2D) PAGE followed by autoradiography revealed a small glycine-rich RNA-binding protein, AtGRP7 as a substrate for ADP-ribosylation by HopU1. In conclusion, according to the authors, post-translational modification of GRP7 impairs its ability to bind mRNAs, which results in

blocked translation. More recently, it was discovered that GRP7 interacts with transcripts from the immune receptor gene *FLS2* and that this binding is prevented by the ADP-RT activity of HopU1 leading to reduced FLS2 protein levels during infection (Nicaise et al., 2013).

HopF2 is another ADP-RT with structural similarity to diphtheria toxin and was found to target MAP kinases MKK4 and MKK5 to suppress MAMP-induced responses (Wang et al., 2010c).

These results highlight that bacterial effectors have the ability to act as post-translational modifiers of host proteins affecting signalling cascades and nuclear processes thus contributing to the infection outcome. Interestingly, Agrobacterium protein 6b associates with histone H3 and according to structural studies it may have ADP-ribosyltransferase activity, which suggests an additional mechanism through which bacterial ADP-ribosyltransferases can interfere with host mechanisms (Ishibashi et al., 2014; Terakura et al., 2007; Tinland et al., 1990; Wang et al., 2011).

a.

	aa	*
HopU1	224	ISGSSQAPS EEEIM
HopO1-1	238	IGPFSKNPYEDEAL
HopO1-2	253	IGPFSKNPYEDEAL

b.

	HopU1	HopO1-1	HopO1-2
HopU1		24%	22%
HopO1-1	36%		75%
HopO1-2	36%	100%	

	Sequence identity of ADP-RT domains
	Sequence identity of full-length protein

Figure 5.1. *Pst* DC3000 effectors with putative ADP-ribosyltransferase domain. (a) An alignment of the conserved regions of mono-ADP-ribosyltransferases (ADP-RTs) from *Pst* DC3000. Conserved residues are shown in red and the invariant amino acids of the cholera toxin group of ADP-RTs are marked with asterisks (adapted from Fu et al 2007); (b) Sequence identities of full-length and ADP-RT domains between HopU1, HopO1-1 and HopO1-2.

Furthermore, the *Pst* DC3000 effector repertoire has been found to contain two additional putative ADP-RTs. There is not much known about these two effectors with regards to their roles during an infection, but given a high sequence similarity with HopU1 (*Fig. 5.1*), it is likely that

HopO1-1 and HopO1-2 have an overlapping set of targets as well as a unique set of target substrates in the host cell (Fu et al., 2007).

These examples highlight how pathogens employ effectors with ADP-ribosyltransferases in order to enhance their virulence. In general, ADP-RTs bind NAD^+ and catalyse the covalent transfer of a single ADP-ribose or poly-ADP ribose usually onto an aspartate or glutamate residue resulting in a change of protein activity. Our understanding of ADP-ribosylation heavily relied on studies of other prokaryotic ADP-RTs with cell damaging properties. For instance, cholera toxin (CT) from *Vibrio cholerae*, a Gram-negative bacterium, which is known to cause cholera and diphtheria toxin (DT) from the Gram-positive *Corynebacterium diphtheriae,* the causative agent of diphtheria are two very well-known ADP-RTs. Their substrates within the host include but are not limited to actin, kinases, cAMP signalling (G-protein coupled receptors) and RNA-recognition motifs (Corda and Di Girolamo, 2003; Fieldhouse et al., 2010; Holbourn et al., 2006; Sun and Barbieri, 2003). In addition, poly-ADP-ribose polymerase 1 (PARP-1) in animals is an ADP-RT that associates with chromatin and acts in response to DNA strand breaks and is capable of ADP-ribosylating histones (Jagtap and Szabo, 2005), which highlights that ADP-ribosylation is important in multiple host processes including chromatin-associated processes. Meanwhile, PARP-1 and PARP-2 in plants were shown to be crucial for MAMP-induced gene activation as double mutants *atparp1 atparp2* displayed compromised immune gene activation as well as enhanced susceptibility to *Pst* DC3000 (Feng et al., 2015).

Overall, it is important to emphasise that despite the identification of host targets for many of the *Pst* DC3000 effectors, there is still a lot to be determined with regards to their sub-cellular localisation profile as well as their interacting partners inside the nucleus. According to our latest understanding of *Pst* DC3000 effector localisation, the vast majority of the effectors are targeted in the cytosol (HopM1, HopZ1, AvrRpt2, Avr-

Rpm1, HopF2 and others), whilst a few have a chloroplastic localisation (HopI1, HopN1). A comprehensive screen to identify nuclear-localised *Pst* DC3000 effectors is lacking and could point towards effectors which interfere with chromatin remodelling.

5.2. Main findings

This chapter presents a comprehensive approach towards identifying *Pst* DC3000 effectors with a role in chromatin remodelling. To this end, a screening approach was employed to first identify nuclear localised effectors and subsequently identify effectors with the capacity to bind chromatin. HopO1-1, a putative ADP-RT localised to the nucleus and appeared to bind chromatin, whilst in the presence of this effector chromatin mobility was significantly affected. Mass spectrometry experiments attempted to test whether HopO1-1 interacts with chromatin, but the results do not support a strong interaction with chromatin or chromatin-associated proteins. Nevertheless, multiple interactors were identified with roles in processes such as protein synthesis (RNA helicases, KH-domain proteins), actin polymerisation and photosynthesis. Evidence for localisation in the chloroplasts as well as the onset of chlorosis in plants expressing HopO1-1 may also point towards a role of this effector in photosynthetic processes.

5.3. Results

5.3.1. *Pst* DC3000 delivers many effectors into the plant nucleus

The completely sequenced genome of *Pseudomonas syringae* DC3000 *pv. tomato* contains approximately 30 effectors, which are delivered into the host cell via a T3SS (Chang et al., 2005; Schechter et al., 2006). Many of these have a known sub-cellular localisation, however, there has been

no study to comprehensively evaluate the sub-cellular localisation profile of all effectors. It is, therefore, reasonable to hypothesise that the *Pst* DC3000 effectorome contains several nuclear localised effectors with the role of promoting virulence. In order to find promising candidates with nuclear localisation as well as functions relating to chromatin remodelling, we followed a comprehensive screening approach as follows.

Firstly, to identify effectors with a putative Nuclear Localisation Signal (NLS), an *in silico* analysis took place using public databases for NLS predictions. The databases used were NLStradamus (Nguyen Ba et al., 2009), NucPred (Brameier et al., 2007) and NLS Mapper (Lin and Hu, 2013), allowing for various methods of NLS prediction. NLS Mapper was able to identify mono-partite as well as bi-partite NLS sequences using a classical NLS functionality screen. The NLStradamus algorithm was used to detect similar residue frequency distribution (different from that of background residues) commonly found in NLS sequences. The algorithm NucPred had the advantage of not being restricted to a predefined set of NLS signatures and could discover non-canonical NLSs. The NLS prediction results are summarised in detail in the *Supplementary Table S5.1*. The variability in the algorithms used resulted in a relatively low coherence amongst the different prediction tools, however, agreement between 2 tools was found in the case of HopO1-1, HopB1, HopH1 and HopY1. Overall, the *in silico* analysis provided an initial prediction of 7 nuclear-localised effector candidates with at least one tool suggesting the presence of a NLS (HopO1-1, HopT1, HopB1, HopH1, HopY1, HopAA1-1, HopG1).

Secondly, to corroborate these results, a biochemical approach was employed to characterize the targeting of *Pst* DC3000 effectors to the nucleus. To this end, a near-complete gene library of 24 *Pst* DC3000 effectors was obtained, cloned downstream of a strong 35S promoter and fused to a sequence encoding three C-terminal hemagglutinin (HA) epi-

tope tags or a single copy of the GFP. After transiently expressing the HA-tagged effectors in *N. benthamiana* leaves, a nuclear isolation protocol took place followed by immunoblotting using an α-HA antibody. The immunoblots presented in *Figure 5.2* showed that at least 14 effectors can be detected in the nucleus of *N. benthamiana,* but only 6 of these (HopO1-1, HopT1, HopB1, HopH1, HopK1 and HopAO1) were exclusively localised in the nucleus. The effectors HopM1 and HopN1 with a well-established purely cytoplasmic localisation were included as negative controls.

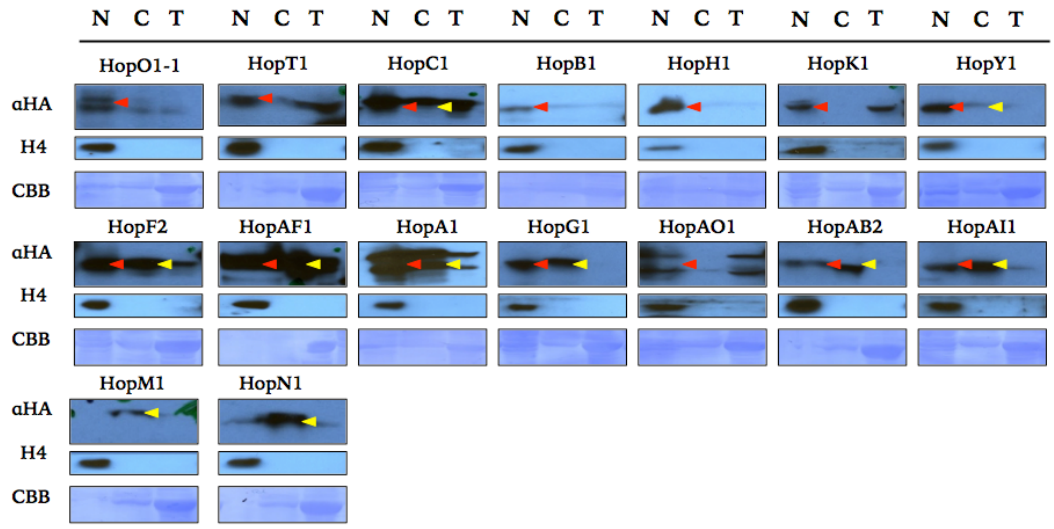

Figure 5.2. Identification of nuclear localised effectors by nuclear isolation and immunoblotting. Nuclear effector ORF sequences were expressed downstream a 35S promoter with a N-ter 3x HA tag. After transient expression in *N. benthamiana,* a nuclear isolation protocol was used to separate Nuclear (N) and Cytoplasmic (C) fractions. A sample of the Total (T) input fraction was loaded as well. Successful isolation of the nuclear fraction is shown by the presence of histone H4 in the N, but not in the C fraction. A yellow arrow is used to indicate the presence of protein in the cytosolic fraction, and a red arrow is used to indicate the presence of protein in the nuclear fraction. A plant cytoplasmic protein has not been used here.

Based on the preliminary data using the *in silico* analysis and the biochemical approach in *N. benthamiana,* a list of 14 candidate effectors was used in the next steps of the nuclear localisation screen using confocal microscopy. Specifically, the aim was to obtain greater resolution as to whether each of these effectors localises strictly to the nucleus or may also localise to the cytoplasm. To this end, GFP-tagged effectors were used to transiently express these GFP-tagged effectors in *N. benthamiana* and in

A. thaliana protoplasts and their subcellular localisation was determined using confocal microscopy. *Figure 5.3* shows confocal images of transiently expressed effectors in *N. benthamiana*. Images of GFP, which is known to have dual localisation in cytosol/nucleus, and GFP-H2B, which is a nuclear-only protein are included as controls. Transient expression in *N. benthamiana* of the complete library of *Pst* DC3000 effectors showed that at least 11 effectors localise to the nucleus including HopO1-1 and HopT1, which were previously found to contain a NLS and to be present in the nuclear fraction according to the immunoblots.

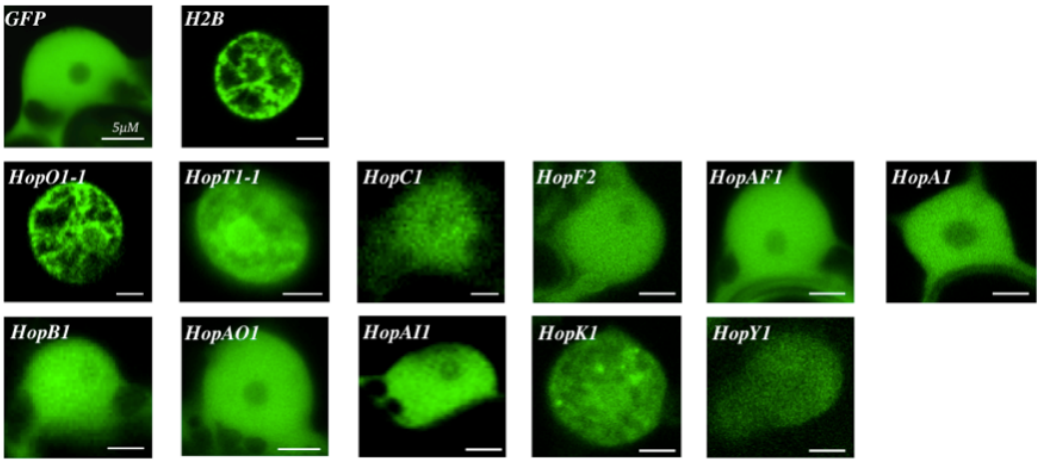

Figure 5.3. Putative nuclear localised effectors transiently expressed in *N. benthamiana*. Leaves were transfected with N-ter GFP fusions of *Pst* DC3000 type III effectors. Only nuclear localised effectors are shown. Effectors included in *Fig. 5.2.* but not in *Fig 5.3.* have been previously tested.

It is interesting to note that in addition to the subcellular localisation of each effector, confocal microscopy experiments allowed us to identify specific nuclear patterns typical of transcription-related proteins. More specifically, effector HopO1-1 displayed a pattern remarkably similar to H2B, which is described by a patchy arrangement. This could potentially suggest that HopO1-1 co-localises with chromatin in the same way as H2B. By contrast, most effectors with the exception of HopT1 and HopK1 converged towards a GFP-like pattern suggesting that they have a more diffused distribution throughout the nucleus and that an interaction or co-localisation with chromatin is lacking. As far as HopT1 and HopK1 are concerned, their localisation pattern stands somewhere between GFP

and H2B, reminiscent of transcription-factors, which are commonly detected as speckles at transcriptional hotspots in the nucleus (Siersbaek et al., 2014). The effectors HopC1, HopF2, HopAF1, HopA1, HopB1, HopAO1, HopY1 displayed a more diffused distribution in the nucleus, whilst it can be clearly observed that none of these effectors localises to the nucleolus, with the exception of HopT1 and HopK1. In the case of HopT1, a much stronger nucleolar signal is observed.

We further confirmed nuclear localisation of effectors by visualising them under a confocal microscope in *A. thaliana* leaf protoplasts transiently expressing the same library of GFP-tagged effectors. *Figure 5.4* shows the results from protoplast-expressed effectors, which are largely in agreement with the results obtained in the *N. benthamiana* screen *(Fig. 5.3)*. Due to lower levels of expression as well as a smaller nucleus size as compared to *N. benthamiana*, the same level of resolution could not be obtained so as to identify whether the effectors displayed a patchy or diffused organization. The protoplast screen identified HopH1 and HopG1 as two additional nuclear localised effectors, which were not successfully expressed in *N. benthamiana* leaves. HopT1 is missing from the protoplast screen due to unsuccessful expression in protoplasts.

The localisation screens presented above showed that 14 effectors (~40% of *Pst* DC3000 effectorome) in total were found to be localised in the nucleus by at least one experimental method (refer to *Fig. 5.7*).

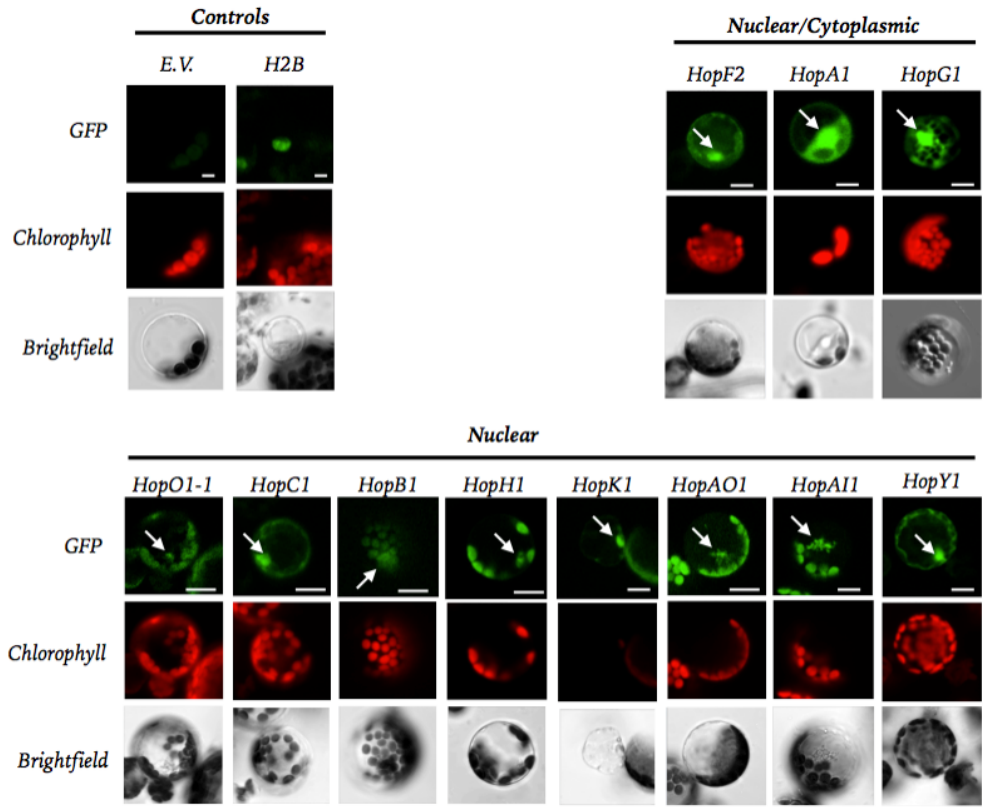

Figure 5.4. Nuclear localised effectors in Arabidopsis protoplasts. Protoplasts from *A. thaliana* leaves were transfected with N-ter GFP fusions of *Pst* DC3000 type III effectors. Only nuclear localised effectors are shown. The remaining effectors from the nuclear localisation screen *Pst DC3000* were previously tested and thus not included this screen. The size bar represents 10µm.

5.3.2. Some nuclear effectors have chromatin binding capacity

The localisation screen was the first step towards identifying effectors with activities relating to host nuclear processes, which could lead us to the identification of virulence mechanisms of *Pst* DC3000. In an attempt to identify effectors with the ability to interfere with DNA/chromatin-related processes we employed Fluorescence Recovery After Photobleaching (FRAP). This technique provides useful information on the kinetics of a protein of interest. The hypothesis is that proteins involved in chromatin-related processes such as gene transcription and DNA replication will interact with basic chromatin components or chromatin-associated proteins and as a result would be largely immobile (H2B-like). In contrast, proteins that diffuse freely inside the nucleus will display high mobility (GFP-like) (Day et al., 2012). The screen involved expressing the

candidate effectors in *N. benthamiana* and performing FRAP experiments. The FRAP screen revealed that 4 effectors (HopT1-1, HopO1-1, HopC1 and HopAI1) recovered in a manner quantitatively similar to the H2B control. By contrast, intermediate/fast recovery was observed for the rest of the effectors (*Figure 5.5*). Due to the inherent variability of FRAP experiments, it was difficult to further characterise the dynamics of the effectors which belong to the 'intermediate/fast recovery' group. In conclusion, the results presented here strongly point towards the presence of multiple *Pst* DC3000 effectors that may be associated with chromatin.

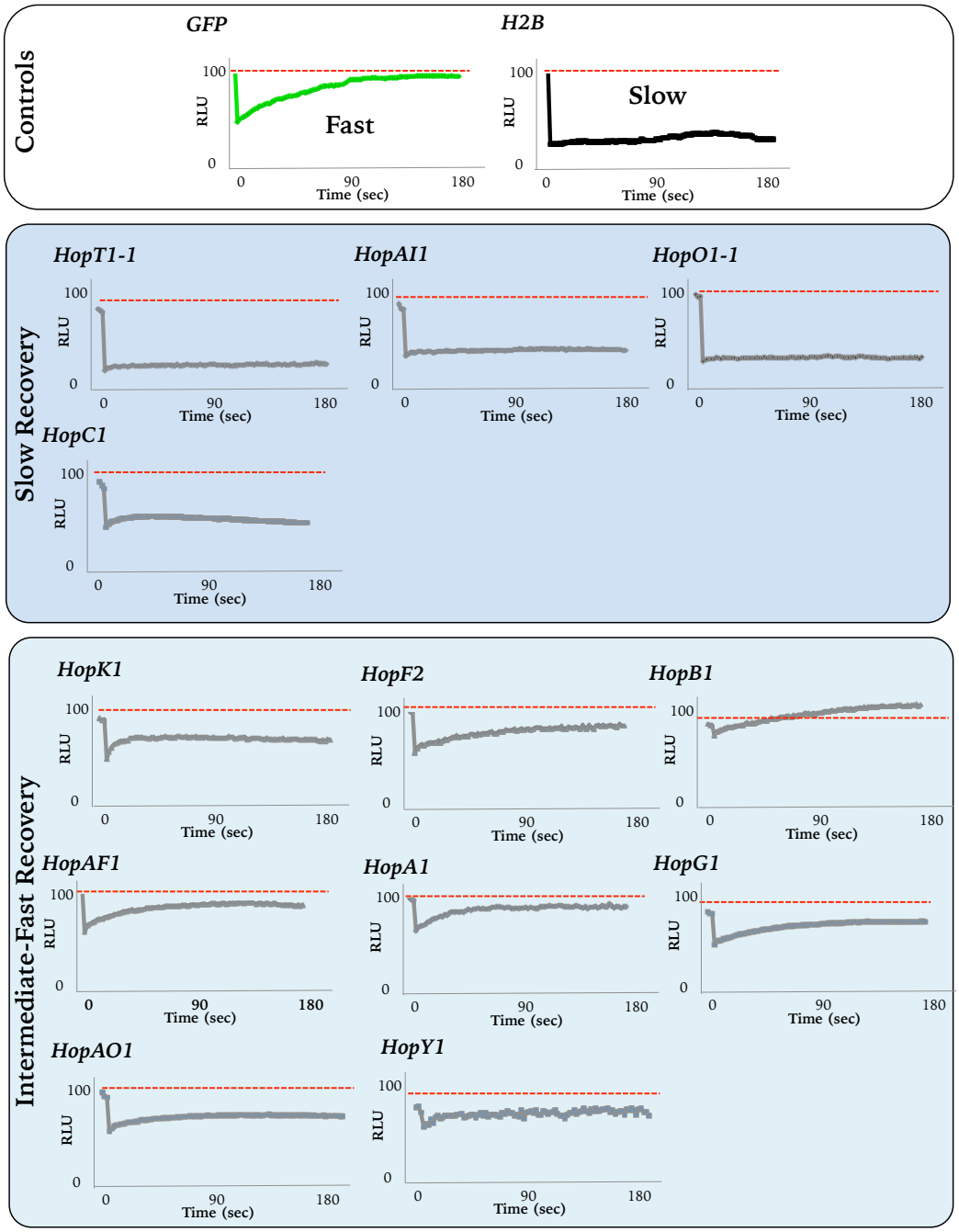

Figure 5.5. Fluorescence recoveries for effectors expressed in *N. benthamiana*. The effectors shown were transiently expressed in leaves from *N. benthamiana* leaves, whilst imaging and FRAP took place 3 days post infiltration. Representative FRAP experiments are shown in the three panels. The effectors are split according to FRAP dynamics broadly in a 'slow' and an 'intermediate-fast' category. The red line represents initial fluorescence prior to photobleaching (maximum fluorescence recovery).

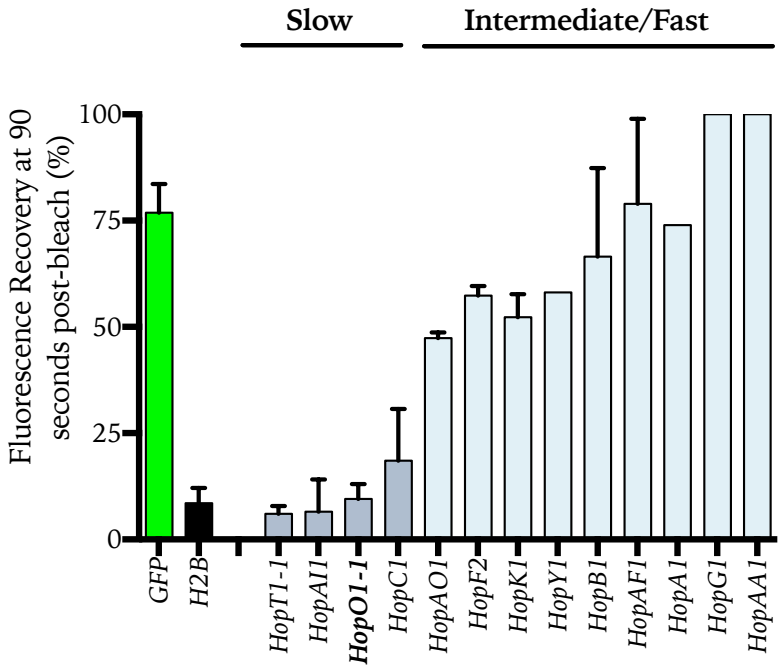

Figure 5.6. Chromatin binding properties of *P. syringae* DC3000 nuclear effectors in *N. benthamiana*. A library of nuclear localised effectors was screened for binding to chromatin (DNA and/or histones) using the FRAP method. GFP-tagged effectors were transiently expressed in *N.benthamiana* leaves and imaged 3 days post-infiltration. For HopY1 and HopA1, FRAP experiments could be conducted successfully only on one nucleus for each construct, due to low transformation rates and low levels of fluorescence. HopG1 and HopAA1 displayed very fast recoveries resulting in total fluorescence recovery of more than 100%.

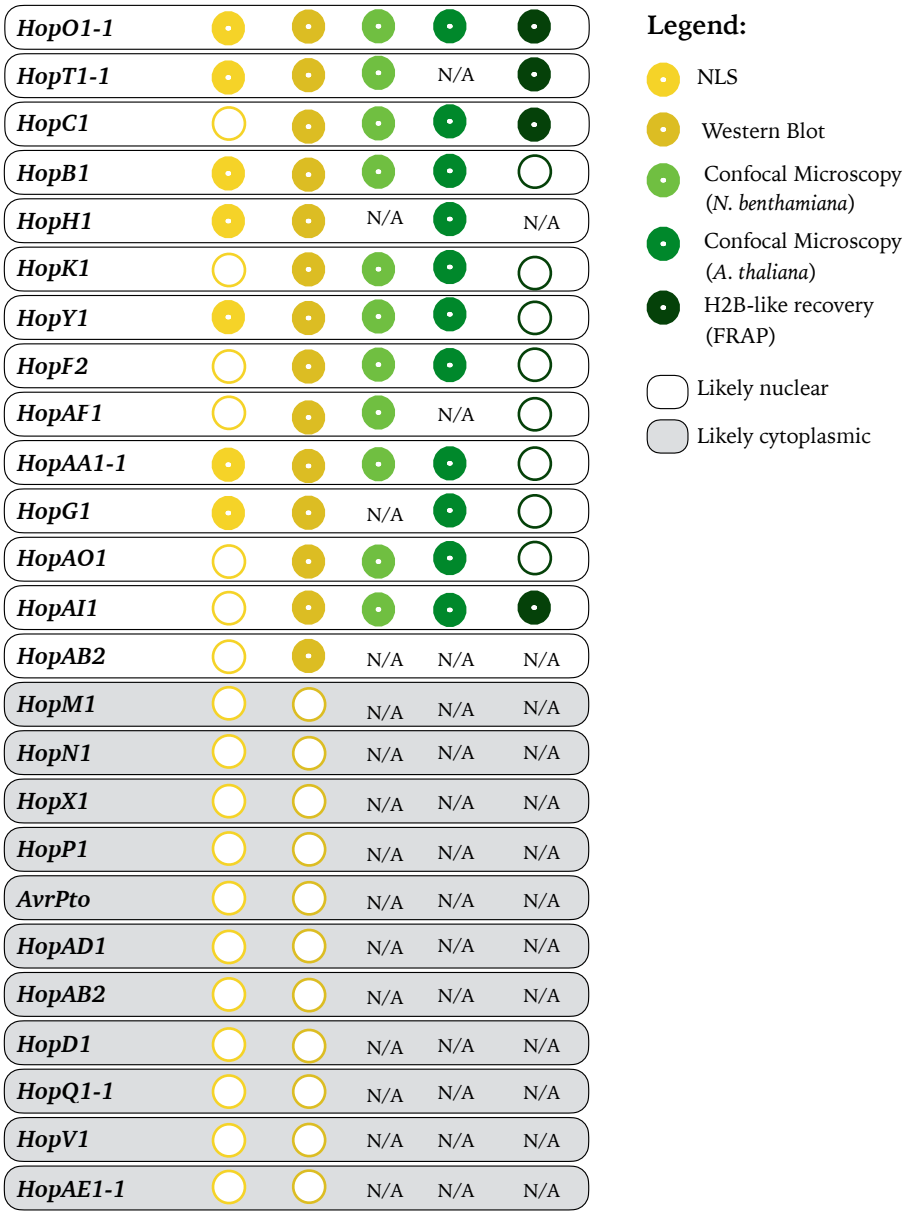

Figure 5.7. A comprehensive screening methodology towards identifying chromatin-associated effectors. *NLS, Nuclear Localisation Signal,* a full circle indicates the presence of a NLS as identified by at least one prediction website; *Western blotting,* a full circle indicates nuclear localisation as identified by immunoblotting after nuclear isolation; *Confocal microscopy*, a full circle indicates nuclear localisation as identified by confocal microscopy either in *N. benthamiana* or *A. thaliana* protoplasts; *H2B-like recovery***,** a full circle indicates an H2B-like recovery as identified by FRAP experiments; *N/A, not available,* indicates that data are not available.

5.3.3. HopO1-1 is a putative ADP-RT and capable of reducing chromatin mobility

Amongst the effectors identified to have an H2B-like recovery in our FRAP experiments, HopO1-1 and HopT1 had highly favourable profiles in terms of nuclear localisation and chromatin binding (*Figure 5.7*), however, more complete data had been collected for HopO1-1. Conducting a literature search on HopT1 showed this effector's role in suppressing miRNA-directed translation inhibition consistent with an involvement of AGO1 (Argonaute 1) (Navarro et al., 2008), which is responsible for inhibiting gene expression transcriptionally or post-transcriptionally (Baulcombe, 2004). HopT1 has thus been shown to interfere with miRNA pathways, which are essential in plant immunity. Meanwhile, a literature search on HopO1-1 showed that very little is known about this effector. However, homology searches identified its close sequence similarity to other well-characterised ADP-ribosyltransferase enzymes with known roles in various cellular processes including chromatin remodelling (Ishibashi et al. 2014). Thus, we focused on HopO1-1, a putative ADP-ribosyltransferase (ADP-RT) bearing homology to the already characterised effector HopU1 (Fu et al., 2007) with a known role in suppressing immunity. Specifically, as shown in *Figure 5.1*, HopO1-1 (as well as the highly related HopO1-2) bear a high degree of sequence similarity both in the putative ADP-RT domain (36%) as well as in the full protein sequence (24%). A search for protein domains on HopO1-1 using the protein homology tool from NCBI (Marchler-Bauer et al., 2011) did not show the presence of any domains in addition to the ADP-RT domain (*Supp. Figure S5.2*).

The putative activity of HopO1-1 as an ADP-RT in combination with its nuclear localisation and in alignment with its potential association with chromatin, led to the hypothesis that HopO1-1 has the ability to interact with chromatin and to post-translationally modify chromatin

or chromatin-associated proteins. For this reason, we decided to further investigate HopO1-1 using a variety of tools to test its role in the pathogenicity of *Pst* DC3000.

Specifically, having found evidence that HopO1-1 is bound to the chromatin, we aimed to investigate whether this effector is able to alter host chromatin dynamics either in resting state or during flg22 elicitation (*as seen in Chapter 3, Fig. 3.2*). The experimental design to address this question involved transient co-expression of HA-tagged HopO1-1 and GFP-H2B in *N. benthamiana* leaves and the subsequent collection of leaf discs 3 days post infiltration. Leaf discs were elicited with 100nM flg22 prior to FRAP. We observed a faster recovery of chromatin in leaves elicited with flg22 in keeping with previous findings. Interestingly, the faster chromatin dynamics upon flg22 elicitation were reduced in the presence of HopO1-1. In other words, the 'chromatin opening' was no longer seen when HopO1-1 was expressed in the leaf despite elicitation with flg22 (*Fig 5.8a*). We verified that HopO1-1 was successfully expressed in the leaves tested by performing immunoblotting using an α-HA antibody (*Fig 5.8b*). This result could suggest that HopO1-1 associates with chromatin leading to slower chromatin dynamics in order to suppress the flg22-induced chromatin remodelling.

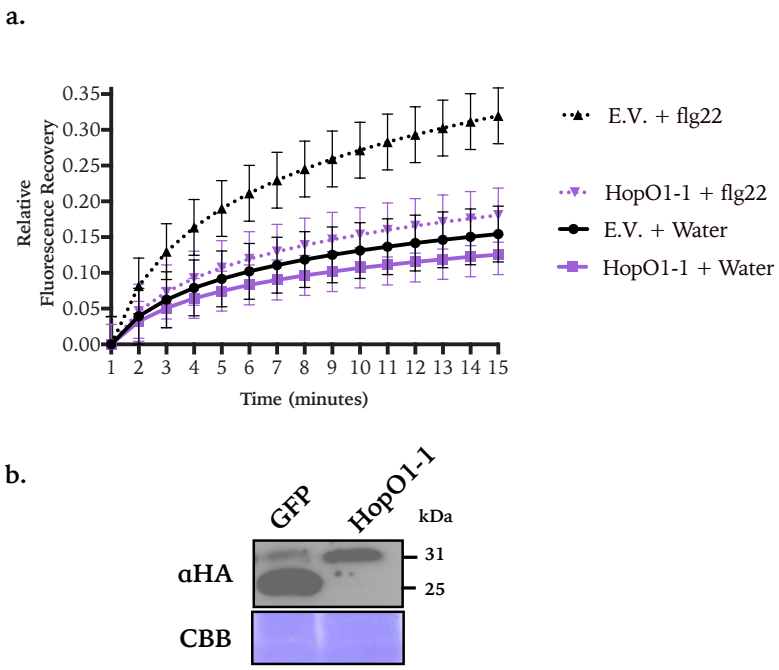

Figure 5.8. Chromatin mobility is reduced in the presence of HopO1-1. (a) *N. benthamiana* leaves transiently expressing H2B-GFP and co-infiltrated with empty vector (E.V) or HA-tagged HopO1-1 and sampled 3 days post infiltration. Leaf discs were removed and treated with water or flg22 (100nM) before FRAP experiment (n=10 nuclei); (b) Expression of HopO1-1 was later confirmed on the same leaves tested by immunoblot analysis using an HA-tagged GFP construct as control. CBB, Coomasie Brilliant Blue. The ladder is denoted by kDa.

5.3.4. HopO1-1 interacts with proteins involved in different processes

The FRAP results raise the question of how HopO1-1 is able to suppress chromatin remodelling. To this end, we performed immunoprecipitation experiments followed by mass spectrometry to identify the interacting partners of HopO1-1 within the nucleus. Specifically, a nuclear enrichment protocol was performed on Arabidopsis seedlings stably expressing a DEX-inducible *HopO1-1* gene with an HA tag. After induction of 14-day old seedlings with DEX or water control, the aerial tissue was formaldehyde cross-linked before nuclear enrichment and immunoprecipitation.

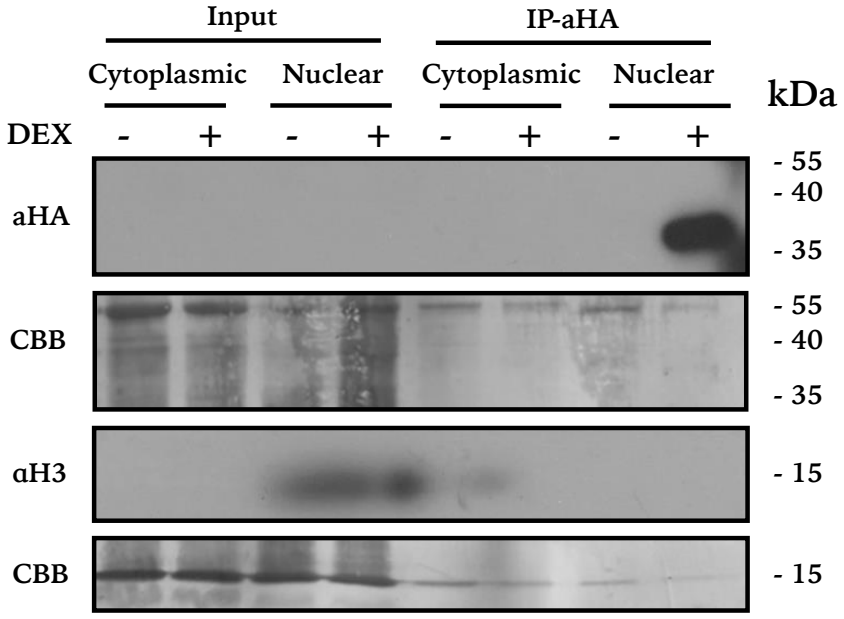

Figure 5.9. HopO1-1 is purified successfully after DEX induction, but does not interact with H3. After DEX-induction of *A. thaliana* seedlings expressing *DEX::HopO1-1-HA,* HopO1-1 was identified in the nuclear fraction (top panel). Anti-histone H3 (αH3) antibody was used to detect the presence of H3, after 'stripping' the membrane from the aHA antibody.

Figure 5.9 shows that HopO1-1 is detected in the nuclear fraction only in the DEX-induced sample. To test for the interaction with nucleosomes, an aH3 antibody was used, which did not show an interaction between HopO1-1 with H3.

After successful purification of HopO1-1, the immunoprecipitated samples were processed by mass spectrometry to identify the interacting partners of HopO1-1. *Figure 5.10* shows the sequence coverage of HopO1-1 from all biological replicates. The sequence coverage varied greatly between experiments, for example, in Experiment 1 HopO1-1 was identified at a 50% sequence coverage, while in Experiment 2 a coverage of 12% was observed in the DEX-induced samples, whereas a coverage of 35% and 15% was found in Experiments 3 and 4, respectively.

a. **HopO1-1 (NP_808677), 31kDa, 140/282 amino acids, 50% coverage**

MGNICGTSGSNHVYSPPISPQHASGSSTPVPSASGTMLSLSHEQILSQNYASN
IKGKYRTNPRKGPSPRLSDTLMKQALSSVITQEKKRLKSQPKSIAQDIQPPNS
MIKNALDEKDSHPFGDCFSDDEFLAIHLYTSCLYRPINHHLRYAPKNDVAPV
VEAMNSGLAKLAQYPDQVSGQLHRGIKQKMDDGEVMSRFKPGNTYRDDA
FMSTSTRMDVTEEFTSDVTLHLQSSSAVNIGPFSKNPYEDEALIPPLTPFKVT
GLHKQDDRWHVHLNEIAESSDE

b. **HopO1-1 (NP_808677), 31kDa, 34/282 amino acids, 12% coverage**

MGNICGTSGSNHVYSPPISPQHASGSSTPVPSASGTMLSLSHEQILSQNYASN
IKGKYRTNPRKGPSPRLSDTLMKQALSSVITQEKKRLKSQPKSIAQDIQPPNS
MIKNALDEKDSHPFGDCFSDDEFLAIHLYTSCLYRPINHHLRYAPKNDVAPV
VEAMNSGLAKLAQYPDQVSGQLHRGIKQKMDDGEVMSRFKPGNTYRDDA
FMSTSTRMDVTEEFTSDVTLHLQSSSAVNIGPFSKNPYEDEALIPPLTPFKVT
GLHKQDDRWHVHLNEIAESSDE

c. **HopO1-1 (NP_808677), 31kDa, 100/282 amino acids, 35% coverage**

MGNICGTSGSNHVYSPPISPQHASGSSTPVPSASGTMLSLSHEQILSQNYASN
IKGKYRTNPRKGPSPRLSDTLMKQALSSVITQEKKRLKSQPKSIAQDIQPPNS
MIKNALDEKDSHPFGDCFSDDEFLAIHLYTSCLYRPINHHLRYAPKNDVAPV
VEAMNSGLAKLAQYPDQVSGQLHRGIKQKMDDGEVMSRFKPGNTYRDDA
FMSTSTRMDVTEEFTSDVTLHLQSSSAVNIGPFSKNPYEDEALIPPLTPFKVT
GLHKQDDRWHVHLNEIAESSDE

d. **HopO1-1 (NP_808677), 31kDa, 46/282 amino acids, 15% coverage**

MGNICGTSGSNHVYSPPISPQHASGSSTPVPSASGTMLSLSHEQILSQNYASN
IKGKYRTNPRKGPSPRLSDTLMKQALSSVITQEKKRLKSQPKSIAQDIQPPNS
MIKNALDEKDSHPFGDCFSDDEFLAIHLYTSCLYRPINHHLRYAPKNDVAPV
VEAMNSGLAKLAQYPDQVSGQLHRGIKQKMDDGEVMSRFKPGNTYRDDA
FMSTSTRMDVTEEFTSDVTLHLQSSSAVNIGPFSKNPYEDEALIPPLTPFKVT
GLHKQDDRWHVHLNEIAESSDE

Figure 5.10. HopO1-1 is detected by mass spectrometry in *A. thaliana*. HopO1-1 sequence coverage is highlighted in yellow for peptides that were uniquely identified at least once. Only the DEX-induced sample is shown. (a) Experiment 1 showed a protein coverage of 50%; (b) Experiment 2 showed a protein coverage of 12%; (c) Experiment 3 showed a protein coverage of 35% and (d) Experiment 4 showed a protein coverage of 15%.

In total, 4 biological replicates were completed to identify the interactors of HopO1-1. *Table 5.2* shows a summary of potential interactors, categorised on the basis of gene ontology. A quantitative analysis was deemed inappropriate in this set of experiments due to the identification of bait protein (HopO1-1) in the un-induced samples (DEX^-) in Experiments 2 and 4. This is likely to be due to leaky transcription from the inducible promoter. The classification of the identified proteins by function as seen on the first column of *Table 5.2*, suggested a number of different

hypotheses regarding the mode of action of HopO1-1. For example, histones H2A, H2B and H3 were identified only in Experiment 1, but in both DEX- and DEX+ samples. Together with the results presented in *Figure 5.9*, it appears unlikely that HopO1-1 directly interacts with histones.

Interestingly, several KH-domain containing proteins were identified, mostly in Experiment 1, but also in Experiment 2, however, due to the presence of these proteins in the un-induced sample of Experiment 1, further supporting evidence is required. Given the involvement of ADP-ribosylating proteins with RNA metabolism and protein translation (Bock et al., 2015), we checked whether any relevant interactions were found in our experiments, but it appears that the interaction with one RNA-binding protein (AT3G15010) was not specific to the induced sample. Evidence for interaction with DEAD/H box RNA helicases was also found here and is supported by findings that these proteins have roles in RNA metabolism and translation (Jankowsky et al., 2001). As mentioned earlier, HopU1 was shown to interfere with protein translation (Fu *et al* 2007), whilst other ADP-RTs have been found to ADP-ribosylate elongation factors (EF-2) to inhibit protein translation (Mateyak and Kinzy, 2013). In our experiments, there was evidence of HopO1-1 interacting with EIF4A1, EIF4A2 and SH3-like protein, which are all known to have roles in translation (Jackson et al., 2010). Therefore, these interactions should be explored further in future work.

In line with the reported interaction of bacterial ADP-RTs with actin (Visschedyk et al., 2010), we showed the interaction with several relevant proteins such as tubulin or actin. Once again, whilst there is some evidence to suggest interaction of tubulins with HopO1-1, the presence of tubulin peptides in the control samples warrants further investigation. Two members of the NB-RR family were found in Experiment 2 to be specific to DEX^+ induced conditions without further confirmation in other biological replicates. Moreover, Experiment 2 yielded a large num-

ber of kinases as putative interactors of HopO1-1, none of which were confirmed in the other repeats. Furthermore, RabGTPases are known regulators of cAMP signalling and ADP-ribosylation is an important process therein, which prompted us to look for any relevant interactors. To this end, we found some evidence supporting that HopO1-1 could interact with ATRAB8D. Given that ExoS, a ADP-ribosyltransferase from *Pseudomonas aeruginosa* interacts with Rab5 GTPase in mammalian cultured cells (Barbieri et al., 2001), this interaction could be explored further in future experiments. Strong interaction of HopO1-1 with a clathrin protein was found in one repeat, which is in agreement with our knowledge of ADP ribosylation being a crucial step in the formation of clathrin-coated vesicles upon vesicle trafficking (Kornfeld and Mellman, 1989).

Probability Legend:
over 95%
80% to 94%
50% to 79%
20% to 49%
0% to 19%

			Exp 1		Exp 2		Exp3		Exp 4	
			Dex-	Dex+	Dex-	Dex+	Dex-	Dex+	Dex-	Dex+
Effector (Bait)	**HopO1-1**	**NP_806677**	4	16	0	9	8	7	0	2
Translation	KH domain	AT2G25970	11	10	0	0	0	0	0	0
	KH domain/Zn finger	AT3G12130	1	2	0	8	0	0	0	0
	KH domain	AT1G33680	1	5	0	0	0	0	0	0
	Poly(A) Binding protein	AT4G34110	0	0	0	3	0	0	0	0
	RNA-binding protein	AT3G15010	12	8	0	0	0	0	0	0
	EIF4A1	AT3G13920	0	0	0	14	0	0	0	0
	EIF4A2	AT1G54270	0	0	0	13	0	0	0	0
	SH3-like protein	AT1G09590	0	0	0	3	0	0	0	0
	DEA(D/H) box RNA heli	AT5G11170	0	0	0	3	0	0	0	0
	DRH1 RNA helicase	AT3G01540	0	0	0	9	0	0	0	0
	DEA(D/H) box RNA heli	AT3G58510	0	0	0	4	0	0	0	0
Histone	Histone H3	AT1G07660	8	9	0	0	0	0	0	0
	Histone H2B	AT1G07790	6	5	0	0	0	0	0	0
	Histone H2A	AT5G27670	2	3	0	0	0	0	0	0
Tubulin & Actin	TUB2	AT5G62690	5	8	0	12	0	0	0	0
	TUB9	AT4G20890	5	8	0	0	8	0	0	0
	TUB4	AT5G44340	0	0	0	9	0	0	0	0
	TUB5	AT1G20010	0	0	0	10	3	3	0	2
	TUB6	AT5G12250	0	0	0	11	0	0	0	0
	Tubulin alpha 3	AT5G19770	7	3	0	0	0	0	0	0
	ACT12	AT3G46520	4	5	0	0	5	2	3	3
NB-LRR	TIR-NBS-LRR Family	AT3G51570	2	0	0	0	0	0	0	0
	CC-NBS-LRR Family	AT5G43470	0	0	0	9	0	0	0	0
	CC-NBS-LRR Family	AT5G48620	0	0	0	5	0	0	0	0
Kinase	LRR Kinase	AT1G51805	0	0	0	10	0	0	0	0
	LRR Kinase	AT4G30520	0	0	0	4	0	0	0	0
	LRR Kinase	AT3G14840	0	0	0	6	0	0	0	0
	LRR Kinase	AT5G10290	0	0	0	0	5	0	0	0
	RLK4	AT4G23180	0	0	0	3	0	0	0	0
	BR-signalling kinase 1	AT4G35230	0	0	0	7	5	0	0	0
	BR-signalling kinase 3	AT4G00710	0	0	0	3	0	0	0	0
	CPK21	AT4G04720	0	0	0	7	0	0	0	0
	CPK9	AT3G20410	0	0	0	3	0	0	0	0
	CPK15	AT4G21940	0	0	0	5	0	0	0	0
	CDPK6	AT4G23650	0	0	0	9	0	0	0	0
Rab GTPase	ATRAB8D	AT4G20360	0	0	0	3	0	0	8	8
Clathrin	Clathrin heavy chain	AT3G11130	0	0	0	6	0	0	0	0

Table 5.1. Interactors of HopO1-1 in *A. thaliana*. The putative interactors from all biological replicates are shown. The number of exclusive unique peptides is displayed with a color code indicating the probability of each peptide. The different proteins are grouped based on known function.

Next, we reasoned that the leaky expression of HopO1-1 from the DEX-inducible promoter was responsible for the lack of clear significant interactors in *A. thaliana*. Thus, we decided to take a complementary approach, which involved the identification of HopO1-1 interactors in *N. benthamiana*. This was also a logical next step, because the phenotypes observed in our FRAP experiments (*Fig. 5.8*) were in the context of *N. benthamiana*.

To this end, we generated HopO1-1 constructs with an N-terminus or C-terminus GFP tag for transient expression. We followed the same protocols for formaldehyde-crosslinking, nuclear extraction and immunoprecipitation and checked for expression of the constructs by western blotting (*Fig. 5.11a*). Although we failed to detect the N-ter GFP-tagged HopO1-1 by western blot, we were confident that the protein was expressed after observing the nuclear localisation of both, using a confocal microscope *(Fig. 5.11b)*. After submitting the samples to mass spectrometry, the baits were identified with a variable sequence coverage (*Fig. 5.12*).

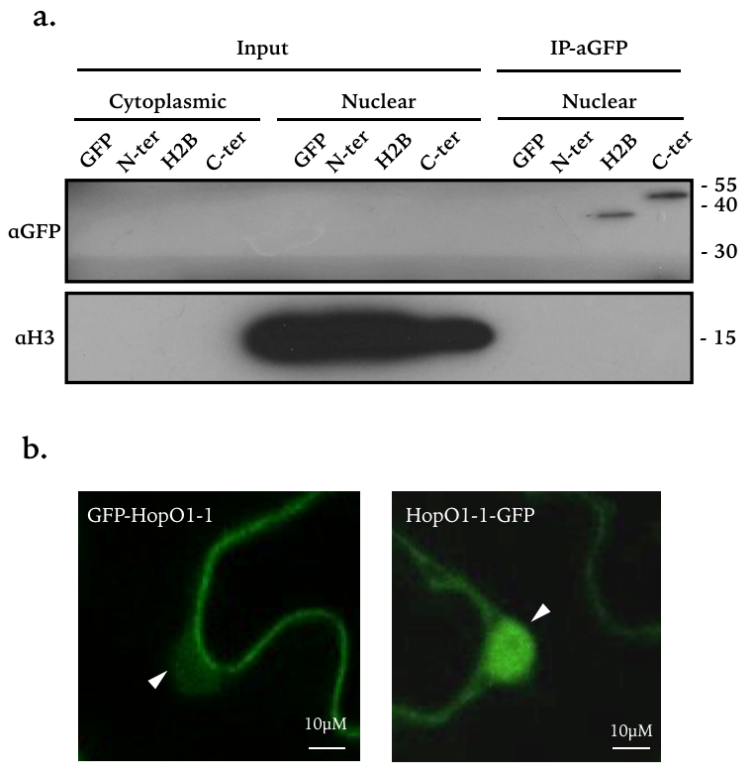

Figure 5.11. HopO1-1 expression and purification from *N. benthamiana* prior to mass spectrometry. a. GFP-tagged HopO1-1 (N-ter and C-ter) were transiently expressed in *N. benthamiana* leaves and purified following a nuclear extraction protocol and GFP-immunoprecipitation. Immunoblot was performed using antibodies against GFP and histone H3; **b**. The same samples were previously visualised under the confocal microscope.

a.

HopO1-1 (NP_808677), 31kDa, 17/282 amino acids, 6% coverage

MGNICGTSGSNHVYSPPISPQHASGSSTPVPSASGTMLSLSHEQILSQNYASN
IKGKYRTNPRKGPSPRLSDTLMKQALSSVITQEKKRLKSQPKSIAQDIQPPNS
MIKNALDEKDSHPFGDCFSDDEFLAIHLYTSCLYRPINHHLRYAPKNDVAPV
VEAMNSGLAKLAQYPDQVSGQLHRGIKQKMDDGEVMSRFKPGNTYRDDA
FMSTSTRMDVTEEFTSDVTLHLQSSSAVNIGPFSKNPYEDEALIPPLTPFKVT
GLHKQDDRWHVHLNEIAESSDE

b.

HopO1-1 (NP_808677), 31kDa, 55/282 amino acids, 20% coverage

MGNICGTSGSNHVYSPPISPQHASGSSTPVPSASGTMLSLSHEQILSQNYASN
IKGKYRTNPRKGPSPRLSDTLMKQALSSVITQEKKRLKSQPKSIAQDIQPPNS
MIKNALDEKDSHPFGDCFSDDEFLAIHLYTSCLYRPINHHLRYAPKNDVAPV
VEAMNSGLAKLAQYPDQVSGQLHRGIKQKMDDGEVMSRFKPGNTYRDDA
FMSTSTRMDVTEEFTSDVTLHLQSSSAVNIGPFSKNPYEDEALIPPLTPFKVT
GLHKQDDRWHVHLNEIAESSDE

Figure 5.12. HopO1-1 is detected by mass spectrometry in *N. benthamiana*. HopO1-1 sequence coverage is highlighted in yellow for peptides that were identified at least once; (a) N-ter GFP-tagged HopO1-1; (b) C-ter GFP-tagged HopO1-1

Table 5.2 shows the MS results from two biological replicates in *N. benthamiana*. Experiment 1 was done using HA-tagged HopO1-1 construct, while Experiment 2 involved both N-ter and C-ter tagged constructs of HopO1-1. A GFP-H2B control was included to identify potential common interactors between H2B and HopO1-1 to assess whether HopO1-1 has a direct or indirect interaction with chromatin. The same grouping as in *Table 5.1* was used in *Table 5.2*.

In these experiments, there was a stronger indication that HopO1-1 interacts with KH-domain proteins. Several RNA-binding and Poly-A-binding proteins showed enrichment in HopO1-1 sample, however, it remains unclear whether these interactions are true, as some RNA-binding proteins were identified in our GFP control. Other proteins with described roles in translation did not show a clear enrichment pattern across the two biological replicates, with the exception of DEAD box RNA helicases, which point towards an interaction with HopO1-1.

With regards to chromatin-associated and histone proteins, there seems to be no enrichment in our HopO1-1 samples, which confirms findings from the MS experiments in *A. thaliana*. Furthermore, tubulin and actin were present to a lesser extent than in our *A. thaliana* MS results with peptides in our control sample for actin and very little enrichment in our HopO1-1 sample for tubulin. Meanwhile, PEPR2 receptor was found to interact with HopO1-1, which could be an interesting interaction to follow up given the role of PEPR2 as a PAMP receptor (albeit an oomycete PAMP receptor) (Yamaguchi et al., 2010).

Probability Legend:
over 95%
80% to 94%
50% to 79%
20% to 49%
0% to 19%

			Exp 1				Exp 2			
			HA-tagged				GFP-tagged			
			GFP		HopO1-1		GFP	H2B	N-ter	C-ter
Effector (Bait)	**HopO1-1**	**NP_806677**	0	0	6	8	0	0	2	5
Protein Translation & RNA metabolism	KH-domain	NICBE_018106.1_TGAC	0	0	0	5	0	0	2	0
	KH-domain / RNA binding	NbS00057914g0013.1_SGN	0	0	0	4	0	0	0	0
	RNA binding protein	NbS00004079g0002.1_SGN	0	0	0	7	0	0	0	0
	RNA binding protein	NbS00043627g0002.1_SGN	7	5	8	25	0	0	0	0
	RNA binding protein	NICBE_156354.1_TGAC	6	5	0	11	0	0	0	0
	RNA binding protein	NbS00011011g0001.1_SGN	0	0	6	15	0	0	0	0
	Nuclear ribonucleoprotein D0	NICBE_106212.1_TGAC	0	0	0	12	0	0	0	0
	Nuclear ribonucleoprotein Q	NICBE_107290.2_TGAC	0	0	0	4	0	0	0	0
	WHI3	NICBE_122568.1_TGAC	0	0	0	8	0	0	0	0
	Nuclear polyadenylated RBP 4	NbS00016009g0003.1_SGN	0	0	0	0	0	0	3	0
	Polyadenylate-binding protein	NICBE_411537.1_TGAC	0	0	0	0	0	0	3	0
	Polyadenylate-binding protein	NbS00001538g0002.1_SGN	0	0	0	6	0	0	0	0
	Polyadenylate-binding protein	NICBE_247741.1_TGAC	0	0	0	4	0	0	0	0
	Polyadenylate-binding protein	NICBE_246621.1_TGAC	0	0	0	12	0	0	0	0
	Polyadenylate-binding protein	NICBE_309056.1_TGAC	0	0	0	4	0	0	0	0
	Polyadenylate-binding protein	NICBE_389866.1_TGAC	0	0	0	2	0	0	0	0
	Polyadenylate-binding protein	NbS00027422g0005.1_SGN	6	0	0	7	0	0	0	0
	RNA binding protein Musashi 1	NbS00015780g0008.1_SGN	0	0	0	0	0	0	2	0
	Elongation factor 1 alpha	NbS00019623g0001.1_SGN	5	7	0	6	0	0	0	0
	Elongation factor 1 alpha	NbS00007372g0013.1_SGN	0	0	0	0	0	0	4	0
	EIF4A-15	NICBE_012093.1_TGAC	4	0	0	0	0	0	0	0
	DEAD DEAD/DEAH box helicase	NICBE_085315.1_TGAC	0	0	0	0	0	0	3	0
	DEAD-box ATP-dependent RNA heli. 56	NICBE_015641.1_TGAC	0	0	0	0	0	2	4	0
	DEAD-box ATP-dependent RNA heli.	NICBE_138517.1_TGAC	0	0	0	14	0	0	0	0
Histones and DNA/chromatin-associated	Histone H1	NICBE_257082.1_TGAC	0	0	0	0	0	0	3	0
	Histone H2A	NbS00001942g0006.1_SGN	0	0	0	0	2	0	3	0
	Histone Deacetylase	NICBE_003162.1_TGAC	0	0	0	0	0	2	2	0
	Histone H2B	NICBE_289597.1_TGAC	0	0	8	0	0	0	0	0
	Histone H3.2	NbS00014992g0013.1_SGN	6	8	0	0	0	0	0	0
	Histone H4	NICBE_153093.1_TGAC	28	19	32	32	0	0	0	0
	Zn Finger CCCH domain protein	NICBE_069509.1_TGAC	0	0	0	5	0	0	0	0
Tubulin & Actin	Tubulin alpha chain	NICBE_040110.1_TGAC	0	0	0	0	0	0	0	2
	Actin-7	NICBE_128693.1_TGAC	0	7	9	6	0	0	0	0
ARF	ADP-ribosylation factor 2	NICBE_020747.1_TGAC	0	0	0	0	0	0	2	0
LRR	PEPR2	NbS00024482g0011.1_SGN	0	0	0	0	0	0	5	0
Photosynthesis	Oxygen-evolving enhancer protein 3-2	NICBE_135957.1_TGAC	0	0	5	0	0	0	0	0
	Oxygen-evolving enhancer protein 3-2	NICBE_170660.1_TGAC	0	0	0	0	0	0	3	0

Table 5.2. Interactors of HopO1-1 in *N. benthamiana*. The putative interactors from all biological replicates are shown. The number of exclusive unique peptides is displayed with a color code indicating the probability of each peptide. The different proteins are grouped based on known function.

5.3.2. HopO1-1 could have roles relating to photosynthesis

The MS experiments aimed to identify interactors that could explain the phenotypes observed previously in our lab. More specifically, (*Supp. Figure S5.3a*) in experiments conducted by Dr. Gimenez-Ibanez, *A. thaliana* plants expressing DEX-inducible HopO1-1 were more susceptible to subsequent *Pst* DC3000 infection as compared to control plants (no DEX induction), suggesting that HopO1-1 contributes to suppression of plant immunity. By infecting Col-0 plants with *Pst* DC3000 and *Pst* DC3000 *hopO1-1* (lacking *HopO1-1* gene) we could not observe a clear difference, which could suggest that in the presence of HopO1-1 prior to an infection, plant immunity is compromised, however, in the absence of HopO1-1 pathogen fitness is not significantly impaired *(Fig. 5.13)*.

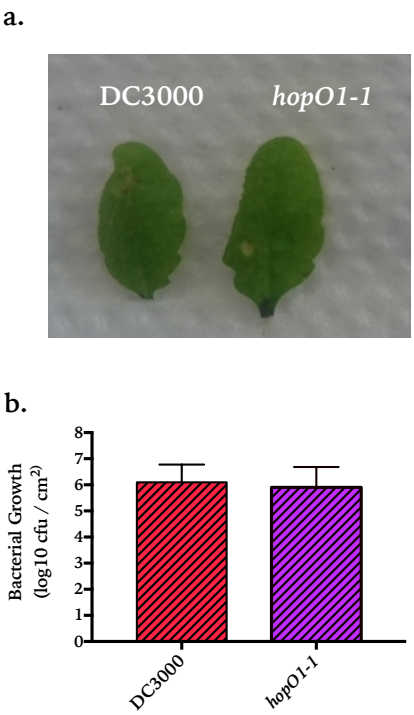

Figure 5.13. Deletion of *HopO1-1* does not reduce *Pst* DC3000 virulence. Syringe-infiltration of *Pst* DC3000 WT and *hopO1-1* has no significant difference in terms of (a) disease symptoms or (b) bacterial growth.

Additional experiments by Dr. Gimenez-Ibanez, pointed towards a role of HopO1-1 in photosynthetic processes. More specifically, in seedlings induced with DEX, expression of DEX-inducible HopO1-1 led

to a chlorotic effect (*Supp. Figure S5.3b*), which was not observed in un-induced plants. These findings could suggest either that HopO1-1 can also localise to the chloroplast or that HopO1-1 can affect the expression of nuclear-encoded chloroplastic genes (NECGs). A search query into the sub-cellular localisation signal database, LOCALIZER (Sperschneider et al., 2017) did not yield reliable outputs to suggest that HopO1-1 contains a chloroplast localisation signal. On one hand, HopO1-1 appeared to have a high probability to localise to chloroplasts, whilst on the other hand, effectors with a published chloroplast localisation such as HopI1 and HopN1 (Xin and He, 2013) yielded a low probability of chloroplast localisation (*Supp.Table S5.1*), suggesting that this approach is not always reliable for bacterial effectors. This is also probably due to the fact that certain effectors, such as AvrRps4 and HopK, employ non-canonical import sequences, which suggests that multiple strategies have evolved for effector localisation into the chloroplasts (Li et al., 2014c). Therefore, we decided to take a closer look into the localisation pattern of HopO1-1 using confocal microscopy to determine whether HopO1-1 can localise to the chloroplasts in addition to the nuclei. The experiments conducted by Dr. Gimenez-Ibanez after transiently expressing HopO1-1 in *N. benthamiana*, determined that the effector could also be localising to the chloroplasts (*Supp. Fig. 5.3c*).

In support of these findings, the interaction of HopO1-1 with Oxygen-evolving enhancer protein 3-2 (OEE3), may further suggest that HopO1-1 not only localises to the chloroplast, but also has *bona fide* targets therein, potentially targeting Photosystem II of which OEE3 is a known component (Umena et al., 2011).

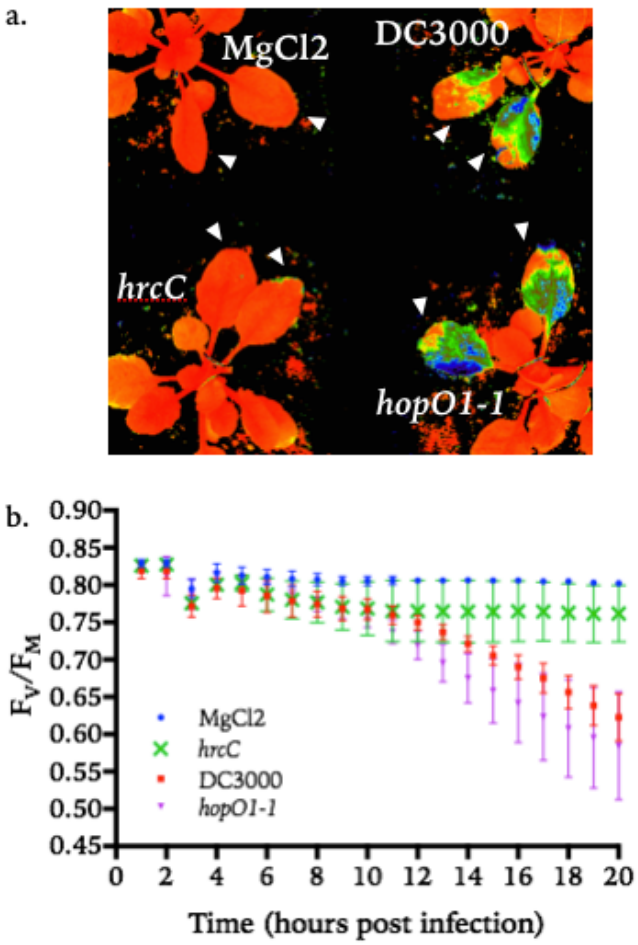

Figure 5.14. Photosynthetic activity is the same after infection with *Pst* DC3000 and *Pst* DC3000 *hopO1-1*. Col-0 plants were infiltrated with $MgCl_2$, *Pst* DC3000, *Pst* DC3000 *hrcC* or *Pst* DC3000 *hopO1-1* and chlorophyll imaging took place immediately after infection; (a) Photosynthetic activity (F_v/F_m) is stronger at the red end of the color spectrum, while blue suggests reduced activity; (b) F_v/F_m is shown after quantification across time. The values represent the mean ± standard error in relative chlorophyll units. The experiment was performed twice with similar results.

Altogether, a role of HopO1-1 in interfering with photosynthetic processes is possible. To further investigate this hypothesis, we attempted to measure whether the photosynthetic activity of *A. thaliana* plants is affected by HopO1-1 by infecting Col-0 plants with *Pst* DC3000 or *Pst* DC3000 *hopO1-1* (lacking HopO1-1). We employed a technique known as 'chlorophyll fluorescence imaging' to measure the photosynthetic activity of plants, which is commonly used as an indicator of plant stress (Zhu et al., 2004). As *Figure 5.14* shows we observed no difference between the two strains, therefore, we cannot claim that HopO1-1 is able to affect the photosynthetic activity of the host.

5.4. Discussion

This chapter explored the possibility that plant chromatin remodelling is a susceptibility factor targeted by *Pst* DC3000 effectors. The effector localisation screen showed that at least 14 effectors localise to the nucleus, which strongly suggests that multiple susceptibility factors are found in the nucleus. It should be noted that many effectors could passively diffuse into the nucleus due to their small size and compact structure i.e. those without a putative NLS (e.g. HopC1, HopK1, HopF2, HopAF1, HopAI1, HopAB2). In addition, despite employing a variety of prediction algorithms to identify NLS in each of the effectors, it is possible that a NLS signal is not found in the primary structure, but in the secondary or tertiary structure of the protein, which would be more challenging to identify using these prediction tools.

Our experimental approach relied on the assumption that effectors interfering with chromatin remodelling would have to be nuclear localised. However, a recent study showed that the cytoplasmic effector PsAvh23 from *Phytophthora sojae* interferes with the association of ADA2 with HAG1 in soybean (*Glycine max*) by binding to ADA2 (Kong et al., 2017). Therefore, chromatin remodelling mechanisms can be targeted by pathogen effectors acting in the cytoplasm. Nuclear localisation of the effector was, however, found to be crucial for virulence as the assembly of ADA2 with GCN5 takes place only inside the nucleus.

It is interesting that GCN5 (albeit from soybean) is targeted by pathogens. Preliminary experiments to test for an interaction between the nuclear effectors presented here and HAG1 from *A. thaliana* have not yielded a positive result so far (Noukakis lab, *data not shown*). Although finding an interaction with HAG1 would be very impactful in the field of chromatin remodelling and plant-pathogen interaction, we focused on taking an unbiased screening approach towards identifying effectors with

the potential to target chromatin remodelling mechanisms in general.

Our localisation screen found a significant number of effectors localising to the nucleus, either exclusively or having also a cytoplasmic localisation. In the case of HopO1-1, which was investigated more thoroughly, evidence for chloroplast localisation was found in *N. benthamiana*. It is possible that the localisation outcomes presented here are sensitive to the effect of the GFP tag, but this is unlikely the case for HopO1-1 since the experiments using an HA tag confirmed the nuclear localisation. In other words, for further confirmation of these results, we could attempt to test the localisation of these effectors using a GFP tag on the C-terminus or an additional tag as in the case of HopO1-1.

Our FRAP screen provided evidence for binding to the chromatin as previously described using the same technique (Pruett et al., 2003). We crudely split our effectors' fluorescence recoveries into 'slow' and 'intermediate-fast'. In the case of the intermediate-fast group of effectors, due to the inherent variability of FRAP experiments, more detailed or alternative experiments could allow us to quantitatively discriminate amongst these effectors in terms of kinetics (*Fig. 5.5*). In other words, this would allow us to identify TF-like effectors with a more transient chromatin interaction than the 4 effectors displaying H2B-like properties (*Fig. 5.6*). Detailed experiments have been published whereby microscopy and computational tools have allowed the quantification of residency times on chromatin for a variety of chromatin-binding proteins (Phair et al., 2004). Phair *et al* (2004) caveated that slow recoveries observed for certain proteins may be due to non-chromatin binding such as binding to a nuclear matrix or to storage compartments. It is possible that this is the case with HopO1-1 given that we have found no evidence for direct interaction with chromatin, but instead there is some evidence that HopO1-1 interacts with actin or tubulin.

As an alternative to the FRAP screen, it would be extremely infor-

mative to perform CoIPs (after expression in *N. benthamiana*) of all nuclear localised effectors with histones after following the same protocol of FA-crosslinking and nuclear enrichment. This would allow us to screen for direct interaction with chromatin, thus complementing the FRAP screens.

HopO1-1 was found to be nuclear and showed evidence for chromatin association according to FRAP experiments. However, we failed to identify an interaction with H3. Although we could argue that interaction with other histones could be tested by using different histone antibodies, our protocol involved FA-crosslinking, which would allow the nucleosome to be intact during our co-IP. In addition, the MS data did not point towards a direct interaction with chromatin or chromatin-associated proteins. More specifically, it is interesting that HopO1-1 is able to alter chromatin dynamics without directly interacting with chromatin. One possibility is that HopO1-1 interferes with upstream components such as signalling proteins.

To this end, multiple kinases may interact with HopO1-1, although the evidence supporting this hypothesis can only be found in one biological replicate in the Arabidopsis experiment.

Our results showed that HopO1-1, HopT1-1, HopC1 and HopAI1 displayed H2B-like recovery and could be promising candidates for interaction with chromatin. We chose not pursue further characterisation of HopT1-1 due to its previously reported role in interfering with miRNA pathways. We also did not choose HopC1 as it had been reported to localise to the plasma membrane with potential roles therein, and considering that we did not identify a NLS for this effector, we reasoned that the nuclear localisation could be a result of diffusion into the nucleus (Wei et al., 2007). Also, HopO1-1 as a putative ADP-RT with the potential to modify other proteins such as histones, had a very interesting profile, which prompted us to investigate its role in plant immunity. Given the lack of information on this effector, we prioritised it over HopAI1, which

also had a promising profile as a phospho-Thr lyase with proven enzymatic activity, MAPKs as its substrates and a nuclear localisation (confirmed by our experiments as well) (Zhang et al 2007) and could thus be a potential modifier of histones.

In this chapter, experiments involving HopO1-1 were conducted in both *N. benthamiana* and *A. thaliana* and to a large extent, results were consistent between the two species. For example, the nuclear localisation of many effectors was the same between the two species (*Figure 5.7*). However, not all experiments could be conducted in both systems. For example, due to lower levels of expression, the FRAP experiments could not be conducted in protoplasts to investigate the chromatin binding properties of the effectors, therefore, we had to rely on the data obtained from *N. benthamiana*. Once transgenic lines expressing GFP-tagged effectors are available, the FRAP experiments can potentially be repeated in *A. thaliana*. Furthermore, the MS data showed that there was some consistency in the groups of proteins identified such as KH-domain proteins and other proteins involved in translation. Nevertheless, comparing results between the two systems should be done with caution as it is possible that the effector behaves somewhat differently in each system.

Research in plant immunity has focused on processes such as pathogen perception, signal transduction, transcriptional and post-translational processes, but other processes such as pre-mRNA splicing, polyadenylation, mRNA silencing and transport have been studied to a lesser extent, despite their established roles in plant immunity. A common denominator in the latter group of processes, is the importance of RNA-binding proteins, which employ RNA-recognition motifs (RRM) and KH domains. Wang *et al* (2015) showed that a KH-domain/RNA-binding protein was a susceptibility factor in potato (*Solanum tuberosum*) infected with *Phytophthora infestans*. Specifically, interaction between *St*KRBP1 and Pi04089 by Y2H and *in planta* was shown in this study

(Wang et al., 2015). Furthermore, the effector Pi04089 localises to the nucleus and upon interaction with *St*KRBP1 a pattern of speckles is visible (*Fig. 5.15*), which is strongly reminiscent of the pattern recorded for HopO1-1. Although we cannot specify what these speckles represent, it is interesting that there is alignment between the observations made by Wang *et al* (2015) and our findings.

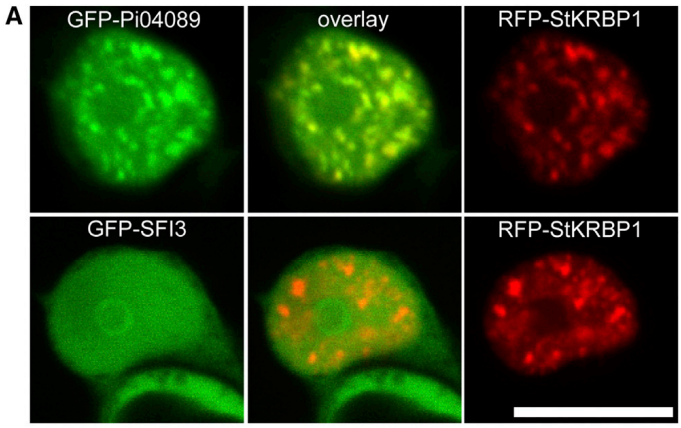

Figure 5.15. *St*KRBP1 Specifically relocalises Pi04089 to nuclear speckles. Single optical sections of *N. benthamiana* leaf epidermal cell nuclei transiently co-expressing the GFP-Pi04089 or GFP-SFI3 with RFP- StKRBP1, showing that GFP-Pi04089 is relocated to nuclear speckles. Scale bar represents 10 µm. Taken from Wang *et al* (2015).

Such RNA-binding proteins have been implicated in defence against *Pst* DC3000 as in the case of RBP-DR1 (Qi et al., 2010). As already mentioned, GRP7 has been found to be targeted by HopU1 (ADP-RT by *Pst* DC3000). GRP7 also belongs to the group of proteins with RNA-binding capacity and it was also found that it binds to mRNA transcripts from the receptor gene FLS2 such that targeting by HopU1 results in compromised immunity. It would be interesting to assess the role of the KH domain-containing proteins identified in our MS results and identify whether the virulence of *Pst* DC3000 is diminished in the absence of these proteins (i.e. in knock-out mutants).

With regards to the finding that RNA helicases may be interacting with HopO1-1, members belonging to this group have been implicated in processes such as mRNA export (Du et al., 2016) or even in the epigenetic silencing of gene expression through the RNA-directed DNA meth-

ylation (RdDM) pathway during abiotic stress (Khan et al., 2014). Based on the literature, DEAD box RNA helicases such as STRS1 (STRESS RESPONSE SUPPRESSOR1) associate with other nucleolar and chromocenter-localized proteins, which could implicate these proteins in chromatin-related processes. Follow-up experiments in the Ntoukakis lab confirmed the direct interaction of HopO1-1 with a RNA helicase candidate (DRH1, AT3G01520) through a Y2H screen (*data not shown*) solidifying our MS results.

Furthermore, we were intrigued to find evidence that HopO1-1 is capable of inducing chlorosis. In general, it is known that suppression of photosynthesis is one of the earliest physiological responses detected following *Pst* DC3000 infection (de Torres Zabala et al., 2015). Chlorophyll fluorescence imaging was an ideal tool to record early changes to photosynthetic activity and we saw a change of activity in the presence of *Pst* DC3000, but not *hrcC* stain, as previously recorded (de Torres Zabala et al. 2015). However, the *hopO1-1* mutant strain did not show reduced capacity to impair photosynthetic activity as compared to *Pst* DC3000. Also, upon infection of Col-0 plants with *Pst* DC3000 and *Pst* DC3000 lacking HopO1-1 we failed to detect a difference. Previously, Fu *et al* (2007) reported a reduction in virulence in the case of *Pst* DC3000 *hopU1,* but Torres-Zabala *et al* (2015) failed to detect a significant difference between *Pst* DC3000 and *Pst* DC3000 *hopN1 (*from *Pseudomonas fluorescens)*. In fact, Torres-Zabala *et al* (2015) found evidence to support that multiple effectors are targeted to the chloroplasts acting concomitantly to alter photosystem function, which may explain the lack of clear phenotypes in the absence of only a single effector. In other words, although both HopU1 and HopN1 are known to have targets within the host, it is possible that the presence of a larger effector repertoire may compensate for the absence of a single effector. This could be the case in the absence of HopO1-1, which our data show that this effector has several targets within the cell, however, in

its absence other effectors are contributing to infection. It is also possible that the closely related HopO1-2 has a large set of overlapping interactors as HopO1-1 and, therefore, their activities are redundant. To this end, we could use a strain that contains a double deletion of both HopO1-1 and HopO1-2, which would perhaps show a stronger phenotype in our infection and chlorophyll imaging experiments.

In line with these findings, follow-up microarray experiments in the Ntoukakis lab showed the down regulation of NECGs in the presence of HopO1-1. Specifically, from the 614 genes differentially expressed upon DEX-induction of HopO1-1, 204 (33%) of these are NECGs. Downregulated genes represented 329 genes, of which 172 (52%) are NECGs (*Supp. Fig. 5.4*). Thus, it appears that HopO1-1 has a role in interfering with photosynthetic processes at the transcriptional level. However, the exact mechanism is still being investigated.

In general, generating viable *Pst* DC3000 with deletions in multiple effector genes is a challenging task because many effector genes are found tandemly organised within polycistronic operons (Petnicki-Ocwieja et al., 2005). Although few experiments have addressed the secretion hierarchy of effector proteins, a study showed that deletion of 18 effector genes was required to impair the *in planta* bacterial growth (Kvitko et al., 2009). Subsequent experiments, showed that a minimal set of 8 effectors contributes to bacterial virulence and plant defence suppression (Cunnac et al., 2011). Although we failed to see a clear phenotype in *in planta* bacterial colonisation when HopO1-1 was mutated, we did see a phenotype upon inducible expression of HopO1-1. Accordingly, subsequent experiments performed in the Ntoukakis lab showed a clear reduction in photosynthetic activity following induction of HopO1-1 (*data not shown*).

In terms of suppressing photosynthetic activity, the two hypotheses are that HopO1-1 has a direct effect inside the chloroplasts by directly interacting with its target protein and/or that HopO1-1 is able to influ-

ence the expression of nuclear-encoded chloroplastic genes (NECGs) (de Torres Zabala et al. 2015). Support for the first hypothesis comes from the fact that we identified interaction with an integral component of the photosystem, namely OEE3-2 (Umena et al. 2011). To test for the second hypothesis, a similar approach to de Torres Zabala *et al* (2015) could be followed, whereby, transcriptional changes in NECGs were analysed in response to infection with *Pst* DC3000 or mutated strains thereof. This would complement the current microarray data in our lab *(Supp. Fig. 5.4)*

To properly distinguish the potential roles of HopO1-1 between the nucleus and chloroplast one approach could involve the addition of a nuclear exclusion signal, which would occlude the effector from the nucleus and only allow its localisation into the chloroplasts. Thus, we could re-assess the outcome of infection as well as the interactome of HopO1-1 within the chloroplasts. This would of course, require a chloroplast isolation protocol and subsequent MS after IP of HopO1-1.

It is interesting that in our MS results we identified a chloroplastic protein such as oxygen evolving enhancer protein 3-2 (OEE3-2), despite following a nuclear enrichment protocol. This could be due to technical reasons, specifically, insufficient washing of the nuclei during nuclear enrichment. Considering that HopO1-1 may localise to the chloroplast, this interaction was identified during IP and MS. To obtain greater granularity into the chloroplast-specific interactors of HopO1-1, we could follow a chloroplast enrichment protocol followed by immunoprecipitation and mass spectrometry as before (Jouhet and Gray, 2009).

Fu *et al* (2007) separated ADP-RT reactions from *A. thaliana* extracts incubated with HopU1 and employed two-dimensional (2D) PAGE and autoradiography to identify proteins ADP-ribosylated by the effector. The identity of the proteins that showed greater separation was further analysed by MS. We could follow a similar approach to confirm ADP-ribosylation targets of HopO1-1 and at the same time show the enzymatic ac-

tivity of HopO1-1. We could also use putative catalytic inactive mutants as controls.

Visschedyk *et al* (2010) reported on a novel ADP-RT from *Photorhabdus luminescens*, called Photox, which specifically ADP-ribosylates skeletal actin and non-muscle actin, inhibiting the polymerisation process of actin filaments. In turn, this appeared to have potent cytotoxic effects. Our MS results suggest that HopO1-1 acts on actin and tubulin in plants. Nuclear actin filaments have been implicated in a variety of processes, which include but are not limited to transcription, mRNA processing and even chromatin remodelling (Chen and Shen, 2007).

Other examples of bacterial ADP-RT proteins exist, whereby interaction with host proteins involved in protein synthesis has been reported. Specifically, the exotoxin A from *P. aeruginosa* was found to ADP-ribosylate elongation factor 2 (EF2), which resulted in inhibition of protein synthesis and killing of the cell (Simon et al., 2014). In our experiments, we found weak evidence for the interaction of HopO1-1 with proteins involved in translation. For example, although in Arabidopsis, interaction with elongation factor (EIF4A1, EIF4A2) was more clear, in *N. benthamiana* it appears that there was no enrichment for such an interaction. This could mean either that HopO1-1 does not interfere with protein synthesis or that it may do so only in Arabidopsis. However, the latter hypothesis may be less likely given that protein translation is a highly conserved biological process across kingdoms.

Overall, the findings of this chapter suggest that HopO1-1 is a nuclear/cytoplasmic effector with strong evidence for localisation to the chloroplast. Its roles may be similar to the previously described ADP-RT HopU1 in that it may interact with RNA-binding proteins, but it may be unique in that it may directly interact with chloroplastic proteins involved in photosynthesis. These findings warrant further investigation as there is

currently no published research in the roles of HopO1-1 in *A. thaliana-Pst* DC3000 interaction.

Chapter 6 - General Discussion

6.1. HAG1 is responsible for the flg22-induced histone acetylation

From an evolutionary point of view, it is interesting that HAG1/GCN5 has maintained a central function in different biological processes across kingdoms. With roles in development and response to different types of stress, we can place HAG1 at the forefront of plant histone acetylation and chromatin remodelling. Our results could support a model in which HAG1 interacts with multiple proteins and can potentially be found in different complexes, which allows this enzyme to perform a variety of functions. Chapter 3 explored the role of histone acetylation in plant immunity and identified HATs specifically involved in the process of PAMP-induced histone acetylation. *Figure 6.1* describes a model in which HAG1 is potentially acetylating histones H3 during resting conditions, however, this activity is increased following flg22 perception leading to higher levels of histone acetylation. According to our immunoblots, comparing the PAMP-induced histone acetylation in wild type and *hag1-6* plants (*Fig. 3.10*), HAG1 is crucial in this process. At the same time, a HDAC is antagonistically removing acetylation from histones. As recently published by Latrasse *et al* (2017), HD2B is a HDAC with roles in immunity possibly acting on a different set of genes as HAG1 (*Fig. 6.1*). Of course, multiple proteins involved in chromatin remodelling are likely to act on chromatin upon flg22 perception, including ATP-dependent chromatin remodellers, kinases phosphorylating histones, histone methyltransferases and more. Last but not least, HD2B was found to be activated by upstream MPK3, but we have not identified whether HAG1 is activated by a similar kinase (MAPK or CDPK).

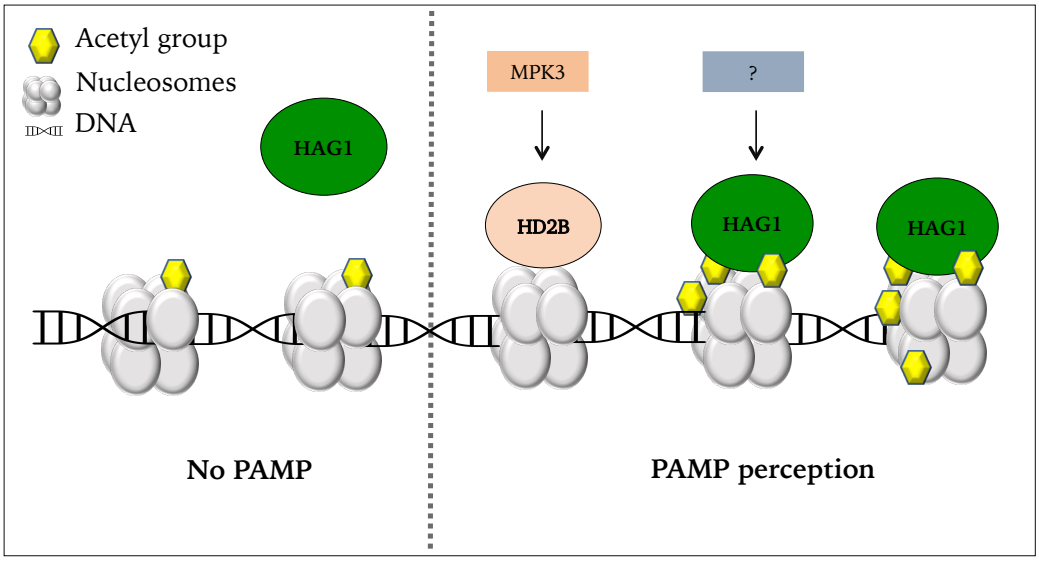

Figure 6.1: HAG1 is responsible for flg22-induced histone acetylation. In resting conditions HAG1 interacts with histones on the promoters of defence genes and may acetylate those genes at an intermediate level. Following flg22 perception, HAG1 is recruited (by an unknown mechanism) onto the promoters of defence genes resulting in increased levels of histone acetylation. Meanwhile, HD2B is responsible for the deacetylation of many genes following flg22 perception, however, the majority of those genes are not involved in defence. The model also shows that although HD2B is activated by MPK3, a similar interaction with an upstream kinase and HAG1 has not been described so far.

6.2. HAG1 complex has core and PTI/ETI-specific interactors

Based on our MS analysis, we identified ADA2a, ADA2b and ADA3 as core components of the putative plant HAG1 complex, similarly to what has been extensively described in other organisms. In addition, we showed the interaction of HAG1 and chromatin remodeller CHR5, the homolog of which (Chd1) is also a SAGA component in yeast (Pray-Grant et al., 2005). Therefore, as shown in *Figure 6.2* four proteins were found to be highly conserved interactors within the plant HAG1 complex. We were not able to identify a MAPK or CDPK responsible for the activation of HAG1, we did find evidence for a possible mechanism by which the role of HAG1 in immunity is regulated by members of the TOPLESS family. According to this model, TPL family proteins (TPL, TPR1, 2 and 4) interact more strongly with the HAG1 complex in resting conditions and this interaction is partially lost during PTI and ETI *(Fig. 6.3)*.

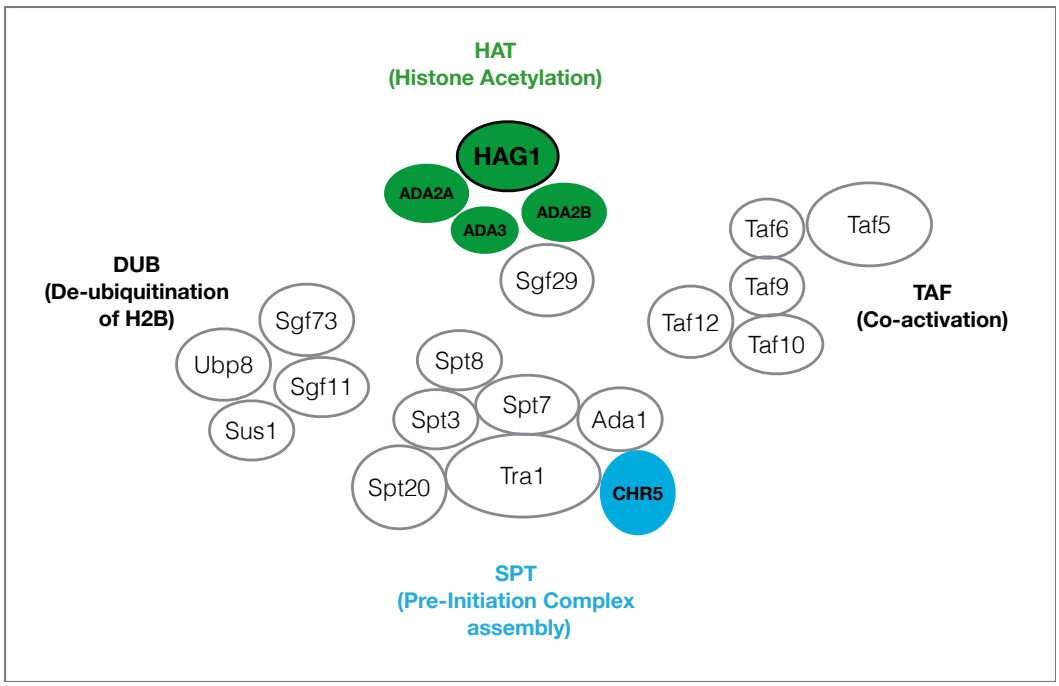

Figure 6.2 : Confirmed components of HAG1 complex in plants compared to yeast SAGA. Proteins shown in white circles have been identified in yeast only. Proteins in coloured circles have been identified both in yeast and in our experiments in *A. thaliana*. Based on Koutelou *et al* (2010).

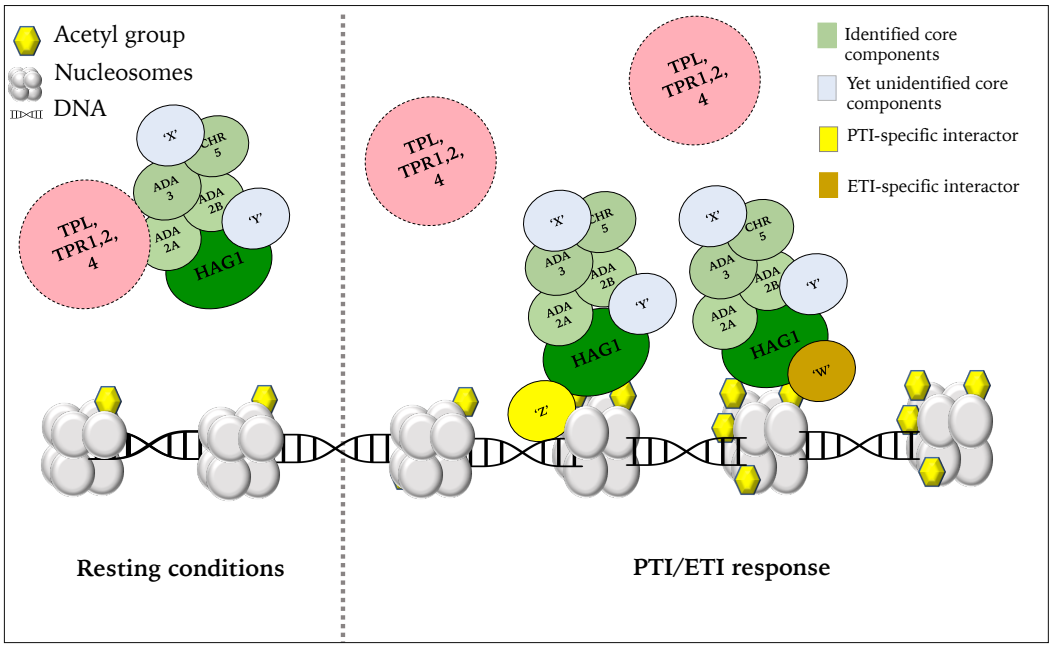

Figure 6.3: HAG1 acts in a multi protein complex, which consists of core interactors and potentially PTI/ETI-specific interactors. The increased levels of histone acetylation after flg22 perception could be explained by the concerted action of HAG1 and its interactors. Core components of HAG1 complex have been identified. The interaction with the corepressor TPL family members could be potentially lost during PTI or ETI responses, thus allowing HAG1 complex to increase the acetylation at the promoters of defence genes. Other proteins, here depicted as 'X' and 'Y' could be additional core components of HAG1 complex, which we failed to identify. Proteins 'Z' and 'W' could be transcription factors guiding the complex to specific DNA sequences or chromatin binding proteins binding specific histone marks.

This could explain the increased levels of histone acetylation observed after flg22 perception. Nevertheless, this model is based on a semi-quantitative approach and warrants further investigation. The value of co-immunoprecipitation and ChIP experiments as previously discussed should be highlighted, as these experiments would allow us to test this hypothesis.

6.3. HopO1-1 is involved in various molecular processes

Chapter 5 aimed to identify effectors that would interfere with chromatin remodelling and in particular, effectors with a role in the interference of histone acetylation. Our approach appears to have narrowed down the search to a few candidates based on the localisation of GFP-tagged effectors and subsequent FRAP assays suggesting binding to chromatin. Despite their meaningful insight, the FRAP results should be interpreted with caution and follow-up experiments such as mass spectrometry can elucidate the interacting partners of the effectors. In the case of HopO1-1, direct interaction with chromatin-associated proteins was not found based on our MS data, however, strong evidence for interaction with proteins involved in different processes was found as summarised in *Figure 6.4*. It is possible that HopO1-1 has the ability to interact with a wide variety of proteins within the host given that it localises to the cytoplasm, nucleus and potentially in the chloroplast. Also the absence of a conserved protein domain other than the putative ADP-RT domain (*Supp. Fig. S5.2*), may explain why HopO1-1 is not highly specific in its interactions.

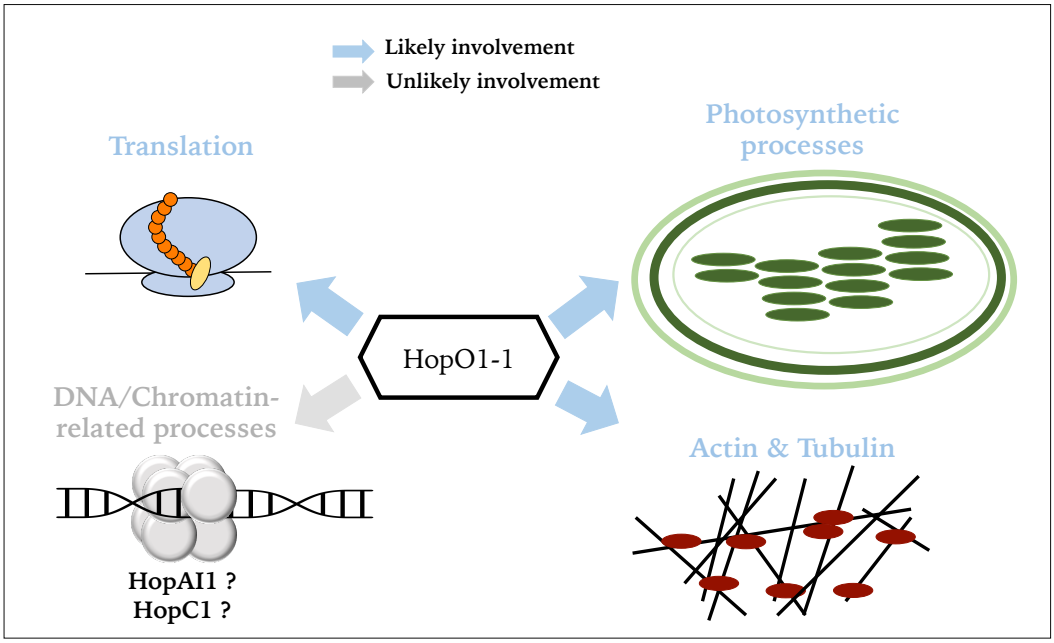

Figure 6.4: HopO1-1 could be involved in various molecular processes. Our experiments have pointed towards a potential involvement of HopO1-1 in various processes such as protein translation, photosynthesis and actin/tubulin metabolism. The model provides a framework for follow-up experiments involving HopO1-1. HopAI1 and HopC1 could be investigated further in terms of interaction with DNA or chromatin according to their profiles as nuclear localised and chromatin bound effectors based on subcellular localisation and FRAP experiments.

Last but not least, in our continued efforts to identify *Pst* DC3000 effectors with chromatin-binding capacity, we could investigate HopAI1 or HopC1. In terms of protein domains, there seems to be no indication that HopAI1 and HopC1 have the capacity to bind chromatin (*Supp. Fig. S5.2)*, however, further experiments are warranted on the basis of their promising profiles from our experiments (*Fig. 5.7*). Stable transgenic lines expressing these effectors would allow us to test for interaction with chromatin. Also, following the approach of Franco-Zorilla *et al* (2014), we could test for the DNA-binding specificities of these effectors using a high-throughput method.

The take-home message for Chapter 5 is that the set of experiments employed here to identify effectors that interfere with host chromatin remodelling, can be applied not only to the rest of the effectors

from *Pst* DC3000, but could also potentially be used across different plant pathogens.

Chapter 7 - Conclusions & Looking Forward

7.1. Epigenetics and chromatin remodelling across organisms

The study of epigenetics and chromatin remodelling has found various applications with the most significant ones in today's medical practice. For example, epigenetic drugs have been approved for the treatment of different cancer types (Sharma et al., 2010). Therefore, it is important to continue to develop our understanding of different mechanisms governing gene expression. The power of using plants as model organisms has been demonstrated throughout centuries of research from Gregor Mendel's plant hybridisation experiments to David Baulcomb's discovery of siRNA. Therefore, research on chromatin remodelling should continue to go 'hand-in-hand' with research in other organisms.

7.2. Benefiting from research in other model organisms

Throughout this PhD project, working on a protein that has been described to a lesser extent in plants than it has in other model organisms could be described as challenging at times. However, it should be highlighted that GCN5 is one of the most well-studied proteins involved in chromatin-remodelling with most of the biochemical research having been conducted in yeast. The abundance of information on GCN5 in yeast spanning 30 years of research was instrumental in progressing our research group's understanding of HAG1 as well as in the design of many of the experiments presented here. To be more specific, a lot of technical knowledge was drawn from the biochemical characterisation of the SAGA complex in the seminal papers by Allis laboratory (Kuo et al., 1996; Trievel et al., 1999). This includes, for example, the use of cross-linking agents as well as the scale at which the experiments would have to be conducted to achieve a desirable level of complex purification. Of course, a consider-

able caveat was the transferability of these technical aspects from a yeast system to a plant system. The key message is that plant researchers have a lot to benefit from transferring knowledge between different model organisms.

Furthermore, Kim *et al* (2015) proposed that improved techniques in epigenomics are needed to allow greater accuracy and resolution, for example, when it comes to tissue-specific alterations during plant stress. Current methodologies such as ChIP may not be able to address changes at the tissue-specific level, nevertheless, this is an important technique in a plant researcher's toolbox.

Crucial in overcoming technical limitations in plant research, will be the use of CRISPR/Cas system to effectively generate mutants without relying on T-DNA-based mutagenesis, which may often result in misleading phenotypes depending on the site of insertion. In the case of *HAG1* T-DNA mutants, *hag1-6* gene may be able to produce a truncated protein, possibly with partial functionality. By being able to effectively delete a gene for a histone writer or eraser, we could more clearly study the effects of this protein on gene expression upon its absence.

7.3. From model plant organisms to commercially important crops

Looking forward from research in model organisms, it would be highly informative to identify the importance of histone acetylation in commercially important crops such as tomato, wheat and rice. Tomato, in particular, lends itself more easily to the study of its interaction with *Pseudomonas syringae* DC3000 *pv* tomato. Logical next steps using this pathosystem would involve generating mutations in tomato HAG1 homolog (using CRISPR/Cas) or silencing of this gene through RNAi. Several examples have already been reported. Undoubtedly, the way forward will involve field trials for transgenic crops, the number of which has been increasing in recent years, however, some countries have stopped con-

ducting trials due to safety concerns. According to a study, only a small percentage of field trials concerns traits relating to fungal or bacterial resistance with the aim of most trials focused on traits such as herbicide tolerance, insect resistance, product quality and others (Pray et al., 2002). Hopefully, new technologies will be able to alleviate some of the safety concerns and will show their potential in improving crop traits.

In addition, the ability of epigenetic regulators to determine basal levels of expression in response to environmental cues provides new avenues of altering plant behaviour via genetic manipulation of major signalling pathways. Epigenetic marks themselves can be selected in a process of epigenetic breeding in which isogenic populations undergo several rounds of selections. This approach has been used in the past with the aim of improving drought tolerance in *Brassica napus* (Verkest et al., 2015). This example supports the incorporation of epigenetics into conventional plant breeding, but it still relies on a thorough understanding of the underlying molecular processes.

In a recent study by Venturelli *et al* (2015), chemical inhibitors of HATs and HDACs were identified in the rhizosphere. These inhibitors, which derived from hydroxamic acid compounds from plants were shown to have potent allelochemical effects by inhibiting HDAC activity and thus affected the growth of nearby plants. These findings add another level of complexity into how chromatin-related processes are regulated by environmental factors, and more specifically in the context of plant-plant interaction. It would be interesting to explore whether HAT or HDAC inhibitors can be used for commercial purposes in the future, although large scale use as well as the selectivity of these molecules could be a challenge.

In conclusion, the scientific community is tasked with solving one of the most challenging problems of today; that of food security. The experiments presented here can be placed within the scope of food security,

however, research and development is only a small part of the solution. A more holistic approach should be followed, which would also aim towards improved scientific communication as well as regulation as a step towards public acceptance of transgenics and other technologies, which appears to be a major barrier in the uptake of this technology.

Appendix - Supplementary Information

The individual chapters contain references to the supplementary figures and tables shown below.

Chapter 1

SAGA Subunits	Yeast	Human	*Arabidopsis thaliana*		*Orzya sativa*	
			Name	Locus	Name	Locus
ADAs	Ada1	ADA1	AtADA1a	At2g14850	OsADA1a	Os12g39090
			AtADA1b	At5g67410	OsADA1b	Os03g55450
	Ada2	ADA2b	AtADA2b	At4g16420	OsADA2b	Os03g53960
	Ada3	ADA3	AtADA3	At4g29790	OsADA3	Os05g28300
	Gcn5 (Ada4)	GCN5	AtGCN5	At3g54610	OsGCN5	Os10g28040
DUBm	Ubp8	USP22	AtUBP22	At5g10790	OsUBP22	Os04g55360
	Sgf11	ATXN7L3	AtSGF11	At5g58575	OsSGF11	Os05g28370
	Sus1	ENY2	AtENY2	At3g27100	OsSUS1	Os01g69110
	Sgf73	ATXN7	AtSGF73	ND	OsSGF73	ND
SPT	Spt3	SPT3	AtSPT3	At1g02680	OsSPT3	Os01g23630
	Spt7	STAF65/ SUPT7L	AtSPT7	At1g32750	OsSPT7	Os06g43790
	Spt8	ND	AtSPT8	ND	OsSPT8	ND
	Spt20 (Ada5)	SPT20	AtSPT20	At1g72390	OsSPT20	Os01g02860
TAFs	Taf5	TAF5L	AtTAF5	At5g25150	OsTAF5	Os06g44030
	Taf6	TAF6L	AtTAF6	At1g04950	OsTAF6	Os01g32750
			AtTAF6b	At1g54360		
	Taf9	TAF9	AtTAF9	At1g54140	OsTAF9	Os03g29470
		TAF9b			OsTAF9b	Os07g42150
	Taf10	TAF10	AtTAF10	At4g31720	OsTAF10	Os09g26180
	Taf12	TAF12	AtTAF12	At3g10070	OsTAF12	Os01g63940
			AtTAF12b	At1g17440	OsTAF12b	Os01g62820
Other Subunits	Chd1	ND	AtCHR5	At2g13370	OsCHD1	OsJ_25446
	Sgf29	STAF36	AtSGF29a	At3g27460	OsSGF29	Os12g19350
			AtSGF29b	At5g40550		
	Tra1	TRRAP	AtTRA1a	At2g17930	OsTRA1	Os07g45064
			AtTRA1b	At4g36080		

ND: Not detected.

Supplementary Table S1.1. Homologous SAGA components across species. Yeast and human SAGA have been biochemically described in greater detail. The table lists protein homologs from *A. thaliana* and *O. sativa*. Taken from Moraga and Aquea (2015).

Code	Description	Sequence (5'—>3')
VN41	LBb1.3	ATTTTGCCGATTTCGGAAC
VN42	RB4	TCACGGGTTGGGGTTTCTACAGGAC
VN88	HAG1-prom-F	AAAAAGCAGGCTCCACCTGTCAAGTGGTGCTTTAAC
VN89	HAG1-F	AAAAAGCAGGCTCCACCGACTCTCACTCTTCCC
VN90	HAG1-RC	AGAAAGCTGGGTCCTATTGAGATTTAGCACCAG
VN91	HAG1-RO	AGAAAGCTGGGTCTTGAGATTTAGCACCAG
VN92	HAG1-pOPIN-F	GGTACCGACTCTCACTCTTCC
VN93	HAG1-pOPIN-R	GTTTAAACCTATTGAGATTTAGCAC
VN94	hag1-6-LP	TTGCACAAAATGCTATTTCCC
VN95	hag1-6-RP	CTCCAACGATGAACTCGAGAG
VN96	hag1-5-LP	AAACGTCTTACCTGGTTGCAC
VN97	hag1-5-RP	ACGTATCAGTTTCTGATCCGG
VN98	M13-F	GTTGTAAAACGACGGCCAGT
VN99	M13-R	CACAGGAAACAGCTATGACC
VN100	HAG1-FS1	ATATGATGTGCTTGATTGG
VN101	HAG1-FS2	CACTGGATCTATGCTAATG
VN102	HAG1-FS3	GATGTTGATGGATTGACGC
VN103	HAG1-FS4	GATACGCCAGCAAAGAAAG
VN104	HAG1-FS5	ACCACGGCAGCGAATGC
VN105	HAG1-FS6	TGCAAGACCATGCTGATGC
VN106	HAG1-F1	ATGGACTCTCACTCTTCCCAC
VN107	HAG1-R1	CTATTGAGATTTAGCACCAGATTGG
VN116	pOPIN-M-FS1	CGAAAACTATCTGCTGACTG
VN117	HAG1-RS1	CCGTCTTAAGTTTAGTGTTGC
VN118	pOPIN-M-RS	TATGTCCTTCCGAGTGAGAG
VN119	HAG1mutKpnI	AGTAAAAGGTTACGGAACCAGATTGATGAACCACTTG
VN120	mutE289Q	TATCACAGTCAGAAGTTTGGGCAAATAGCATTTTGTGC
VN121	mutE289H	CCATATCACAGTCAGAAGTTTGGGCATATAGCATTTTGTGC
VN295	LP hda19	TGACGGTTACAACCTAGTGGG
VN296	RP hda19	TTTCCTCTTCACACCATCAGG
VN298	mutgDNAE289H	GATTCAGTCAGAAGTTTGGG**C**A**U**ATAGCATTTTGTGCAATCAC
VN299	revHAG1mutKpnI	CAAGTGGTTCATCAATCTGGTTCCGTAACCTTTTACT
VN300	revmutE289Q	GCACAAAATGCTATTTGCCCAAACTTCTGACTGTGATA
VN301	GFPCter-F	AGAAGAACGGCATCAAGG
VN302	RFPCter-F	GGGCGAGATCAAGATGAG
VN338	nahG F	CACCGGGCGGATTTCAT
VN339	nahG R	CCCGAATTGGGCGATACC
VN336	sid2-1 F	GCAGTCCGAAAGACGACCTCGAG
VN337	sid2-1 R	CTATCGAATGATTCTAGAAGAAGC
VN338	nahG F	CACCGGGCGGATTTCAT
VN339	nahG R	CCCGAATTGGGCGATACC

Supplementary Table 2.2. Primers used throughout this project

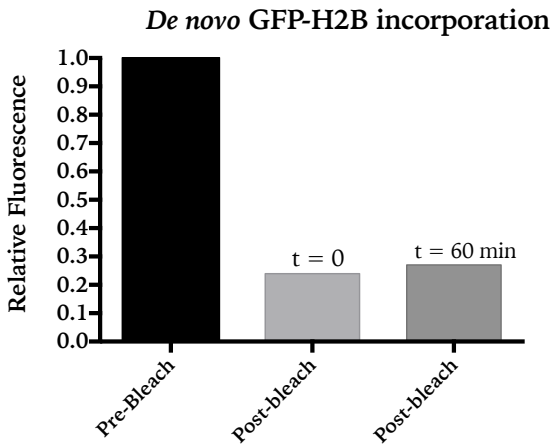

Supplementary Figure S3.1. There is no *de novo* GFP-H2B incorporation into chromatin. Nuclei expressing GFP-H2B were fully bleached to cancel all fluorescence and fluorescence recovery was monitored over 1 hour to record the rate of GFP-H2B synthesis, which could show whether FRAP recovery in our experiments is due to *de novo* protein synthesis or due to protein mobility within the nucleus.

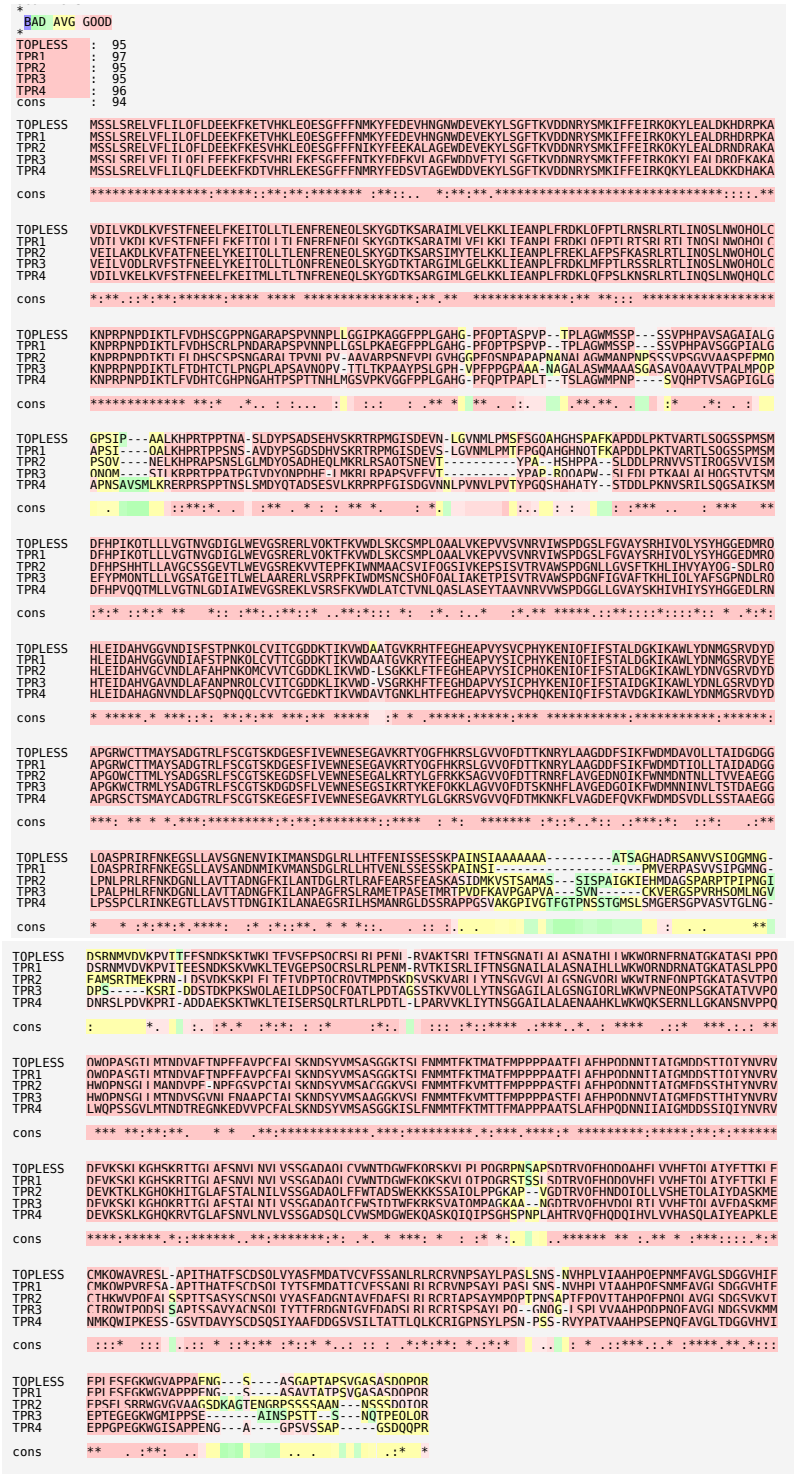

Supplementary Figure S4.1. Protein sequence alignment of TOPLESS family members. The symbols below the sequences denote degree of conservation, for example, '*' means complete conservation of the amino acid, ':' suggests strong conservation and '.' suggests low conservation. The color coding from blue to red denotes 'bad' to 'good' level of alignment. The alignment was performed using T-COFFEE alignment software (http://tcoffee.crg.cat).

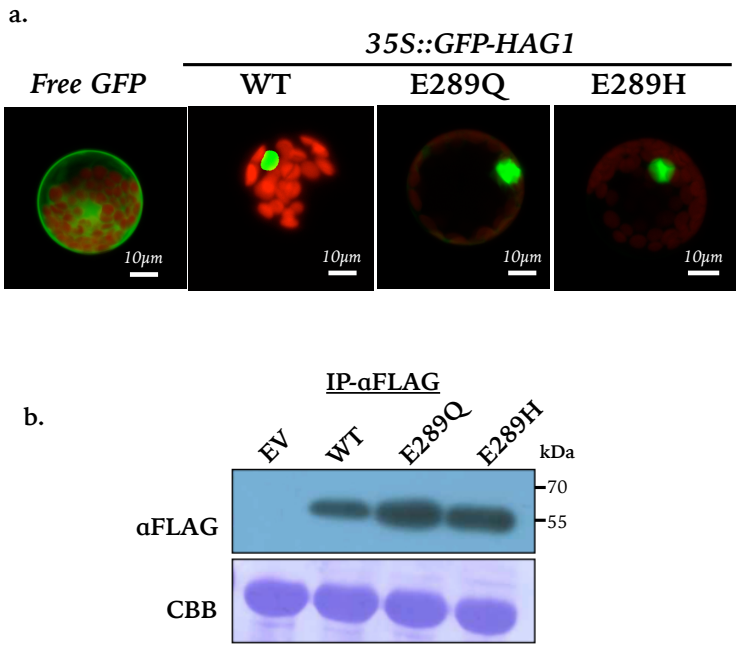

Supplementary Figure S4.2. HAG1 catalytic inactive mutants were generated. Localisation and protein expression were confirmed by expression in protoplasts and confocal imaging (Panel a) as well as by transient expression in *N. benthamiana* and immunoblotting (Panel b)

BAIT	HAG1	*AT3G54610*	*Bromo, HAT*
Published Interactors	ADA2A	*AT3G07740*	*RNAP C-ter domain, ADA2*
	ADA2B	*AT4G16420*	*ADA2*
	ADA3	*AT4G29790*	*No domains identified*
	CHR5	*AT2G13370*	*SNF2, DUF4208, Chromo*
TOPLESS Family	TOPLESS	*AT1G15750*	*WD40, LisH, CBP*
	TPR1	*AT1G80490*	*WD40, LisH, Vir28*
	TPR2	*AT3G16830*	*WD40, LisH*
	TPR4	*AT3G15880*	*WD40, LisH*
Chromatin Remodelling	HAC1	*AT1G79000*	*HAT, PHD, Zn finger*
	PKL	*AT2G25170*	*SNF2, DUF, Chromo, PHD*
	CHR11	*AT3G06400*	*Probable CRC ATPase*
	CHR2	*AT2G46020*	*SNF2, Bromo, QLQ*
	HD2B	*AT5G22650*	*No domains identified*
Proteins with chromatin binding, DNA binding, protein modification properties	ARGAH2	*AT4G08870*	*Arginine HDAC*
	Tudor1	*AT5G07350*	*Tudor*
	PHD finger	*AT1G77800*	*PHD Zn finger, PHD finger*
	RNA Pol α	*ATCG00740*	*RNAP alpha subunit*
	TFIIB	*AT2G41630*	*SUA7 (TF2B subunit)*
	NFA03	*AT5G56950*	*Nucleosome assembly domain*
	SMP2	*AT4G37120*	*Slu7 (pre-mRNA splicing)*
	HMGB2	*AT1G20693*	*HMG (High mobility group) box*
	Zn Finger (CCCH)	*AT3G27700*	*RRM, DUF*
	WD40-Transducin	*AT3G63460*	*WD40, PAT1, ACE1*
	Cyclophilin-like	*AT2G36130*	*Cyclophilin superfamily*
	Cyclophilin71	*AT3G44600*	*WD40, Cyclophilin superfamily*
	WLIM1	*AT1G10200*	*Lim superfamily*
	Global TF B1	*AT1G65440*	*SPT6*
	CwfJ-like protein	*AT5G56900*	*CwfJ, YTH1*
	RNA binding plectin	*AT4G25740*	*S10 plectin domain*
	Nucleic Acid Binding	*AT2G02570*	*No domains identified*
	ING1	*AT3G24010*	*ING histone-binding*
	Zn Knuckle (CCHC)	*AT5G49400*	*Zinc knuckle*
	WRKY1	*AT2G04880*	*WRKY domain*
	LRR	*AT3G20820*	*LRR domains*
	PP2A	*AT3G09880*	*Phosphatase B56 domain*
	Protein Kinase	*AT3G13670*	*Ser/Thr catalytic domain*
	Protein Kinase	*AT1G67580*	*Ser/Thr catalytic domain*
Nuclear Import/Export	Transportin1	*AT2G16950*	*Karyopherin domain*
	NUA	*AT1G79280*	*Chromosomal maintenance domain*
	NRP1	*AT2G03440*	*No domains identified*
Other proteins	ACX1	*AT4G16760*	*Acyl-coenzyme A oxidase*
	NRP1	*AT2G03440*	*No domains identified*
	ATMIN7	*AT3G43300*	*Sec7 domain*
	PLD	*AT3G15730*	*Phospholipase D domain*
	SRP30	*AT1G09140*	*RNA recognition motif*
	CXIP4	*AT2G28910*	*No domains identified*
	SHM4	*AT4G13930*	*Ser Hydroxymethyltransferase domain*
	DDB1A	*AT4G05420*	*DNA damage replication domain*
	MFP2	*AT3G06860*	*Fatty acid oxidation domain*

Supplementary Figure S4.3. Conserved protein domains in HAG1 interactors. A search on Pubmed for the presence of conserved protein domains is shown. Domains with probable roles in DNA or chromatin binding or chromatin modification are highlighted in blue font.

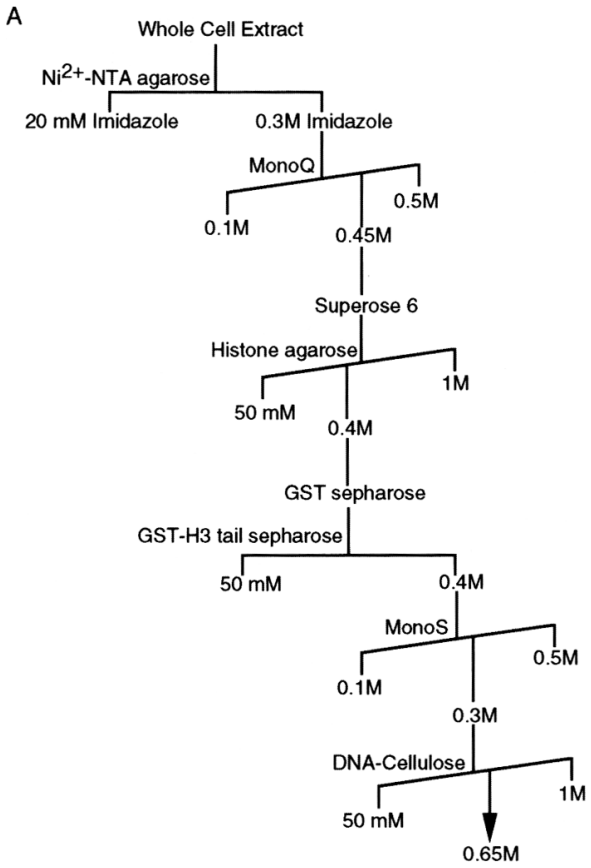

Supplementary Figure S4.4. Purification scheme for the 1.8-MD nucleosomal HAT complex, SAGA. Taken from Grant *et al* (1997).

	NLS Mapper		NLStradamus	NucPred
	Monopartite	Bipartite		
HopO1-1	✗	✓	✓	✗
HopT1	✗	✓	✗	✗
HopC1	✗	✗	✗	✗
HopB1	✗	✗	✓	✓
HopH1	✗	✓	✗	✗
HopK1	✗	✗	✗	✗
HopY1	✗	✗	✓	✓
HopF2	✗	✗	✗	✗
HopAF1	✗	✗	✗	✗
HopA1	✗	✗	✗	✗
HopG1	✗	✗	✗	✗
HopAO1	✗	✗	✗	✗
HopAA1-1	✗	✓	✗	✗
HopG1	✗	✓	✗	✗
HopAB2	✗	✗	✗	✗
HopM1	✗	✗	✗	✗
HopN1	✗	✗	✗	✗

Supplementary Table S5.1. NLS Mapper was able to identify mono-partite as well as bipartite NLS sequences using a classical NLS functionality screen. NLStradamus algorithm was able to detect similar residue frequency distribution (different from that of background residues) commonly found in NLS sequences. The algorithm NucPred is not restricted to a predefined set of NLS signatures allowing the discovery of new NLSs. Overall, the variability in the algorithms resulted in relatively low coherence amongst the different prediction tools, however, agreement between 2 tools was found in the case of HopO1-1, HopB1, HopH1 and HopY1.

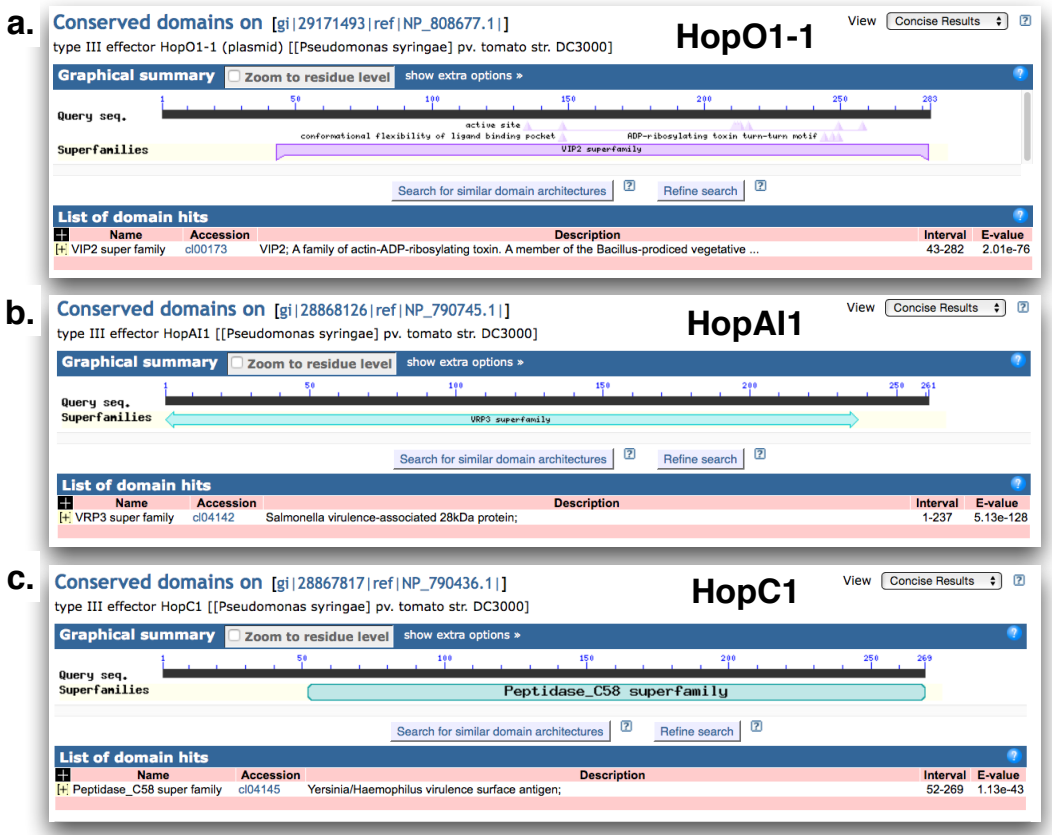

Supplementary Figure S5.2. Conserved domains in HopO1-1, HopAI1 and HopC1. A 'conserved domain' search on PubMed was performed in order to identify additional domains in the protein sequence of HopO1-1, HopA1 and HopC1 effectors. (a) HopO1-1 contains only a ADP-RT conserved domain; (b) HopAI1 contains only a VRP3 superfamily domain; (c) HopC1 contains only a peptidase domain from the C58 superfamily.

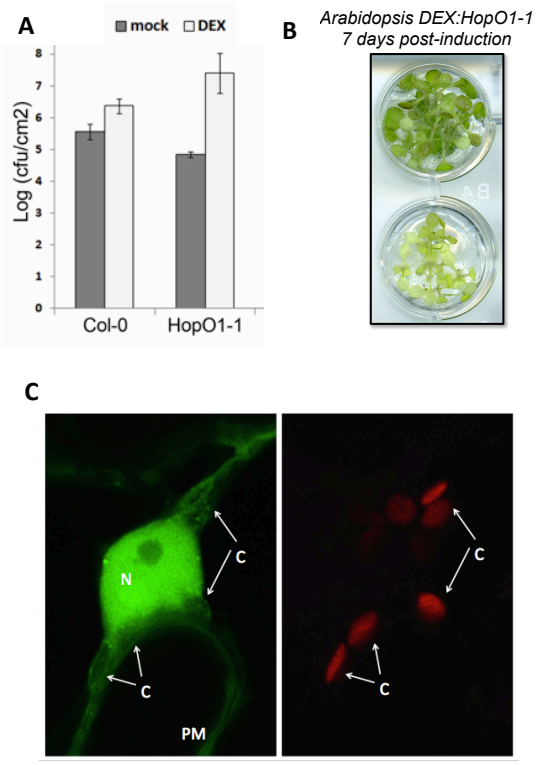

Supplementary Figure S5.3. HopO1-1 could localise to the nucleus and chloroplasts leading to a chlorotic effect and contributing to host colonisation; (a) bacterial growth in Col-0 is lower than in DEX-induced plants expressing a DEX-inducible HopO1-1 construct (b) chlorosis is observed after DEX induction in plants expressing a DEX-inducible HopO1-1 construct (c) HopO1-1 appears to localise to the chloroplasts in addition to the nucleus. C, Chloroplasts; N, Nuclei; PM, Plasma membrane. Images kindly provided by Dr. Gimenez-Ibanez from the Ntoukakis lab.

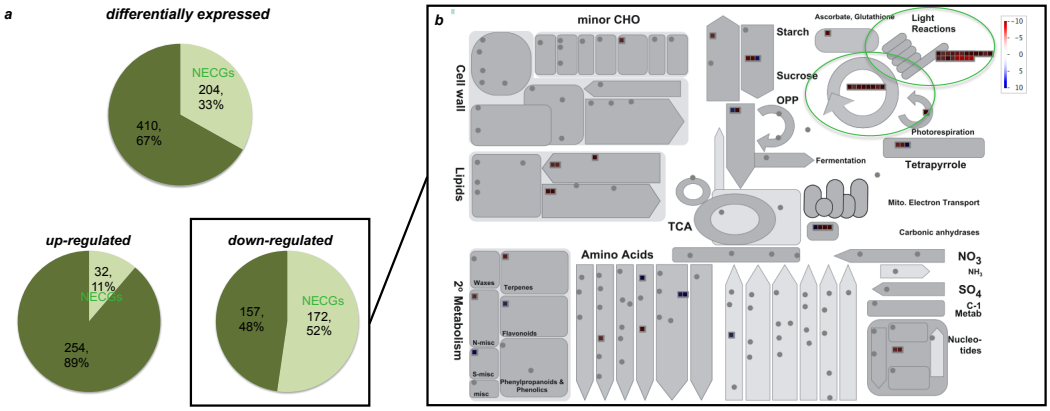

Supplementary Figure S5.4. HopO1-1 interferes with the expression of genes involved in photosynthetic processes.(a) Results from microarray experiments after DEX-induction of HopO1-1; (b) enrichment in NECGs encoding for proteins in the light reactions of photosynthesis. Images kindly provided by Dr. Gimenez-Ibanez from the Ntoukakis lab.

Effector	Published Localisation	Length	*Probability of Localisation*		Match (published vs. predicted)
			Chloroplast	Mitochondrion	
HopO1-1	N/A	283	0.86	0.05	N/A
HopO1-2	N/A	298	0.86	0.04	N/A
HopI1	Chloroplast	276	0.07	0.08	Low
HopN1	Chloroplast	350	0.15	0.34	Low
HopF2	Cytosol	204	0.57	0.42	Medium
HopM1	Cytosol	211	0.31	0.142	High
HopAI1	Cytosol	261	0.46	0.21	High

Supplementary Table S5.1. Predicting localisation to the chloroplast or mitochondrion using LOCALIZER software. Different effectors were queried for potential to localise to the chloroplasts or mitochondria. The published localisation of these effectors is shown to compare with the prediction outcome. Probability of localisation ranges from 0 (low) to 1 (high). The match between published localisation and prediction outcome is provided on the last column.

Bibliography

· 2BladesFoundation (2004). Projects and Technology.

· Aasland, R., Gibson, T.J., and Stewart, A.F. (1995). The PHD finger: implications for chromatin-mediated transcriptional regulation. Trends Biochem Sci *20*, 56-59.

· Abbo, S., Pinhasi van-Oss, R., Gopher, A., Saranga, Y., Ofner, I., and Peleg, Z. (2014). Plant domestication versus crop evolution: a conceptual framework for cereals and grain legumes. Trends Plant Sci *19*, 351-360.

· Abreu, M.E., and Munne-Bosch, S. (2009). Salicylic acid deficiency in NahG transgenic lines and sid2 mutants increases seed yield in the annual plant Arabidopsis thaliana. J Exp Bot *60*, 1261-1271.

· Aktar, M.W., Paramasivam, M., Sengupta, D., Purkait, S., Ganguly, M., and Banerjee, S. (2009). Impact assessment of pesticide residues in fish of Ganga river around Kolkata in West Bengal. Environ Monit Assess *157*, 97-104.

· Alajem, A., Biran, A., Harikumar, A., Sailaja, B.S., Aaronson, Y., Livyatan, I., Nissim-Rafinia, M., Sommer, A.G., Mostoslavsky, G., Gerbasi, V.R., *et al.* (2015). Differential association of chromatin proteins identifies BAF60a/SMARCD1 as a regulator of embryonic stem cell differentiation. Cell Rep *10*, 2019-2031.

· Alinsug, M.V., Chen, F.F., Luo, M., Tai, R., Jiang, L., and Wu, K. (2012). Subcellular localization of class II HDAs in Arabidopsis thaliana: nucleocytoplasmic shuttling of HDA15 is driven by light. PLoS One *7*, e30846.

· Alvarez, M., Nota, F., and Cambiagno, D. (2010). Epigenetic control of plant immunity. Molecular Plant Pathology ***11***, 563-576.

· Anzola, J.M., Sieberer, T., Ortbauer, M., Butt, H., Korbei, B., Weinhofer, I., Mullner, A.E., and Luschnig, C. (2010). Putative Arabidopsis transcriptional adaptor protein (PROPORZ1) is required to modulate histone acetylation in response to auxin. Proc Natl Acad Sci U S A *107*, 10308-10313.

· Appel, W. (1986). Chymotrypsin: molecular and catalytic properties. Clin Biochem *19*, 317-322.

· Asai, T., Tena, G., Plotnikova, J., Willmann, M.R., Chiu, W.L., Gomez-Gomez, L., Boller, T., Ausubel, F.M., and Sheen, J. (2002). MAP kinase signalling cascade in Arabidopsis innate immunity. Nature *415*, 977-983.

· Audenaert, K., Pattery, T., Cornelis, P., and Hofte, M. (2002). Induction of systemic resistance to Botrytis cinerea in tomato by Pseudomonas aeruginosa 7N-

SK2: role of salicylic acid, pyochelin, and pyocyanin. Mol Plant Microbe Interact *15*, 1147-1156.

· Barbieri, A.M., Sha, Q., Bette-Bobillo, P., Stahl, P.D., and Vidal, M. (2001). ADP-ribosylation of Rab5 by ExoS of Pseudomonas aeruginosa affects endocytosis. Infect Immun *69*, 5329-5334.

· Baulcombe, D. (2004). RNA silencing in plants. Nature *431*, 356-363.

· Baumgarten, A., Cannon, S., Spangler, R., and May, G. (2003). Genome-level evolution of resistance genes in Arabidopsis thaliana. Genetics *165*, 309-319.

· Benhamed, M., Bertrand, C., Servet, C., and Zhou, D.X. (2006). Arabidopsis GCN5, HD1, and TAF1/HAF2 interact to regulate histone acetylation required for light-responsive gene expression. Plant Cell *18*, 2893-2903.

· Benhamed, M., Martin-Magniette, M., Taconnat, L., Bitton, F., Servet, C., De Clercq, R., De Meyer, B., Buysschaert, C., Rombauts, S., Villarroel, R., *et al.* (2008). Genome-scale Arabidopsis promoter array identifies targets of the histone acetyltransferase GCN5. Plant Journal *56*, 493-504.

· Berger, S. (2007). The complex language of chromatin regulation during transcription. Nature *447*, 407-412.

· Bernstein, B.E., Mikkelsen, T.S., Xie, X., Kamal, M., Huebert, D.J., Cuff, J., Fry, B., Meissner, A., Wernig, M., Plath, K., *et al.* (2006). A bivalent chromatin structure marks key developmental genes in embryonic stem cells. Cell *125*, 315-326.

· Berr, A., McCallum, E.J., Alioua, A., Heintz, D., Heitz, T., and Shen, W.H. (2010). Arabidopsis histone methyltransferase SET DOMAIN GROUP8 mediates induction of the jasmonate/ethylene pathway genes in plant defense response to necrotrophic fungi. Plant Physiol *154*, 1403-1414.

· Bertrand, C., Bergounioux, C., Domenichini, S., Delarue, M., and Zhou, D. (2003). Arabidopsis histone acetyltransferase AtGCN5 regulates the floral meristem activity through the WUSCHEL/AGAMOUS pathway. Journal of Biological Chemistry *278*, 28246-28251.

· Bhat, R.A., Borst, J.W., Riehl, M., and Thompson, R.D. (2004). Interaction of maize Opaque-2 and the transcriptional co-activators GCN5 and ADA2, in the modulation of transcriptional activity. Plant Mol Biol *55*, 239-252.

· Bhat, R.A., Riehl, M., Santandrea, G., Velasco, R., Slocombe, S., Donn, G., Steinbiss, H.H., Thompson, R.D., and Becker, H.A. (2003). Alteration of GCN5 levels in maize reveals dynamic responses to manipulating histone acetylation. Plant J *33*, 455-469.

· Biel, M., Kretsovali, A., Karatzali, E., Papamatheakis, J., and Giannis, A. (2004). Design, synthesis, and biological evaluation of a small-molecule inhibitor of the histone acetyltransferase Gcn5. Angew Chem Int Ed Engl *43*, 3974-3976.
· Boch, J., and Bonas, U. (2010). Xanthomonas AvrBs3 family-type III effectors: discovery and function. Annu Rev Phytopathol *48*, 419-436.
· Boch, J., Bonas, U., and Lahaye, T. (2014). TAL effectors--pathogen strategies and plant resistance engineering. New Phytol *204*, 823-832.
· Bock, F.J., Todorova, T.T., and Chang, P. (2015). RNA Regulation by Poly(ADP-Ribose) Polymerases. Mol Cell *58*, 959-969.
· Boller, T., and Felix, G. (2009). A Renaissance of Elicitors: Perception of Microbe-Associated Molecular Patterns and Danger Signals by Pattern-Recognition Receptors. Annual Review of Plant Biology *60*, 379-406.
· Bolwell, G.P., Davies, D.R., Gerrish, C., Auh, C.K., and Murphy, T.M. (1998). Comparative biochemistry of the oxidative burst produced by rose and french bean cells reveals two distinct mechanisms. Plant Physiol *116*, 1379-1385.
· Boudsocq, M., Willmann, M., McCormack, M., Lee, H., Shan, L., He, P., Bush, J., Cheng, S., and Sheen, J. (2010). Differential innate immune signalling via Ca2+ sensor protein kinases. Nature *464*, 418-U116.
· Boutrot, F., Segonzac, C., Chang, K.N., Qiao, H., Ecker, J.R., Zipfel, C., and Rathjen, J.P. (2010). Direct transcriptional control of the Arabidopsis immune receptor FLS2 by the ethylene-dependent transcription factors EIN3 and EIL1. Proc Natl Acad Sci U S A *107*, 14502-14507.
· Boyer, L.A., Latek, R.R., and Peterson, C.L. (2004). The SANT domain: a unique histone-tail-binding module? Nat Rev Mol Cell Biol *5*, 158-163.
· Bradley, D.J., Kjellbom, P., and Lamb, C.J. (1992). Elicitor- and wound-induced oxidative cross-linking of a proline-rich plant cell wall protein: a novel, rapid defense response. Cell *70*, 21-30.
· Brameier, M., Krings, A., and MacCallum, R.M. (2007). NucPred--predicting nuclear localization of proteins. Bioinformatics *23*, 1159-1160.
· Braunstein, M., Sobel, R.E., Allis, C.D., Turner, B.M., and Broach, J.R. (1996). Efficient transcriptional silencing in Saccharomyces cerevisiae requires a heterochromatin histone acetylation pattern. Mol Cell Biol *16*, 4349-4356.
· Bretz, J.R., Mock, N.M., Charity, J.C., Zeyad, S., Baker, C.J., and Hutcheson, S.W. (2003). A translocated protein tyrosine phosphatase of Pseudomonas syringae

pv. tomato DC3000 modulates plant defence response to infection. Mol Microbiol *49*, 389-400.

· Brodersen, P., Petersen, M., Bjorn Nielsen, H., Zhu, S., Newman, M.A., Shokat, K.M., Rietz, S., Parker, J., and Mundy, J. (2006). Arabidopsis MAP kinase 4 regulates salicylic acid- and jasmonic acid/ethylene-dependent responses via EDS1 and PAD4. Plant J *47*, 532-546.

· Brouwer, A., Longnecker, M.P., Birnbaum, L.S., Cogliano, J., Kostyniak, P., Moore, J., Schantz, S., and Winneke, G. (1999). Characterization of potential endocrine-related health effects at low-dose levels of exposure to PCBs. Environ Health Perspect *107 Suppl 4*, 639-649.

· Brownell, J.E., and Allis, C.D. (1995). An activity gel assay detects a single, catalytically active histone acetyltransferase subunit in Tetrahymena macronuclei. Proc Natl Acad Sci U S A *92*, 6364-6368.

· Cabal, G.G., Genovesio, A., Rodriguez-Navarro, S., Zimmer, C., Gadal, O., Lesne, A., Buc, H., Feuerbach-Fournier, F., Olivo-Marin, J.C., Hurt, E.C., *et al.* (2006). SAGA interacting factors confine sub-diffusion of transcribed genes to the nuclear envelope. Nature *441*, 770-773.

· Cao, W., Bao, C., Padalko, E., and Lowenstein, C.J. (2008). Acetylation of mitogen-activated protein kinase phosphatase-1 inhibits Toll-like receptor signaling. J Exp Med *205*, 1491-1503.

· Carre, C., Szymczak, D., Pidoux, J., and Antoniewski, C. (2005). The histone H3 acetylase dGcn5 is a key player in Drosophila melanogaster metamorphosis. Mol Cell Biol *25*, 8228-8238.

· Catinot, J., Buchala, A., Abou-Mansour, E., and Metraux, J.P. (2008). Salicylic acid production in response to biotic and abiotic stress depends on isochorismate in Nicotiana benthamiana. FEBS Lett *582*, 473-478.

· Causier, B., Ashworth, M., Guo, W., and Davies, B. (2012). The TOPLESS interactome: a framework for gene repression in Arabidopsis. Plant Physiol *158*, 423-438.

· Chang, J.H., Urbach, J.M., Law, T.F., Arnold, L.W., Hu, A., Gombar, S., Grant, S.R., Ausubel, F.M., and Dangl, J.L. (2005). A high-throughput, near-saturating screen for type III effector genes from Pseudomonas syringae. Proc Natl Acad Sci U S A *102*, 2549-2554.

· Chen, M., and Shen, X. (2007). Nuclear actin and actin-related proteins in chromatin dynamics. Curr Opin Cell Biol *19*, 326-330.

· Chinchilla, D., Zipfel, C., Robatzek, S., Kemmerling, B., Nurnberger, T., Jones, J.D., Felix, G., and Boller, T. (2007). A flagellin-induced complex of the receptor FLS2 and BAK1 initiates plant defence. Nature *448*, 497-500.
· Chini, A., Fonseca, S., Fernandez, G., Adie, B., Chico, J.M., Lorenzo, O., Garcia-Casado, G., Lopez-Vidriero, I., Lozano, F.M., Ponce, M.R., *et al.* (2007). The JAZ family of repressors is the missing link in jasmonate signalling. Nature *448*, 666-671.
· Chittoor, J.M., Leach, J.E., and White, F.F. (1997). Differential induction of a peroxidase gene family during infection of rice by Xanthomonas oryzae pv. oryzae. Mol Plant Microbe Interact *10*, 861-871.
· Choi, S.M., Song, H.R., Han, S.K., Han, M., Kim, C.Y., Park, J., Lee, Y.H., Jeon, J.S., Noh, Y.S., and Noh, B. (2012). HDA19 is required for the repression of salicylic acid biosynthesis and salicylic acid-mediated defense responses in Arabidopsis. Plant J *71*, 135-146.
· Churchill, A.C. (2011). Mycosphaerella fijiensis, the black leaf streak pathogen of banana: progress towards understanding pathogen biology and detection, disease development, and the challenges of control. Mol Plant Pathol *12*, 307-328.
· Cigliano, R.A., Cremona, G., Paparo, R., Termolino, P., Perrella, G., Gutzat, R., Consiglio, M.F., and Conicella, C. (2013). Histone deacetylase AtHDA7 is required for female gametophyte and embryo development in Arabidopsis. Plant Physiol *163*, 431-440.
· Clark, D.J., and Felsenfeld, G. (1991). Formation of nucleosomes on positively supercoiled DNA. EMBO J *10*, 387-395.
· Clark, D.J., and Kimura, T. (1990). Electrostatic mechanism of chromatin folding. J Mol Biol *211*, 883-896.
· Conrath, U. (2011). Molecular aspects of defence priming. Trends Plant Sci *16*, 524-531.
· Corda, D., and Di Girolamo, M. (2003). Functional aspects of protein mono-ADP-ribosylation. EMBO J *22*, 1953-1958.
· Cote, J., Peterson, C.L., and Workman, J.L. (1998). Perturbation of nucleosome core structure by the SWI/SNF complex persists after its detachment, enhancing subsequent transcription factor binding. Proc Natl Acad Sci U S A *95*, 4947-4952.

· Crane, Y.M., and Gelvin, S.B. (2007). RNAi-mediated gene silencing reveals involvement of Arabidopsis chromatin-related genes in Agrobacterium-mediated root transformation. Proc Natl Acad Sci U S A *104*, 15156-15161.
· Crisp, T.M., Clegg, E.D., Cooper, R.L., Wood, W.P., Anderson, D.G., Baetcke, K.P., Hoffmann, J.L., Morrow, M.S., Rodier, D.J., Schaeffer, J.E.*, et al.* (1998). Environmental endocrine disruption: an effects assessment and analysis. Environ Health Perspect *106 Suppl 1*, 11-56.
· Cronauer-Mitra, S.S., and Krikorian, A.D. (1987). Adventitious shoot production from calloid cultures of banana. Plant Cell Rep *6*, 443-445.
· Cui, H., Tsuda, K., and Parker, J.E. (2015). Effector-triggered immunity: from pathogen perception to robust defense. Annu Rev Plant Biol *66*, 487-511.
· Cui, Y., Fang, X., and Qi, Y. (2016). TRANSPORTIN1 Promotes the Association of MicroRNA with ARGONAUTE1 in Arabidopsis. Plant Cell *28*, 2576-2585.
· Cunnac, S., Chakravarthy, S., Kvitko, B.H., Russell, A.B., Martin, G.B., and Collmer, A. (2011). Genetic disassembly and combinatorial reassembly identify a minimal functional repertoire of type III effectors in Pseudomonas syringae. Proc Natl Acad Sci U S A *108*, 2975-2980.
· Dangl, J.L., and Jones, J.D. (2001). Plant pathogens and integrated defence responses to infection. Nature *411*, 826-833.
· Day, C.A., Kraft, L.J., Kang, M., and Kenworthy, A.K. (2012). Analysis of protein and lipid dynamics using confocal fluorescence recovery after photobleaching (FRAP). Curr Protoc Cytom *Chapter 2*, Unit2 19.
· de la Cruz, X., Lois, S., Sanchez-Molina, S., and Martinez-Balbas, M.A. (2005). Do protein motifs read the histone code? Bioessays *27*, 164-175.
· de Torres Zabala, M., Littlejohn, G., Jayaraman, S., Studholme, D., Bailey, T., Lawson, T., Tillich, M., Licht, D., Bolter, B., Delfino, L.*, et al.* (2015). Chloroplasts play a central role in plant defence and are targeted by pathogen effectors. Nat Plants *1*, 15074.
· Defraia, C.T., Wang, Y., Yao, J., and Mou, Z. (2013). Elongator subunit 3 positively regulates plant immunity through its histone acetyltransferase and radical S-adenosylmethionine domains. BMC Plant Biol *13*, 102.
· DeFraia, C.T., Zhang, X., and Mou, Z. (2010). Elongator subunit 2 is an accelerator of immune responses in Arabidopsis thaliana. Plant J *64*, 511-523.

· Delaney, T.P., Uknes, S., Vernooij, B., Friedrich, L., Weymann, K., Negrotto, D., Gaffney, T., Gut-Rella, M., Kessmann, H., Ward, E., *et al.* (1994). A central role of salicylic Acid in plant disease resistance. Science *266*, 1247-1250.
· Dempsey, D.A., Vlot, A.C., Wildermuth, M.C., and Klessig, D.F. (2011). Salicylic Acid biosynthesis and metabolism. Arabidopsis Book *9*, e0156.
· Deng, W.L., and Huang, H.C. (1999). Cellular locations of Pseudomonas syringae pv. syringae HrcC and HrcJ proteins, required for harpin secretion via the type III pathway. J Bacteriol *181*, 2298-2301.
· Denis, A. (2015). From liability to opportunity: How to build food security and nourish growth. (London, McKinsey & Co).
· Deslandes, L., Olivier, J., Peeters, N., Feng, D.X., Khounlotham, M., Boucher, C., Somssich, I., Genin, S., and Marco, Y. (2003). Physical interaction between RRS1-R, a protein conferring resistance to bacterial wilt, and PopP2, a type III effector targeted to the plant nucleus. Proc Natl Acad Sci U S A *100*, 8024-8029.
· Devoto, A., Nieto-Rostro, M., Xie, D., Ellis, C., Harmston, R., Patrick, E., Davis, J., Sherratt, L., Coleman, M., and Turner, J.G. (2002). COI1 links jasmonate signalling and fertility to the SCF ubiquitin-ligase complex in Arabidopsis. Plant J *32*, 457-466.
· Dhawan, R., Luo, H., Foerster, A.M., Abuqamar, S., Du, H.N., Briggs, S.D., Mittelsten Scheid, O., and Mengiste, T. (2009). HISTONE MONOUBIQUITINATION1 interacts with a subunit of the mediator complex and regulates defense against necrotrophic fungal pathogens in Arabidopsis. Plant Cell *21*, 1000-1019.
· Ding, B., Bellizzi, M., Ning, Y., Meyers, B., and Wang, G. (2012). HDT701, a Histone H4 Deacetylase, Negatively Regulates Plant Innate Immunity by Modulating Histone H4 Acetylation of Defense-Related Genes in Rice. Plant Cell *24*, 3783-3794.
· Dolan, L., Janmaat, K., Willemsen, V., Linstead, P., Poethig, S., Roberts, K., and Scheres, B. (1993). Cellular organisation of the Arabidopsis thaliana root. Development *119*, 71-84.
· Du, J., Gao, Y., Zhan, Y., Zhang, S., Wu, Y., Xiao, Y., Zou, B., He, K., Gou, X., Li, G., *et al.* (2016). Nucleocytoplasmic trafficking is essential for BAK1- and BKK1-mediated cell-death control. Plant J *85*, 520-531.
· Dubiella, U., Seybold, H., Durian, G., Komander, E., Lassig, R., Witte, C.P., Schulze, W.X., and Romeis, T. (2013). Calcium-dependent protein kinase/

NADPH oxidase activation circuit is required for rapid defense signal propagation. Proc Natl Acad Sci U S A *110*, 8744-8749.

· Dundr, M., Hoffmann-Rohrer, U., Hu, Q., Grummt, I., Rothblum, L.I., Phair, R.D., and Misteli, T. (2002). A kinetic framework for a mammalian RNA polymerase in vivo. Science *298*, 1623-1626.

· Durrant, W., and Dong, X. (2004a). Systemic acquired resistance. Annual Review of Phytopathology *42*, 185-209.

· Durrant, W.E., and Dong, X. (2004b). Systemic acquired resistance. Annu Rev Phytopathol *42*, 185-209.

· Durrin, L.K., Mann, R.K., Kayne, P.S., and Grunstein, M. (1991). Yeast histone H4 N-terminal sequence is required for promoter activation in vivo. Cell *65*, 1023-1031.

· Earley, K.W., Haag, J.R., Pontes, O., Opper, K., Juehne, T., Song, K., and Pikaard, C.S. (2006). Gateway-compatible vectors for plant functional genomics and proteomics. Plant J *45*, 616-629.

· Earley, K.W., Shook, M.S., Brower-Toland, B., Hicks, L., and Pikaard, C.S. (2007). In vitro specificities of Arabidopsis co-activator histone acetyltransferases: implications for histone hyperacetylation in gene activation. Plant J *52*, 615-626.

· Eberharter, A., and Becker, P.B. (2002). Histone acetylation: a switch between repressive and permissive chromatin. Second in review series on chromatin dynamics. EMBO Rep *3*, 224-229.

· Espinosa, A., Guo, M., Tam, V.C., Fu, Z.Q., and Alfano, J.R. (2003). The Pseudomonas syringae type III-secreted protein HopPtoD2 possesses protein tyrosine phosphatase activity and suppresses programmed cell death in plants. Mol Microbiol *49*, 377-387.

· Felix, G., Duran, J., Volko, S., and Boller, T. (1999a). Plants have a sensitive perception system for the most conserved domain of bacterial flagellin. Plant Journal *18*, 265-276.

· Felix, G., Duran, J.D., Volko, S., and Boller, T. (1999b). Plants have a sensitive perception system for the most conserved domain of bacterial flagellin. Plant J *18*, 265-276.

· Feng, B., Liu, C., de Oliveira, M.V., Intorne, A.C., Li, B., Babilonia, K., de Souza Filho, G.A., Shan, L., and He, P. (2015). Protein poly(ADP-ribosyl)ation regulates

arabidopsis immune gene expression and defense responses. PLoS Genet *11*, e1004936.

· Fieldhouse, R.J., Turgeon, Z., White, D., and Merrill, A.R. (2010). Cholera- and anthrax-like toxins are among several new ADP-ribosyltransferases. PLoS Comput Biol *6*, e1001029.

· Finnegan, E.J., Peacock, W.J., and Dennis, E.S. (2000). DNA methylation, a key regulator of plant development and other processes. Curr Opin Genet Dev *10*, 217-223.

· Fisher, M.C., Henk, D.A., Briggs, C.J., Brownstein, J.S., Madoff, L.C., McCraw, S.L., and Gurr, S.J. (2012). Emerging fungal threats to animal, plant and ecosystem health. Nature *484*, 186-194.

· Franco-Zorrilla, J.M., Lopez-Vidriero, I., Carrasco, J.L., Godoy, M., Vera, P., and Solano, R. (2014). DNA-binding specificities of plant transcription factors and their potential to define target genes. Proc Natl Acad Sci U S A *111*, 2367-2372.

· Franks, T.M., Benner, C., Narvaiza, I., Marchetto, M.C., Young, J.M., Malik, H.S., Gage, F.H., and Hetzer, M.W. (2016). Evolution of a transcriptional regulator from a transmembrane nucleoporin. Genes Dev *30*, 1155-1171.

· Frei dit Frey, N., Garcia, A.V., Bigeard, J., Zaag, R., Bueso, E., Garmier, M., Pateyron, S., de Tauzia-Moreau, M.L., Brunaud, V., Balzergue, S., *et al.* (2014). Functional analysis of Arabidopsis immune-related MAPKs uncovers a role for MPK3 as negative regulator of inducible defences. Genome Biol *15*, R87.

· Frye, C.A., and Innes, R.W. (1998). An Arabidopsis mutant with enhanced resistance to powdery mildew. Plant Cell *10*, 947-956.

· Fu, Z.Q., Guo, M., Jeong, B.R., Tian, F., Elthon, T.E., Cerny, R.L., Staiger, D., and Alfano, J.R. (2007). A type III effector ADP-ribosylates RNA-binding proteins and quells plant immunity. Nature *447*, 284-288.

· Fu, Z.Q., Yan, S., Saleh, A., Wang, W., Ruble, J., Oka, N., Mohan, R., Spoel, S.H., Tada, Y., Zheng, N., *et al.* (2012). NPR3 and NPR4 are receptors for the immune signal salicylic acid in plants. Nature *486*, 228-232.

· Fuglie, K., Heisey, P., King, J., Pray, C.E., and Schimmelpfennig, D. (2012). Research funding. The contribution of private industry to agricultural innovation. Science *338*, 1031-1032.

· Gao, M.J., Hegedus, D.D., Sharpe, A.G., Robinson, S.J., Lydiate, D.J., and Hannoufa, A. (2007). Isolation and characterization of a GCN5-interacting protein from Arabidopsis thaliana. Planta *225*, 1367-1379.

· Gao, X., Chen, X., Lin, W., Chen, S., Lu, D., Niu, Y., Li, L., Cheng, C., McCormack, M., Sheen, J., *et al.* (2013). Bifurcation of Arabidopsis NLR immune signaling via Ca(2)(+)-dependent protein kinases. PLoS Pathog *9*, e1003127.
· Gaspar-Maia, A., Alajem, A., Meshorer, E., and Ramalho-Santos, M. (2011). Open chromatin in pluripotency and reprogramming. Nat Rev Mol Cell Biol *12*, 36-47.
· Gaspar-Maia, A., Alajem, A., Polesso, F., Sridharan, R., Mason, M.J., Heidersbach, A., Ramalho-Santos, J., McManus, M.T., Plath, K., Meshorer, E., *et al.* (2009). Chd1 regulates open chromatin and pluripotency of embryonic stem cells. Nature *460*, 863-868.
· Georgakopoulos, T., and Thireos, G. (1992). Two distinct yeast transcriptional activators require the function of the GCN5 protein to promote normal levels of transcription. EMBO J *11*, 4145-4152.
· Gimenez-Ibanez, S., Hann, D.R., Ntoukakis, V., Petutschnig, E., Lipka, V., and Rathjen, J.P. (2009). AvrPtoB targets the LysM receptor kinase CERK1 to promote bacterial virulence on plants. Curr Biol *19*, 423-429.
· Glazebrook, J. (2005). Contrasting mechanisms of defense against biotrophic and necrotrophic pathogens. Annu Rev Phytopathol *43*, 205-227.
· Glozak, M.A., Sengupta, N., Zhang, X., and Seto, E. (2005). Acetylation and deacetylation of non-histone proteins. Gene *363*, 15-23.
· Gomez-Gomez, L., and Boller, T. (2000). FLS2: An LRR receptor-like kinase involved in the perception of the bacterial elicitor flagellin in Arabidopsis. Molecular Cell *5*, 1003-1011.
· Grant, P.A., Duggan, L., Cote, J., Roberts, S.M., Brownell, J.E., Candau, R., Ohba, R., Owen-Hughes, T., Allis, C.D., Winston, F., *et al.* (1997). Yeast Gcn5 functions in two multisubunit complexes to acetylate nucleosomal histones: characterization of an Ada complex and the SAGA (Spt/Ada) complex. Genes Dev *11*, 1640-1650.
· Grant, P.A., Eberharter, A., John, S., Cook, R.G., Turner, B.M., and Workman, J.L. (1999). Expanded lysine acetylation specificity of Gcn5 in native complexes. J Biol Chem *274*, 5895-5900.
· Grant, P.A., Schieltz, D., Pray-Grant, M.G., Steger, D.J., Reese, J.C., Yates, J.R., 3rd, and Workman, J.L. (1998). A subset of TAF(II)s are integral components of the SAGA complex required for nucleosome acetylation and transcriptional stimulation. Cell *94*, 45-53.

· Gregory, P.D., Schmid, A., Zavari, M., Lui, L., Berger, S.L., and Horz, W. (1998). Absence of Gcn5 HAT activity defines a novel state in the opening of chromatin at the PHO5 promoter in yeast. Mol Cell *1*, 495-505.
· Gruenbaum, Y., Naveh-Many, T., Cedar, H., and Razin, A. (1981). Sequence specificity of methylation in higher plant DNA. Nature *292*, 860-862.
· Guo, W., Yang, H., Liu, Y., Gao, Y., Ni, Z., Peng, H., Xin, M., Hu, Z., Sun, Q., and Yao, Y. (2015). The wheat transcription factor TaGAMyb recruits histone acetyltransferase and activates the expression of a high-molecular-weight glutenin subunit gene. Plant J *84*, 347-359.
· Hamon, M., and Cossart, P. (2008). Histone modifications and chromatin remodeling during bacterial infections. Cell Host & Microbe *4*, 100-109.
· Hark, A.T., Vlachonasios, K.E., Pavangadkar, K.A., Rao, S., Gordon, H., Adamakis, I.D., Kaldis, A., Thomashow, M.F., and Triezenberg, S.J. (2009). Two Arabidopsis orthologs of the transcriptional coactivator ADA2 have distinct biological functions. Biochim Biophys Acta *1789*, 117-124.
· Holbourn, K.P., Shone, C.C., and Acharya, K.R. (2006). A family of killer toxins. Exploring the mechanism of ADP-ribosylating toxins. FEBS J *273*, 4579-4593.
· Homrich, M.S., Wiebke-Strohm, B., Weber, R.L., and Bodanese-Zanettini, M.H. (2012). Soybean genetic transformation: A valuable tool for the functional study of genes and the production of agronomically improved plants. Genet Mol Biol *35*, 998-1010.
· Hopkins, A.L. (2008). Network pharmacology: the next paradigm in drug discovery. Nat Chem Biol *4*, 682-690.
· Ishibashi, N., Kitakura, S., Terakura, S., Machida, C., and Machida, Y. (2014). Protein encoded by oncogene 6b from Agrobacterium tumefaciens has a reprogramming potential and histone chaperone-like activity. Front Plant Sci *5*, 572.
· Jackson, R.J., Hellen, C.U., and Pestova, T.V. (2010). The mechanism of eukaryotic translation initiation and principles of its regulation. Nat Rev Mol Cell Biol *11*, 113-127.
· Jacob, F., Vernaldi, S., and Maekawa, T. (2013). Evolution and Conservation of Plant NLR Functions. Front Immunol *4*, 297.
· Jacobson, R.H., Ladurner, A.G., King, D.S., and Tjian, R. (2000). Structure and function of a human TAFII250 double bromodomain module. Science *288*, 1422-1425.

· Jagtap, P., and Szabo, C. (2005). Poly(ADP-ribose) polymerase and the therapeutic effects of its inhibitors. Nat Rev Drug Discov *4*, 421-440.
· Jankowsky, E., Gross, C.H., Shuman, S., and Pyle, A.M. (2001). Active disruption of an RNA-protein interaction by a DExH/D RNA helicase. Science *291*, 121-125.
· Jaskiewicz, M., Conrath, U., and Peterhansel, C. (2011). Chromatin modification acts as a memory for systemic acquired resistance in the plant stress response. Embo Reports *12*, 50-55.
· Jenuwein, T., and Allis, C.D. (2001). Translating the histone code. Science *293*, 1074-1080.
· Jones, J., and Dangl, J. (2006). The plant immune system. Nature *444*, 323-329.
· Jouhet, J., and Gray, J.C. (2009). Interaction of actin and the chloroplast protein import apparatus. J Biol Chem *284*, 19132-19141.
· Kadota, Y., Sklenar, J., Derbyshire, P., Stransfeld, L., Asai, S., Ntoukakis, V., Jones, J.D., Shirasu, K., Menke, F., Jones, A., *et al.* (2014). Direct regulation of the NADPH oxidase RBOHD by the PRR-associated kinase BIK1 during plant immunity. Mol Cell *54*, 43-55.
· Kaldis, A., Tsementzi, D., Tanriverdi, O., and Vlachonasios, K.E. (2011). Arabidopsis thaliana transcriptional co-activators ADA2b and SGF29a are implicated in salt stress responses. Planta *233*, 749-762.
· Kassem, S., Villanyi, Z., and Collart, M.A. (2017). Not5-dependent co-translational assembly of Ada2 and Spt20 is essential for functional integrity of SAGA. Nucleic Acids Res *45*, 1186-1199.
· Khan, A., Garbelli, A., Grossi, S., Florentin, A., Batelli, G., Acuna, T., Zolla, G., Kaye, Y., Paul, L.K., Zhu, J.K., *et al.* (2014). The Arabidopsis STRESS RESPONSE SUPPRESSOR DEAD-box RNA helicases are nucleolar- and chromocenter-localized proteins that undergo stress-mediated relocalization and are involved in epigenetic gene silencing. Plant J *79*, 28-43.
· Kim, D.S., and Hwang, B.K. (2014). An important role of the pepper phenylalanine ammonia-lyase gene (PAL1) in salicylic acid-dependent signalling of the defence response to microbial pathogens. J Exp Bot *65*, 2295-2306.
· Kim, G.W., and Yang, X.J. (2011). Comprehensive lysine acetylomes emerging from bacteria to humans. Trends Biochem Sci *36*, 211-220.

· Kim, J.M., Sasaki, T., Ueda, M., Sako, K., and Seki, M. (2015). Chromatin changes in response to drought, salinity, heat, and cold stresses in plants. Front Plant Sci *6*, 114.
· Kliebenstein, D.J., Rowe, H.C., and Denby, K.J. (2005). Secondary metabolites influence Arabidopsis/Botrytis interactions: variation in host production and pathogen sensitivity. Plant J *44*, 25-36.
· Kloek, A.P., Verbsky, M.L., Sharma, S.B., Schoelz, J.E., Vogel, J., Klessig, D.F., and Kunkel, B.N. (2001). Resistance to Pseudomonas syringae conferred by an Arabidopsis thaliana coronatine-insensitive (coi1) mutation occurs through two distinct mechanisms. Plant J *26*, 509-522.
· Klose, R.J., and Bird, A.P. (2006). Genomic DNA methylation: the mark and its mediators. Trends Biochem Sci *31*, 89-97.
· Kong, L., Qiu, X., Kang, J., Wang, Y., Chen, H., Huang, J., Qiu, M., Zhao, Y., Kong, G., Ma, Z., *et al.* (2017). A Phytophthora Effector Manipulates Host Histone Acetylation and Reprograms Defense Gene Expression to Promote Infection. Curr Biol *27*, 981-991.
· Koornneef, M., and Meinke, D. (2010). The development of Arabidopsis as a model plant. Plant J *61*, 909-921.
· Kornberg, R.D. (1974). Chromatin structure: a repeating unit of histones and DNA. Science *184*, 868-871.
· Kornet, N., and Scheres, B. (2009). Members of the GCN5 Histone Acetyltransferase Complex Regulate PLETHORA-Mediated Root Stem Cell Niche Maintenance and Transit Amplifying Cell Proliferation in Arabidopsis. Plant Cell *21*, 1070-1079.
· Kornfeld, S., and Mellman, I. (1989). The biogenesis of lysosomes. Annu Rev Cell Biol *5*, 483-525.
· Koutelou, E., Hirsch, C.L., and Dent, S.Y. (2010). Multiple faces of the SAGA complex. Curr Opin Cell Biol *22*, 374-382.
· Kouzarides, T. (2007). Chromatin modifications and their function. Cell *128*, 693-705.
· Kruger, W., Peterson, C.L., Sil, A., Coburn, C., Arents, G., Moudrianakis, E.N., and Herskowitz, I. (1995). Amino acid substitutions in the structured domains of histones H3 and H4 partially relieve the requirement of the yeast SWI/SNF complex for transcription. Genes Dev *9*, 2770-2779.

· Kumar, S., and Wigge, P. (2010). H2A.Z-Containing Nucleosomes Mediate the Thermosensory Response in Arabidopsis. Cell *140*, 136-147.
· Kunze, G., Zipfel, C., Robatzek, S., Niehaus, K., Boller, T., and Felix, G. (2004). The N terminus of bacterial elongation factor Tu elicits innate immunity in Arabidopsis plants. Plant Cell *16*, 3496-3507.
· Kuo, M.H., Brownell, J.E., Sobel, R.E., Ranalli, T.A., Cook, R.G., Edmondson, D.G., Roth, S.Y., and Allis, C.D. (1996). Transcription-linked acetylation by Gcn5p of histones H3 and H4 at specific lysines. Nature *383*, 269-272.
· Kvitko, B.H., Park, D.H., Velasquez, A.C., Wei, C.F., Russell, A.B., Martin, G.B., Schneider, D.J., and Collmer, A. (2009). Deletions in the repertoire of Pseudomonas syringae pv. tomato DC3000 type III secretion effector genes reveal functional overlap among effectors. PLoS Pathog *5*, e1000388.
· Lacombe, S., Rougon-Cardoso, A., Sherwood, E., Peeters, N., Dahlbeck, D., van Esse, H.P., Smoker, M., Rallapalli, G., Thomma, B.P., Staskawicz, B., *et al.* (2010). Interfamily transfer of a plant pattern-recognition receptor confers broad-spectrum bacterial resistance. Nat Biotechnol *28*, 365-369.
· Latrasse, D., Benhamed, M., Henry, Y., Domenichini, S., Kim, W., Zhou, D.X., and Delarue, M. (2008). The MYST histone acetyltransferases are essential for gametophyte development in Arabidopsis. BMC Plant Biol *8*, 121.
· Latrasse, D., Jegu, T., Li, H., de Zelicourt, A., Raynaud, C., Legras, S., Gust, A., Samajova, O., Veluchamy, A., Rayapuram, N., *et al.* (2017). MAPK-triggered chromatin reprogramming by histone deacetylase in plant innate immunity. Genome Biol *18*, 131.
· Lebreton, A., Lakisic, G., Job, V., Fritsch, L., Tham, T.N., Camejo, A., Mattei, P.J., Regnault, B., Nahori, M.A., Cabanes, D., *et al.* (2011). A bacterial protein targets the BAHD1 chromatin complex to stimulate type III interferon response. Science *331*, 1319-1321.
· Lecourieux, D., Mazars, C., Pauly, N., Ranjeva, R., and Pugin, A. (2002). Analysis and effects of cytosolic free calcium increases in response to elicitors in Nicotiana plumbaginifolia cells. Plant Cell *14*, 2627-2641.
· Lecourieux, D., Ranjeva, R., and Pugin, A. (2006). Calcium in plant defence-signalling pathways. New Phytol *171*, 249-269.
· Lewis, L.A., Polanski, K., de Torres-Zabala, M., Jayaraman, S., Bowden, L., Moore, J., Penfold, C.A., Jenkins, D.J., Hill, C., Baxter, L., *et al.* (2015). Transcriptional Dynamics Driving MAMP-Triggered Immunity and Pathogen Effector-

Mediated Immunosuppression in Arabidopsis Leaves Following Infection with Pseudomonas syringae pv tomato DC3000. Plant Cell *27*, 3038-3064.

· Li, C., Xu, J., Li, J., Li, Q., and Yang, H. (2014a). Involvement of Arabidopsis HAC family genes in pleiotropic developmental processes. Plant Signal Behav *9*, e28173.

· Li, F., Cheng, C., Cui, F., de Oliveira, M.V., Yu, X., Meng, X., Intorne, A.C., Babilonia, K., Li, M., Li, B., *et al.* (2014b). Modulation of RNA polymerase II phosphorylation downstream of pathogen perception orchestrates plant immunity. Cell Host Microbe *16*, 748-758.

· Li, G., Froehlich, J.E., Elowsky, C., Msanne, J., Ostosh, A.C., Zhang, C., Awada, T., and Alfano, J.R. (2014c). Distinct Pseudomonas type-III effectors use a cleavable transit peptide to target chloroplasts. Plant J *77*, 310-321.

· Li, X., Jiang, Y., Ji, Z., Liu, Y., and Zhang, Q. (2015). BRHIS1 suppresses rice innate immunity through binding to monoubiquitinated H2A and H2B variants. EMBO Rep *16*, 1192-1202.

· Ligterink, W., Kroj, T., zur Nieden, U., Hirt, H., and Scheel, D. (1997). Receptor-mediated activation of a MAP kinase in pathogen defense of plants. Science *276*, 2054-2057.

· Lin, J.R., and Hu, J. (2013). SeqNLS: nuclear localization signal prediction based on frequent pattern mining and linear motif scoring. PLoS One *8*, e76864.

· Lin, W., Li, B., Lu, D., Chen, S., Zhu, N., He, P., and Shan, L. (2014). Tyrosine phosphorylation of protein kinase complex BAK1/BIK1 mediates Arabidopsis innate immunity. Proc Natl Acad Sci U S A *111*, 3632-3637.

· Lindeberg, M., Myers, C.R., Collmer, A., and Schneider, D.J. (2008). Roadmap to new virulence determinants in Pseudomonas syringae: insights from comparative genomics and genome organization. Mol Plant Microbe Interact *21*, 685-700.

· Liu, X., Luo, M., Zhang, W., Zhao, J., Zhang, J., Wu, K., Tian, L., and Duan, J. (2012). Histone acetyltransferases in rice (Oryza sativa L.): phylogenetic analysis, subcellular localization and expression. BMC Plant Biol *12*, 145.

· Liu, Z., and Karmarkar, V. (2008). Groucho/Tup1 family co-repressors in plant development. Trends Plant Sci *13*, 137-144.

· Long, J.A., Ohno, C., Smith, Z.R., and Meyerowitz, E.M. (2006). TOPLESS regulates apical embryonic fate in Arabidopsis. Science *312*, 1520-1523.

· Lorenzo, O., Piqueras, R., Sanchez-Serrano, J.J., and Solano, R. (2003). ETHYLENE RESPONSE FACTOR1 integrates signals from ethylene and jasmonate pathways in plant defense. Plant Cell *15*, 165-178.
· Low, J.C., and Donachie, W. (1997). A review of Listeria monocytogenes and listeriosis. Vet J *153*, 9-29.
· Luger, K., Mader, A.W., Richmond, R.K., Sargent, D.F., and Richmond, T.J. (1997). Crystal structure of the nucleosome core particle at 2.8 A resolution. Nature *389*, 251-260.
· Luna, E., Pastor, V., Robert, J., Flors, V., Mauch-Mani, B., and Ton, J. (2011). Callose deposition: a multifaceted plant defense response. Mol Plant Microbe Interact *24*, 183-193.
· Luque, A., Collepardo-Guevara, R., Grigoryev, S., and Schlick, T. (2014). Dynamic condensation of linker histone C-terminal domain regulates chromatin structure. Nucleic Acids Res *42*, 7553-7560.
· Lusser, A. (2002). Acetylated, methylated, remodeled: chromatin states for gene regulation. Curr Opin Plant Biol *5*, 437-443.
· Lusser, A., Kolle, D., and Loidl, P. (2001). Histone acetylation: lessons from the plant kingdom. Trends Plant Sci *6*, 59-65.
· Ma, W., and Berkowitz, G.A. (2007). The grateful dead: calcium and cell death in plant innate immunity. Cell Microbiol *9*, 2571-2585.
· Macaluso, M., Montanari, M., and Giordano, A. (2006). Rb family proteins as modulators of gene expression and new aspects regarding the interaction with chromatin remodeling enzymes. Oncogene *25*, 5263-5267.
· Macek, B., Waanders, L.F., Olsen, J.V., and Mann, M. (2006). Top-down protein sequencing and MS3 on a hybrid linear quadrupole ion trap-orbitrap mass spectrometer. Mol Cell Proteomics *5*, 949-958.
· Macho, A.P., Schwessinger, B., Ntoukakis, V., Brutus, A., Segonzac, C., Roy, S., Kadota, Y., Oh, M.H., Sklenar, J., Derbyshire, P., *et al.* (2014). A bacterial tyrosine phosphatase inhibits plant pattern recognition receptor activation. Science *343*, 1509-1512.
· Mahrez, W., Arellano, M.S., Moreno-Romero, J., Nakamura, M., Shu, H., Nanni, P., Kohler, C., Gruissem, W., and Hennig, L. (2016). H3K36ac Is an Evolutionary Conserved Plant Histone Modification That Marks Active Genes. Plant Physiol *170*, 1566-1577.

· Makandar, R., Essig, J.S., Schapaugh, M.A., Trick, H.N., and Shah, J. (2006). Genetically engineered resistance to Fusarium head blight in wheat by expression of Arabidopsis NPR1. Mol Plant Microbe Interact *19*, 123-129.
· Mao, Y., Pavangadkar, K.A., Thomashow, M.F., and Triezenberg, S.J. (2006). Physical and functional interactions of Arabidopsis ADA2 transcriptional coactivator proteins with the acetyltransferase GCN5 and with the cold-induced transcription factor CBF1. Biochim Biophys Acta *1759*, 69-79.
· March-Diaz, R., Garcia-Dominguez, M., Lozano-Juste, J., Leon, J., Florencio, F.J., and Reyes, J.C. (2008). Histone H2A.Z and homologues of components of the SWR1 complex are required to control immunity in Arabidopsis. Plant J *53*, 475-487.
· Marchler-Bauer, A., Lu, S., Anderson, J.B., Chitsaz, F., Derbyshire, M.K., DeWeese-Scott, C., Fong, J.H., Geer, L.Y., Geer, R.C., Gonzales, N.R., *et al.* (2011). CDD: a Conserved Domain Database for the functional annotation of proteins. Nucleic Acids Res *39*, D225-229.
· Marfella, C.G., and Imbalzano, A.N. (2007). The Chd family of chromatin remodelers. Mutat Res *618*, 30-40.
· Marois, E., Van den Ackerveken, G., and Bonas, U. (2002). The xanthomonas type III effector protein AvrBs3 modulates plant gene expression and induces cell hypertrophy in the susceptible host. Mol Plant Microbe Interact *15*, 637-646.
· Mateyak, M.K., and Kinzy, T.G. (2013). ADP-ribosylation of translation elongation factor 2 by diphtheria toxin in yeast inhibits translation and cell separation. J Biol Chem *288*, 24647-24655.
· Matzinger, P. (2007). Friendly and dangerous signals: is the tissue in control? Nat Immunol *8*, 11-13.
· McHale, L., Tan, X., Koehl, P., and Michelmore, R.W. (2006). Plant NBS-LRR proteins: adaptable guards. Genome Biol *7*, 212.
· Melotto, M., Underwood, W., Koczan, J., Nomura, K., and He, S.Y. (2006). Plant stomata function in innate immunity against bacterial invasion. Cell *126*, 969-980.
· Messner, S., Altmeyer, M., Zhao, H., Pozivil, A., Roschitzki, B., Gehrig, P., Rutishauser, D., Huang, D., Caflisch, A., and Hottiger, M.O. (2010). PARP1 ADP-ribosylates lysine residues of the core histone tails. Nucleic Acids Res *38*, 6350-6362.

· Millet, Y.A., Danna, C.H., Clay, N.K., Songnuan, W., Simon, M.D., Werck-Reichhart, D., and Ausubel, F.M. (2010). Innate immune responses activated in Arabidopsis roots by microbe-associated molecular patterns. Plant Cell *22*, 973-990.
· Misteli, T. (2001). Nuclear structure - Protein dynamics: Implications for nuclear architecture and gene expression. Science *291*, 843-847.
· Moore, J.W., Loake, G.J., and Spoel, S.H. (2011). Transcription dynamics in plant immunity. Plant Cell *23*, 2809-2820.
· Moraga, F., and Aquea, F. (2015). Composition of the SAGA complex in plants and its role in controlling gene expression in response to abiotic stresses. Front Plant Sci *6*, 865.
· Mosher, R.A., Durrant, W.E., Wang, D., Song, J., and Dong, X. (2006). A comprehensive structure-function analysis of Arabidopsis SNI1 defines essential regions and transcriptional repressor activity. Plant Cell *18*, 1750-1765.
· Mou, Z., Fan, W., and Dong, X. (2003). Inducers of plant systemic acquired resistance regulate NPR1 function through redox changes. Cell *113*, 935-944.
· Mueller, F., Mazza, D., Stasevich, T.J., and McNally, J.G. (2010). FRAP and kinetic modeling in the analysis of nuclear protein dynamics: what do we really know? Curr Opin Cell Biol *22*, 403-411.
· Narusaka, M., Kubo, Y., Hatakeyama, K., Imamura, J., Ezura, H., Nanasato, Y., Tabei, Y., Takano, Y., Shirasu, K., and Narusaka, Y. (2013). Interfamily transfer of dual NB-LRR genes confers resistance to multiple pathogens. PLoS One *8*, e55954.
· Navarro, L., Jay, F., Nomura, K., He, S.Y., and Voinnet, O. (2008). Suppression of the microRNA pathway by bacterial effector proteins. Science *321*, 964-967.
· Navarro, L., Zipfel, C., Rowland, O., Keller, I., Robatzek, S., Boller, T., and Jones, J.D. (2004). The transcriptional innate immune response to flg22. Interplay and overlap with Avr gene-dependent defense responses and bacterial pathogenesis. Plant Physiol *135*, 1113-1128.
· Neely, K.E., and Workman, J.L. (2002). Histone acetylation and chromatin remodeling: which comes first? Mol Genet Metab *76*, 1-5.
· Nguyen Ba, A.N., Pogoutse, A., Provart, N., and Moses, A.M. (2009). NLStradamus: a simple Hidden Markov Model for nuclear localization signal prediction. BMC Bioinformatics *10*, 202.
· Nicaise, V., Joe, A., Jeong, B.R., Korneli, C., Boutrot, F., Westedt, I., Staiger, D., Alfano, J.R., and Zipfel, C. (2013). Pseudomonas HopU1 modulates plant im-

mune receptor levels by blocking the interaction of their mRNAs with GRP7. EMBO J *32*, 701-712.

· Nicaise, V., Roux, M., and Zipfel, C. (2009). Recent advances in PAMP-triggered immunity against bacteria: pattern recognition receptors watch over and raise the alarm. Plant Physiol *150*, 1638-1647.

· Nomura, K., Debroy, S., Lee, Y.H., Pumplin, N., Jones, J., and He, S.Y. (2006). A bacterial virulence protein suppresses host innate immunity to cause plant disease. Science *313*, 220-223.

· Olsen, J.V., Ong, S.E., and Mann, M. (2004). Trypsin cleaves exclusively C-terminal to arginine and lysine residues. Mol Cell Proteomics *3*, 608-614.

· Paine, J.A., Shipton, C.A., Chaggar, S., Howells, R.M., Kennedy, M.J., Vernon, G., Wright, S.Y., Hinchliffe, E., Adams, J.L., Silverstone, A.L., *et al.* (2005). Improving the nutritional value of Golden Rice through increased pro-vitamin A content. Nat Biotechnol *23*, 482-487.

· Pandey, R., Muller, A., Napoli, C., Selinger, D., Pikaard, C., Richards, E., Bender, J., Mount, D., and Jorgensen, R. (2002). Analysis of histone acetyltransferase and histone deacetylase families of Arabidopsis thaliana suggests functional diversification of chromatin modification among multicellular eukaryotes. Nucleic Acids Research *30*, 5036-5055.

· Paul, J.Y., Khanna, H., Kleidon, J., Hoang, P., Geijskes, J., Daniells, J., Zaplin, E., Rosenberg, Y., James, A., Mlalazi, B., *et al.* (2017). Golden bananas in the field: elevated fruit pro-vitamin A from the expression of a single banana transgene. Plant Biotechnol J *15*, 520-532.

· Pauwels, L., Barbero, G.F., Geerinck, J., Tilleman, S., Grunewald, W., Perez, A.C., Chico, J.M., Bossche, R.V., Sewell, J., Gil, E., *et al.* (2010). NINJA connects the co-repressor TOPLESS to jasmonate signalling. Nature *464*, 788-791.

· Pavet, V., Quintero, C., Cecchini, N.M., Rosa, A.L., and Alvarez, M.E. (2006). Arabidopsis displays centromeric DNA hypomethylation and cytological alterations of heterochromatin upon attack by pseudomonas syringae. Mol Plant Microbe Interact *19*, 577-587.

· Perdivara, I., Deterding, L.J., Przybylski, M., and Tomer, K.B. (2010). Mass spectrometric identification of oxidative modifications of tryptophan residues in proteins: chemical artifact or post-translational modification? J Am Soc Mass Spectrom *21*, 1114-1117.

· Pereira, S.F., Goss, L., and Dworkin, J. (2011). Eukaryote-like serine/threonine kinases and phosphatases in bacteria. Microbiol Mol Biol Rev *75*, 192-212.
· Petersen, M., Brodersen, P., Naested, H., Andreasson, E., Lindhart, U., Johansen, B., Nielsen, H.B., Lacy, M., Austin, M.J., Parker, J.E., *et al.* (2000). Arabidopsis map kinase 4 negatively regulates systemic acquired resistance. Cell *103*, 1111-1120.
· Petnicki-Ocwieja, T., van Dijk, K., and Alfano, J.R. (2005). The hrpK operon of Pseudomonas syringae pv. tomato DC3000 encodes two proteins secreted by the type III (Hrp) protein secretion system: HopB1 and HrpK, a putative type III translocator. J Bacteriol *187*, 649-663.
· Phair, R.D., Scaffidi, P., Elbi, C., Vecerova, J., Dey, A., Ozato, K., Brown, D.T., Hager, G., Bustin, M., and Misteli, T. (2004). Global nature of dynamic protein-chromatin interactions in vivo: three-dimensional genome scanning and dynamic interaction networks of chromatin proteins. Mol Cell Biol *24*, 6393-6402.
· Pieterse, C.M., Van der Does, D., Zamioudis, C., Leon-Reyes, A., and Van Wees, S.C. (2012). Hormonal modulation of plant immunity. Annu Rev Cell Dev Biol *28*, 489-521.
· Piquerez, S.J., Balmuth, A.L., Sklenar, J., Jones, A.M., Rathjen, J.P., and Ntoukakis, V. (2014). Identification of post-translational modifications of plant protein complexes. J Vis Exp, e51095.
· Pitzschke, A., and Hirt, H. (2009). Disentangling the complexity of mitogen-activated protein kinases and reactive oxygen species signaling. Plant Physiol *149*, 606-615.
· Pitzschke, A., Schikora, A., and Hirt, H. (2009). MAPK cascade signalling networks in plant defence. Curr Opin Plant Biol *12*, 421-426.
· Pray, C.E., Courtmanche, A., and Govindasamy, R. (2002). The importance of interllectual property rights in the interantional spread of private sector agricultural biotechnology. 6th International Conference by ICABR on Agricultural Biotechnologies *New Avenues for Production, Consumption and Technology Transfer*.
· Pray-Grant, M.G., Daniel, J.A., Schieltz, D., Yates, J.R., 3rd, and Grant, P.A. (2005). Chd1 chromodomain links histone H3 methylation with SAGA- and SLIK-dependent acetylation. Nature *433*, 434-438.
· Pray-Grant, M.G., Schieltz, D., McMahon, S.J., Wood, J.M., Kennedy, E.L., Cook, R.G., Workman, J.L., Yates, J.R., 3rd, and Grant, P.A. (2002). The novel SLIK his-

tone acetyltransferase complex functions in the yeast retrograde response pathway. Mol Cell Biol *22*, 8774-8786.

· Pruett, S.B., Fan, R., and Zheng, Q. (2003). Characterization of glucocorticoid receptor translocation, cytoplasmic IkappaB, nuclear NFkappaB, and activation of NFkappaB in T lymphocytes exposed to stress-inducible concentrations of corticosterone in vivo. Int Immunopharmacol *3*, 1-16.

· Qi, Y., Tsuda, K., Joe, A., Sato, M., Nguyen le, V., Glazebrook, J., Alfano, J.R., Cohen, J.D., and Katagiri, F. (2010). A putative RNA-binding protein positively regulates salicylic acid-mediated immunity in Arabidopsis. Mol Plant Microbe Interact *23*, 1573-1583.

· Qian, W., Miki, D., Zhang, H., Liu, Y., Zhang, X., Tang, K., Kan, Y., La, H., Li, X., Li, S., *et al.* (2012). A histone acetyltransferase regulates active DNA demethylation in Arabidopsis. Science *336*, 1445-1448.

· Qiu, J.L., Fiil, B.K., Petersen, K., Nielsen, H.B., Botanga, C.J., Thorgrimsen, S., Palma, K., Suarez-Rodriguez, M.C., Sandbech-Clausen, S., Lichota, J., *et al.* (2008). Arabidopsis MAP kinase 4 regulates gene expression through transcription factor release in the nucleus. EMBO J *27*, 2214-2221.

· Redenbaugh, K., Hiatt, B., Martineau, B., Kramer, M., Sheehy, R., Sanders, R., Houck, C. and Emlay, D. (1992). Safety Assessment of Genetically Engineered Fruits and Vegetables: A Case Study of the Flavr Savr Tomato. CRC Press, 288.

· Reinke, H., and Horz, W. (2003). Histones are first hyperacetylated and then lose contact with the activated PHO5 promoter. Mol Cell *11*, 1599-1607.

· Robatzek, S., Chinchilla, D., and Boller, T. (2006). Ligand-induced endocytosis of the pattern recognition receptor FLS2 in Arabidopsis. Genes Dev *20*, 537-542.

· Roberts, S.M., and Winston, F. (1997). Essential functional interactions of SAGA, a Saccharomyces cerevisiae complex of Spt, Ada, and Gcn5 proteins, with the Snf/Swi and Srb/mediator complexes. Genetics *147*, 451-465.

· Rodriguez-Navarro, S., Fischer, T., Luo, M.J., Antunez, O., Brettschneider, S., Lechner, J., Perez-Ortin, J.E., Reed, R., and Hurt, E. (2004). Sus1, a functional component of the SAGA histone acetylase complex and the nuclear pore-associated mRNA export machinery. Cell *116*, 75-86.

· Rojas, A.L., Nagem, R.A., Neustroev, K.N., Arand, M., Adamska, M., Eneyskaya, E.V., Kulminskaya, A.A., Garratt, R.C., Golubev, A.M., and Polikarpov, I. (2004). Crystal structures of beta-galactosidase from Penicillium sp. and its complex with galactose. J Mol Biol *343*, 1281-1292.

· Rolando, M., Sanulli, S., Rusniok, C., Gomez-Valero, L., Bertholet, C., Sahr, T., Margueron, R., and Buchrieser, C. (2013). Legionella pneumophila effector RomA uniquely modifies host chromatin to repress gene expression and promote intracellular bacterial replication. Cell Host Microbe *13*, 395-405.
· Rosa, S., Ntoukakis, V., Ohmido, N., Pendle, A., Abranches, R., and Shaw, P. (2014). Cell differentiation and development in Arabidopsis are associated with changes in histone dynamics at the single-cell level. Plant Cell *26*, 4821-4833.
· Routh, A., Sandin, S., and Rhodes, D. (2008). Nucleosome repeat length and linker histone stoichiometry determine chromatin fiber structure. Proc Natl Acad Sci U S A *105*, 8872-8877.
· Rushton, P.J., Somssich, I.E., Ringler, P., and Shen, Q.J. (2010). WRKY transcription factors. Trends Plant Sci *15*, 247-258.
· Sadeghi, M., Dehghan, S., Fischer, R., Wenzel, U., Vilcinskas, A., Kavousi, H.R., and Rahnamaeian, M. (2013). Isolation and characterization of isochorismate synthase and cinnamate 4-hydroxylase during salinity stress, wounding, and salicylic acid treatment in Carthamus tinctorius. Plant Signal Behav *8*, e27335.
· Samara, N.L., and Wolberger, C. (2011). A new chapter in the transcription SAGA. Curr Opin Struct Biol *21*, 767-774.
· Sano, S., Aoyama, M., Nakai, K., Shimotani, K., Yamasaki, K., Sato, M.H., Tojo, D., Suwastika, I.N., Nomura, H., and Shiina, T. (2014). Light-dependent expression of flg22-induced defense genes in Arabidopsis. Front Plant Sci *5*, 531.
· Sarris, P.F., and Jones, J.D. (2015). Plant immune receptors mimic pathogen virulence targets. Oncotarget *6*, 16824-16825.
· Sawicka, A., and Seiser, C. (2012). Histone H3 phosphorylation - a versatile chromatin modification for different occasions. Biochimie *94*, 2193-2201.
· Schaub, P., Al-Babili, S., Drake, R., and Beyer, P. (2005). Why is golden rice golden (yellow) instead of red? Plant Physiol *138*, 441-450.
· Schechter, L.M., Vencato, M., Jordan, K.L., Schneider, S.E., Schneider, D.J., and Collmer, A. (2006). Multiple approaches to a complete inventory of Pseudomonas syringae pv. tomato DC3000 type III secretion system effector proteins. Mol Plant Microbe Interact *19*, 1180-1192.
· Schulze, B., Mentzel, T., Jehle, A.K., Mueller, K., Beeler, S., Boller, T., Felix, G., and Chinchilla, D. (2010). Rapid heteromerization and phosphorylation of ligand-activated plant transmembrane receptors and their associated kinase BAK1. J Biol Chem *285*, 9444-9451.

· Scofield, S.R., Tobias, C.M., Rathjen, J.P., Chang, J.H., Lavelle, D.T., Michelmore, R.W., and Staskawicz, B.J. (1996). Molecular Basis of Gene-for-Gene Specificity in Bacterial Speck Disease of Tomato. Science *274*, 2063-2065.
· Searle, B.C. (2010). Scaffold: a bioinformatic tool for validating MS/MS-based proteomic studies. Proteomics *10*, 1265-1269.
· Servet, C., Benhamed, M., Latrasse, D., Kim, W., Delarue, M., and Zhou, D.X. (2008). Characterization of a phosphatase 2C protein as an interacting partner of the histone acetyltransferase GCN5 in Arabidopsis. Biochim Biophys Acta *1779*, 376-382.
· Servet, C., Conde e Silva, N., and Zhou, D.X. (2010a). Histone acetyltransferase AtGCN5/HAG1 is a versatile regulator of developmental and inducible gene expression in Arabidopsis. Mol Plant *3*, 670-677.
· Servet, C., Silva, N., and Zhou, D. (2010b). Histone Acetyltransferase AtGCN5/HAG1 Is a Versatile Regulator of Developmental and Inducible Gene Expression in Arabidopsis. Molecular Plant *3*, 670-677.
· Sharma, S., Kelly, T.K., and Jones, P.A. (2010). Epigenetics in cancer. Carcinogenesis *31*, 27-36.
· Sheard, L.B., Tan, X., Mao, H., Withers, J., Ben-Nissan, G., Hinds, T.R., Kobayashi, Y., Hsu, F.F., Sharon, M., Browse, J., *et al.* (2010). Jasmonate perception by inositol-phosphate-potentiated COI1-JAZ co-receptor. Nature *468*, 400-405.
· Shen, Q.H., Saijo, Y., Mauch, S., Biskup, C., Bieri, S., Keller, B., Seki, H., Ulker, B., Somssich, I.E., and Schulze-Lefert, P. (2007). Nuclear activity of MLA immune receptors links isolate-specific and basal disease-resistance responses. Science *315*, 1098-1103.
· Siersbaek, R., Baek, S., Rabiee, A., Nielsen, R., Traynor, S., Clark, N., Sandelin, A., Jensen, O.N., Sung, M.H., Hager, G.L., *et al.* (2014). Molecular architecture of transcription factor hotspots in early adipogenesis. Cell Rep *7*, 1434-1442.
· Simon, N.C., Aktories, K., and Barbieri, J.T. (2014). Novel bacterial ADP-ribosylating toxins: structure and function. Nat Rev Microbiol *12*, 599-611.
· Singh, P., Yekondi, S., Chen, P.W., Tsai, C.H., Yu, C.W., Wu, K., and Zimmerli, L. (2014). Environmental History Modulates Arabidopsis Pattern-Triggered Immunity in a HISTONE ACETYLTRANSFERASE1-Dependent Manner. Plant Cell *26*, 2676-2688.

· Singh, R.P., Hodson, D.P., Jin, Y., Lagudah, E.S., Ayliffe, M.A., Bhavani, S., Rouse, M.N., Pretorius, Z.A., Szabo, L.J., Huerta-Espino, J., *et al.* (2015). Emergence and Spread of New Races of Wheat Stem Rust Fungus: Continued Threat to Food Security and Prospects of Genetic Control. Phytopathology *105*, 872-884.
· Smale, S.T. (2014). Transcriptional regulation in the immune system: a status report. Trends Immunol *35*, 190-194.
· Spange, S., Wagner, T., Heinzel, T., and Kramer, O.H. (2009). Acetylation of non-histone proteins modulates cellular signalling at multiple levels. Int J Biochem Cell Biol *41*, 185-198.
· Sperschneider, J., Catanzariti, A.M., DeBoer, K., Petre, B., Gardiner, D.M., Singh, K.B., Dodds, P.N., and Taylor, J.M. (2017). LOCALIZER: subcellular localization prediction of both plant and effector proteins in the plant cell. Sci Rep *7*, 44598.
· Sridha, S., and Wu, K. (2006). Identification of AtHD2C as a novel regulator of abscisic acid responses in Arabidopsis. Plant J *46*, 124-133.
· Stasevich, T.J., and McNally, J.G. (2011). Assembly of the transcription machinery: ordered and stable, random and dynamic, or both? Chromosoma *120*, 533-545.
· Steger, D.J., and Workman, J.L. (1996). Remodeling chromatin structures for transcription: what happens to the histones? Bioessays *18*, 875-884.
· Sterner, D.E., and Berger, S.L. (2000). Acetylation of histones and transcription-related factors. Microbiol Mol Biol Rev *64*, 435-459.
· Stockinger, E., Mao, Y., Regier, M., Triezenberg, S., and Thomashow, M. (2001). Transcriptional adaptor and histone acetyltransferase proteins in Arabidopsis and their interactions with CBF1, a transcriptional activator involved in cold-regulated gene expression. Nucleic Acids Research *29*, 1524-1533.
· Strahl, B., and Allis, C. (2000). The language of covalent histone modifications. Nature *403*, 41-45.
· Stroud, H., Otero, S., Desvoyes, B., Ramirez-Parra, E., Jacobsen, S.E., and Gutierrez, C. (2012). Genome-wide analysis of histone H3.1 and H3.3 variants in Arabidopsis thaliana. Proc Natl Acad Sci U S A *109*, 5370-5375.
· Subirana, J.A. (1990). Analysis of the charge distribution in the C-terminal region of histone H1 as related to its interaction with DNA. Biopolymers *29*, 1351-1357.
· Sudarsanam, P., and Winston, F. (2000). The Swi/Snf family nucleosome-remodeling complexes and transcriptional control. Trends Genet *16*, 345-351.

· Sun, J., and Barbieri, J.T. (2003). Pseudomonas aeruginosa ExoT ADP-ribosylates CT10 regulator of kinase (Crk) proteins. J Biol Chem *278*, 32794-32800.
· Svejstrup, J.Q. (2003). Rescue of arrested RNA polymerase II complexes. J Cell Sci *116*, 447-451.
· Szemenyei, H., Hannon, M., and Long, J.A. (2008). TOPLESS mediates auxin-dependent transcriptional repression during Arabidopsis embryogenesis. Science *319*, 1384-1386.
· Tanner, K.G., Trievel, R.C., Kuo, M.H., Howard, R.M., Berger, S.L., Allis, C.D., Marmorstein, R., and Denu, J.M. (1999). Catalytic mechanism and function of invariant glutamic acid 173 from the histone acetyltransferase GCN5 transcriptional coactivator. J Biol Chem *274*, 18157-18160.
· Tee, W.W., Shen, S.S., Oksuz, O., Narendra, V., and Reinberg, D. (2014). Erk1/2 activity promotes chromatin features and RNAPII phosphorylation at developmental promoters in mouse ESCs. Cell *156*, 678-690.
· Tena, G., Boudsocq, M., and Sheen, J. (2011). Protein kinase signaling networks in plant innate immunity. Current Opinion in Plant Biology *14*, 519-529.
· Terakura, S., Ueno, Y., Tagami, H., Kitakura, S., Machida, C., Wabiko, H., Aiba, H., Otten, L., Tsukagoshi, H., Nakamura, K., *et al.* (2007). An oncoprotein from the plant pathogen Agrobacterium has histone chaperone-like activity. Plant Cell *19*, 2855-2865.
· Thilmony, R., Underwood, W., and He, S.Y. (2006). Genome-wide transcriptional analysis of the Arabidopsis thaliana interaction with the plant pathogen Pseudomonas syringae pv. tomato DC3000 and the human pathogen Escherichia coli O157:H7. Plant J *46*, 34-53.
· Thines, B., Katsir, L., Melotto, M., Niu, Y., Mandaokar, A., Liu, G., Nomura, K., He, S.Y., Howe, G.A., and Browse, J. (2007). JAZ repressor proteins are targets of the SCF(COI1) complex during jasmonate signalling. Nature *448*, 661-665.
· Thomma, B.P., Eggermont, K., Penninckx, I.A., Mauch-Mani, B., Vogelsang, R., Cammue, B.P., and Broekaert, W.F. (1998). Separate jasmonate-dependent and salicylate-dependent defense-response pathways in Arabidopsis are essential for resistance to distinct microbial pathogens. Proc Natl Acad Sci U S A *95*, 15107-15111.
· Tinland, B., Rohfritsch, O., Michler, P., and Otten, L. (1990). Agrobacterium tumefaciens T-DNA gene 6b stimulates rol-induced root formation, permits

growth at high auxin concentrations and increases root size. Mol Gen Genet *223*, 1-10.

· Tiwari, S.B., Hagen, G., and Guilfoyle, T.J. (2004). Aux/IAA proteins contain a potent transcriptional repression domain. Plant Cell *16*, 533-543.

· Torres, M.A., Dangl, J.L., and Jones, J.D. (2002). Arabidopsis gp91phox homologues AtrbohD and AtrbohF are required for accumulation of reactive oxygen intermediates in the plant defense response. Proc Natl Acad Sci U S A *99*, 517-522.

· Trievel, R.C., Rojas, J.R., Sterner, D.E., Venkataramani, R.N., Wang, L., Zhou, J., Allis, C.D., Berger, S.L., and Marmorstein, R. (1999). Crystal structure and mechanism of histone acetylation of the yeast GCN5 transcriptional coactivator. Proc Natl Acad Sci U S A *96*, 8931-8936.

· Turner, B.M., Birley, A.J., and Lavender, J. (1992). Histone H4 isoforms acetylated at specific lysine residues define individual chromosomes and chromatin domains in Drosophila polytene nuclei. Cell *69*, 375-384.

· Turriziani, B., Garcia-Munoz, A., Pilkington, R., Raso, C., Kolch, W., and von Kriegsheim, A. (2014). On-beads digestion in conjunction with data-dependent mass spectrometry: a shortcut to quantitative and dynamic interaction proteomics. Biology (Basel) *3*, 320-332.

· Tyler, R.C., Bitto, E., Berndsen, C.E., Bingman, C.A., Singh, S., Lee, M.S., Wesenberg, G.E., Denu, J.M., Phillips, G.N., Jr., and Markley, J.L. (2006). Structure of Arabidopsis thaliana At1g77540 protein, a minimal acetyltransferase from the COG2388 family. Biochemistry *45*, 14325-14336.

· Umena, Y., Kawakami, K., Shen, J.R., and Kamiya, N. (2011). Crystal structure of oxygen-evolving photosystem II at a resolution of 1.9 A. Nature *473*, 55-60.

· Umezawa, T., Sugiyama, N., Takahashi, F., Anderson, J.C., Ishihama, Y., Peck, S.C., and Shinozaki, K. (2013). Genetics and phosphoproteomics reveal a protein phosphorylation network in the abscisic acid signaling pathway in Arabidopsis thaliana. Sci Signal *6*, rs8.

· Uppalapati, S.R., Ishiga, Y., Wangdi, T., Kunkel, B.N., Anand, A., Mysore, K.S., and Bender, C.L. (2007). The phytotoxin coronatine contributes to pathogen fitness and is required for suppression of salicylic acid accumulation in tomato inoculated with Pseudomonas syringae pv. tomato DC3000. Mol Plant Microbe Interact *20*, 955-965.

· Ustun, S., Sheikh, A., Gimenez-Ibanez, S., Jones, A., Ntoukakis, V., and Bornke, F. (2016). The Proteasome Acts as a Hub for Plant Immunity and Is Targeted by Pseudomonas Type III Effectors. Plant Physiol *172*, 1941-1958.
· van den Burg, H.A., and Takken, F.L. (2009). Does chromatin remodeling mark systemic acquired resistance? Trends Plant Sci *14*, 286-294.
· Van der Biezen, E.A., and Jones, J.D. (1998). Plant disease-resistance proteins and the gene-for-gene concept. Trends Biochem Sci *23*, 454-456.
· Venturelli, S., Belz, R.G., Kamper, A., Berger, A., von Horn, K., Wegner, A., Bocker, A., Zabulon, G., Langenecker, T., Kohlbacher, O., *et al.* (2015). Plants Release Precursors of Histone Deacetylase Inhibitors to Suppress Growth of Competitors. Plant Cell *27*, 3175-3189.
· Verkest, A., Byzova, M., Martens, C., Willems, P., Verwulgen, T., Slabbinck, B., Rombaut, D., Van de Velde, J., Vandepoele, K., Standaert, E., *et al.* (2015). Selection for Improved Energy Use Efficiency and Drought Tolerance in Canola Results in Distinct Transcriptome and Epigenome Changes. Plant Physiol *168*, 1338-1350.
· Visschedyk, D.D., Perieteanu, A.A., Turgeon, Z.J., Fieldhouse, R.J., Dawson, J.F., and Merrill, A.R. (2010). Photox, a novel actin-targeting mono-ADP-ribosyltransferase from Photorhabdus luminescens. J Biol Chem *285*, 13525-13534.
· Vlachonasios, K.E., Thomashow, M.F., and Triezenberg, S.J. (2003). Disruption mutations of ADA2b and GCN5 transcriptional adaptor genes dramatically affect Arabidopsis growth, development, and gene expression. Plant Cell *15*, 626-638.
· Vlot, A.C., Dempsey, D.A., and Klessig, D.F. (2009). Salicylic Acid, a multifaceted hormone to combat disease. Annu Rev Phytopathol *47*, 177-206.
· Wallberg, A.E., Flinn, E.M., Gustafsson, J.A., and Wright, A.P. (2000). Recruitment of chromatin remodelling factors during gene activation via the glucocorticoid receptor N-terminal domain. Biochem Soc Trans *28*, 410-414.
· Walley, J.W., Rowe, H.C., Xiao, Y., Chehab, E.W., Kliebenstein, D.J., Wagner, D., and Dehesh, K. (2008). The chromatin remodeler SPLAYED regulates specific stress signaling pathways. PLoS Pathog *4*, e1000237.
· Wang, C., Gao, F., Wu, J., Dai, J., Wei, C., and Li, Y. (2010a). Arabidopsis putative deacetylase AtSRT2 regulates basal defense by suppressing PAD4, EDS5 and SID2 expression. Plant Cell Physiol *51*, 1291-1299.

· Wang, L., Liu, L., and Berger, S.L. (1998). Critical residues for histone acetylation by Gcn5, functioning in Ada and SAGA complexes, are also required for transcriptional function in vivo. Genes Dev *12*, 640-653.
· Wang, M., Soyano, T., Machida, S., Yang, J.Y., Jung, C., Chua, N.H., and Yuan, Y.A. (2011). Molecular insights into plant cell proliferation disturbance by Agrobacterium protein 6b. Genes Dev *25*, 64-76.
· Wang, S., Durrant, W.E., Song, J., Spivey, N.W., and Dong, X. (2010b). Arabidopsis BRCA2 and RAD51 proteins are specifically involved in defense gene transcription during plant immune responses. Proc Natl Acad Sci U S A *107*, 22716-22721.
· Wang, X., Boevink, P., McLellan, H., Armstrong, M., Bukharova, T., Qin, Z., and Birch, P.R. (2015). A Host KH RNA-Binding Protein Is a Susceptibility Factor Targeted by an RXLR Effector to Promote Late Blight Disease. Mol Plant *8*, 1385-1395.
· Wang, Y., Li, J., Hou, S., Wang, X., Li, Y., Ren, D., Chen, S., Tang, X., and Zhou, J.M. (2010c). A Pseudomonas syringae ADP-ribosyltransferase inhibits Arabidopsis mitogen-activated protein kinase kinases. Plant Cell *22*, 2033-2044.
· Wei, C.F., Kvitko, B.H., Shimizu, R., Crabill, E., Alfano, J.R., Lin, N.C., Martin, G.B., Huang, H.C., and Collmer, A. (2007). A Pseudomonas syringae pv. tomato DC3000 mutant lacking the type III effector HopQ1-1 is able to cause disease in the model plant Nicotiana benthamiana. Plant J *51*, 32-46.
· Weinmann, A.S., Mitchell, D.M., Sanjabi, S., Bradley, M.N., Hoffmann, A., Liou, H.C., and Smale, S.T. (2001). Nucleosome remodeling at the IL-12 p40 promoter is a TLR-dependent, Rel-independent event. Nat Immunol *2*, 51-57.
· Weinmann, A.S., Plevy, S.E., and Smale, S.T. (1999). Rapid and selective remodeling of a positioned nucleosome during the induction of IL-12 p40 transcription. Immunity *11*, 665-675.
· Weiste, C., and Droge-Laser, W. (2014). The Arabidopsis transcription factor bZIP11 activates auxin-mediated transcription by recruiting the histone acetylation machinery. Nat Commun *5*, 3883.
· WHO (1990). Public Health Impact of Pesticides Used in Agriculture. World Heatlh Organization, Geneva *88*.
· Wildermuth, M.C., Dewdney, J., Wu, G., and Ausubel, F.M. (2001). Isochorismate synthase is required to synthesize salicylic acid for plant defence. Nature *414*, 562-565.

· Windram, O., Madhou, P., McHattie, S., Hill, C., Hickman, R., Cooke, E., Jenkins, D., Penfold, C., Baxter, L., Breeze, E., *et al.* (2012). Arabidopsis Defense against Botrytis cinerea: Chronology and Regulation Deciphered by High-Resolution Temporal Transcriptomic Analysis. Plant Cell *24*, 3530-3557.
· Workman, J.L., and Kingston, R.E. (1998). Alteration of nucleosome structure as a mechanism of transcriptional regulation. Annu Rev Biochem *67*, 545-579.
· Wu, Y., Zhang, D., Chu, J.Y., Boyle, P., Wang, Y., Brindle, I.D., De Luca, V., and Despres, C. (2012). The Arabidopsis NPR1 protein is a receptor for the plant defense hormone salicylic acid. Cell Rep *1*, 639-647.
· Xin, X.F., and He, S.Y. (2013). Pseudomonas syringae pv. tomato DC3000: a model pathogen for probing disease susceptibility and hormone signaling in plants. Annu Rev Phytopathol *51*, 473-498.
· Xu, F., Zhang, K., and Grunstein, M. (2005). Acetylation in histone H3 globular domain regulates gene expression in yeast. Cell *121*, 375-385.
· Xu, W., Edmondson, D.G., Evrard, Y.A., Wakamiya, M., Behringer, R.R., and Roth, S.Y. (2000). Loss of Gcn5l2 leads to increased apoptosis and mesodermal defects during mouse development. Nat Genet *26*, 229-232.
· Xu, X.M., Rose, A., and Meier, I. (2007). NUA Activities at the Plant Nuclear Pore. Plant Signal Behav *2*, 553-555.
· Yamaguchi, Y., Huffaker, A., Bryan, A.C., Tax, F.E., and Ryan, C.A. (2010). PEPR2 is a second receptor for the Pep1 and Pep2 peptides and contributes to defense responses in Arabidopsis. Plant Cell *22*, 508-522.
· Yano, R., Takebayashi, Y., Nambara, E., Kamiya, Y., and Seo, M. (2013). Combining association mapping and transcriptomics identify HD2B histone deacetylase as a genetic factor associated with seed dormancy in Arabidopsis thaliana. Plant J *74*, 815-828.
· Yoo, S.D., Cho, Y.H., and Sheen, J. (2007). Arabidopsis mesophyll protoplasts: a versatile cell system for transient gene expression analysis. Nat Protoc *2*, 1565-1572.
· Yoshida, M., Horinouchi, S., and Beppu, T. (1995). Trichostatin A and trapoxin: novel chemical probes for the role of histone acetylation in chromatin structure and function. Bioessays *17*, 423-430.
· Zhang, J., Shao, F., Li, Y., Cui, H., Chen, L., Li, H., Zou, Y., Long, C., Lan, L., Chai, J., *et al.* (2007). A Pseudomonas syringae effector inactivates MAPKs to suppress PAMP-induced immunity in plants. Cell Host Microbe *1*, 175-185.

· Zhao, J., Herrera-Diaz, J., and Gross, D.S. (2005). Domain-wide displacement of histones by activated heat shock factor occurs independently of Swi/Snf and is not correlated with RNA polymerase II density. Mol Cell Biol *25*, 8985-8999.
· Zheng, Y., Ding, Y., Sun, X., Xie, S., Wang, D., Liu, X., Su, L., Wei, W., Pan, L., and Zhou, D.X. (2016). Histone deacetylase HDA9 negatively regulates salt and drought stress responsiveness in Arabidopsis. J Exp Bot *67*, 1703-1713.
· Zhu, X.G., Ort, D.R., Whitmarsh, J., and Long, S.P. (2004). The slow reversibility of photosystem II thermal energy dissipation on transfer from high to low light may cause large losses in carbon gain by crop canopies: a theoretical analysis. J Exp Bot *55*, 1167-1175.
· Zhu, Z., Xu, F., Zhang, Y., Cheng, Y.T., Wiermer, M., Li, X., and Zhang, Y. (2010). Arabidopsis resistance protein SNC1 activates immune responses through association with a transcriptional corepressor. Proc Natl Acad Sci U S A *107*, 13960-13965.
· Zipfel, C. (2008). Pattern-recognition receptors in plant innate immunity. Curr Opin Immunol *20*, 10-16.
· Zipfel, C., Robatzek, S., Navarro, L., Oakeley, E., Jones, J., Felix, G., and Boller, T. (2004). Bacterial disease resistance in Arabidopsis through flagellin perception. Nature *428*, 764-767.
· Zou, B., Yang, D.L., Shi, Z., Dong, H., and Hua, J. (2014). Monoubiquitination of histone 2B at the disease resistance gene locus regulates its expression and impacts immune responses in Arabidopsis. Plant Physiol *165*, 309-318.
· Zurawski, D.V., Mumy, K.L., Faherty, C.S., McCormick, B.A., and Maurelli, A.T. (2009). Shigella flexneri type III secretion system effectors OspB and OspF target the nucleus to downregulate the host inflammatory response via interactions with retinoblastoma protein. Mol Microbiol *71*, 350-368.